Orchestration of viral replication by norovirus NS4 via host membrane rearrangement and interaction with viral NS1-2

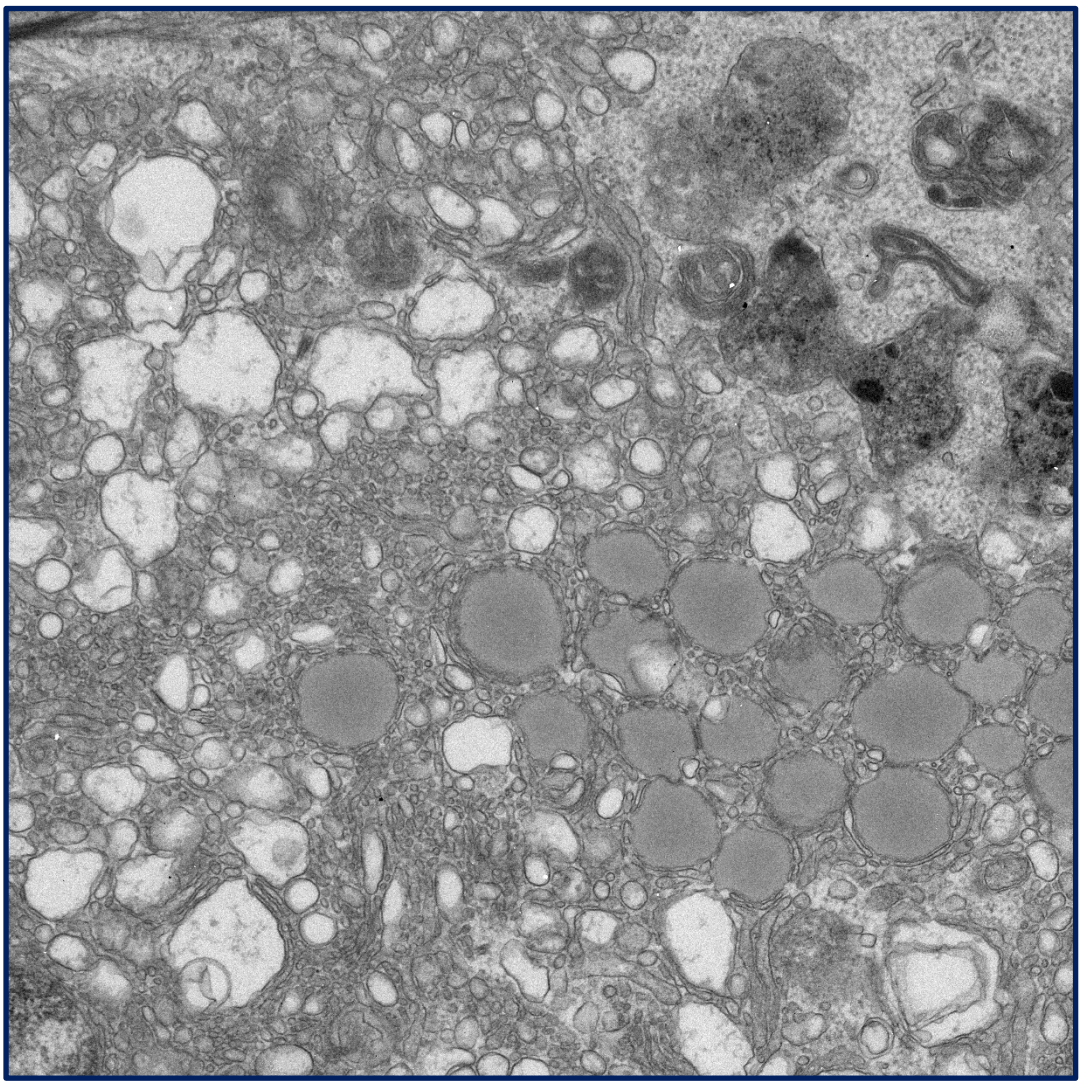

Robin Veenstra

Inaugural dissertation

for

obtaining the doctoral degree

of the

Combined Faculty of Mathematics, Engineering and Natural Sciences

of the

Ruprecht-Karls-University

Heidelberg

Presented by Robin Veenstra, MSc

born on the 2nd of August, 1994

in Delft, The Netherlands

Oral examination: February 18, 2025 at 11:00

Orchestration of viral replication by norovirus NS4 via host membrane rearrangement and interaction with viral NS1-2

Referees: Prof. dr. Ralf Bartenschlager

Prof. dr. Volker Lohmann

“The feeling of awed wonder that science can give us is one of the highest experiences of which the human psyche is capable. It is a deep aesthetic passion to rank with the finest that music and poetry can deliver.”

— Richard Dawkins (1941), *Unweaving the Rainbow*

I dedicate this doctoral thesis to my parents and grandparents, who always supported my scientific and academic endeavors with love and kindness, and to my former biology teacher, Dr. A.F. Weidema, who taught me to never stop asking difficult questions about life.

Abstract

Norovirus is the leading cause of acute gastroenteritis worldwide with over half a billion infections each year. Belonging to the positive-sense, single-stranded RNA viruses, norovirus is categorized in the order of *Picornavirales* in the family of *Caliciviridae*. Similar to other positive-sense, single-stranded RNA viruses, norovirus infection is characterized by the vesicular rearrangement of intracellular membranes. As these vesicular structures colocalize with viral nonstructural (NS) proteins and double-stranded RNA, these membranous alterations harbor the norovirus replication complex (RC). Although norovirus RC biogenesis remains poorly understood, the membrane-associated nonstructural proteins NS1-2, NS3 and NS4 are involved in this process. In particular, NS4 has been shown to induce a variety of membrane rearrangements, hinting at a key role for this protein in membrane remodeling during norovirus infection. However, little is known about the exact mechanism by which NS4 induces membrane alterations or how NS4 interacts with other nonstructural proteins in the norovirus RC. Therefore, this thesis aimed to unravel the molecular determinants of the membrane-rearranging and membrane-associating properties of NS4 as well as to explore protein-protein interactions between NS4 and other norovirus nonstructural proteins.

The first objective of this thesis was to identify amino acid residues within NS4 essential for viral replication. To this end, an amino acid alignment was performed to identify residues which are conserved among multiple genogroups. The reverse genetics model of GV murine norovirus (MNV)-1.CW1 was used to assess the importance of these residues for viral replication. Several of these amino acids were shown to be indispensable for viral replication. However, single mutation of these residues in the context of GII.4 New Orleans (NO) NS4 or ORF1 did not significantly impact membrane remodeling upon expression.

The second objective of this thesis was to identify and to characterize the NS4 domain responsible for the membrane-associating and membrane-rearranging abilities of NS4. First, *in silico* analyses predicted three distinct regions in NS4: an N-terminal structured region (SR), a large alpha helix (AH4) and a C-terminal nonstructured region (NSR). GFP fusion proteins of these regions were expressed in Huh7-T7 Lunet cells and subsequent immunofluorescence identified AH4 as the major determinant of membrane association of NS4. Since membrane-associating alpha helices are often amphipathic, the amphipathicity of AH4 of GII.4 NO and GV MNV-1.CW1 was

examined *in silico*. Interestingly, AH4 displayed comparable amphipathicity in both noroviruses. To explore the importance of the amphipathicity of AH4 for viral replication and the induction of membrane alterations, amphipathic mutants of GII.4 NO NS4 were designed and expressed in Huh7-T7 Lunet cells, followed by immunofluorescence and electron microscopy (EM). GII.4 NO NS4 mutants with a decreased amphipathic moment lost membrane association and did not induce membrane enwrapment of lipid droplets, a hallmark of membrane remodeling observed upon NS4 expression. However, deletion of AH4 from GII.4 NO ORF1 did not seem to impact membrane remodeling, challenging the view that AH4 is the main determinant of membrane rearrangements. Nevertheless, mutations in MNV.CW-1 which impaired the amphipathicity of AH4 abolished membrane association of NS4 as well as viral replication, highlighting the importance of the amphipathicity of AH4 for norovirus replication.

The third and final aim of this thesis was to identify and to characterize the protein-protein interactions between NS4 and other nonstructural proteins. Co-expression and immunoprecipitation revealed a strong interaction between GII.4 NO NS1-2 and NS4. Further mapping of NS4 pointed to the C-terminus of AH4 as the minimal binding region for NS1-2. Moreover, alanine scanning of this minimal binding region identified five specific amino acid residues that facilitated the interaction with NS1-2. Since many of these amino acid residues are conserved among multiple genogroups, corresponding sites were mutated in the MNV-1.CW1 genome to study the effect on the NS1-2-NS4 interaction during MNV infection. In line with the findings for GII.4 NO, mutation of corresponding amino acid residues in MNV-1.CW1 NS4 indeed abrogated the interaction between NS1-2 and NS4 and abolished viral replication. Finally, guided by AlphaFold predictions of the NS1-2-NS4 interaction, the C-terminal hydrophobic region of NS1-2 was found to bind to NS4 via specific residues within this region.

In conclusion, this thesis provides evidence that a large alpha helix in norovirus NS4 is essential for viral replication. The amphipathicity of this alpha helix determines the membrane association and is critical for the membrane-rearranging properties of NS4. In addition, this alpha helix interacts through specific residues with norovirus NS1-2. Breaking the NS1-2-NS4 interaction renders MNV replication-deficient, indicating that this interaction is pivotal for viral replication. Future research should therefore examine the use of this interaction as a druggable target against norovirus infection.

Zusammenfassung

Das Norovirus ist mit über einer halben Milliarde Infektionen pro Jahr weltweit die häufigste Ursache für akute Gastroenteritis. Das Norovirus gehört zu den einzelsträngigen RNA-Viren mit positiver Polarität und wird in die Ordnung *Picornavirales* in der Familie *Caliciviridae* eingeordnet. Ähnlich wie bei anderen einzelsträngigen RNA-Viren mit positiver Polarität ist die Infektion mit Noroviren durch eine vesikuläre Umstrukturierung der intrazellulären Membranen gekennzeichnet. Da diese vesikulären Strukturen mit viralen Nichtstrukturproteinen (NS) und doppelsträngiger RNA kollokalisieren, beherbergen diese membranösen Veränderungen den Norovirus-Replikationskomplex (RC). Obwohl die Biogenese des Norovirus-RC nur unzureichend verstanden ist, sind die membrangebundenen NS1-2, NS3 und NS4 an diesem Prozess beteiligt. Insbesondere NS4 induziert nachweislich eine Vielzahl von Membranumbauvorgängen, was auf eine Schlüsselrolle dieses Proteins bei Membranumstrukturierungen während der Norovirusinfektion hindeutet. Allerdings ist nur wenig über den genauen Mechanismus bekannt, durch den NS4 die Membranumstrukturierung auslöst, oder darüber, wie NS4 mit anderen nicht-strukturellen Proteinen im Norovirus RC interagiert. Daher zielt diese Arbeit darauf ab, die molekularen Determinanten der Membranumlagerung und der Assoziation der Membranen mit NS4 aufzudecken. Des Weiteren wird die Protein-Protein-Interaktion zwischen NS4 und anderen Nicht-Strukturproteinen des Norovirus zu untersuchen.

Das erste Ziel dieser Arbeit war die Identifizierung von Regionen in den Aminosäuresequenzen innerhalb von NS4, die für die virale Replikation wesentlich sind. Zu diesem Zweck wurde ein Aminosäure-Alignment durchgeführt, um Regionen zu identifizieren, die in mehreren Genogruppen konserviert sind. Das Modell der reversen Genetik des GV murinen Norovirus (MNV)-1.CW1 wurde verwendet, um die Bedeutung dieser Regionen für die virale Replikation zu evaluieren. Es zeigte sich, dass einige dieser Aminosäuren für die virale Replikation essenziell sind. Eine einzelne Mutation dieser Region im Kontext von GII.4 New Orleans (NO) NS4 oder des offenen Leserahmens (ORF) 1 hatte jedoch keine signifikanten Auswirkungen auf die Membranumstrukturierung während der Expression.

Das zweite Ziel dieser Arbeit war die Identifizierung und Charakterisierung der NS4-Domäne, die für die Membranassoziation und -umstrukturierung verantwortlich ist. Zunächst wurden durch *In-silico-Analysen* drei verschiedene Regionen in NS4

vorhergesagt: eine strukturierte N-terminale (SR), eine große Alpha-Helix (AH4) und eine C-terminale nicht-strukturierte Region (NSR). GFP-Fusionsproteine dieser Regionen wurden in Huh7-T7 Lunet-Zellen exprimiert, und die anschließende Immunfluoreszenz identifizierte AH4 als die Hauptdeterminante der Membranassoziation von NS4. Da membranassoziierte Alpha-Helices häufig amphipathisch sind, wurde die Amphipathie von AH4 von GII.4 NO und GV MNV-1.CW1 *in silico* untersucht. Interessanterweise zeigte AH4 in beiden Noroviren eine vergleichbare Amphipathie. Um die Bedeutung der Amphipathie von AH4 für die virale Replikation und die Induktion von Membranveränderungen zu untersuchen, wurden amphipathische Mutanten von GII.4 NO NS4 erstellt und in Huh7-T7 Lunet-Zellen exprimiert, gefolgt von Immunofluoreszenz und Elektronenmikroskopie (EM). GII.4 NO NS4-Mutanten mit einem reduzierten amphipathischen Moment verloren die Membranassoziation und induzierten keine Umhüllung der Lipidtröpfchen mit Membranen, ein Merkmal der Membranumstrukturierung, das bei der NS4-Expression beobachtet wurde. Die Deletion von AH4 aus GII.4 NO ORF1 scheint jedoch die Membranumstrukturierung nicht zu beeinträchtigen, was die Hypothese in Frage stellt, dass AH4 die Hauptdeterminante der Membranumstrukturierung ist. Mutationen in MNV.CW-1, die die AH4-Amphipathizität beeinträchtigten, führten zur Aufhebung der Membranassoziation von NS4 und der viralen Replikation, was die Bedeutung der AH4-Amphipathizität für die Norovirus-Replikation unterstreicht.

Das dritte und letzte Ziel dieser Arbeit war die Identifizierung und Charakterisierung von Protein-Protein-Interaktionen zwischen NS4 und anderen nicht-strukturellen Proteinen. Koexpression und Immunpräzipitation zeigten eine starke Interaktion zwischen GII.4 NO NS1-2 und NS4. Weitere Analyse von NS4 ergab, dass der C-Terminus von AH4 eine minimale Bindungsregion für NS1-2 darstellt. Darüber hinaus wurden bei einem Alanin-Scan dieser minimalen Bindungsregion fünf spezifische Aminosäuren identifiziert, die die Interaktion mit NS1-2 fördern. Da ein Großteil dieser Aminosäuren in mehreren Genogruppen konserviert sind, wurden die entsprechenden Stellen im MNV-1.CW1-Genom mutiert, um ihre Auswirkungen auf die NS1-2-NS4-Interaktion während der MNV-Infektion zu untersuchen. In Übereinstimmung mit den Ergebnissen für GII.4 NO führte die Mutation der entsprechenden Aminosäurereste in MNV-1.CW1 NS4 tatsächlich zur Aufhebung der Interaktion zwischen NS1-2 und NS4 und virale Replikation war nichtmehr nachweisbar. Schließlich wurde anhand von

AlphaFold-Vorhersagen der NS1-2-NS4-Interaktion festgestellt, dass die C-terminale hydrophobe Region von NS1-2 an spezifische Regionen innerhalb von NS4 bindet.
Zusammenfassend lässt sich sagen, dass diese Arbeit Beweise dafür liefert, dass ein großer Alpha-Helix in Norovirus NS4 für die virale Replikation essentiell ist. Die Amphipathie dieses Alpha-Helix bestimmt die Membranassoziation und ist entscheidend für die Membranumstrukturierung mittels NS4. Darüber hinaus interagiert dieser Alpha-Helix über spezifische Regionen mit Norovirus NS1-2, und mangelnde Interaktion zwischen NS1-2-NS4 führt zu reduzierter MNV-Replikation, was darauf hindeutet, dass diese Interaktion für die virale Replikation entscheidend ist. Für die Zukunft ist diese Interaktion zwischen NS1-2 und NS4 daher ein möglicher Angriffspunkt für antivirale Therapien und sollte weiter erforscht werden.

Table of contents

Chapter 1

Introduction

"*Science is more than a body of knowledge; it is a way of thinking.*"

— Carl Sagan (1934-1996), *The Demon-Haunted World*

---

1 Introduction

1.1 Norovirus disease

1.1.1 History and clinical manifestation of human noroviruses

Acute, non-bacterial gastroenteritis was first described by Zahorsky in 1929 and described as “winter vomiting disease” (1). Almost four decades later, human norovirus was isolated for the first time from stool collected from an outbreak of gastroenteritis in an elementary school in Norwalk, Ohio, in 1968 (2). Oral administration of these stool filtrates in healthy male prisoners resulted in the same clinical manifestation, further fueling the hypothesis that the disease might be caused by a non-bacterial pathogen (3,4). Electron microscopy (EM) in 1972 indeed confirmed the presence of small, 27-nm viral particles in stool samples of the outbreak and the virus was subsequently called “the Norwalk virus”, which later became known as the prototype of all norovirus strains (5). Noroviruses are now widely recognized as the leading cause of acute, non-bacterial gastroenteritis with over half a billion cases and more than 200,000 deaths each year worldwide (6). Even though the overall mortality of norovirus infection remains low in developed countries, the total economic costs of these infections are over ten billion US dollars each year in the United States alone, surpassing the societal costs of various other common infectious diseases (7). Despite the societal and economic burden, no vaccines or antiviral therapies against norovirus infection are commercially available.

The primary route of transmission of noroviruses is the fecal-oral route, where infected hosts spread the virus by directly contaminating foods or surfaces. In addition, transmission through aerosols generated by vomiting and transmission via the consumption of certain raw foods that have a high rate of norovirus contamination, such as raw oysters and other bivalve mollusks, are also implicated in norovirus transmission (8). Given this route of transmission, norovirus outbreaks occur often in restaurants or semi-closed settings such as schools, daycare centers, cruise ships, hospitals or nursing homes. Moreover, noroviruses are highly contagious as less than hundred particles might be sufficient to infect a new host (9). Although asymptomatic

infection occurs in an estimated 30 percent of all norovirus infections, the average incubation time of most symptomatic norovirus infection lies between 24 and 48 hours, depending on the norovirus strain and the infected host (10–12). The most frequent symptoms of norovirus infection include nausea, vomiting, diarrhea and abdominal cramps, whereas less common, but clinically relevant symptoms include fever and headache (13–15). Symptoms typically last for two to three days, but in rare cases can persist for weeks in immunocompromised hosts such as transplant patients (16–21).

1.1.2 Classification and epidemiology of noroviruses

At first, the Norwalk virus was characterized as a picornavirus or parvovirus based on appearance by electron microscopy alone (5). Later analyses carefully placed the Norwalk virus in the *Caliciviridae* family using virion morphology, nucleic acid composition and protein properties (Figure 1.1A) (22–24). However, final proof that the Norwalk virus indeed belongs to the *Caliciviridae* family was not provided until sequencing of the whole viral genome in the early 1990s (25). Initially, novel viruses showing high morphological similarity to the Norwalk virus were classified in the genus of “Norwalk-like viruses”, which was later renamed to the genus Norovirus (26). Prior to the rise of viral genome sequencing, the classification of different Norwalk-like viruses was based on cross-challenge studies, which initially led to the identification of three distinct antigenic classes: the Norwalk virus, the Hawaii virus and the Snow Mountain virus, all named after the place of the gastroenteritis outbreak (27–29). In the early 1990s, this number of antigenic classes was expanded to nine different antigenic entities (24). However, soon after viral genome sequencing became readily available, classification of Norwalk-like viruses based on antigenicity was abandoned and replaced with a classification based on nucleic acid sequence similarity. Initially, noroviruses were divided into five different genogroups based on nucleic acid sequences of the RNA-dependent RNA-polymerase (RdRp) region in open reading frame 1 (ORF1) or the major capsid protein (VP1) gene in ORF2, but this has been updated and reclassified recently to ten different genogroups with 48 distinct genotypes (Figure 1.1B) (30). Nomenclature of a norovirus strain is typically shown with both the genogroup and genotype in the form of “Ga.A”, where lowercase “a” is representing the genogroup in Roman numbers and the capital “A” is representing the genotype in Arabic numbers.

Of all ten genogroups, genogroup II is responsible for the vast majority of human norovirus infections worldwide, ranging up to 90 percent of all norovirus infections (31–33). Especially genogroup II genotype 4 (GII.4) is overrepresented in these statistics: over two-thirds of human norovirus infections seem to be caused by a strain of this particular genogroup and genotype (Figure 1.1C) (33). For the last decades, various GII.4 noroviruses have succeeded each other as the predominant pandemic strain in

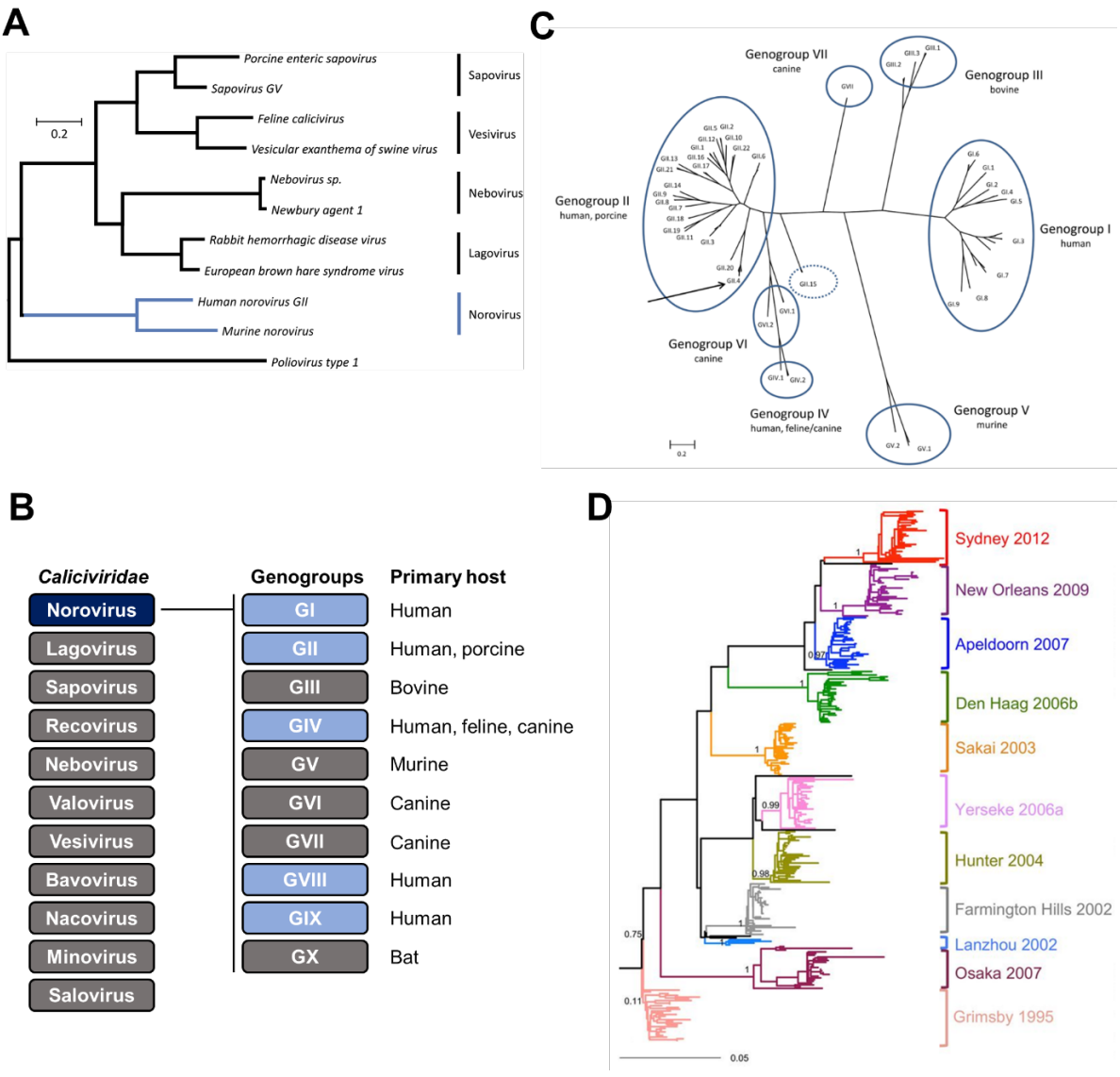

Figure 1.1 Phylogeny and classification of noroviruses

(A) Phylogenetic tree for the RdRp protein sequences of the family *Caliciviridae* and poliovirus type 1 (branch length represents number of substitutions per site, adapted from (102)). (B) Genogroups of norovirus and their known hosts. (C) Phylogenetic tree of genogroup I to VII. Arrow indicates the genogroup II genotype 4 (GII.4) (taken from (38)). (D) Phylogenetic tree of the pandemic GII.4 strains (figure taken from (260)).

humans, such as the GII.4 Den Haag 2006b strain, the GII.4 New Orleans 2009 strain and the GII.4 Sydney 2012 strain (Figure 1.1D) (34–38). Moreover, most strains causing large outbreaks belong to GII.4 and often result in higher mortality than strains of other genogroups or genotypes (39,40). In addition to GII.4, other clinically significant strains of human noroviruses belong to genogroup I, II, IV, GVIII and GIX (41,42). For example, the Norwalk virus strain belongs to GI.1 (43). Interestingly, sequencing of wastewater for norovirus sequences reveals a more diverse genetic pool, suggesting that infections with non-GII.4 noroviruses might be overlooked, since they display milder clinical manifestations (44).

1.2 Norovirus genomic organization

1.2.1 RNA genome

Noroviruses are non-enveloped viruses with a positive-sense, single-stranded RNA genome (Figure 1.2). The exact length of the viral genome is variable but usually ranges between 7.3 and 7.7 kb (45). Most norovirus genomes including those of human noroviruses contain three ORFs with the exception of GV MNV, which consists of four ORFs (46). Before the start of the first ORF, human noroviruses have a small 5' untranslated region (UTR), typically encompassing four nucleotides, whereas the GV MNV genome contains a small UTR of five nucleotides in length (47). As for all members of the *Caliciviridae* family, the norovirus genome is covalently linked at the 5' end with the viral protein VPg (NS5) (48). Downstream of the last ORF, which is ORF3, norovirus genomes contain a 3' UTR varying from 46 to 78 nucleotides in size, followed by a poly(A) tail at the very 3' end (47).

ORF1 is translated directly from the full-length viral genome as a large polyprotein and encodes the nonstructural proteins. This polyprotein of around 200 kDa is cleaved after translation by the norovirus protease Pro (NS6), which is encoded inside ORF1, giving rise to the six individual nonstructural proteins which will be elaborated on in more detail later in this thesis (49,50). The major capsid protein (VP1) and the minor capsid protein (VP2) are encoded by ORF2 and ORF3 respectively. ORF4 has so far only been described for MNV and is encoding a protein called virulence factor 1 (VF1),

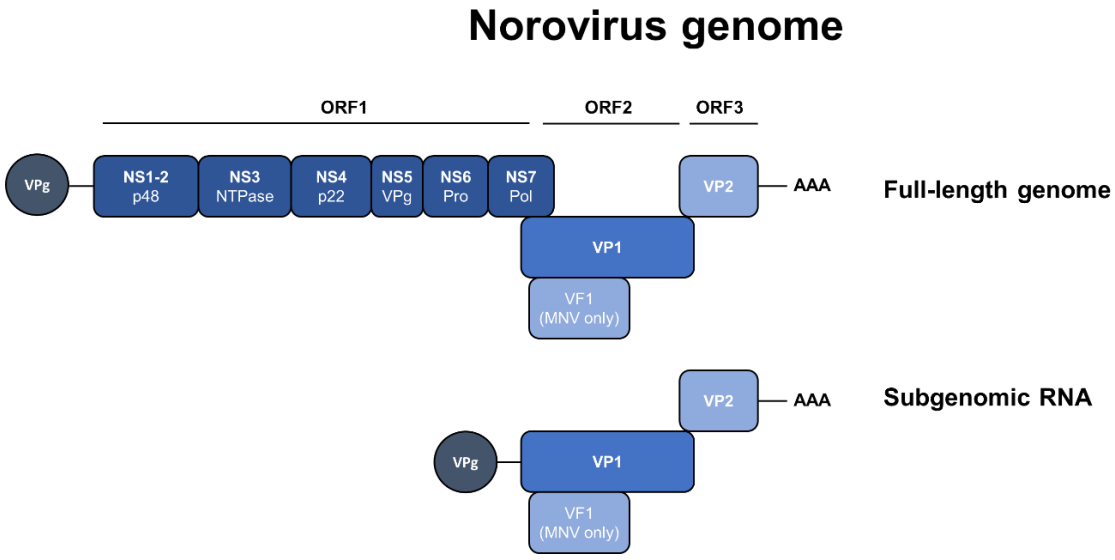

Figure 1.2 Schematic overview of the norovirus genome

The positive-sense, single-stranded RNA genome is covalently linked to the VPg protein at the 5' end. The very short 5' UTR is followed by ORF1, encoding the norovirus nonstructural proteins. ORF2 and ORF3 are located downstream of ORF1 and encode the structural proteins VP1 and VP2. In the case of MNV, a small ORF4 encoding VF1 is present within ORF2. ORF2, ORF3 and ORF4 are not translated directly from the viral genome, but require a subgenomic RNA for translation. The translation of ORF3 is facilitated by termination-reinitiation during translation of ORF2, whereas ORF4 seems to be expressed as an alternative ORF.

which is involved in regulating the host innate immune response and host cell apoptosis (46). ORF2 and ORF3 (and in MNV, ORF4) are not translated directly from the viral genome, but require a VPg-linked subgenomic RNA intermediate for translation (51,52). Direct translation of ORF2 from these subgenomic RNAs will yield VP1, whereas a translation termination-reinitiation strategy is utilized to translate ORF3, producing VP2 (53). In MNV, ORF4 is overlapping with ORF2 and the translation is most likely started directly as an alternative ORF, since the start codon of ORF4 is in close proximity to the ORF2 start codon (46).

1.2.2 NS1-2 or p48

The first protein encoded in ORF1 of the norovirus genome is NS1-2. In human noroviruses, this protein is typically referred to as p48. However, for purposes of consistency, this thesis will henceforth apply NS1-2 for both MNV and human noroviruses. Secondary structure analysis of NS1-2 show a disordered N-terminal

region, which is rich in proline and serine residues, followed by an H-box and NC sequence motif and an ordered C-terminal region, which is proposed to contain a hydrophobic region (54,55). No specific enzymatic activities of NS1-2 have been demonstrated so far, but a putative hydrolase domain has been identified *in silico* (56). In addition, human norovirus NS1-2 has been suggested to function as a viroporin that disrupts host calcium signaling kinetics, similar to NS1-2 homologues of other caliciviruses, such as TV NS1-2 and rabbit haemorrhagic disease virus (RHDV) p23 (57–62). Furthermore, two caspase cleavage sites have been identified in MNV NS1-2, which are crucial for the cleavage of NS1-2 into NS1 and NS2 and facilitate persistent infection of MNV in intestinal epithelial cells (63). Cleavage of human norovirus NS1-2 by caspase 7 has been observed *in vitro*, but it is not understood yet whether this occurs during natural infection as well (64). Interestingly, a single amino acid change in the NS1-2 protein of the nonpersistent CW3 MNV strain can confer colonic tropism and persistence (65).

Expression of human norovirus and MNV NS1-2 show a filamentous or reticular ER-like localization pattern and human norovirus NS1-2 seems to induce ER tubule formation in Huh7-T7 Lunet cells (56,61,66). Colocalization of NS1-2 with the replication intermediate double-stranded RNA (dsRNA) during MNV infection has been investigated and validated (67). Moreover, Norwalk NS1-2 has been shown to behave like an integral membrane protein and associates tightly with VAPA, an integral membrane protein of the ER that is implicated in the biogenesis of HCV RCs as well (68–71). In addition, the FCV NS1-2 analogue p32 has been shown to interact with the analogues of NS3 and NS4, p39 and p30, and is present in FCV RCs (72–74). These observations have led to the hypothesis that NS1-2, together with NS3 and NS4, is responsible for the biogenesis of the norovirus RCs.

1.2.3 NS3 or NTPase

Based on amino acid sequence alignments, NS3 was first proposed to function as a viral helicase. For a long time, this was challenging to proof experimentally and most studies could only convincingly demonstrate nucleotide triphosphatase (NTPase) and RNA chaperone activities in both MNV and human norovirus (75,76). However, almost all of these studies were using a bacterial expression system for the production of NS3,

which does not mimic all post-translational modification made in eukaryotic cells. A more recent paper therefore utilized the baculovirus expression system to produce NS3 in insect cells and this study was able to demonstrate helicase activity of GI.1 NS3 (77). This highlights the importance of post-translational modifications on the helicase activity of GI.1 NS3, which is in line with similar findings for the expression and helicase activity of human enterovirus $2C^{ATPase}$ (78). Still, higher resolution structures are needed to draw definite conclusions.

In addition to its putative helicase activity, NS3 has also been implicated in the generation of norovirus RCs. For example, NS3 has been shown to localize to LDs and ER membranes via two N-terminal amphipathic helices (79). Binding of NS3 to NS1-2 and NS4 has also been demonstrated, providing a mechanism by which these proteins can form the norovirus RC (79,80). Interestingly, NS3 of GII, but not GI, has also been shown to colocalize with mitochondrial markers and the C-terminus of GII NS3 seems involved in this mitochondrial targeting (80). Finally, NS3 is also the first norovirus nonstructural protein reported to be directly involved in viral egress by permeabilizing host membranes and facilitating apoptosis (81).

1.3.4 NS4 or p22

The exact function of NS4 is poorly understood. The expression pattern of GII.4 NS4 in Huh7-T7 Lunet cells shows colocalization with markers of the ER, Golgi and LDs. Furthermore, expression of GII.4 NS4 can induce the formation of both SMVs and DMVs, hinting at an important role for GII.4 NS4 in the biogenesis of norovirus replication complexes (RCs) (56). For MNV, NS4 has been shown to colocalize with markers of the ER and Golgi as well, however, prominent colocalization has also been observed for endosomal markers (66). Moreover, EM and immunofluorescence (IF) experiments on MNV infected cells have not only shown that the replication-intermediate dsRNA and MNV NS4 colocalize to a high degree, but also that dsRNA resides in vesicles adjacent to the nucleus and in close proximity of the Golgi apparatus, which is in line with the hypothesis that NS4 is part of the vesicular norovirus RC (67).

The mechanism by which NS4 rearranges membranes is not known. However, the NS4 protein of human noroviruses, but not of murine noroviruses, contains a mimic of an MERES in their NS4. This MERES seems to induce Golgi disassembly and inhibition the secretory pathway, which might be important for the induction of membrane alterations by NS4 (82). In addition, the NS4 protein of all noroviruses seems to contain an amphipathic alpha helix, which might facilitate the tethering of NS4 to membranes (83).

1.2.5 NS5 or VPg

NS5, more commonly known as VPg, is a protein covalently linked to the 5' end of the norovirus genome that serves multiple purposes in the viral life cycle. After translation of ORF1 and cleavage of the polyprotein, VPg is coupled to free nucleotides in a process which is called nucleotidylylation (84). This process is facilitated by the precursor NS6-NS7 and mature NS7 and seems to favor the linkage of VPg with GMP and UMP over linkage with CMP and AMP (85,86). Furthermore, biochemical analysis shows that the linkage between VPg and free nucleotides is greatly dependent on a tyrosine present in VPg (Y27 in human noroviruses, Y26 in MNV, Figure 1.3) (85,87,88). The preference of linkage to GMP and UMP over CMP or AMP seems in line with the hypothesis that nucleotidylylation is important for the start of genomic replication, since virtually all norovirus genomes start with a guanine at the 5' end and end at the 3' end with a poly(A) tail (47).

The priming of the 5' end of the norovirus genome with VPg is itself essential for translation of the norovirus genome. VPg binds directly to eIF4G, which leads to the recruitment of the host cell translation machinery and translation of ORF1 (89). Furthermore, proteinase K treatment of VPg-linked replicon RNA prior to transfection results in complete loss of colony formation ability, arguing that VPg-linkage is essential for translation and/or replication of the incoming viral RNA (90).

1.2.6 NS6 or Pro

NS6 or Pro functions as the norovirus protease. After initial translation, the ORF1 polyprotein cleavage is immediately initiated by the protease domain within NS6 (49,50). The structure of many human norovirus proteases has been determined using

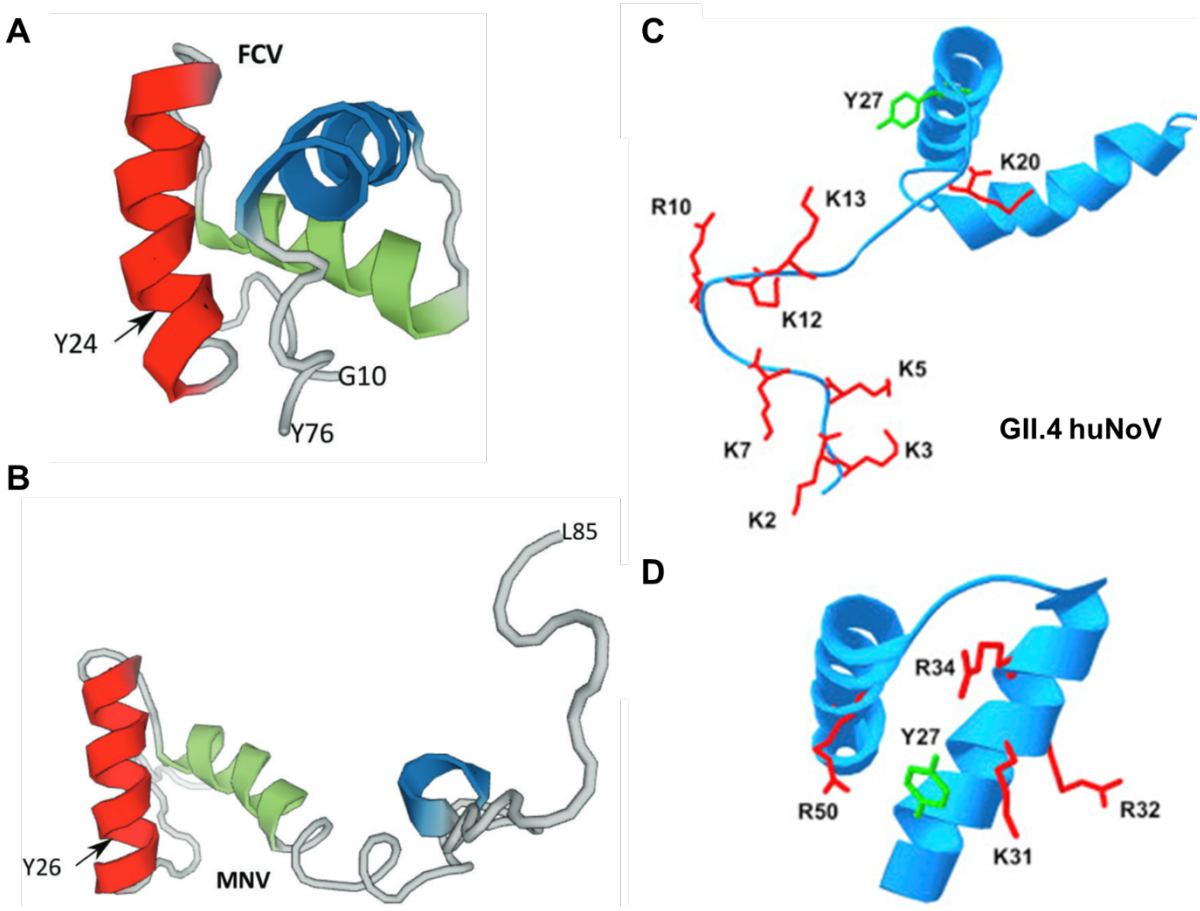

Figure 1.3 VPg structures of *Caliciviridae* members

(A) NMR structure of FCV VPg (PDB: 2M4H) spanning from G10 to Y76. The tyrosine at position 24 is critical for nucleotidylylation. (B) NMR structure of MNV VPg (PDB: 2MG4) spanning from G11 to L85. The tyrosine at position 26 is critical for nucleotidylylation. (C) Structure prediction of the N-terminus and central core of GII.4 human norovirus VPg, spanning from G1 to E56. For GII.4 human noroviruses, the tyrosine at position 27 in VPg is essential for nucleotidylylation and genome replication. (D) Structure prediction of the core domain of VPg in GII.4 human norovirus, spanning from residue D24 to E56. Figures adapted from (88, 86).

X-ray crystallography and they all consist of two domains, the N-terminal domain I and the C-terminal domain II, which are linked together by a large loop region (91–93). The active site of human norovirus proteases lies at the cleft between domain I and II and a reactive cysteine at this site is essential for protease activity, indicating that human norovirus proteases belong to the family of chymotrypsin-like cysteine proteases (94). Interestingly, X-ray crystallography of the MNV protease has revealed a high degree of structural homology to the structures found for human norovirus proteases (95).

Given the high similarity between different norovirus proteases, the NS6 protein serves as the prime target in many studies for the development of antivirals (96–98).
Like many viral proteases, the norovirus protease has preferential cleavage sites. For example, the MNV protease cleaves the junction between NS1-2/NS3 and NS3/NS4 most efficiently, whereas the junction between NS4/NS5, NS5/NS6 and NS6/NS7 are proteolytically cleaved at reduced rates (99). These preferential cleavage sites give rise to temporarily expressed viral protein precursors which often have independent functions, such as the role of the NS6-NS7 precursor in the nucleotidylylation of VPg (85).

1.2.7 NS7 or Pol

NS7, Pol or RNA-dependent RNA polymerase (RdRp) is arguably one of the most characterized nonstructural proteins of noroviruses. NS7 serves as the polymerase and is therefore responsible for the transcription of the novel norovirus genomes as well as norovirus antigenomic RNA and (anti)subgenomic RNA (100–104). X-ray crystallographic analysis have determined the structure of the polymerase of multiple noroviruses in depth (105–109). This structure shows high homology to the RdRp of other positive-sense, single-stranded RNA viruses and consists of fingers, thumb and palm subdomains, forming the canonical ‘right-hand’ structure (Figure 1.4) (100). Of note, multiple aspartate residues within the active site of the norovirus RdRp play a key role in directing metal ions such as manganese to the active site, facilitating the nucleotide polymerization (110). Since inhibition of the viral RdRp is often an effective antiviral strategy, many potential inhibitors have been screened against norovirus infection (110–122).

1.3 Norovirus cell culture models

1.3.1 RNA replicon-based models

Since RNA replicons have been developed successfully for many other positive-sense, single-stranded RNA viruses, such as HCV, poliovirus and more recently severe acute respiratory syndrome coronavirus 2 (SARS-CoV-2), the construction of such an RNA replicon for human noroviruses would greatly facilitate the development of novel antivirals (123–125). One of the first efforts to generate a norovirus RNA replicon led

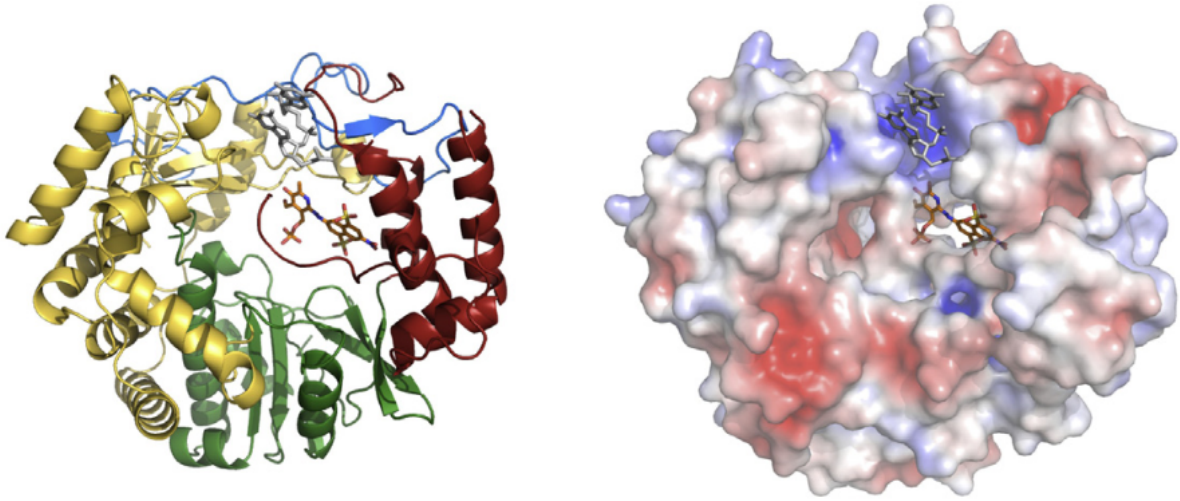

Figure 1.4 Crystal structure of the GII.4 human norovirus RdRp

The crystal structure of the GII.4 human norovirus RdRp in complex with the RdRp inhibitor PPNDS. The figure on the left shows the N-terminal domain of the RdRp in blue, the thumb domain in red, fingers domain in yellow and the palm domain in green. The figure on the right shows the electrostatic potential (negative potential in red, positive potential in blue). Figure taken from (122).

to the establishment of the GI.1 Norwalk replicon in BHK cells (Figure 1.5) (126). In this replicon, a part of ORF2 in the GI.1 Norwalk genome was replaced with the neomycin phosphotransferase gene, removing the region encoding VP1 but retaining the subgenomic promoter. Subsequent *in vitro* RNA transcription and electroporation in Huh7 or baby hamster kidney (BHK) cells resulted in expression of nonstructural proteins and the formation of colonies. Moreover, replicon RNA isolated after initial electroporation generated even more colonies than *in vitro* transcribed replicon RNA. Since treatment of this isolated replicon RNA with proteinase K completely abolished the capacity to form colonies, it is possible that the enhanced 'infectivity' of this isolated replicon RNA is caused by linkage of the replicon RNA to VPg.

Unfortunately, this GI.1 Norwalk replicon is thus far the only stable, selectable and reproducible RNA replicon of a human norovirus published, but it has proven to be a useful tool for antiviral screening. For example, the enterovirus protease inhibitor rupintrivir has been shown to effectively eradicate the GI.1 Norwalk replicon from Huh7 cells (97). The hepatitis C virus polymerase inhibitor 2'-C-methylcytidine (2CMC) reduces viral RNA in replicon-bearing cells in a dose-dependent manner (116).

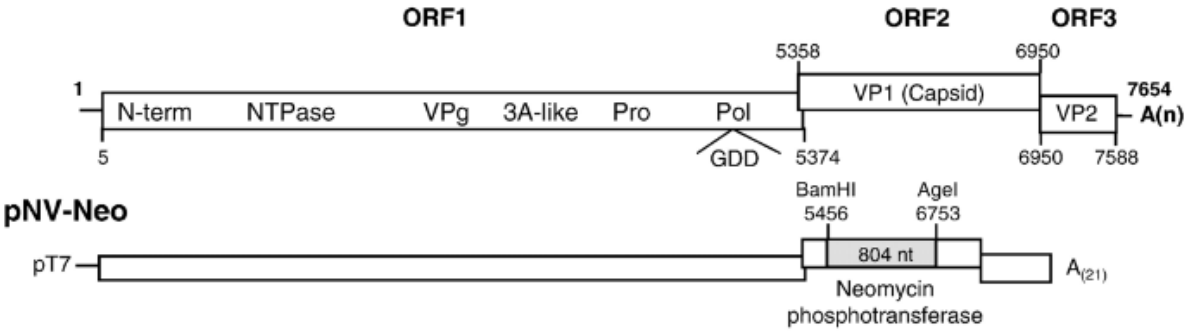

Figure 1.5 Design of the GI.1 Norwalk RNA replicon

A large part of GI.1 Norwalk ORF2 was replaced by the gene encoding neomycin phosphotransferase. The replicon was transcribed and capped using a T7-based kit and the capped RNA was electroporated in BHK cells. Selection of cells harboring the replicon was performed by addition of neomycin to the cell culture medium. RNA from these selected cells, which is presumably VPg-linked, could be harvested and transfected into other cell types to efficiently select for new replicon-bearing cells. Taken from (126).

Similarly, the adenosine analogue NITD008 can clear the Norwalk replicon from replicon-bearing cells without significant toxicity, most likely by blocking the active site of the norovirus RdRp (127). In addition to antiviral screening, the Norwalk replicon has been of help in understanding the norovirus lifecycle as well. For example, replicon-harboring human gastric tumor (HGT) cells showed reduced expression of the interferon lambda receptor 1 (IFNLR1) through epigenetic methylation of the *IFNLR1* promoter, hinting at the importance of type III interferons in the control of human noroviruses (128). Furthermore, knockdown of MDA5 in replicon-bearing cells has been demonstrated to increase replicon RNA. Although MDA5 typically acts through MAVS, it was found that in cells harboring the Norwalk replicon, MDA5 might induce a non-canonical antiviral response through activation of the JAK-STAT pathway (129). However, a main bottleneck of the system is its low efficiency regarding the establishment of cell lines based on *in vitro* transcribed RNA, which limits its applicability for reverse genetic studies, aiming at the understanding of the function of viral proteins by site-directed mutagenesis.

1.3.2 Cell culture models for infection with stool-derived virus

The establishment of a norovirus cell culture model has been a hot topic in the research field for decades, but only recently major progress has been made. In 2004, MNV was found to replicate in murine dendritic cells and macrophages, such as RAW264.7 and

BV2 cells (130). Since no cell culture system existed for any other noroviruses at the time, this cell culture system was soon adopted as a surrogate model for the study of human noroviruses. Even more, the use of this model has intensified after the discovery of the MNV receptor in 2016, enabling infection of non-murine cells with MNV (131,132). This paved the way for genome-wide knockout screenings which led to the discovery of multiple host proteins implicated in the MNV replication cycle, such as TRIM7, IFIT1 and G3BP1 (90,133,134). However, to study human noroviruses directly, the search for a suitable cell culture system continued. This resulted in the publication of the first human norovirus cell culture model in 2014 (135). This model consisted of BJAB cells, a cell line of human B lymphoma origin, and HBGA-expressing enteric bacteria and was infectable with GII.4 Sydney human norovirus derived from stool. However, viral replication in this model was modest and it was widely debated whether B cells are the primary target of human norovirus infection and replication *in vivo* (136). With the rise of induced pluripotent stem cells (iPSCs) and the introduction of organoid systems, the first human enteroid model capable of cultivating human noroviruses was introduced in 2016 (137). This enteroid model was quickly adopted and adapted by the research field and is now widely used in many domains of the norovirus research area (138–141).

1.3.3 Reverse genetics models

To evaluate the effect of mutations in the norovirus genome on viral replication, reverse genetics models are of great importance to the field. To date, only the MNV infection model is able to efficiently facilitate reverse genetics of the MNV genome (142,143). Two types of MNV reverse genetics models exist, although both systems are very similar in nature. In the first model, a plasmid encoding the MNV genome is used for *in vitro* transcription to produce capped MNV genomic RNA, which can be transfected into permissive cells to study the MNV replication cycle (Figure 1.6A). In the second model, a plasmid encoding the MNV genome under a mammalian promoter is directly transfected into cells to study MNV replication. Transcription and capping in this second system is therefore not performed *in vitro*, but rather directly *in cellulo* using a mammalian promoter like the cytomegalovirus (CMV) promoter or the Elongation Factor 1-alpha (EF-1α) promoter (Figure 1.6B).

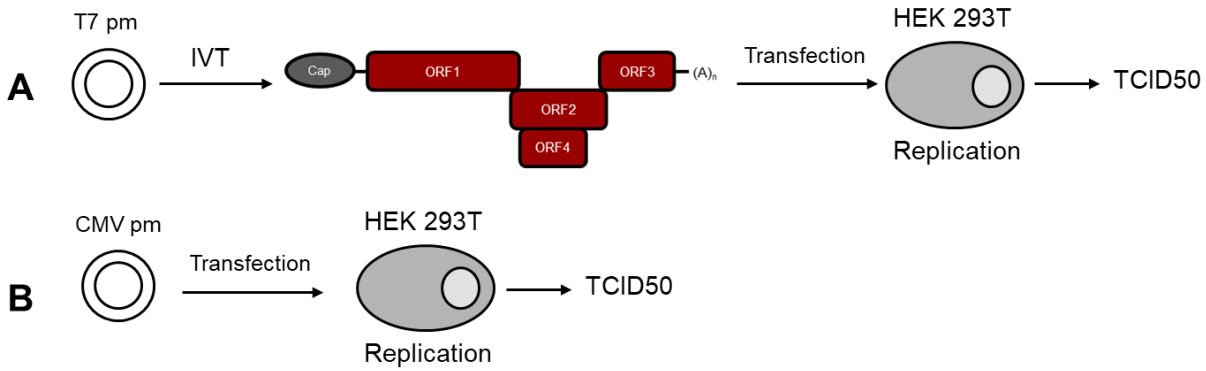

Figure 1.6 Reverse genetics of MNV

(A) A plasmid encoding the MNV genome under the T7 promotor is *in vitro* transcribed and the obtained capped RNA is transfected into HEK293T cells. These cells subsequently facilitate replication of the capped MNV genome and the viral titer can be determined using $TCID_{50}$.

(B) A plasmid encoding the MNV genome under the CMV promotor is directly transfected in HEK293T cells, which facilitate transcription and replication of capped MNV genomes. A viral titer can be determined using $TCID_{50}$.

1.4 Norovirus life cycle

1.4.1 Norovirus receptors and host cell tropism

The life cycle of human noroviruses presumably starts with the binding of virions to glycan groups on histo-blood group antigens (HBGAs) on human cells in the intestine (144–147). Numerous studies have used X-ray crystallography to study and confirm the binding of dimers of the protruding domain (P domain) of VP1 with multiple HBGAs (Figure 1.7) (147–149). Overall, the binding patterns of different norovirus strains is highly strain-specific and can be divided into two distinct binding categories: the A/B binding group that mostly recognizes A, B and H epitopes but not Lewis epitopes, whereas the Lewis binding group can recognize Lewis epitopes but not A and B epitopes (146,150,151). Furthermore, the host enzyme galactoside 2-alpha-L-fucosyltransferase 2 (FUT2) seems to play a crucial role in HBGA biosynthesis and human norovirus infection: functional FUT2 results in HBGAs expressed on intestinal cells and secreted HBGAs in bodily fluids, known as the “secretor” phenotype. Homozygosity for a nonsense mutation in *FUT2* (428G>A), which is present in roughly 20 percent of the population, leads to dramatically reduced expression and secretion

of HBGA, giving rise to the “non-secretor” phenotype and conferring resistance to infection with various human norovirus strains (152,153). Interestingly, recent research suggests that human noroviruses can also bind to bacterial HBGA-like ligands present in the gut, further complicating the research field on the role of HBGA and HBGA-like ligands in norovirus pathogenesis (154–156).

The exact mechanism of binding of human norovirus virions to HBGAs remains elusive. Some studies hint on a role for bile acids, which might alter the conformation of the P domain in VP1 to favor binding between VP1 and HBGAs (157,158). Interestingly, bile acids seem to facilitate GV murine norovirus (MNV) infection as well by enhancing the binding of VP1 to the proteinaceous MNV receptor CD300lf (159,160). Other studies point to the importance of sialic acid residues on HBGAs for the binding to norovirus virions (161–163). One study even demonstrates that dimers of the P domain of VP1 can directly interact with alpha2,3-linked sialic acid residues of 3’-sialyllactose on HBGAs (164). Other viruses within the family of *Caliciviridae*, such as Tulane virus and feline calicivirus (FCV), are known to interact with sialic acid residues on glycans as well (165–167). However, another study found no interaction between P domains of MNV or GII.4 norovirus and sialylated glycans. Moreover, introduction of the MNV receptor, CD300lf, was shown to be sufficient to render sialic acid deficient CHO cells susceptible to MNV infection and replication (131,132,168). Whether sialylated glycans are thus responsible for human norovirus attachment to HBGAs and whether these HBGAs serve as coreceptors or as the main receptors for host cell entry therefore remain a topic of debate and ongoing research in the field.

Since the receptor for MNV is known, various murine cell types have been identified as naturally permissive for MNV, such as cells of macrophagic and dendritic origin (130–132). Other lymphocytes in the gut, such as T cells and B cells in the gut-associated lymphoid tissue (GALT), are also targeted by MNV upon oral norovirus inoculation in mice (169). More recently, the chronic strain MNV-CR6 has been shown to infect the rare chemosensory tuft cells, the only intestinal epithelial cells expressing the MNV receptor CD300lf (170).

By contrast, the host cell tropism of human noroviruses is less clear. One study points in the direction of enterocytes as the main cell type for human norovirus replication, a

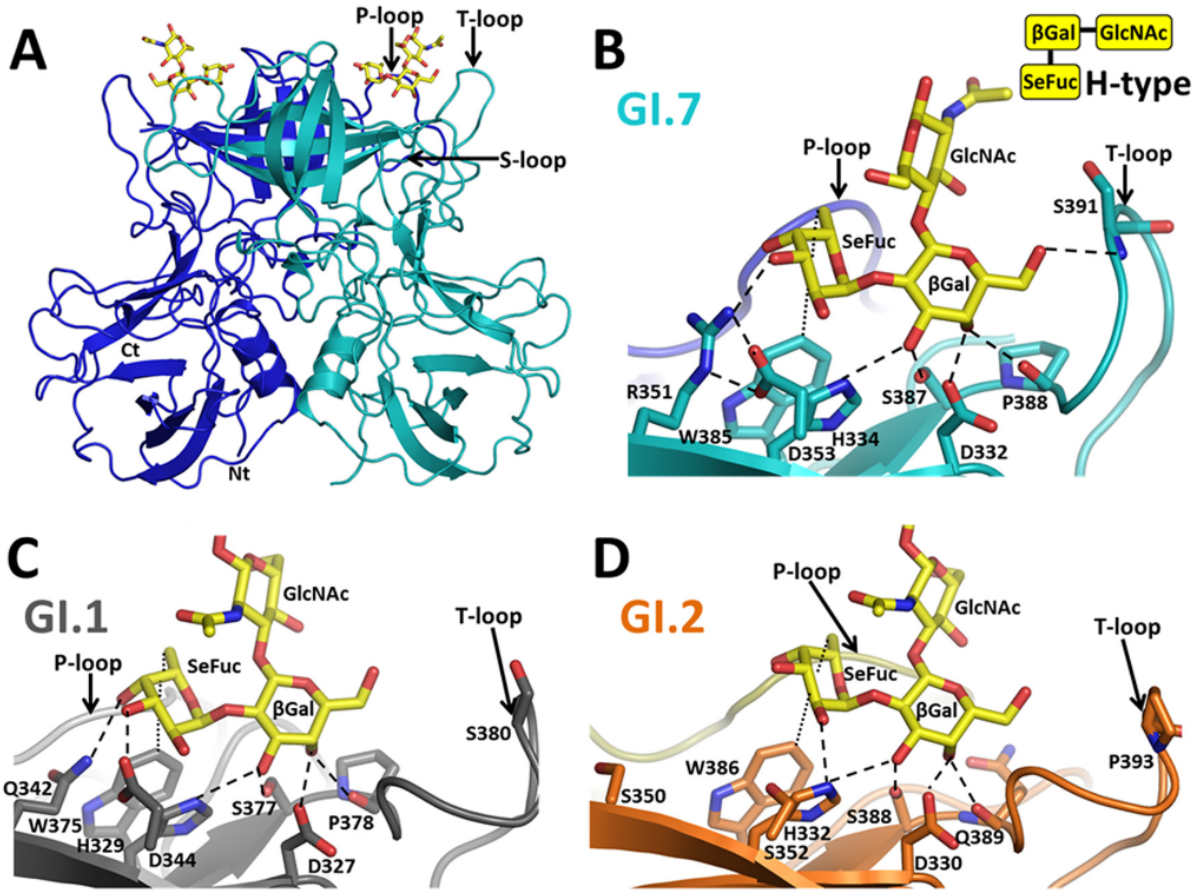

Figure 1.7 H-type HBGA binding among GI norovirus strains

(A) Dimer of the GI.7 P domain with the two subunits in blue and cyan. The HBGA interaction site is indicated with black arrows. (B) Binding of GI.7 P domain to H-type 2. (C) Binding of GI.1 P domain to H-type 1. (D) Binding of GI.2 P domain to H-type 1. Taken from (149).

finding that was later confirmed in the stem cell-derived intestinal enteroid cell culture systems (137,171). On the other hand, replication of human noroviruses has also been documented in B cells, giving rise to the B cell infection model for human noroviruses (135). Since many of the cell culture models of human noroviruses are quite artificial and often allow only low levels of replication, it is therefore still elusive whether the identified cell types for human norovirus replication also function as primary sites of replication *in vivo*. Interestingly, a recent study stained intestinal tissues of a patient with severe norovirus gastroenteritis for viral RNA and cell-type specific markers and found that human norovirus replication occurs in the enteroendocrine epithelial cells of the gut, a rare cell type that represents less than 1% of all cell types in the gut epithelium (172).

1.4.2 ORF1 translation and polyprotein processing

After cell surface attachment, norovirus virions are endocytosed and the viral genomic RNA is released into the cytosol. The exact mechanism by which noroviruses release their viral genome is unknown, but MNV uncoating is independent of pH, which suggest that it does not require the acidity of endosomes for uncoating (173). Furthermore, adding the dynamin inhibitor dynasor or the cholesterol-removing agent methyl-beta-cyclodextrin to MNV upon infection inhibits entry, suggesting that cholesterol-sensitive lipid drafts and dynamin might play a role in MNV entry (174). However, a more recent study demonstrates the importance of other pathways in the entry of GII.4 virions, such as the dynamin-independent, clathrin-independent endocytosis pathway and the wound repair pathway, highlighting possible heterogeneity across the entry mechanisms of different noroviruses (175).

The release of the norovirus genome into the cytosol makes it possible for the VPg-linked RNA genome to be translated. The linkage of VPg to the RNA genome seems crucial for this process: the C-terminal region of VPg directly interacts with the eukaryotic translation initiation factor 4G (eIF4G) and thereby recruits the eukaryotic translation initiation factor 4F (eIF4F) complex, bringing the starting components of translation to the 5' end of the norovirus genome (89). Other host cell factors bind to the viral genome as well and might further regulate translation and/or replication of the viral genome. For example, the heterogeneous nuclear ribonucleoprotein A1 (hnRNP A1) and poly(rC)-binding protein 2 (PCBP2) have been shown to bind to the 5' and 3' end of the MNV genome and facilitate genome circularization and MNV replication (176). Interestingly, very similar host factors have been found to bind *in vitro* to the Norwalk genome (human norovirus, GI.1) (177). Moreover, many other positive-sense, single-stranded RNA viruses are known to circularize their genomes in order to regulate translation and replication. For example, the circularization of many flavivirus genomes inhibits translation in order to favor genome replication (178). Other viruses, such as coxsackievirus, presumable circularize their genomes to enhance IRES-dependent translation initiation (179). Since eukaryotic mRNAs can also be circularized to enhance or regulate protein translation, it is very likely that circularization of the norovirus genome by host proteins plays an important role in regulating viral translation and replication (180).

Once the eIF4F complex has been recruited to the 5' end of the VPg-linked RNA genome, translation of ORF1 will be initiated. This results in a large polyprotein of around 200 kDa, which is subsequently cleaved by the norovirus protease NS6. Since cleavage of NS6 is not equally efficient for all junctions between the nonstructural proteins, multiple precursor proteins are present during infection (49,50,181,182). *In vitro* polyprotein processing of the MD145-12 strain (GII.4) revealed p22-VPg (NS4-NS5) and Pro-Pol (NS6-NS7) to be the most stable precursor proteins, but less stable precursors such as p22-VPg-Pro-Pol (NS4-NS7), p22-VPg-Pro (NS4-NS6) and VPg-Pro (NS5-NS6) were also detectable (Figure 1.8) (181). This is in line with data for GV MNV, where it is hypothesized that NS4 is important for the membrane-localization of NS4-containing precursors (50). In addition, the precursor Pro-Pol seems to play a unique role in the nucleotidylylation of VPg, since its nucleotidylylation activity is a hundred times more efficient than that of the mature Pol protein, emphasizing the importance of protein precursors in the norovirus replication (85,86). After translation of the ORF1 polyprotein, intracellular membranes of the host are rearranged by the norovirus nonstructural proteins to form membrane-associated RCs, which serve as platforms for norovirus genomic replication.

1.4.4 Genomic replication and generation of subgenomic RNA

Since the structural proteins of norovirus are not encoded in ORF1, but in ORF2 and ORF3, subgenomic RNA is generated to facilitate translation of these ORFs. As a first step towards subgenomic RNA synthesis, a negative-sense RNA copy of the genome is synthesized by the viral polymerase NS7 or the precursor NS6-NS7 (101). The exact mechanisms by which the norovirus negative-sense RNA is generated from the positive-sense, single-stranded RNA genome is largely unknown, but *in vitro* studies have shown that this process seems to occur either *de novo* or VPg-mediated (Figure 1.9) (183,184). However, in contrast to poliovirus, there is no evidence that negative-sense, intermediate RNAs of noroviruses are linked to VPg, arguing that *de novo* synthesis might be the prime mechanism for norovirus negative-sense RNA synthesis (185,186).

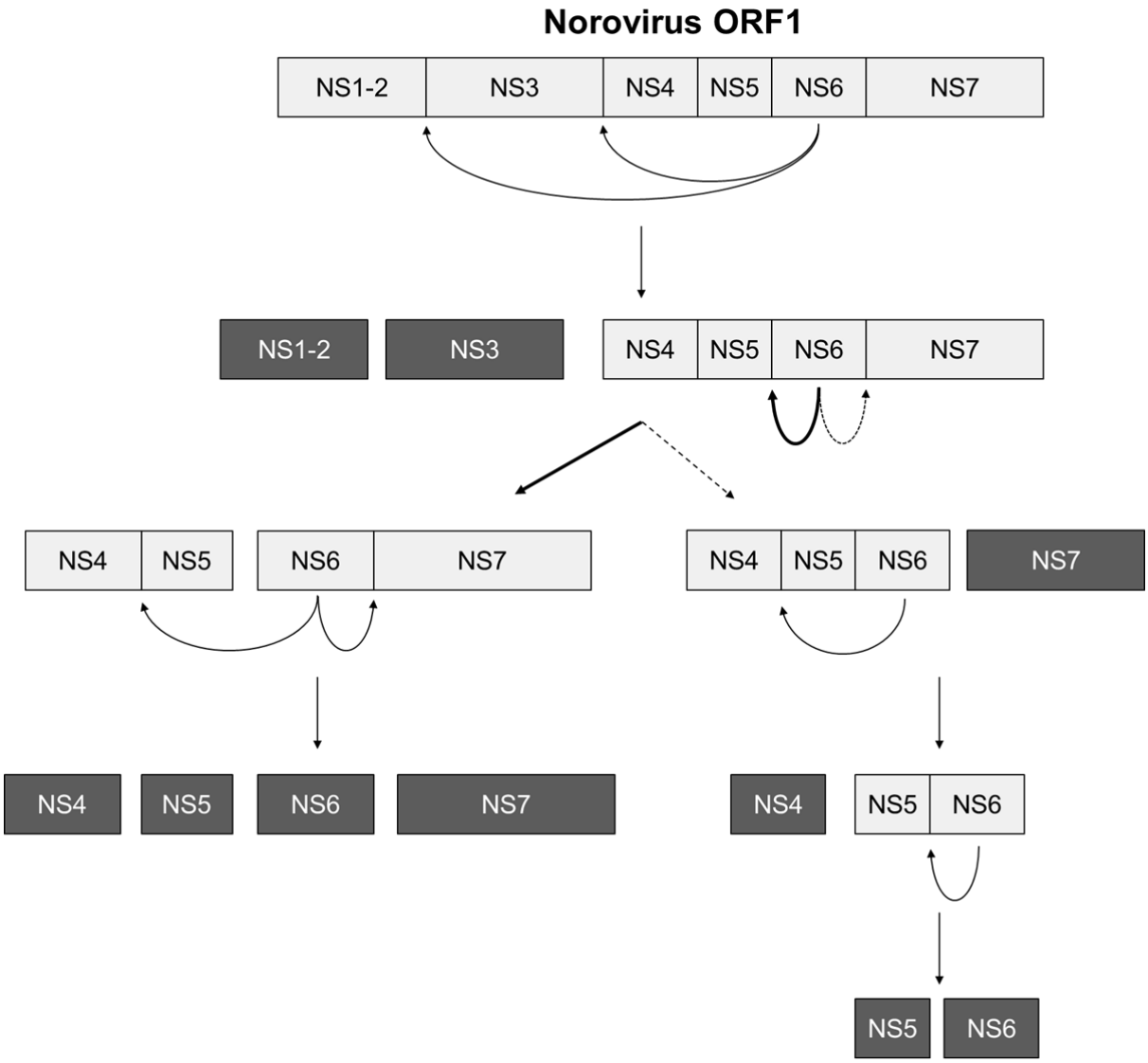

Figure 1.8 Proposed polyprotein cleavage map of norovirus

Although variance exists between genogroups, genotypes and even strains, the order of proteolytic cleavage of the norovirus ORF1 polyprotein has been proposed based on experimental data. Early in infection, both NS1-2 and NS3 are cleaved off from the polyprotein to form mature proteins. The remaining precursor NS4-NS7 can subsequently be cleaved in two distinct manners. First, the NS4-NS7 precursor is cleaved into the stable precursors NS4-5 and NS6-7. These precursors can later be cleaved in the mature proteins NS4, NS5, NS6 and NS7. Experimental evidence from infected cells suggest that most of the NS4-NS7 precursor is processed in this first manner. Second, as an alternative proteolytic order, the NS7 protein is cleaved off from the NS4-NS7 precursor giving rise to mature NS7 and the precursor NS4-NS6. NS4-NS6 is then cleaved to NS5-6 and finally to NS5 and NS6 to produce mature nonstructural proteins. Adapted from (181).

For the generation of more positive-sense, single-stranded RNA genomes, a VPg-dependent initiation of replication is presumably utilized, ensuring that novel norovirus genomes are coupled to VPg (184,185,187). A crucial step for this VPg-mediated initiation of replication is the nucleotidylylation of VPg, a process where the precursor NS6-NS7 or the mature NS7 links a nucleotide monophosphate to the VPg protein, enabling VPg to serve as a protein primer for viral replication (85,86). A specific tyrosine of the VPg protein (Y27 in human noroviruses, Y26 in MNV) has been identified as the target residue for this linkage (85,87). Furthermore, it is worth mentioning that, although positive-sense norovirus RNA is linked to VPg, *in vitro* studies have shown that the norovirus RdRp is able to generate genomic RNA without the use of VPg as well, depending on a stem-loop structure in the 3'-end of the antigenomic sequence (188,189).

The generation of norovirus subgenomic RNA is proposed to follow two mechanisms (102,185). The premature termination model was first proposed and states that premature termination of negative-sense RNA synthesis gives rise to negative-sense, subgenomic RNA. This negative-sense subgenomic RNA could serve as a template for VPg-mediated synthesis of positive-sense subgenomic RNA. Studies on a Norwalk RNA replicon and MNV infected cells have confirmed the presence of negative-sense subgenomic RNA, providing evidence that premature termination might take place during norovirus replication, although a termination sequence that facilitates such premature termination has yet to be identified (52,126).

On the other hand, the internal initiation model points to the identification of a subgenomic promoter on the norovirus antigenomic RNA which is recognized by the viral RdRp and facilitates VPg- mediated synthesis of positive-sense, single-stranded subgenomic RNA (51,52). The positive-sense subgenomic RNA can be directly translated to give rise to VP1 and VP2, but it can also serve as a template for the generation of negative-sense subgenomic RNA, followed by another round of positive-sense subgenomic RNA synthesis. Since the subgenomic promoter has been identified and investigated more intensively, the internal initiation model seems most plausible, although the two models are not mutually exclusive.

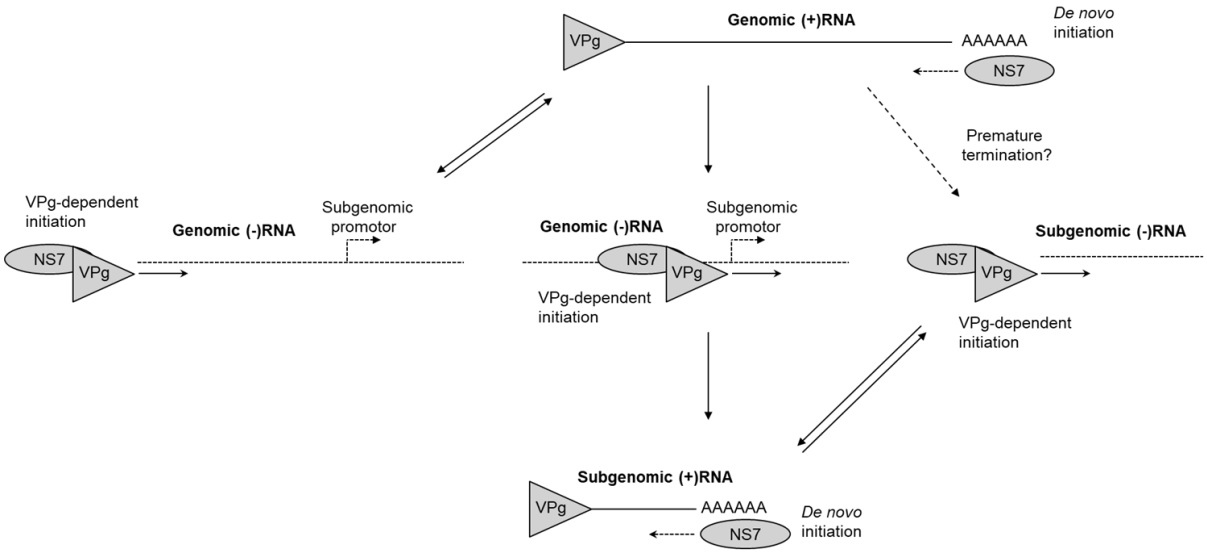

Figure 1.9 Proposed norovirus genomic replication

Upon entry, the positive-sense, single-stranded RNA genome of norovirus is released in the cell. Since this RNA genome is linked to VPg at the 5' end, translation can start directly, giving rise to the nonstructural proteins. *De novo* initiation of RNA synthesis by the viral RdRp (NS7) on the positive-sense RNA genome generates a negative-sense RNA intermediate of the norovirus genome. VPg-dependent initiation of RNA synthesis on this negative-sense RNA intermediate will subsequently lead to the generation of new positive-sense norovirus genomes or to the production of positive-sense subgenomic RNA via the subgenomic promotor. Negative-sense subgenomic RNA intermediates can be generated from positive-sense subgenomic RNA via *de novo* initiation of RNA synthesis and serve as a platform to quickly generate more positive-sense subgenomic RNA. Alternatively, negative-sense subgenomic RNA might be produced from the positive-sense genomic RNA via a process of premature termination of the RNA synthesis, although no termination signal for this process has been found so far.

1.4.5 Translation of subgenomic RNA

After the synthesis of positive-sense subgenomic RNA, the translation of ORF2 and ORF3 (and in MNV, ORF4) can take place. Since the positive-sense, subgenomic RNA is linked to VPg, translation is initiated by recruitment of eIF4G by the VPg and thereby recruitment of the complete eIF4F complex (89). ORF2 is first translated, which gives rise to the VP1, the major capsid protein. The translation of ORF3 seems to involve a termination-reinitiation mechanism (53). ORF2 and ORF3 share a small overlap sequence (UAAUG) containing the stop codon of ORF2 and start codon of ORF3. In MNV, the forty-five nucleotides upstream of the start codon of ORF3 are essential for

this termination-reinitiation process. This region contains a sequence that is complementary to 18S rRNA and mutation of this sequence abolishes ORF2 translation (53). It seems therefore plausible that MNV utilizes this sequence to bind the 40S subunit to the end of ORF2, bringing the translation machinery in close proximity to the start codon of ORF3. Translation of ORF3 will give rise to VP2, the minor capsid protein.

Although absent in human noroviruses, the MNV genome contains a fourth ORF (46). Since the start codon of ORF4 is positioned around ten nucleotides upstream of the start codon of ORF2, the most likely explanation for ORF4 translation is alternative initiation of translation. The product of ORF4 translation, VF1, is present during MNV replication, but does not seem to have an impact on viral replication in cell culture (46). However, disruption of ORF4 leads to lower viral titers during infection *in vivo* and seems to impact the viral fitness (190). This discrepancy between *in vitro* and *in vivo* studies might be explained by the properties of VF1, which is implicated in host cell apoptosis and antagonization of the innate immune system.

1.4.6 Virus assembly and exit

Little is known about the assembly of noroviruses, especially during natural infection conditions. VP1 alone is capable of self-assembly and sole expression of VP1 results in the production of virus-like particles (VLPs) with a T=3 icosahedral symmetry and a diameter of 38.0 nm, closely resembling other *Caliciviridae* members (191). Mutational analysis indicates that the N-terminal shell domain (S domain) of VP1 contains all requirements for the capacity to self-assemble, whereas the C-terminal P domain seems to regulate the size and stability of the capsid (Figure 1.10) (192,193).

Although VP2 is not required for capsid assembly, it is present in norovirus virions and deletion of ORF3 and thus VP2 in FCV abolishes the production of infectious virions (194). In addition, VP2 interacts with VP1 via the S domain of VP1, ensuring the encapsidation of VP2 (195). The basic nature of VP2 and its position within the virion has led to the hypothesis that it might interact with the acidic backbone of the norovirus RNA genome and ensure genome encapsidation. However, direct interaction between VP2 and the viral RNA has never been proven (185).

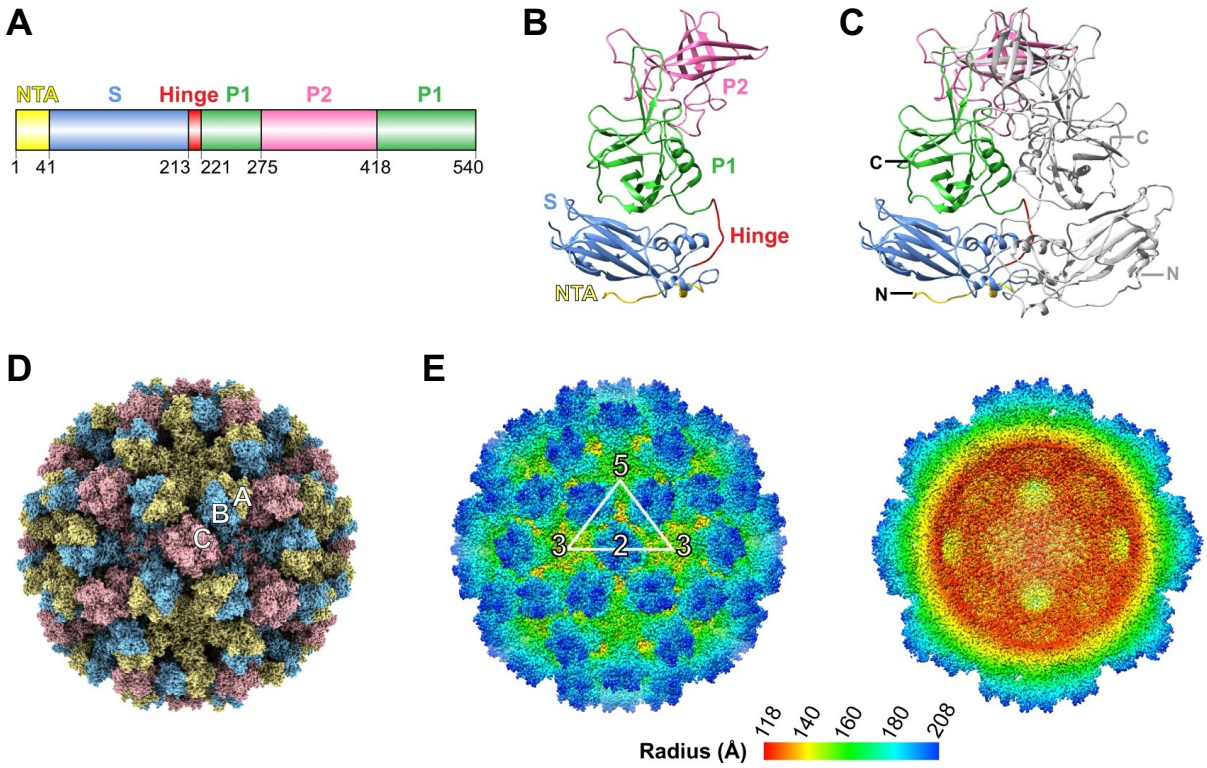

Figure 1.10 Assembly of GII.4 norovirus VP1 in virus-like particles

(A) Schematic depiction of the subdomains of norovirus VP1. (B) VP1 monomer with the NTA subdomain in yellow, S in blue, hinge in red, P1 in green and P2 in pink. (C) VP1 dimer with N- and C-termini indicated. (D) VP1-induced virus-like particles display a T=3 icosahedral symmetry similar to norovirus virions. The subunit A, B and C are colored here respectively with yellow, blue and pink. (E) External and internal view on the VP1-induced virus-like particle. Inner diameter is approximately 230 Å, whereas the outer diameter measures around 410 Å. Taken from (193).

Although few studies have been performed on the exit strategy of noroviruses, other members of the *Caliciviridae* family have been reported to use apoptosis as an exit mechanism to complete the life cycle (196,197). MNV infection is known as well to induce apoptosis by caspase activation, mediated by the downregulation of the pro-survival protein Survivin, activation of the cysteine protease cathepsin B and release of cytochrome *c* release (198,199). Caspases cleave the MNV NS1-2 protein into NS1 and NS2 in later stages of the viral life cycle and inhibition of this cleavage compromises viral persistence and shedding in mice, emphasizing the importance of caspase activity for MNV pathology (63). Furthermore, biopsies taken from patients infected with human noroviruses show a significant increase in apoptosis of enterocytes as well (200–202). A more recent study identified a MLKL-like four-helix bundle domain in the N-terminal part of NS3 which was shown to permeabilize the

mitochondrial membrane, resulting in apoptosis and viral egress (81). Finally, nonlytic release of noroviruses has been shown to occur during infection as well (203). This exit strategy gives rise to vesicle-cloaked norovirus particles, which have been found in stool of infected hosts and are significantly more infectious than non-enveloped virus.

1.4.7 Host innate immune responses to norovirus

As for all viruses, the host is equipped with molecular tools to detect norovirus infection. To examine the detection of noroviruses by membrane-bound pattern recognition receptors (PRRs), such as Toll-like receptors (TLRs), VLPs and MNV have been used as experimental surrogates for human norovirus infection. One study using GII.4 VLPs demonstrates binding of VLPs to TLR2 and TLR5, whereas other studies using MNV show antiviral effects of TLR4 and TLR7 agonists (204–206). However, although *TLR3* knockout mice develop slightly higher MNV titers upon infection *in vivo*, experimental knockout of *TLR3, TLR5, TLR7* or *MyD88* in bone marrow-derived dendritic cells seems to have little impact on the interferon (IFN) response after infection *in vitro*, obscuring the role of these membrane-bound PRRs in natural infection and moving the scientific scoop to the role of cytosolic PRRs in the innate immunity against noroviruses (207–209).

Numerous studies have investigated the role of cytosolic PRRs in the innate immunity against noroviruses, still, the function of particular cytosolic PRRs in the recognition of noroviruses is still debated (Figure 1.11). Although retinoic acid-inducible gene I (RIG-I) has been shown to detect RNA transcripts generated by the MNV polymerase and overexpression of the MNV polymerase alone augments RIG-I-triggered IFN response, direct antagonism of RIG-I does not seem to alter MNV titers *in vitro* (187,210,211). By contrast, the detection of noroviruses the RIG-I-like receptor melanoma differentiation-associated protein 5 (MDA5) is widely accepted to play a key role in the innate immune response against MNV strains (207,209,212). Moreover, although MNV infection in *MDA5* knockout mice is generally pathogenic but not lethal, significant mortality is observed upon MNV infection of *STAT1* knockout mice, suggesting that MDA5 is not the only cytosolic PRR capable of sensing MNV infection (209,213,214). Nucleotide-binding oligomerization domain (NOD)-like receptor family pyrin domain containing 6

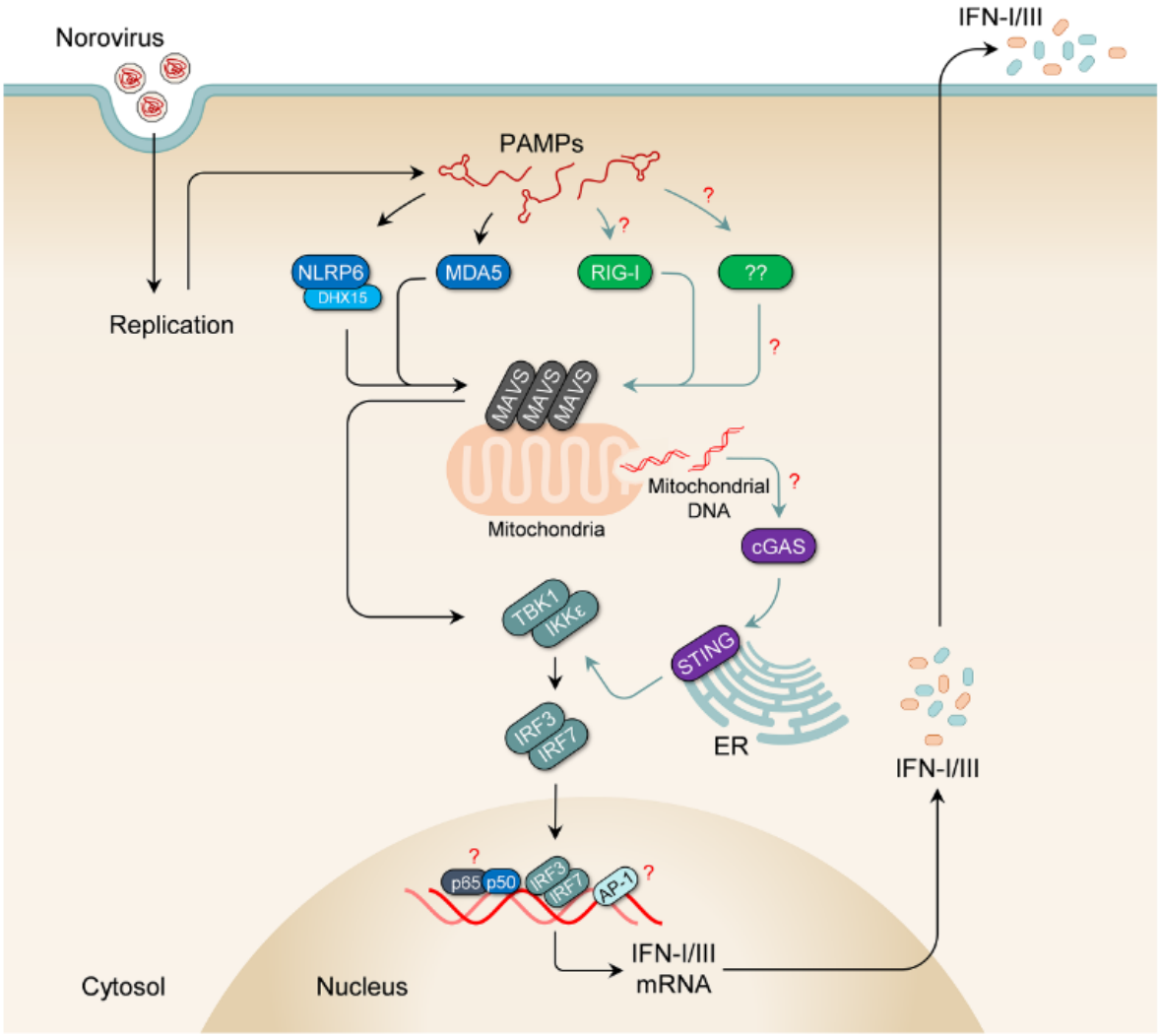

Figure 1.11 Innate immune response to norovirus infection

Pathogen-associated molecular patterns (PAMPs) associated with norovirus infection, such as double-stranded RNA, are detected by MDA5, NLRP6 and possibly RIG-I, leading to cleavage of MAVS, activation of downstream signaling and expression of type I and type III interferons. In addition, NS4 induces leakage of mitochondrial DNA into the cytosol, thereby activating cGAS signaling. Taken from (209).

(NLRP6) has subsequently been identified as another cytosolic PPR stimulating the IFN response upon MNV infection, most likely via its binding partner DEAH-box RNA helicase DHX15 (215,216). More recently, the cyclic GMP-AMP synthase (cGAS)-stimulator of IFN genes (STING) pathway has been found to induce an IFN response during norovirus infection as well (217,218). Interestingly, since cGAS detects cytosolic, double-stranded DNA, it was found that the norovirus protein NS4 promotes leakage of mitochondrial and nuclear DNA into the cytosol (217).

Detection of MNV infection by cytosolic PRRs results in downstream signaling via proteins such as mitochondrial antiviral-signaling protein (MAVS), IFN regulated factor 3 (IRF-3) and IRF-7 (207,219). Although not fully understood, it is believed that the MNV protein VF1 suppresses innate immunity by antagonizing this signaling cascade, most likely downstream of TBK1 (46,220). In case of inadequate antagonism, this signaling cascade leads to strain-specific expression of type I and type III IFNs, most notably IFN-α, IFN-β and IFN-λ, as has been shown for multiple MNV strains both *in vitro* and *in vivo* (208,213,219,221–223). In contrast to MNV, IFN responses to human norovirus infection are more controversial. In some studies, replication of human noroviruses *in vitro* does not seem to induce any IFN response, although pretreatment with IFN-α or IFN-β inhibits replication (224). However, experimental infections in humans demonstrate elevated blood levels of IFN- α and IFN-γ during infection (225–227). More recently, studies with human enteroid models have indicated a pivotal role for IFN-λ, further complicating the study of the IFN response against human noroviruses (228).

1.5 Biogenesis of the norovirus replication complex

1.5.1 Membrane rearrangements during viral infection

Similar to other positive-sense, single-stranded RNA viruses, norovirus replication is associated with virus-induced membranous compartments within the host cell (229–231). These RCs spatially concentrate host and viral factors required for viral propagation and thus function as platforms for viral replication. In addition, the membranous nature of RCs shields viral replication from detection by the innate immune system and enhances immune evasion (232–235).

Although RC morphology of different viruses vary substantially, these membrane alterations can roughly be divided into two morphological groups: one group consists of spherical invagination called spherules, whereas the second group consists of clusters of single, double or even multi-membrane vesicles (SMVs, DMVs and MMVs) (236,237). For example, replication of *Togaviridae* such as Sindbis virus (SINV) and Chikungunya virus (CHIKV) takes place in virus-induced spherules at the plasma membrane, whereas the replication of *Picornaviridae* like poliovirus and coxsackievirus

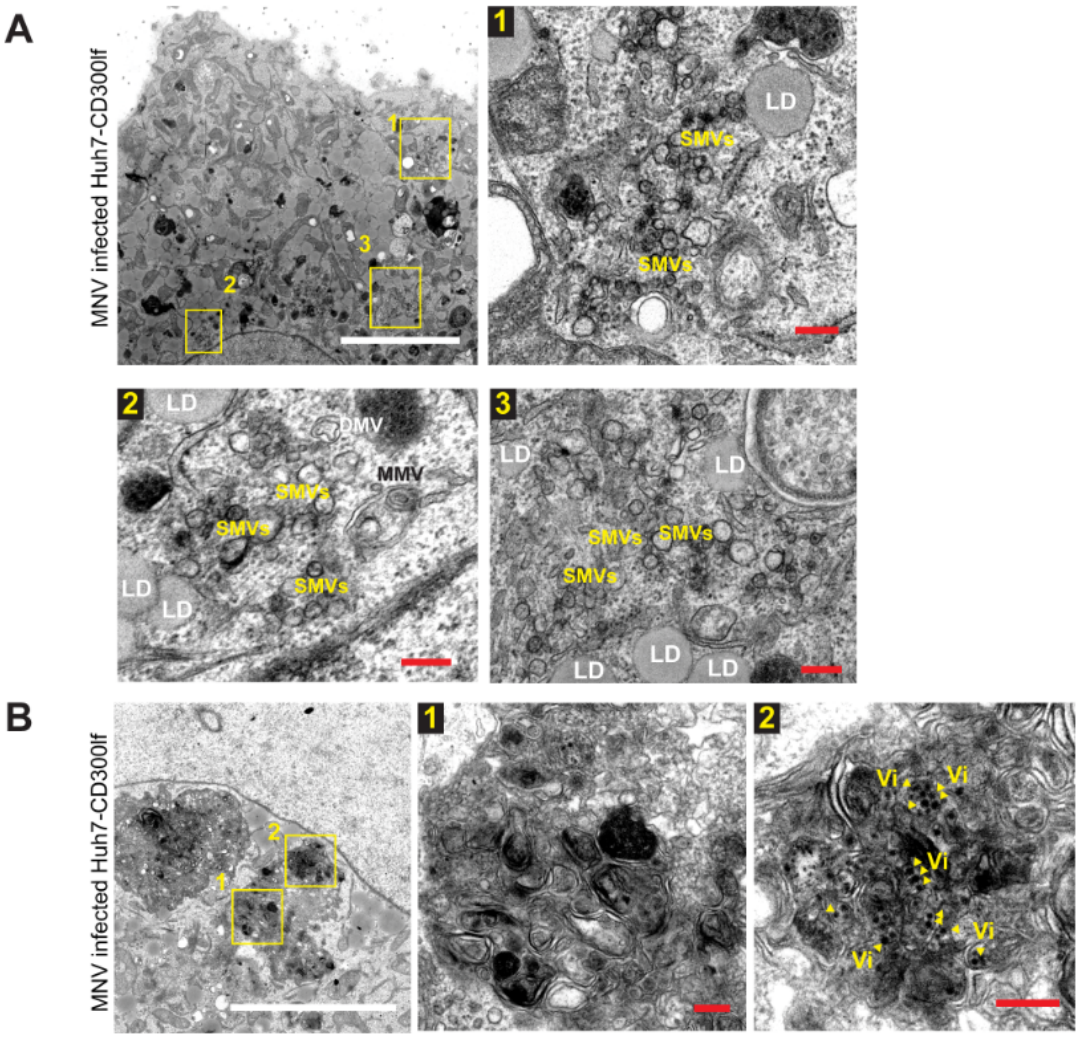

Figure 1.12 Membrane rearrangements during MNV infection

(A) Around 16 hours after MNV infection, large clusters of SMVs, DMVs and even MMVs can be found in the infected cell. These membrane rearrangements are often found around clusters of LDs in the perinuclear region of the cell. (B) Virions can be observed in close association with these membranous structures. White scale bars 5 µm, red scale bars 200 nm. Figure taken from (56).

occurs at virus-induced vesicles (238–242). EM studies on cells infected with MNV or cells expressing the ORF1 polyprotein of GII.4 human norovirus reveal that the norovirus RC belongs morphologically to the vesicular type, which is in line with similar findings for other members of the *Caliciviridae* family such as FCV (Figure 1.12) (56,67,73).

1.5.2. Initiation of the replication complex formation

The exact mechanism by which norovirus triggers the formation of RCs is an ongoing field of research, but the process starts directly after translation and cleavage of the

ORF1 polyprotein. For FCV, the viral proteins p32, p39 and p30 localize to the ER membrane to initiate the formation of RCs (72). The norovirus homologues of these three proteins, NS1-2, NS3 and NS4, seem to play a key role in orchestrating RC formation as well (56). For example, NS1-2 is known to bind the protein vesicle-associated membrane protein-associated protein A (VAPA), a protein involved in membrane trafficking. VAPA is also known to associate with hepatitis C virus (HCV) NS5A, a viral protein with a crucial role in the biogenesis of HCV RCs (68–71,243,244). In addition, sole expression of GII.4 NS1-2 in Huh7-T7 Lunet cells induces ER tubules and expression of MNV NS1-2 in Vero cells shows an ER-like reticular staining pattern as well, further implicating a membrane-associated role of NS1-2 in the norovirus life cycle (56,66). However, although NS1-2 has a putative hydrolase domain in GII.4, no enzymatic activities of NS1-2 have been reported (56).

Besides functioning as a putative helicase, NTPase and RNA chaperon, NS3 has also been implicated in the formation of norovirus RCs. NS3 of both MNV and human norovirus have been shown to form vesicle clusters, surrounding structures that were later identified as lipid droplets (LDs) (56,66,79,245). A recent study shows that the docking of NS3 to LDs is mediated by two amphipathic alpha helices (79). Since other positive-sense, single-stranded RNA viruses, such as enteroviruses and coronaviruses, are known as well to interact with LDs and are speculated to utilize the lipids stored in LDs to fuel the biogenesis of RCs, it is possible that norovirus NS3 serves a similar purpose as well (246–248). Interestingly, NS3 and NS4 of GII.4 norovirus seems to interact with each other via the N-terminus of NS3, a function which could facilitate the formation of multiprotein complexes required for the biogenesis of RCs (79).

Of all nonstructural proteins, norovirus NS4 seems to be most important for driving the formation of membrane alterations. Sole expression of GII.4 NS4 in Huh7-T7 Lunet cells can induce both SMVs and DMVs (56). The exact mechanism by which NS4 is able to induce these membranous rearrangements is unknown, but it seems that a mimic of an ER export signal (MERES) is important for the disruption of the host secretory pathway (249). Since the membranes of MNV RCs have been shown to

derive from the host secretory pathway, it is possible that NS4 can rearrange these membranes to form RCs (67).

Taken together, these first three nonstructural proteins of norovirus ORF1 seem to be vital for the biogenesis of norovirus RCs and structural models have been proposed for these proteins (Figure 1.13) (56). A better understanding of the norovirus RC biogenesis could greatly help the research field and aid in the development of novel antivirals.

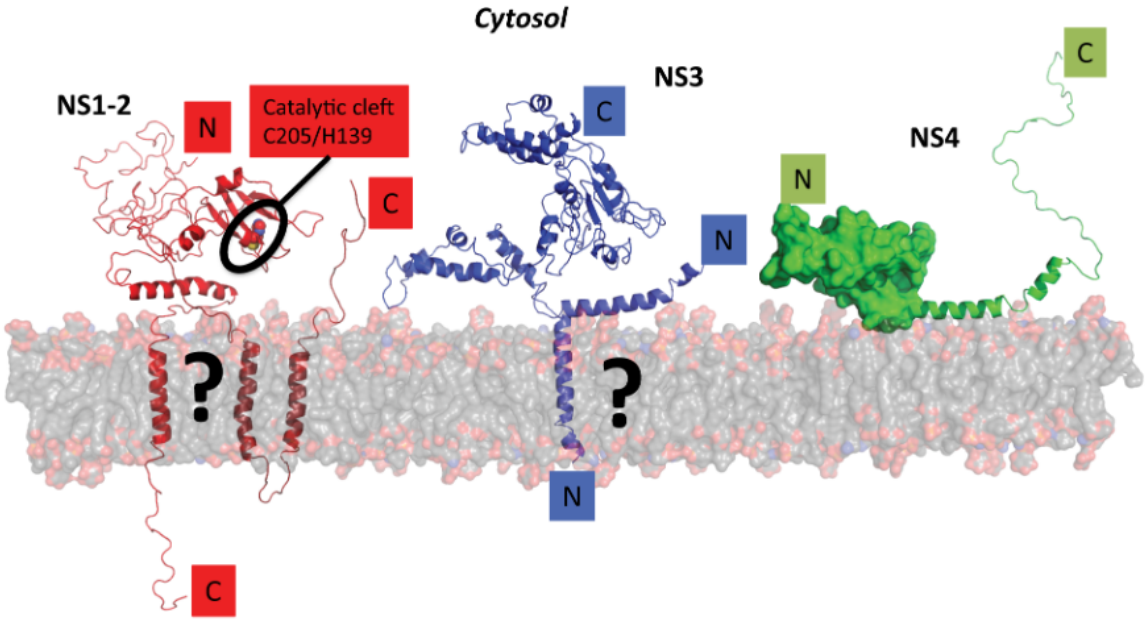

Figure 1.13 Proposed models of GII.4 human norovirus NS1-2, NS3 and NS4

Three *in sicilo* models of NS1-2, NS3 and NS4 of GII.4 New Orleans norovirus. Modeling of the C-terminus of NS1-2 gives two alternatives: one with a peripheral membrane helix and a transmembrane helix or one with two transmembrane helices. Similarly, the N-terminus of NS3 might be folded as a peripheral membrane helix or a transmembrane helix. The model of NS4 suggest a N-terminal structured region with a large, center alpha helix and an unstructured C-terminus. Figure taken from (56).

1.6 Aim of this thesis

RC biogenesis and host membrane reorganization are crucial steps in the life cycle of all positive-sense, single-stranded RNA viruses, but the exact mechanisms initiating these processes during norovirus infection are ill-defined. NS4 is the only norovirus

protein known to induce both SMVs and DMVs upon expression, hinting at a pivotal role of this protein in norovirus RC biogenesis and rearrangement of intracellular membranes. Since pharmacological inhibition of similar proteins of related viruses, such as the HCV protein NS5A, constitute a highly potent class of antivirals, a deeper understanding of the membrane and protein-protein interactions of norovirus NS4 would help to assess its potential as an antiviral target. Since NS4 remains poorly characterized, the overall aim of this thesis was to unravel the molecular determinants of the membrane-rearranging and membrane-associating properties of NS4 as well as to explore protein-protein interactions between NS4 and other norovirus nonstructural proteins.

The first objective of this thesis was to identify amino acids residues within norovirus NS4 essential for viral replication. A domain analysis and an amino acid alignment should provide insight in the homology of NS4 among different norovirus genogroups. Alanine scanning of conserved amino acid sites should assess the impact of mutation of these conserved residues on viral replication.

The second goal of this thesis was to identify and to characterize the NS4 domain responsible for the membrane-associating and membrane-rearranging abilities of NS4. To this end, I aimed to overexpress NS4 domains to analyze their membrane association using immunofluorescence, membrane floatation and extraction assays and site-directed mutagenesis. In addition, electron microscopy should be performed to study the effect of mutations on membrane alterations.

The third and last aim of this thesis was to identify and to characterize the protein-protein interactions between NS4 and other norovirus nonstructural proteins. Co-immunoprecipitation and site-directed mutagenesis should be used to identify these interactions and to map important amino acid residues. Moreover, MNV was taken as a surrogate model for human norovirus replication to study the effect of loss-of-binding between interacting norovirus proteins on viral replication.

Chapter 2

Materials and methods

"*The method of scientific investigation is nothing but the expression of the necessary mode of working of the human mind. It is simply the mode at which all phenomena are reasoned about, rendered precise and exact.*"

— Thomas Henry Huxley (1825-1895), *The Method of Scientific Investigation*

---

2 Materials and methods

2.1 Materials

2.1.1 Antibodies and stains

Table 2.1 Primary antibodies

Protein	Species	Manufacturer	Article number	Dilution
GFP	Rabbit polyclonal IgG	Sigma Aldrich	SAB4301138	WB 1:1000
HA	Rabbit polyclonal IgG	ThermoFischer	PA1-985	WB 1:1000
FLAG	Rabbit polyclonal IgG	Sigma Aldrich	F7425-2MG	WB 1:4000
GAPDH	Mouse monoclonal IgG_1	Santa Cruz	Sc-47724	WB 1:5000
CANX	Rabbit polyclonal	Enzo	ADI-SPA-860-F	WB 1:2000
GM130	Rabbit monoclonal IgG	Cell Signaling	12480S	WB 1:1000

Table 2.2 Secondary antibodies

Label	Species	Manufacturer	Article number	Dilution
HRP	Goat α-mouse	Sigma Aldrich	A4416	WB 1:10000
HRP	Goat α-rabbit	Sigma Aldrich	A6154	WB 1:5000

Table 2.3 Lipid stains and other stains

Staining	Name	Manufacturer	Article number	Dilution
Neutral lipids	HCS LipidTox Deep Red	ThermoFischer	H34477	1:200
DNA	DAPI	Invitrogen	D1306	1:500

2.1.2 Magnetic immunoprecipitation beads

Table 2.4 Magnetic immunoprecipitation beads

Target	Species	Manufacturer	Article number
HA epitope	Monoclonal mouse IgG1	ThermoFischer	88836
FLAG epitope	Monoclonal rat IgG	ThermoFischer	A36797

2.1.3 Kits and buffers

Table 2.5 Kits

Application	Name	Manufacturer	Article number
PCR clean up and gel extraction of DNA	NucleoSpin Gel and PCR Clean-up	Macherey-Nagel	740609.50
Miniprep kit for DNA extraction	NucleoSpin Plasmid	Macherey-Nagel	740588.50
Maxiprep kit for DNA extraction	NucleoBond Xtra Maxi	Macherey-Nagel	740414.50

Table 2.6 Solutions and buffers

Name	Ingredients	Dilution
Laemmli buffer	200 mM Tris-HCL (pH 8.8), 3% SDS, 5 mM EDTA, 10% sucrose, 5% β-mercaptoethanol, 0.1% bromophenol blue	1x
Hypotonic solution	10 mM Tris-HCL (pH 7.4), 2 mM $MgCl_2$	1x
NTE buffer	100 mM NaCl, 10 mM Tris-HCL (pH 8.0), 1 mM EDTA	1x
IP buffer	20 mM Tris-HCL (pH 7.4), 150 mM NaCl, 0.1% NP-40	1x
PBS	1.37 M NaCl, 27 mM KCl, 100 mM Na_2HPO_4, 18 mM KH_2PO_4	10x
SDS resolving gel buffer	1.5 M Tris-HCL (pH 8.8), 0.4% SDS	1x

Name	Ingredients	Dilution
SDS stacking gel buffer	1 M Tris-HCL (pH 6.8), 0.8% SDS	1x
TAE buffer	242.2 g Tris, 18.6 g $Na_2EDTA•2\ H_2O$, 60.5 mL acetic acid and fill up to 1 L with water	50x
TGS Buffer	250 mM Tris, 1.92 M glycine, 1% SDS	10x
DMEM complete	Dulbecco's modified eagle medium, 1% non-essential amino acids, 2 mM L-glutamine, 100 U/mL penicillin, 100 mg/mL streptomycin, 10% FCS	1x
Western blot buffer	25 mM Tris, 192 mM glycine (pH 8.3). For working dilution 1x, add 100 mL Western blot buffer to 200 mL methanol and 700 mL water	10x
Annealing buffer	50 mM HEPES pH 7.4 and 100 mM NaCl	2x
Luciferase assay buffer	25 mM glycylglycine pH 7.8, 15 mM K_3PO_4 pH 7.8, 15 mM $MgSO_4$ and 4 mM EGTA	1x
Crystal violet staining	1.25 grams of crystal violet powder in 75 mL of water and 25 mL of ethanol	1x
EM fixative solution	50 mM sodium cacodylate (pH 7.2), 1 M KCl, 0.1 M $CaCl_2$, 0.1 M $MgCl_2$, 2.5% glutaraldehyde (v/v) and 2% sucrose (w/v)	

2.1.4 Cells

Table 2.7 Eukaryotic cell lines

Name	Description	Selection marker
Huh7-Lunet	Human hepatoma cell line permissive for HCV	N/A
Huh7-T7 Lunet	Huh7-Lunet expressing T7 polymerase	Zeocin
Huh7-Lunet mCherry-ADRP	Huh7-Lunet expressing mCherry-ADRP	Blasticidin
Huh7-T7 Lunet mCherry-ADRP	Huh7-Lunet expressing T7 polymerase and mCherry-ADRP	Blasticidin and puromcycin

Name	Description	Selection marker
HEK 293T	Human embryonic kidney cells expressing large T antigen of SV40	N/A
RAW264.7	Murine macrophage cell line permissive for MNV	N/A
BV-2	Murine microglial cell line permissive for MNV	N/A

2.1.5 Oligonucleotides and plasmids

Table 2.8 Oligonucleotide primers

Name	5'-3' sequence
pSP73MNVCW1_4654_4671_FW	gggcggctttgaccgtca
pSP73MNVCW1_5790_5807_RV	ccccgctggaagtgacag
pSP73MNVCW1_F6A_FW	gaacaaggtctatgacgctgatgccg
pSP73MNVCW1_F6A_RV	cggcatcagcgtcatagaccttgttc
pSP73MNVCW1_D7A_FW	gaacaaggtctatgactttgctgccg
pSP73MNVCW1_D7A_RV	cggcagcaaagtcatagaccttgttc
pSP73MNVCW1_A13S_FW	gcaagatcacctccttcaaagcca
pSP73MNVCW1_A13S_RV	tggctttgaaggaggtgatcttgc
pSP73MNVCW1_A13W_FW	ggcaagatcacctggttcaaagcc
pSP73MNVCW1_A13W_RV	ggctttgaaccaggtgatcttgcc
pSP73MNVCW1_F14A_FW	gatcaccgccgccaaagccat
pSP73MNVCW1_F14A_RV	atggctttggcggcggtgatc
pSP73MNVCW1_A18S_FW	caaagccatgtcggctgacgc
pSP73MNVCW1_A18S_RV	gcgtcagccgacatggctttg
pSP73MNVCW1_A18W_FW	caaagccatgtgggctgacgc
pSP73MNVCW1_A18W_RV	gcgtcagcccacatggctttg
pSP73MNVCW1_G32A_FW	cagctattgcgtgcaaagcaatgg
pSP73MNVCW1_G32A_RV	ccattgctttgcacgcaatagctg
pSP73MNVCW1_C56A_FW	ggctcccgctcaggtgatctacaa

Name	5’-3’ sequence
pSP73MNVCW1_C56A_RV	ttgtagatcacctgagcgggagcc
pSP73MNVCW1_Y65A_FW	caatggtgccaccgctaatgtgag
pSP73MNVCW1_Y65A_FW	ctcacattagcggtggcaccattg
pSP73MNVCW1_A98S_FW	ggataaaggagtcccgcctcc
pSP73MNVCW1_A98S_RV	ggaggcgggactcctttatcc
pSP73MNVCW1_A98W_FW	ggataaaggagtggcgcctcc
pSP73MNVCW1_A98W_RV	ggaggcgccactcctttatcc
pSP73MNVCW1_R99A_FW	gataaaggaggccgccctccg
pSP73MNVCW1_R99A_RV	cggagggcggcctcctttatc
pSP73MNVCW1_Y103A_FW	ctgcgcctgtaggatggctgc
pSP73MNVCW1_Y103A_RV	gcagccatcctacaggcgcag
pSP73MNVCW1_Q116A_FW	catcacgtccattctggcggc
pSP73MNVCW1_Q116A_RV	gccgccagaatggacgtgatg
pSP73MNVCW1_A118S_FW	cattctgcaggcgtccggca
pSP73MNVCW1_A118S_RV	tgccggacgcctgcagaatg
pSP73MNVCW1_A118W_FW	cattctgcaggcgtggggcac
pSP73MNVCW1_A118W_RV	gtgccccacgcctgcagaatg
pSP73MNVCW1_G119A_FW	ccgccacggccttctctatttacc
pSP73MNVCW1_G119A_RV	ggtaaatagagaaggccgtggcgg
pSP73MNVCW1_A121S_FW	ggcacgtccttctctatttaccaccag
pSP73MNVCW1_A121S_RV	ctggtggtaaatagagaaggacgtgcc
pSP73MNVCW1_A121W_FW	ggcacgtggttctctatttaccaccag
pSP73MNVCW1_A121W_RV	ctggtggtaaatagagaaccacgtgcc
pSP73MNVCW1_R131A_FW	ccaccagattgagaaggcgtctagacc
pSP73MNVCW1_R131A_RV	ggtctagacgccttctcaatctggtgg
pSP73MNV_CW1_NS4FLAG_FW	gattacaaggatgacgacgataagtggtaccactctgagggaaagaagg
pSP73MNV_CW1_NS4FLAG_RV	cttatcgtcgtcatccttgtaatccccatcatcgtcatcctcaaagatgtca
pTM_eGFP_NO_ORF1_FW	ggaaaggtctttgacagcgatg
pTM_eGFP_NO_ORF1_RV	gcctcctcctcttcacagaag

Name	5’-3’ sequence
pTM_eGFP_NO_ORF1_F9A_FW	ctctcaccaccttcaatgccg
pTM_eGFP_NO_ORF1_F9A_RV	cggcattgaaggtggtgagag
pTM_eGFP_NO_ORF1_D10A_FW	ctcaccaccttcaatttcgctcg
pTM_eGFP_NO_ORF1_D10A_RV	cgagcgaaattgaaggtggtgag
pTM_eGFP_NO_ORF1_F17A_FW	gtgcttgccgctagacag
pTM_eGFP_NO_ORF1_F17A_RV	ctgtctagcggcaagcac
pTM_eGFP_NO_ORF1_C59A_FW	caagaaggcccaaatagtgtatagtgg
pTM_eGFP_NO_ORF1_C59A_RV	ccactatacactatttgggccttcttg
pTM_eGFP_NO_ORF1_Y68A_FW	caccgccatgcttgagtc
pTM_eGFP_NO_ORF1_Y68A_RV	gactcaagcatggcggtg
pTM_eGFP_NO_ORF1_R105A_FW	cgccgcaatcagatactatgtcaag
pTM_eGFP_NO_ORF1_R105A_RV	cttgacatagtatctgattgcggcg
pTM_eGFP_NO_ORF1_Q112A_FW	gccctgtactccatcattgca
pTM_eGFP_NO_ORF1_Q112A_RV	tgcaatgatggagtacagggc
pTM_eGFP_NO_ORF1_A124S_FW	caaattagcggggctgcatttgtc
pTM_eGFP_NO_ORF1_A124S_RV	gacaaatgcagccccgctaatttg
pTM_eGFP_NO_ORF1_A127S_FW	gggctagttttgtcaccacgc
pTM_eGFP_NO_ORF1_A127S_RV	gcgtggtgacaaaactagccc
pTM_NO_ORF1_FW1_22_46	ggatcacaaccagtatctcttaacg
pTM_NO_ORF1_FW2_503_527	ggcggacatattcagttgataatcg
pTM_NO_ORF1_FW3_1083_1104	caacgtcgttagcgacccttg
pTM_NO_ORF1_FW4_1658_1677	gcacgacttcttcaagtccg
pTM_NO_ORF1_FW5_2267_2283	gcctaaacagcctcccc
pTM_NO_ORF1_FW6_2851_2870	ggaataggaaacccttccc
pTM_NO_ORF1_FW7_3401_3423	gaccaccttgctcaaagacaaag
pTM_NO_ORF1_FW8_3980_3999	cgtgtatgcagaagcccctg
PTM_NO_ORF1_FW9_4513_4532	gtgccctacaccatttgagg
pTM_NO_ORF1_FW10_5102_5120	ggggaagttgtgggctgac
pTM_NO_ORF1_FW11_5703_5723	gaaggtggtgacaacaagggg
pTM_NO_ORF1_FW12_6307_6330	gcctaatggatgaactcaaagcac
pTM_NO_ORF1_FW13_6878_6895	gcggagaactgtgacccg

Name	5’-3’ sequence
pTM_NO_ORF1_FW14_7445_7465	ccgcactcgatgggacatttc
pTM_NO_ORF1_FW15_8038_8062	gattgcgtgatgtgactctagtgac
pTM_NO_ORF1_FW16_8608_8625	cctttctcgccacgttcg
pTM_NO_ORF1_FW17_9105_9122	ccgtgtcgcccttattcc
pTM_NO_ORF1_FW18_9667_9691	ggcgaactacttactctagcttccc
pTM_NO_ORF1_FW19_10227_10247	ggtaactggcttcagcagagc
pTM_NO_ORF1_FW20_10803_10825	ccgtattaccgcctttgagtgag
HAV_2B_FW	gacgagctgtacaagaccggtggtgttggattaatagcagagtgtagaactttc
HAV_2B_RV	gggatccactagtacgcgtttactgagtccttaactccatcattctggag
HAV_2C_FW	gacgagctgtacaagaccggtagtttttccaactggttaagagatattgttctg
HAV_2C_RV	gggatccactagtacgcgtttactgagaccacaactccatgaattcag
HCV_NS4B_FW	gacgagctgtacaagaccggtgcctctagggcggctctc
HCV_NS4B_RV	gggatccactagtacgcgtttagcatgggatggggcagtc
HCV_NS5A_FW	gacgagctgtacaagaccggt tccggatcctggctccg
HCV_NS5A_RV	gggatccactagtacgcgtttagcagcacacggtggtatcg
Swap_FW1	gtcaagtgtgagcaggtcgcc
Swap_RV1	ggcgacctgctcacacttgac
Identical_FW1	gtcaagtgtctccaggacgcc
Identical_RV1	ggcgtcctggagacacttgac
Triple_FW1	cagatactatgtcgtgtgtgagcaggtcgccctg
Triple_RV1	cagggcgacctgctcacacacgacatagtatctg
Stronger_FW1	gtgtccaggaggtcctgacctccatc
Stronger_RV1	gatggaggtcaggacctcctggacac
MNV_AH_MFW1	gcgagagcggttgcactag
MNV_AH_MRV1	cgctcacccaaaagcccc
Swap1_MNV_FW1	ctgctactgtaggatggctgctatcgtcgacacgtccattctgcaggcg

Name	5’-3’ sequence
Swap1_MNV_RV1	cgcctgcagaatggacgtgtcgacgatagcagccatcctacagtagcag
Swap2_MNV_FW1	caaaacacttgtcaactgtgtcagaagggagaagatagcccgcctccgc
Swap2_MNV_RV1	gcggaggcgggctatcttctcccttctgacacagttgacaagtgtttttg
Identical1_MNV_FW1	ctgctactgtaggatggctgctgaggtccttacgtccattctgcaggcg
Identical1_MNV_RV1	cgcctgcagaatggacgtaaggacctcagcagccatcctacagtagcag
Identical2_MNV_FW1	caaaacacttgtcaactgtgtcagaaggcttaaggacgcccgcctccgc
Identical2_MNV_RV1	gcggaggcgggcgtccttaagccttctgacacagttgacaagtgtttttg
FW_MNV_SR	gattacgctaccggtaacaaggtctatgactttgatgccg
FW_MNV_SR	tggcttcacgcgtttacaattcaggctccttgacctttttcaacc
FW_MNV_NSR	ccggttctagaccatccttttattgggatcgtggatacacctaccgtgacggacctggatcctttgacatctttgaggatgacgatgatgggtggtaccactctgagtaaa
RV_MNV_NSR	cgcgtttactcagagtggtaccacccatcatcgtcatcctcaaagatgtcaaaggatccaggtccgtcacggtaggtgtatccacgatcccaataaaaggatggtctagaa
NS4_FW_WOTAG	gataataccatgggcccagctctcacc
NS4_RV_WOTAG	gggatccactagtacgcgtttactcag
WT (d1-20) FW	ccggttactatgtcaagtgtgtccaggaggccctgtactccatcattcaaattgccggggctgcatttgtcaccacgcgcattgccaagcgcatgtaaa
WT (d1-20) RV	cgcgtttacatgcgcttggcaatgcgcgtggtgacaaatgcagcccccggcaatttgaatgatggagtacagggcctcctggacacacttgacatagtaa

Name	5’-3’ sequence
Y1A FW	ccggtgcctatgtcaagtgtgtccaggaggccctgtactccatcatt caaattgccggggctgcatttgtcaccacgcgcattgccaagcgc atgtaaa
Y1A RV	cgcgtttacatgcgcttggcaatgcgcgtggtgacaaatgcagccc cggcaatttgaatgatggagtacagggcctcctggacacacttga cataggca
Y2A FW	ccggttacgctgtcaagtgtgtccaggaggccctgtactccatcatt caaattgccggggctgcatttgtcaccacgcgcattgccaagcgc atgtaaa
Y2A RV	cgcgtttacatgcgcttggcaatgcgcgtggtgacaaatgcagccc cggcaatttgaatgatggagtacagggcctcctggacacacttga cagcgtaa
V3A FW	ccggttactatgccaagtgtgtccaggaggccctgtactccatcatt caaattgccggggctgcatttgtcaccacgcgcattgccaagcgc atgtaaa
V3A RV	cgcgtttacatgcgcttggcaatgcgcgtggtgacaaatgcagccc cggcaatttgaatgatggagtacagggcctcctggacacacttgg catagtaa
K4A FW	ccggttactatgtcgcgtgtgtccaggaggccctgtactccatcattc aaattgccggggctgcatttgtcaccacgcgcattgccaagcgcat gtaaa
K4A RV	cgcgtttacatgcgcttggcaatgcgcgtggtgacaaatgcagccc cggcaatttgaatgatggagtacagggcctcctggacacacgcg acatagtaa
C5A FW	ccggttactatgtcaaggctgtccaggaggccctgtactccatcatt caaattgccggggctgcatttgtcaccacgcgcattgccaagcgc atgtaaa
C5A RV	cgcgtttacatgcgcttggcaatgcgcgtggtgacaaatgcagccc cggcaatttgaatgatggagtacagggcctcctggacagccttga catagtaa

Name	5’-3’ sequence
V6A FW	ccggttactatgtcaagtgtgcccaggaggccctgtactccatcatt caaattgccggggctgcatttgtcaccacgcgcattgccaagcgc atgtaaa
V6A RV	cgcgtttacatgcgcttggcaatgcgcgtggtgacaaatgcagccc cggcaatttgaatgatggagtacagggcctcctgggcacacttga catagtaa
Q7A FW	ccggttactatgtcaagtgtgtcgcggaggccctgtactccatcattc aaattgccggggctgcatttgtcaccacgcgcattgccaagcgcat gtaaa
Q7A RV	cgcgtttacatgcgcttggcaatgcgcgtggtgacaaatgcagccc cggcaatttgaatgatggagtacagggcctccgcgacacacttga catagtaa
E8A FW	ccggttactatgtcaagtgtgtccaggcggccctgtactccatcattc aaattgccggggctgcatttgtcaccacgcgcattgccaagcgcat gtaaa
E8A RV	cgcgtttacatgcgcttggcaatgcgcgtggtgacaaatgcagccc cggcaatttgaatgatggagtacagggccgcctggacacacttga catagtaa
A9S FW	ccggttactatgtcaagtgtgtccaggagagcctgtactccatcattc aaattgccggggctgcatttgtcaccacgcgcattgccaagcgcat gtaaa
A9S RV	cgcgtttacatgcgcttggcaatgcgcgtggtgacaaatgcagccc cggcaatttgaatgatggagtacaggctctcctggacacacttgac atagtaa
L10A FW	ccggttactatgtcaagtgtgtccaggaggccgcgtactccatcatt caaattgccggggctgcatttgtcaccacgcgcattgccaagcgc atgtaaa
L10A RV	cgcgtttacatgcgcttggcaatgcgcgtggtgacaaatgcagccc cggcaatttgaatgatggagtacgcggcctcctggacacacttgac atagtaa

Name	5’-3’ sequence
Y11A FW	ccggttactatgtcaagtgtgtccaggaggccctggcctccatcatt caaattgccggggctgcatttgtcaccacgcgcattgccaagcgc atgtaaa
Y11A RV	cgcgtttacatgcgcttggcaatgcgcgtggtgacaaatgcagccc cggcaatttgaatgatggaggccagggcctcctggacacacttga catagtaa
S12A FW	ccggttactatgtcaagtgtgtccaggaggccctgtacgccatcatt caaattgccggggctgcatttgtcaccacgcgcattgccaagcgc atgtaaa
S12A RV	cgcgtttacatgcgcttggcaatgcgcgtggtgacaaatgcagccc cggcaatttgaatgatggcgtacagggcctcctggacacacttgac atagtaa
I13A FW	ccggttactatgtcaagtgtgtccaggaggccctgtactccgccatt caaattgccggggctgcatttgtcaccacgcgcattgccaagcgc atgtaaa
I13A RV	cgcgtttacatgcgcttggcaatgcgcgtggtgacaaatgcagccc cggcaatttgaatggcggagtacagggcctcctggacacacttga catagtaa
I14A FW	ccggttactatgtcaagtgtgtccaggaggccctgtactccatcgct caaattgccggggctgcatttgtcaccacgcgcattgccaagcgc atgtaaa
I14A RV	cgcgtttacatgcgcttggcaatgcgcgtggtgacaaatgcagccc cggcaatttgagcgatggagtacagggcctcctggacacacttga catagtaa
Q15A FW	ccggttactatgtcaagtgtgtccaggaggccctgtactccatcattg caattgccggggctgcatttgtcaccacgcgcattgccaagcgcat gtaaa
Q15A RV	cgcgtttacatgcgcttggcaatgcgcgtggtgacaaatgcagccc cggcaattgcaatgatggagtacagggcctcctggacacacttga catagtaa

Name	5’-3’ sequence
I16A FW	ccggttactatgtcaagtgtgtccaggaggccctgtactccatcattc aagctgccggggctgcatttgtcaccacgcgcattgccaagcgca tgtaaa
I16A RV	cgcgtttacatgcgcttggcaatgcgcgtggtgacaaatgcagccc ccggcagcttgaatgatggagtacagggcctcctggacacacttga catagtaa
A17S FW	ccggttactatgtcaagtgtgtccaggaggccctgtactccatcattc aaattagcggggctgcatttgtcaccacgcgcattgccaagcgcat gtaaa
A17S RV	cgcgtttacatgcgcttggcaatgcgcgtggtgacaaatgcagccc cgctaatttgaatgatggagtacagggcctcctggacacacttgac atagtaa
G18A FW	ccggttactatgtcaagtgtgtccaggaggccctgtactccatcattc aaattgccgcggctgcatttgtcaccacgcgcattgccaagcgcat gtaaa
G18A RV	cgcgtttacatgcgcttggcaatgcgcgtggtgacaaatgcagccg cggcaatttgaatgatggagtacagggcctcctggacacacttga catagtaa
A19S FW	ccggttactatgtcaagtgtgtccaggaggccctgtactccatcattc aaattgccgggagtgcatttgtcaccacgcgcattgccaagcgcat gtaaa
A19S RV	cgcgtttacatgcgcttggcaatgcgcgtggtgacaaatgcactcc cggcaatttgaatgatggagtacagggcctcctggacacacttga catagtaa
A20S FW	ccggttactatgtcaagtgtgtccaggaggccctgtactccatcattc aaattgccggggcttcatttgtcaccacgcgcattgccaagcgcat gtaaa
A20S RV	cgcgtttacatgcgcttggcaatgcgcgtggtgacaaatgaagccc cggcaatttgaatgatggagtacagggcctcctggacacacttga catagtaa

Name	5’-3’ sequence
F21A FW	ccggttactatgtcaagtgtgtccaggaggccctgtactccatcattc aaattgccggggctgcagctgtcaccacgcgcattgccaagcgc atgtaaa
F21A RV	cgcgtttacatgcgcttggcaatgcgcgtggtgacagctgcagccc cggcaatttgaatgatggagtacagggcctcctggacacacttga catagtaa
V22A FW	ccggttactatgtcaagtgtgtccaggaggccctgtactccatcattc aaattgccggggctgcatttGCCaccacgcgcattgccaagcgc atgtaaa
V22A RV	cgcgtttacatgcgcttggcaatgcgcgtggtggcaaatgcagccc cggcaatttgaatgatggagtacagggcctcctggacacacttga catagtaa
T23A FW	ccggttactatgtcaagtgtgtccaggaggccctgtactccatcattc aaattgccggggctgcatttgtcgccacgcgcattgccaagcgcat gtaaa
T23A RV	cgcgtttacatgcgcttggcaatgcgcgtggcgacaaatgcagcc ccggcaatttgaatgatggagtacagggcctcctggacacacttg acatagtaa
T24A FW	ccggttactatgtcaagtgtgtccaggaggccctgtactccatcattc aaattgccggggctgcatttgtcaccGCGcgcattgccaagcgc atgtaaa
T24A RV	cgcgtttacatgcgcttggcaatgcgcgcggtgacaaatgcagcc ccggcaatttgaatgatggagtacagggcctcctggacacacttg acatagtaa
R25A FW	ccggttactatgtcaagtgtgtccaggaggccctgtactccatcattc aaattgccggggctgcatttgtcaccacggcgattgccaagcgcat gtaaa
R25A RV	cgcgtttacatgcgcttggcaatcgccgtggtgacaaatgcagccc cggcaatttgaatgatggagtacagggcctcctggacacacttga catagtaa

Name	5’-3’ sequence
I26A FW	ccggttactatgtcaagtgtgtccaggaggccctgtactccatcattc aaattgccggggctgcatttgtcaccacgcgcgctgccaagcgca tgtaaa
I26A RV	cgcgtttacatgcgcttggcagcgcgcgtggtgacaaatgcagcc ccggcaatttgaatgatggagtacagggcctcctggacacacttg acatagtaa
A27S FW	ccggttactatgtcaagtgtgtccaggaggccctgtactccatcattc aaattgccggggctgcatttgtcaccacgcgcatttccaagcgcat gtaaa
A27S RV	cgcgtttacatgcgcttggaaatgcgcgtggtgacaaatgcagccc cggcaatttgaatgatggagtacagggcctcctggacacacttga catagtaa
K28A FW	ccggttactatgtcaagtgtgtccaggaggccctgtactccatcattc aaattgccggggctgcatttgtcaccacgcgcattgccgcgcgcat gtaaa
K28A RV	cgcgtttacatgcgcgcggcaatgcgcgtggtgacaaatgcagcc ccggcaatttgaatgatggagtacagggcctcctggacacacttg acatagtaa
R29A FW	ccggttactatgtcaagtgtgtccaggaggccctgtactccatcattc aaattgccggggctgcatttgtcaccacgcgcattgccaaggccat gtaaa
R29A RV	cgcgtttacatggccttggcaatgcgcgtggtgacaaatgcagccc cggcaatttgaatgatggagtacagggcctcctggacacacttga catagtaa
M30A FW	ccggttactatgtcaagtgtgtccaggaggccctgtactccatcattc aaattgccggggctgcatttgtcaccacgcgcattgccaagcgcg cgtaaa
M30A RV	cgcgtttacgcgcgcttggcaatgcgcgtggtgacaaatgcagcc ccggcaatttgaatgatggagtacagggcctcctggacacacttg acatagtaa

Name	5’-3’ sequence
R25AR29A FW	ccggttactatgtcaagtgtgtccaggaggccctgtactccatcattc aaattgccggggctgcatttgtcaccacggcgattgccaaggccat gtaaa
R25AR29A RV	cgcgtttacatggccttggcaatcgccgtggtgacaaatgcagccc cggcaatttgaatgatggagtacagggcctcctggacacacttga catagtaa
R25KR29K FW	ccggttactatgtcaagtgtgtccaggaggccctgtactccatcattc aaattgccggggctgcatttgtcaccacgaaaattgccaagaaaa tgtaaa
R25KR29K RV	cgcgtttacattttcttggcaattttcgtggtgacaaatgcagccccgg caatttgaatgatggagtacagggcctcctggacacacttgacata gtaa
R25ER29E FW	ccggttactatgtcaagtgtgtccaggaggccctgtactccatcattc aaattgccggggctgcatttgtcaccacggaaattgccaaggaaa tgtaaa
R25ER29E RV	cgcgtttacatttccttggcaatttccgtggtgacaaatgcagccccg gcaatttgaatgatggagtacagggcctcctggacacacttgacat agtaa
F21AV22A FW	ccggttactatgtcaagtgtgtccaggaggccctgtactccatcattc aaattgccggggctgcagctgccaccacgcgcattgccaagcgc atgtaaa
F21AV22A RV	cgcgtttacatgcgcttggcaatgcgcgtggtggcagctgcagccc cggcaatttgaatgatggagtacagggcctcctggacacacttga catagtaa
F21AV22AI26A FW	ccggttactatgtcaagtgtgtccaggaggccctgtactccatcattc aaattgccggggctgcagctgccaccacgcgcgctgccaagcgc atgtaaa
F21AV22AI26A RV	cgcgtttacatgcgcttggcagcgcgcgtggtggcagctgcagcc ccggcaatttgaatgatggagtacagggcctcctggacacacttg acatagtaa

Name	5’-3’ sequence
F21AI26A FW	ccggttactatgtcaagtgtgtccaggaggccctgtactccatcattc aaattgccggggctgcagctgtcaccacgcgcgctgccaagcgc atgtaaa
F21AI26A RV	cgcgtttacatgcgcttggcagcgcgcgtggtgacagctgcagcc ccggcaatttgaatgatggagtacagggcctcctggacacacttg acatagtaa
V22AI26A FW	ccggttactatgtcaagtgtgtccaggaggccctgtactccatcattc aaattgccggggctgcatttgccaccacgcgcgctgccaagcgc atgtaaa
V22AI26A RV	cgcgtttacatgcgcttggcagcgcgcgtggtggcaaatgcagcc ccggcaatttgaatgatggagtacagggcctcctggacacacttg acatagtaa
V22L FW	ccggttactatgtcaagtgtgtccaggaggccctgtactccatcattc aaattgccggggctgcatttctcaccacgcgcattgccaagcgcat gtaaa
V22L RV	cgcgtttacatgcgcttggcaatgcgcgtggtgagaaatgcagccc cggcaatttgaatgatggagtacagggcctcctggacacacttga catagtaa
I26L FW	ccggttactatgtcaagtgtgtccaggaggccctgtactccatcattc aaattgccggggctgcatttgtcaccacgcgccttgccaagcgcat gtaaa
I26L RV	cgcgtttacatgcgcttggcaaggcgcgtggtgacaaatgcagcc ccggcaatttgaatgatggagtacagggcctcctggacacacttg acatagtaa
F21Y FW	ccggttactatgtcaagtgtgtccaggaggccctgtactccatcattc aaattgccggggctgcatatgtcaccacgcgcattgccaagcgca tgtaaa
F21Y RV	cgcgtttacatgcgcttggcaatgcgcgtggtgacatatgcagccc cggcaatttgaatgatggagtacagggcctcctggacacacttga catagtaa

Name	5’-3’ sequence
G18V FW	ccggttactatgtcaagtgtgtccaggaggccctgtactccatcattcaaattgccgtggctgcatttgtcaccacgcgcattgccaagcgcatgtaaa
G18V RV	cgcgtttacatgcgcttggcaatgcgcgtggtgacaaatgcagccacggcaatttgaatgatggagtacagggcctcctggacacacttgacatagtaa
NS12_1_111_FW	gtacaagaccggtatgaagatggcg
NS12_1_111_RV	cactagtacgcgtttaagggacactgaaggccgtg
NS12_112_222_FW	gtacaagaccggtccactcaatcagagggagagtagagatg
NS12_112_222_RV	cactagtacgcgtttacctgctcagccacgagtcattaag
NS12_223_334_FW	gtacaagaccggtagaatgatccagagaacaactggtttcttcag
NS12_223_334_RV	gggatccactagtacgcgtttactgtag
2B_Full_FW	gtaactaccggtgccaatatttctctttttatactgaggagcatgaaatg
2B_Full_RV	ctcattacgcgtttactgagtccttaactccatcattctggagtc

Table 2.9 Plasmids

Plasmid name	Backbone	Protein to be expressed
pTM_eGFP_NO_NS4_Coil1_AH1/2	pTM eGFP Nterm	GII.4 NO NS4 aa(1-38)
pTM_eGFP_NO_NS4_Coil1_AH1/2/3	pTM eGFP Nterm	GII.4 NO NS4 aa(1-51)
pTM_eGFP_NO_NS4_SR	pTM eGFP Nterm	GII.4 NO NS4 aa(1-82)
pTM_eGFP_NO_NS4_SR_AH4	pTM eGFP Nterm	GII.4 NO NS4 aa(1-137)
pTM_eGFP_NO_NS4_ΔCoil1	pTM eGFP Nterm	GII.4 NO NS4 aa(13-179)
pTM_eGFP_NO_NS4_ΔCoil1_AH1	pTM eGFP Nterm	GII.4 NO NS4 aa(28-179)
pTM_eGFP_NO_NS4_ΔCoil1_AH1/2	pTM eGFP Nterm	GII.4 NO NS4 aa(44-179)
pTM_eGFP_NO_NS4_ΔCoil1_AH1/2/3	pTM eGFP Nterm	GII.4 NO NS4 aa(59-179)
pTM_eGFP_NO_NS4_AH4	pTM eGFP Nterm	GII.4 NO NS4 aa(88-137)

Plasmid name	Backbone	Protein to be expressed
pTM_eGFP_NO_NS4_AH4_NSR	pTM eGFP Nterm	GII.4 NO NS4 aa(88-179)
pTM_eGFP_NO_NS4_NSR	pTM eGFP Nterm	GII.4 NO NS4 aa(138-179)
pTM_eGFP_NO_NS4_Coil1	pTM eGFP Nterm	GII.4 NO NS4 aa(1-12)
pTM_eGFP_NO_NS4_AH1	pTM eGFP Nterm	GII.4 NO NS4 aa(13-23)
pTM_eGFP_NO_NS4_Coil1_AH1	pTM eGFP Nterm	GII.4 NO NS4 aa(1-23)
pTM_eGFP_NO_NS4_AH2	pTM eGFP Nterm	GII.4 NO NS4 aa(28-38)
pTM_eGFP_NO_NS4_AH1/2	pTM eGFP Nterm	GII.4 NO NS4 aa(13-38)
pTM_eGFP_NO_NS4_AH3	pTM eGFP Nterm	GII.4 NO NS4 aa(44-51)
pTM_eGFP_NO_NS4_β strands	pTM eGFP Nterm	GII.4 NO NS4 aa(59-82)
pTM_eGFP_NO_NS4_AH4_Δ1-10	pTM eGFP Nterm	GII.4 NO NS4 aa(98-137)
pTM_eGFP_NO _AH4_Δ1-20	pTM eGFP Nterm	GII.4 NO NS4 aa(108-137)
pTM_eGFP_NO_ AH4_Δ1-30	pTM eGFP Nterm	GII.4 NO NS4 aa(118-137)
pTM_eGFP_NO_ AH4_Δ1-40	pTM eGFP Nterm	GII.4 NO NS4 aa(128-137)
pTM_eGFP_NO_ AH4_Δ40-50	pTM eGFP Nterm	GII.4 NO NS4 aa(88-127)
pTM_eGFP_NO_ AH4_Δ30-50	pTM eGFP Nterm	GII.4 NO NS4 aa(88-117)
pTM_eGFP_NO_ AH4_Δ20-50	pTM eGFP Nterm	GII.4 NO NS4 aa(88-107)
pTM_eGFP_NO_ AH4_Δ10-50	pTM eGFP Nterm	GII.4 NO NS4 aa(88-97)
pTM_eGFP_NO_ AH4_Δ1-20_Y108A	pTM eGFP Nterm	GII.4 NO NS4 aa(108-137) with Y108A (Y1A)
pTM_eGFP_NO_ AH4_Δ1-20_Y109A	pTM eGFP Nterm	GII.4 NO NS4 aa(108-137) with Y109A (Y2A)
pTM_eGFP_NO_ AH4_Δ1-20_V110A	pTM eGFP Nterm	GII.4 NO NS4 aa(108-137) with V110A (V3A)
pTM_eGFP_NO_ AH4_Δ1-20_K111A	pTM eGFP Nterm	GII.4 NO NS4 aa(108-137) with K111A (K4A)
pTM_eGFP_NO_ AH4_Δ1-20_C112A	pTM eGFP Nterm	GII.4 NO NS4 aa(108-137) with C112A (C5A)
pTM_eGFP_NO_ AH4_Δ1-20_V113A	pTM eGFP Nterm	GII.4 NO NS4 aa(108-137) with V113A (V6A)

Plasmid name	Backbone	Protein to be expressed
pTM_eGFP_NO_ AH4_Δ1-20_Q114A	pTM eGFP Nterm	GII.4 NO NS4 aa(108-137) with Q114A (Q7A)
pTM_eGFP_NO_ AH4_Δ1-20_E115A	pTM eGFP Nterm	GII.4 NO NS4 aa(108-137) with E115A (E8A)
pTM_eGFP_NO_ AH4_Δ1-20_A116S	pTM eGFP Nterm	GII.4 NO NS4 aa(108-137) with A116S (A9S)
pTM_eGFP_NO_ AH4_Δ1-20_L117A	pTM eGFP Nterm	GII.4 NO NS4 aa(108-137) with L117A (L10A)
pTM_eGFP_NO_ AH4_Δ1-20_Y118A	pTM eGFP Nterm	GII.4 NO NS4 aa(108-137) with Y118A (Y11A)
pTM_eGFP_NO_ AH4_Δ1-20_S119A	pTM eGFP Nterm	GII.4 NO NS4 aa(108-137) with S119A (S12A)
pTM_eGFP_NO_ AH4_Δ1-20_I120A	pTM eGFP Nterm	GII.4 NO NS4 aa(108-137) with I120A (I13A)
pTM_eGFP_NO_ AH4_Δ1-20_I121A	pTM eGFP Nterm	GII.4 NO NS4 aa(108-137) with I121A (I14A)
pTM_eGFP_NO_ AH4_Δ1-20_Q122A	pTM eGFP Nterm	GII.4 NO NS4 aa(108-137) with Q122A (Q15A)
pTM_eGFP_NO_ AH4_Δ1-20_I123A	pTM eGFP Nterm	GII.4 NO NS4 aa(108-137) with I123A (I16A)
pTM_eGFP_NO_ AH4_Δ1-20_A124S	pTM eGFP Nterm	GII.4 NO NS4 aa(108-137) with A124S (A17S)
pTM_eGFP_NO_ AH4_Δ1-20_G125A	pTM eGFP Nterm	GII.4 NO NS4 aa(108-137) with G125A (G18A)
pTM_eGFP_NO_ AH4_Δ1-20_A126S	pTM eGFP Nterm	GII.4 NO NS4 aa(108-137) with A126S (A19S)
pTM_eGFP_NO_ AH4_Δ1-20_A127S	pTM eGFP Nterm	GII.4 NO NS4 aa(108-137) with A127S (A20S)
pTM_eGFP_NO_ AH4_Δ1-20_F128A	pTM eGFP Nterm	GII.4 NO NS4 aa(108-137) with F128A (F21A)
pTM_eGFP_NO_ AH4_Δ1-20_V129A	pTM eGFP Nterm	GII.4 NO NS4 aa(108-137) with V129A (V22A)
pTM_eGFP_NO_ AH4_Δ1-20_T130A	pTM eGFP Nterm	GII.4 NO NS4 aa(108-137) with T130A (T23A)
pTM_eGFP_NO_ AH4_Δ1-20_T131A	pTM eGFP Nterm	GII.4 NO NS4 aa(108-137) with T131A (T24A)
pTM_eGFP_NO_ AH4_Δ1-20_R132A	pTM eGFP Nterm	GII.4 NO NS4 aa(108-137) with R132A (R25A)
pTM_eGFP_NO_ AH4_Δ1-20_I133A	pTM eGFP Nterm	GII.4 NO NS4 aa(108-137) with I133A (I26A)
pTM_eGFP_NO_ AH4_Δ1-20_A134S	pTM eGFP Nterm	GII.4 NO NS4 aa(108-137) with A134S (A27S)
pTM_eGFP_NO_ AH4_Δ1-20_K135A	pTM eGFP Nterm	GII.4 NO NS4 aa(108-137) with K135A (K28A)
pTM_eGFP_NO_ AH4_Δ1-20_R136A	pTM eGFP Nterm	GII.4 NO NS4 aa(108-137) with R136A (R29A)

Plasmid name	Backbone	Protein to be expressed
pTM_eGFP_NO_ AH4_Δ1-20_M137A	pTM eGFP Nterm	GII.4 NO NS4 aa(108-137) with M137A (M30A)
pTM_eGFP_NO_ AH4_Δ1-20_G125V	pTM eGFP Nterm	GII.4 NO NS4 aa(108-137) with G125V (G18V)
pTM_eGFP_NO_ AH4_Δ1-20_F128Y	pTM eGFP Nterm	GII.4 NO NS4 aa(108-137) with F128Y (F21Y)
pTM_eGFP_NO_ AH4_Δ1-20_V129L	pTM eGFP Nterm	GII.4 NO NS4 aa(108-137) with V129L (V22L)
pTM_eGFP_NO_ AH4_Δ1-20_I133L	pTM eGFP Nterm	GII.4 NO NS4 aa(108-137) with I133L (I26L)
pTM_eGFP_NO_ AH4_Δ1-20_F128A_V129A	pTM eGFP Nterm	GII.4 NO NS4 aa(108-137) with F128A and V129A (F21A and V22A)
pTM_eGFP_NO_ AH4_Δ1-20_F128A_I133A	pTM eGFP Nterm	GII.4 NO NS4 aa(108-137) with F128A and I133A (F21A and I26A)
pTM_eGFP_NO_ AH4_Δ1-20_V129A_I133A	pTM eGFP Nterm	GII.4 NO NS4 aa(108-137) with V129A and I133A (V22A and I26A)
pTM_eGFP_NO_ AH4_Δ1-20_F128A_V129A_I133A	pTM eGFP Nterm	GII.4 NO NS4 aa(108-137) with F128A, V129A and I133A (F21A, V22A and I26A)
pTM_eGFP_NO_ AH4_Δ1-20_R132A_R136A	pTM eGFP Nterm	GII.4 NO NS4 aa(108-137) with R132A and R136A (R25A and R29A)
pTM_eGFP_NO_ AH4_Δ1-20_R132K_R136K	pTM eGFP Nterm	GII.4 NO NS4 aa(108-137) with R132A and R136A (R25K and R29K)
pTM_eGFP_NO_ AH4_Δ1-20_R132E_R136E	pTM eGFP Nterm	GII.4 NO NS4 aa(108-137) with R132A and R136A (R25E and R29E)
pTM_eGFP_NO_NS4_F9A	pTM eGFP Nterm	Full length GII.4 NO NS4 with F9A
pTM_eGFP_NO_NS4_D10A	pTM eGFP Nterm	Full length GII.4 NO NS4 with D10A
pTM_eGFP_NO_NS4_F17A	pTM eGFP Nterm	Full length GII.4 NO NS4 with F17A
pTM_eGFP_NO_NS4_C59A	pTM eGFP Nterm	Full length GII.4 NO NS4 with C59A
pTM_eGFP_NO_NS4_Y68A	pTM eGFP Nterm	Full length GII.4 NO NS4 with Y68A
pTM_eGFP_NO_NS4_R105A	pTM eGFP Nterm	Full length GII.4 NO NS4 with R105A
pTM_eGFP_NO_NS4_Q122A	pTM eGFP Nterm	Full length GII.4 NO NS4 with Q122A

Plasmid name	Backbone	Protein to be expressed
pTM_eGFP_NO_NS4_A124S	pTM eGFP Nterm	Full length GII.4 NO NS4 with A124S
pTM_eGFP_NO_NS4_A127S	pTM eGFP Nterm	Full length GII.4 NO NS4 with A127S
pTM_eGFP_NO_NS4_K111V_V113E_E115V	pTM eGFP Nterm	Full length GII.4 NO NS4 with triple mutant K111V, V113E and E115V
pTM_eGFP_NO_NS4_V113E_E115V	pTM eGFP Nterm	Full length GII.4 NO NS4 with V113E and E115V
pTM_eGFP_NO_NS4_A116V_E115D	pTM eGFP Nterm	Full length GII.4 NO NS4 with V113L and E115D
pTM_eGFP_NO_NS4_A116V_Y118T	pTM eGFP Nterm	Full length GII.4 NO NS4 with A116V and Y118T
pTM_eGFP	pTM	eGFP
pTM_eGFP_NO_ORF1	pTM eGFP Nterm	Full length GII.4 NO ORF1
pTM_eGFP_NO_ORF1_F9A	pTM eGFP Nterm	Full length GII.4 NO ORF1 with NS4 mutation F9A
pTM_eGFP_NO_ORF1_D10A	pTM eGFP Nterm	Full length GII.4 NO ORF1 with NS4 mutation D10A
pTM_eGFP_NO_ORF1_F17A	pTM eGFP Nterm	Full length GII.4 NO ORF1 with NS4 mutation F17A
pTM_eGFP_NO_ORF1_C59A	pTM eGFP Nterm	Full length GII.4 NO ORF1 with NS4 mutation C59A
pTM_eGFP_NO_ORF1_Y68A	pTM eGFP Nterm	Full length GII.4 NO ORF1 with NS4 mutation Y68A
pTM_eGFP_NO_ORF1_R105A	pTM eGFP Nterm	Full length GII.4 NO ORF1 with NS4 mutation R105A
pTM_eGFP_NO_ORF1_Q122A	pTM eGFP Nterm	Full length GII.4 NO ORF1 with NS4 mutation Q122A
pTM_eGFP_NO_ORF1_A124S	pTM eGFP Nterm	Full length GII.4 NO ORF1 with NS4 mutation A124S
pTM_eGFP_NO_ORF1_A127S	pTM eGFP Nterm	Full length GII.4 NO ORF1 with NS4 mutation A127S
pTM_eGFP_NO_ORF1_ΔSR	pTM eGFP Nterm	Full length GII.4 NO ORF1 with deletion of SR of NS4

Plasmid name	Backbone	Protein to be expressed
pTM_eGFP_NO_ORF1_ΔAH4	pTM eGFP Nterm	Full length GII.4 NO ORF1 with deletion of AH4 of NS4
pTM_eGFP_NO_ORF1_ΔNSR	pTM eGFP Nterm	Full length GII.4 NO ORF1 with deletion of NSR of NS4
pSP73_MNV_NS4_F6A	pSP73 SpeI	Full genome MNV with NS4 mutation F6A
pSP73_MNV_NS4_D7A	pSP73 SpeI	Full genome MNV with NS4 mutation D7A
pSP73_MNV_NS4_A13S	pSP73 SpeI	Full genome MNV with NS4 mutation A13S
pSP73_MNV_NS4_A13W	pSP73 SpeI	Full genome MNV with NS4 mutation A13W
pSP73_MNV_NS4_F14A	pSP73 SpeI	Full genome MNV with NS4 mutation F14A
pSP73_MNV_NS4_A18S	pSP73 SpeI	Full genome MNV with NS4 mutation A18S
pSP73_MNV_NS4_A18W	pSP73 SpeI	Full genome MNV with NS4 mutation A18W
pSP73_MNV_NS4_G32A	pSP73 SpeI	Full genome MNV with NS4 mutation G32A
pSP73_MNV_NS4_C56A	pSP73 SpeI	Full genome MNV with NS4 mutation C56A
pSP73_MNV_NS4_Y65A	pSP73 SpeI	Full genome MNV with NS4 mutation Y65A
pSP73_MNV_NS4_A98S	pSP73 SpeI	Full genome MNV with NS4 mutation A98S
pSP73_MNV_NS4_A98W	pSP73 SpeI	Full genome MNV with NS4 mutation A98W
pSP73_MNV_NS4_R99A	pSP73 SpeI	Full genome MNV with NS4 mutation R99A
pSP73_MNV_NS4_Y103A	pSP73 SpeI	Full genome MNV with NS4 mutation Y103A
pSP73_MNV_NS4_Q116A	pSP73 SpeI	Full genome MNV with NS4 mutation Q116A
pSP73_MNV_NS4_A118S	pSP73 SpeI	Full genome MNV with NS4 mutation A118S
pSP73_MNV_NS4_A118W	pSP73 SpeI	Full genome MNV with NS4 mutation A118W
pSP73_MNV_NS4_G119A	pSP73 SpeI	Full genome MNV with NS4 mutation G119A
pSP73_MNV_NS4_A121S	pSP73 SpeI	Full genome MNV with NS4 mutation A121S
pSP73_MNV_NS4_A121W	pSP73 SpeI	Full genome MNV with NS4 mutation A121W

Plasmid name	Backbone	Protein to be expressed
pSP73_MNV_NS4_R131A	pSP73 SpeI	Full genome MNV with NS4 mutation R131A
pGL-SV40	pGL-SV40	Gaussia luciferase
pSP73_MNV	pSP73 SpeI	Full genome MNV WT
pSP73_MNV_HA	pSP73 SpeI	Full genome MNV with HA in NS1-2
pSP73_MNV_FLAG	pSP73 SpeI	Full genome MNV with FLAG in NS4
pSP73_MNV_HA/FLAG	pSP73 SpeI	Full genome MNV with HA in NS1-2 and FLAG in NS4
pSP73_MNV_NS4_H126A_R131A	pSP73 SpeI	Full genome MNV with NS4 mutation H126A and R131A (AA)
pSP73_MNV_NS4_F122A_S123A_I128A	pSP73 SpeI	Full genome MNV with NS4 mutation F122A, S123A and I128A (AAA)
pSP73_MNV_NS4_F122A_S123A_H126A_ I128A_R131A	pSP73 SpeI	Full genome MNV with NS4 mutation F122A, S123A, H126A, I128A and R131A (AAAAA)
pSP73_MNV_HA/FLAG_NS4_H126A_R131A	pSP73 SpeI	Full genome MNV with HA/FLAG tags and NS4 mutation H126A and R131A (AA)
pSP73_MNV_HA/FLAG_NS4_F122A_S123A _I128A	pSP73 SpeI	Full genome MNV with HA/FLAG tags and NS4 mutation F122A, S123A and I128A (AAA)
pSP73_MNV_HA/FLAG_NS4_F122A_S123A _H126A_I128A_R131A	pSP73 SpeI	Full genome MNV with HA/FLAG tags and NS4 mutation F122A, S123A, H126A, I128A and R131A (AAAAA)
pSP73_MNV_ NS4_D109E_I111L	pSP73 SpeI	Full genome MNV with NS4 AH4 mutation D109E and I111L (Identical 1)
pSP73_MNV_ NS4_D109I_I111D	pSP73 SpeI	Full genome MNV with NS4 AH4 mutation D109I and I111D (Swap 1)
pSP73_MNV_ NS4_I95L_E97D	pSP73 SpeI	Full genome MNV with NS4 AH4 mutation I95L and E97D (Identical 2)
pSP73_MNV_ NS4_I95E_E97I	pSP73 SpeI	Full genome MNV with NS4 AH4 mutation I95E and E97I (Swap 2)

Plasmid name	Backbone	Protein to be expressed
pTM_eGFP_ MNV_ NS4_D109E_I111L	pTM eGFP Nterm	Full length MNV NS4 with NS4 AH4 mutation D109E and I111L (Identical 1)
pTM_eGFP_ MNV_ NS4_D109I_I111D	pTM eGFP Nterm	Full length MNV NS4 with NS4 AH4 mutation D109I and I111D (Swap 1)
pTM_eGFP_ MNV_ NS4_I95L_E97D	pTM eGFP Nterm	Full length MNV NS4 with NS4 AH4 mutation I95L and E97D (Identical 2)
pTM_eGFP_ MNV_ NS4_I95E_E97I	pTM eGFP Nterm	Full length MNV NS4 with NS4 AH4 mutation I95E and E97I (Swap 2)
pTM_eGFP_MNV_NS4_SR	pTM eGFP Nterm	MNV NS4 SR, aa(1-84)
pTM_eGFP_MNV_NS4_AH4a	pTM eGFP Nterm	MNV NS4 Nterm of AH4, aa(85-120)
pTM_eGFP_MNV_NS4_AH4b	pTM eGFP Nterm	MNV NS4 Cterm of AH4, aa(121-131)
pTM_eGFP_MNV_NS4_AH4	pTM eGFP Nterm	MNV NS4 AH4, aa(85-131)
pTM_eGFP_MNV_NS4_NSR	pTM eGFP Nterm	MNV NS4 NSR, aa(132-165)
pTM_eGFP_MNV_NS4	pTM eGFP Nterm	Full length MNV NS4
pTM_HA_MNV_NS4	pTM HA Nterm	Full length MNV NS4
pTM_HA_MNV_NS12	pTM HA Nterm	Full length MNV NS1-2
pTM_eGFP_NO_NS4	pTM eGFP Nterm	Full length GII.4 NO NS4
pTM_HA_NO_NS4	pTM HA Nterm	Full length GII.4 NO NS4
pTM_HA_NO_NS12	pTM HA Nterm	Full length GII.4 NO NS1-2
pTM_mCherry_NO_NS12	pTM mCherry Nterm	Full length GII.4 NO NS1-2
pTM_eGFP_NO_NS12_1_111	pTM eGFP Nterm	GII.4 NO NS1-2 aa(1-111) (dom1)
pTM_eGFP_NO_NS12_112_222	pTM eGFP Nterm	GII.4 NO NS1-2 aa(112-222) (dom2)
pTM_eGFP_NO_NS12_223_334	pTM eGFP Nterm	GII.4 NO NS1-2 aa(223-334) (dom3)
pTM_eGFP_NO_NS12_223_250	pTM eGFP Nterm	GII.4 NO NS1-2 aa(223-250) (dom3a)
pTM_eGFP_NO_NS12_251_278	pTM eGFP Nterm	GII.4 NO NS1-2 aa(251-278) (dom3b)
pTM_eGFP_NO_NS12_279_306	pTM eGFP Nterm	GII.4 NO NS1-2 aa(279-306) (dom3c)

Plasmid name	Backbone	Protein to be expressed
pTM_eGFP_NO_NS12_307_334	pTM eGFP Nterm	GII.4 NO NS1-2 aa(307-334) (dom3d)
pTM_eGFP_NO_NS12_223_278	pTM eGFP Nterm	GII.4 NO NS1-2 aa(223-278) (dom3ab)
pTM_eGFP_NO_NS12_251_306	pTM eGFP Nterm	GII.4 NO NS1-2 aa(251-306) (dom3bc)
pTM_eGFP_NO_NS12_279_334	pTM eGFP Nterm	GII.4 NO NS1-2 aa(279-334) (dom3cd)
pTM_eGFP_NO_NS12_277_313	pTM eGFP Nterm	GII.4 NO NS1-2 aa(277-313) (minimal binding region)
pTM_eGFP_NO_NS12_290_326	pTM eGFP Nterm	GII.4 NO NS1-2 aa(290-326)
pTM_eGFP_NO_NS12_277_313_D290A	pTM eGFP Nterm	GII.4 NO NS1-2 (277-313) with NS1-2 mutation D290A (min1a)
pTM_eGFP_NO_NS12_277_313_E298A	pTM eGFP Nterm	GII.4 NO NS1-2 (277-313) with NS1-2 mutation E298A (min1b)
pTM_eGFP_NO_NS12_277_313_E305A	pTM eGFP Nterm	GII.4 NO NS1-2 (277-313) with NS1-2 mutation E305A (min1c)
pTM_eGFP_NO_NS12_277_313_W291A	pTM eGFP Nterm	GII.4 NO NS1-2 (277-313) with NS1-2 mutation W291A (min1d)
pTM_eGFP_NO_NS12_277_313_D290A_E298A	pTM eGFP Nterm	GII.4 NO NS1-2 (277-313) with NS1-2 mutation D290A and E298A (min1e)
pSP73_MNV_HA/FLAG_NS1-2_D301A	pSP73 SpeI	Full genome MNV with HA in NS1-2 and FLAG in NS4, NS1-2 mutation D301A (1A1)
pSP73_MNV_HA/FLAG_NS1-2_N309A	pSP73 SpeI	Full genome MNV with HA in NS1-2 and FLAG in NS4, NS1-2 mutation N309A (1A2)
pSP73_MNV_HA/FLAG_NS1-2_E316A	pSP73 SpeI	Full genome MNV with HA in NS1-2 and FLAG in NS4, NS1-2 mutation E316A (1A3)
pSP73_MNV_HA/FLAG_NS1-2_D301A_N309A	pSP73 SpeI	Full genome MNV with HA in NS1-2 and FLAG in NS4, NS1-2 mutation D301A and N309A (2A1)
pSP73_MNV_HA/FLAG_NS1-2_N309A_E316A	pSP73 SpeI	Full genome MNV with HA in NS1-2 and FLAG in

Plasmid name	Backbone	Protein to be expressed
		NS4, NS1-2 mutation N309A and E316A (2A2)
pSP73_MNV_HA/FLAG_NS1-2_D301A_ E316A	pSP73 SpeI	Full genome MNV with HA in NS1-2 and FLAG in NS4, NS1-2 mutation D301A and E316A (2A3)
pSP73_MNV_HA/FLAG_NS1-2_D301A_ N309A_E316A	pSP73 SpeI	Full genome MNV with HA in NS1-2 and FLAG in NS4, NS1-2 mutation D301A, N309A and E316A (3A)
pSP73_MNV_NS1-2_D301A	pSP73 SpeI	Full genome MNV with NS1-2 mutation D301A (1A1)
pSP73_MNV_NS1-2_N309A	pSP73 SpeI	Full genome MNV with NS1-2 mutation N309A (1A2)
pSP73_MNV_NS1-2_E316A	pSP73 SpeI	Full genome MNV with NS1-2 mutation E316A (1A3)
pSP73_MNV_NS1-2_D301A_N309A	pSP73 SpeI	Full genome MNV with NS1-2 mutation D301A and N309A (2A1)
pSP73_MNV_NS1-2_N309A_E316A	pSP73 SpeI	Full genome MNV with NS1-2 mutation N309A and E316A (2A2)
pSP73_MNV_NS1-2_D301A_E316A	pSP73 SpeI	Full genome MNV with NS1-2 mutation D301A and E316A (2A3)
pSP73_MNV_NS1-2_D301A_N309A_E316A	pSP73 SpeI	Full genome MNV with NS1-2 mutation D301A, N309A and E316A (3A)
pTM_eGFP_MNV_NS12	pTM eGFP Nterm	Full length MNV NS1-2
pTM_eGFP_NO_NS12	pTM eGFP Nterm	Full length GII.4 NO NS1-2
pTM_YFP_NO_ORF1	pTM YFP Nterm	Full length GII.4 NO ORF1
pTM_YFP_NO_NS4	pTM YFP Nterm	Full length GII.4 NO NS4
pTM_NO_NS4	pTM	Full length GII.4 NO NS4
pTM_NO_VpG	pTM	Full length GII.4 NO VpG
pTM_GFP_MNV_VF1	pTM eGFP Nterm	Full length MNV VF1
pTM_eGFP_NO_NS4/NS5_FLAG	pTM eGFP Nterm	Full length GII.4 NO NS4-NS5 with C-terminal FLAG tag

Plasmid name	Backbone	Protein to be expressed
pTM_VAPA_FLAG	pTM	Full length human VAPA with C-terminal FLAG tag
pTM_MTS_eGFP	pTM	EGFP with N-terminal mitochondrial targeting sequence (first 29 aa of human cox subunit 8a)
pTM_MTS_eGFP_NO_NS4	pTM	EGFP-GII.4 NO NS4 with N-terminal mitochondrial targeting sequence (first 29 aa of human cox subunit 8a)
pTM_MTS_eGFP_NO_NS4_AH4	pTM	EGFP-AH4 with N-terminal mitochondrial targeting sequence (first 29 aa of human cox subunit 8a)
pTM_HA_NO_NS7	pTM HA Nterm	Full length GII.4 NO NS7
pTM_eGFP_HCV_JFH_NS4B	pTM eGFP Nterm	HCV JFH NS4B
pTM_eGFP_HCV_JFH_NS5A	pTM eGFP Nterm	HCV JFH NS5A
pTM_eGFP_HAV_2B_145_251	pTM eGFP Nterm	HAV 2B aa(145-251)
pTM_eGFP_HAV_2B	pTM eGFP Nterm	Full length HAV 2B
pTM_HA_HCV_JFH_NS5A	pTM HA Nterm	HCV JFH NS5A
pCD300lf_puro	Lentivirus puro	Lentiviral CD300lf plasmid
pWPI_CANX_HA_blr	pWPI BLR	Calnexin HA
pWPI_CANX_HA_puro	pWPI PURO	Calnexin HA
pWPI_T7_zeo	pWPI ZEO	T7 polymerase
pWPI_T7_puro	pWPI PURO	T7 polymerase
pWPI_mCherry_NO_NS12_blr	pWPI BLR	mCherry-GII.4 NO NS1-2
pWPI_mito_mTurquoise_zeo	pWPI ZEO	Mito-mTurquoise
pWPI_GFP_hygro	pWPI Hygro	GFP
pWPI_eGFP_NO_NS6_hygro	pWPI Hygro	GFP-GII.4 NO NS6
pWPI_NO_NS6_hygro	pWPI Hygro	GII.4 NO NS6
pWPI_eGFP_NO_NS4_puro	pWPI PURO	GFP-GII.4 NO NS4

2.2 Methods

2.2.1 Polymerase chain reaction (PCR)

First, both primer stocks were diluted to 10 µM. From these 10 µM dilutions, 1.5 µl of both primers were added to 1 ng of DNA template in an PCR tube. This mixture was filled up with distilled water to 15 µl total volume. Next, 15 µl of 2x Phusion Flash High-Fidelity PCR Master Mix (ThermoFischer) was added to this mixture. The PCR mixture was placed in a PCR machine and the PCR program shown below was started.

Table 2.10 PCR protocol

Step	Temperature	Duration	Repeats
1	95	5 min	
2	95	1 sec	25x
3	50-60	5 sec	
4	72	15 sec/kb	
5	72	1 min	
6	4	hold	

2.2.2 Agarose gel electrophoresis and DNA extraction

Agarose gels were made with a percentage of agarose (0.8-2%) depending on the size of the PCR product. For an average size PCR product of around 1kb, 1 gram of agarose was dissolved in 100 ml 1x TAE buffer. This agarose solution was boiled by microwave heating and the nucleic acid stain GelRed® (NIPPON Genetics) was added to the agarose solution (1:10,000). This mixture was poured into a cast and incubated at room temperature to solidify into a 1% agarose gel. Samples of the PCR reactions were mixed with a DNA Gel Loading Dye (ThermoFischer) and an appropriate DNA ladder was loaded together with the PCR reactions to estimate the size of the PCR products (DNA ladder GeneRuler 100 bp or 1kb, ThermoFischer). Agarose gels were run at 120 V until the DNA ladder was separated sufficiently. The INTAS Gel iX Imager

(INTAS) was used to visualize and photograph the DNA bands on the agarose gel and the correct PCR products were excised with a scalpel on the blue/green LED transilluminator (NIPPON Genetics). The gel fragment with the correct PCR product was transferred in a tube and extracted using the NucleoSpin® Gel and PCR Clean-up kit (Macherey-Nagel) according to the supplier's protocol.

2.2.3 DNA restriction digestion

For most restriction digestions, High-Fidelity (HF®) restriction endonucleases (New England BioLabs) were used, since these enzymes are all compatible with the rCutSmart™ buffer (New England BioLabs) and therefore allow for the simultaneous digestion of the DNA by two restriction enzymes. In case other restriction enzymes were used, a buffer compatible for both restriction enzymes was chosen. Five to ten units of restriction enzyme were added per µg of DNA and the restriction digestion was performed according to the manufacturer's protocol. After full digestion of vector DNA, five units of Quick CIP (calf intestinal phosphatase, New England BioLabs) were added to the digestion mixture and incubated at 37 °C for ten minutes to remove 5'-phosphates from the restriction cleavage sites of the vector, preventing religation of the vector during subsequent DNA ligation.

2.2.4 Hybridization of two oligonucleotide primers

Instead of producing a DNA insert via PCR, a DNA insert can also be generated by annealing two long oligonucleotide primers. To this end, two complementary primers were designed with 5' and 3' overhang sites that can anneal with restriction digestion sites. First, 10 µl of 100 µM of sense oligonucleotide and 10 µl of 100 µM of antisense oligonucleotide were mixed in a tube together with 20 µl of 2x annealing buffer. Next, this annealing mixture was incubated for 10 minutes at 95 °C, followed by incubation at room temperature for at least 30 minutes to obtain hybridized oligonucleotides. To add 5'-phosphates at the restriction ends of hybridized oligonucleotides, 1 µl of hybridized oligonucleotides was added in a tube together with 1 µl of T4 DNA ligase buffer (in house), 1 µl of T4 polynucleotide kinase (PNK, ThermoFischer) and 7 µl of distilled water to obtain a total volume of 10 µl. This mixture was incubated for 1 hour at 37 °C and stopped at 60 °C for 20 minutes. The obtained mixture now contained

hybridized oligonucleotides with 5'-phosphates and can be used for ligation into a vector without further need for purification.

2.2.5 DNA ligation

Vector DNA and insert DNA with compatible restriction ends were added to an Eppendorf tube (1:3 molar ratio) and mixed with one unit of T4 DNA ligase (ThermoFischer) and T4 DNA ligase buffer. This mixture was adjusted to a total of 20 µl using distilled water and incubated at room temperature for 15 minutes in case of sticky ends and 2 hours in case of blunt ends or single base overhangs.

2.2.6 Transformation of competent *Escherichia coli*

To transform one ligation reaction, 80 µl of competent DH5α *Escherichia coli* (*E. coli*) cells were thawed and added to the 20 µl of ligation reaction mixture. This transformation mixture of 100 µl was then incubated on ice for 5 minutes. After incubation on ice, a heat shock treatment was performed by incubating the transformation mixture at 42 °C for 45 seconds, followed by another 5 minutes incubation on ice. Next, 900 µl of LB medium was added to the transformation mixture, followed by incubation at 37 °C for 30 minutes. Finally, the transformation mixture was centrifuged for 5 minutes at 6,000 rpm and the bacterial pellet was resuspended in 100 µl of LB medium and plated on LB agar plates containing ampicillin (100 µg/ml). The LB agar plates were then incubated overnight at 37 °C to grow bacterial colonies.

2.2.7 Plasmid isolation from *Escherichia coli* (*E. coli*) and DNA sequencing

Plasmid DNA was isolated from a picked *E. coli* colony. Depending on the required amount of DNA, the *E. coli* colony was picked and cultured overnight at 37 °C in either 4 ml of LB medium supplemented with ampicillin (100 µg/ml) for a miniprep or in 400 ml LB medium with ampicillin (100 µg/ml) for a maxiprep. The plasmid DNA was isolated with either the miniprep kit NucleoSpin Plasmid (Macherey-Nagel) or the maxiprep kit NucleoBond Xtra Maxi (Macherey-Nagel) according to manufacturer's protocol. Maxiprep isolated plasmid DNA was diluted to a concentration around 1 µg/µl. Both miniprep and maxiprep isolated DNA was sent for sequencing to verify the correct sequence of the plasmid according to the provider's protocol (GATC, Eurofins Genomics).

2.2.8 Cell culture of mammalian cell lines

All cell lines were cultured with DMEM complete at 37 °C with 5% CO_2. For some human cell lines stably expressing certain proteins, the DMEM complete was supplemented with a corresponding selection antibiotic (10 µg/ml blasticidin S, 1 mg/ml G418, 3 µg/ml puromycin, 5 µg/ml zeocin, 100 µg/ml hygromycin B). In case murine cells (RAW264.7 or BV-2) were cultured with the intention of infecting these cells with MNV, the DMEM complete was supplemented additionally with L-glutamine (4 mM final concentration) and HEPES (10 mM final concentration). Passaging cells was done around 80% confluency. The cells were first washed with PBS, after which the cells were trypsinized with 5 ml of 0.05% trypsin-EDTA (Gibco, ThermoFischer) for each 15 cm tissue culture dish (Corning). The trypsinized cells were incubated at 37 °C for 5 minutes, followed by detachment and resuspension of the cells in 5 ml of DMEM complete. Finally, the cells were passaged in a new 15 cm dish with a 1:2 to 1:10 dilution, depending on cell type. Optionally, cell count was measured with a TC20 cell counter (Bio-Rad).

2.2.9 Liquid nitrogen storing and thawing of cells

Fully confluent 15-cm dishes were trypsinized and pelleted for 5 minutes at 700 rpm, followed by a PBS wash and another pelleting round. Cells were then resuspended in cold cryosolution (90% FCS, 10% DMSO) and aliquoted in cryotubes (Greiner). These cryotubes were stored at -80°C for at least one day, followed by long-term storage in liquid nitrogen.

Thawing of cells in cryosolution started with incubation of the cryotubes at 37 °C for 2-3 minutes. Next, the cells in cryosolution were resuspended in DMEM complete, after which the cells were pelleted for 5 minutes at 700 rpm. Cells were then resuspended in new DMEM complete and passaged in a 10 cm cell culture dish (Falcon®, Corning) or a 15 cm cell culture dish depending on the amount of cells thawed.

2.2.10 DNA transfection of mammalian cells

For most DNA transfection applications, except for transfections regarding the MNV reverse genetics model, polyethyleneimine (PEI) was used as the DNA transfection reagent. As a rule, 1 µg of plasmid DNA was mixed with 3 µl of PEI (1 mg/ml) in 100 µl of Opti-MEM (Gibco, ThermoFischer). This amount can be adjusted or upscaled as

long as the ratio DNA:PEI remains approximately 1:3 (w/v ratio). For the transfection of a 24-well plate (Corning), 0.5 µg of DNA was used per well, whereas for a 6-well plate (Corning), 1 µg of DNA was transfected per well. For a 10 cm dish, 5 µg of DNA dish was transfected per, whereas for a 15 cm dish, 10 µg of DNA was used per dish. After addition of the correct amount of plasmid DNA and PEI to Opti-MEM, the transfection mixture was vortexed and left on the bench for an incubation of 15 minutes. Finally, the correct amount of transfection mixture was added dropwise to the cell culture plates (typically 50 µl for a 24-well plate, 100 µl for a 6-well plate, 0.5 ml for a 10 cm dish and 1 ml for a 15 cm dish) and mixed in by swirling the plate or dish.

2.2.11 Lentivirus production

One day prior to transfection, $1 \cdot 10^6$ HEK 293T cells were seeded in a 10 cm dish. On the day of transfection, the cells were transfected with 6.4 µg of pCMV, 2.14 µg of pMD2.G and 6.42 µg of the lentiviral vector (pWPI) using PEI transfection. One day after transfection, the medium of the cells was removed and refreshed with new DMEM complete medium. Two and three days after transfection, medium supernatant contained lentiviruses and was collected and filtered using a 0.45 µm filter. Filtered supernatant was stored for short-term at 4 °C and for long-term at -20 °C.

2.2.12 Lentiviral transduction

Cells that were meant to be transduced were seeded in a 6-well plate at a density of $1 \cdot 10^5$ cells per well one day prior to transduction. On the day of transduction, polybrene was added to the filtered lentivirus supernatant (10 µg/ml final concentration). All medium was aspirated from the wells and 1 ml of filtered lentivirus supernatant was added to each well to start the transduction. Over the course of the next two days, the cells were subjected to one round of lentiviral transduction per day. One day after the last transduction, the cells were provided with fresh DMEM complete medium supplemented with the corresponding antibiotic. Surviving cells were carefully expanded in the presence of the selection antibiotic and were frozen in liquid nitrogen as described in section 2.2.9 for long-term storage.

2.2.13 MNV production

One day prior to transfection, HEK 293T cells were seeded in a 6-well plate with $7.5 \cdot 10^5$ cells per well in 2.5 ml DMEM complete. On the day of transfection, the cells were transfected using TransIT®-LT1 Transfection Reagent (Mirus Bio). As a general rule for one well, 250 µl of Opti-MEM was added in a tube together with 2.375 µg of MNV plasmid DNA (pSP73), 0.125 µg of a plasmid DNA encoding Gaussia luciferase (pGL) and 7.5 µl of TransIT®-LT1 Transfection Reagent. The transfection mixture was vortexed and incubated at room temperature for 15 minutes, followed by dropwise addition of the mixture to the well. Two days after transfection, the 6-well plate was placed in the -80 °C until the supernatants of the wells were frozen. Next, the plate was thawed at room temperature and the lysates containing MNV were centrifuged at 2,500 rpm for 5 minutes. Around 5 percent of the supernatants was collected and diluted in PBS (1:100) for an optional luciferase assay, whereas the remaining supernatant (passage 0 MNV) was used directly for further $TCID_{50}$ analysis or stored at -80 °C for other experiments.

2.2.14 Generating MNV stocks

In order to obtain MNV stocks, the passage 0 (P0) MNV as obtained in 2.2.13 was subjected to serial passaging. The P0 MNV was passaged three times on BV-2 cells to generate a passage 3 (P3) virus. To produce a HA/FLAG tagged MNV stock, a P0 HA/FLAG MNV was passaged three times to obtain a P3 HA/FLAG MNV for subsequent IP experiments.

2.2.15 Luciferase assay

Before the start of the experiment, luciferase assay buffer was supplemented with fresh 1 mM DTT and 2 mM ATP. The luciferin coelenterazine (PJK) was then diluted in luciferase assay buffer to a concentration of 1.5 µM to obtain a working stock of luciferin mixture. Of this luciferin mixture, 100 µl were added in a reaction tube together with 20 µl of MNV supernatant diluted 1:100 in PBS as described earlier. Luminescence was measured with an acquisition time of 10 seconds in a Lumat LB 9607 single tube reader (Berthold).

2.2.16 Fifty percent tissue culture infection dose ($TCID_{50}$)

One day prior to infection, RAW264.7 or BV-2 cells were seeded in a 96-well plate (Corning) with 100 µl DMEM complete and $2 \cdot 10^4$ cells per well. On the day of infection, the cells were infected in serial dilutions in quadruplicates with the MNV containing supernatant harvested earlier. After three days, medium was aspirated from the wells and the wells were washed once with PBS. The wells were incubated with 100 µl of crystal violet staining (1x) per well and incubated at room temperature for at least 15 minutes. Next, crystal violet staining was removed and the wells were washed thoroughly with water. $TCID_{50}$ per mL was calculated using the Reed-Muench method.

2.2.17 SDS-PAGE gel

First, an SDS-PAGE gel was casted. The percentage of resolving gel depended on the size of the proteins needed to be separated. For most purposes (15-100 kDa), a 10 percent gel was casted. To prepare one 10 percent gel of around 15 ml resolving gel solution, 6.25 mL of distilled water, 5 ml of acrylamide/bis-acrylamide (30%, Carl Roth), 3.75 ml of SDS resolving gel buffer, 15 µl of tetramethylethylenediamine (TEMED, Sigma Aldrich) and 60 µl of ammonium persulfate (APS, 25% solution, Sigma Aldrich) were mixed in a reaction tube. Gels with other percentages were prepared according to Table 2.2.11.

Table 2.11 Protocol for SDS-PAGE resolving gels

	10%	x%
Distilled water	6.25 mL	11.25 – 0.5·x mL
Acrylamide/bis-acrylamide (30%)	5 mL	0.5·x mL
SDS resolving buffer (1x)	3.75 mL	3.75 mL
TEMED	15 µL	15 µL
APS (25%)	60 µL	60 µL

The resolving gel solution was swirled and quickly casted in a Mini-PROTEAN® Casting Stand (Bio-Rad), followed by sealing of the gel solution with isopropanol. After at least 15 minutes of incubation, the isopropanol was removed and the stacking gel could be prepared. In order to make stacking gel solution for one gel, 3.7 ml distilled water, 0.67

ml of acrylamide/bisacrylamide (30%), 0.63 ml of SDS stacking gel buffer, 5 µl of TEMED and 30 µl of APS (25% solution) were added in a new reaction tube. The stacking gel solution was mixed and pipetted on top of the solidified resolving gel and the whole gel was now sealed with the appropriate combs.

2.2.18 Western blot

Cell lysates were obtained after transfection, transduction, infection or another setting and diluted with 6x laemmli buffer (in house). Next, the samples were cooked for at least 5 minutes at 95 °C and then cooled down to room temperature. After this cooldown, the samples were loaded on an SDD-PAGE gel together with the Color Prestained Protein Standard, Broad Range (10-250 kDa, New England BioLabs) in a Mini-PROTEAN® Tetra Vertical Electrophoresis Cell tank (Bio-Rad) for 4 gels and the tank was filled up with 1x TGS buffer (in house). The gel was run at least at 80 V until the proteins of the ladder were separated. Next, the gel was transferred to a Mini Trans-Blot® gel holder (Bio-Rad) and covered with a polyvinylidene difluoride (PVDF) membrane and placed between two Whatman papers and foam pads (Bio-Rad). The gel was then transferred in a new electrophoresis tank, which was filled up to the top with Western Blot buffer. An ice pack and magnetic stirrer was added in the tank to keep the temperature of the Western Blot buffer as low as possible. Next, the gel was run at 4 °C for at least 1,5 hour at 360 mA to allow for successful protein transfer from the gel to the membrane. After blotting, the PVDF membrane was transferred to a new reaction tube and incubated for blocking with PBS supplemented with 0.5% Tween 20 (PBST) and 5% milk for one hour at room temperature. The PVDF membrane was then washed quickly twice with PBST, followed by incubation with the primary antibody in PBST supplemented with 3% milk overnight at 4 °C. The next day, the PVDF membrane was again washed two times with PBST and incubated with the secondary antibody for 1 hour at room temperature in PBST supplemented with 3% milk. After incubation with the secondary antibody, the PVDF membrane was washed another two times with PBST and the Clarity™ Western ECL Substrate (Bio-Rad) was pipetted on top of the PVDF membrane to visualize the antibody signal under the Advanced ECL imaging system (INTAS).

2.2.19 Co-immunoprecipitation (Co-IP)

Two days prior to the IP experiment, Huh7-T7 Lunet cells were seeded in a 10 cm dish with a density of $2 \cdot 10^6$ cells per dish. The next day, the cells were transfected as described in section 2.2.10 with one or two plasmids in order to express a certain protein or proteins. On the day of the IP, the cells were first washed twice with PBS, followed by aspiration of the PBS and addition of 1 ml of IP buffer supplemented with the protease inhibitor cOmplete™ (1 pill per 500 ml of buffer, Sigma Aldrich). Next, the cells were scraped of the dishes or plates and transferred to a reaction tube. The cell lysate was put on ice and regularly vortexed for at least 30 minutes to promote lysis of the cells. Around 10 percent of the lysate was then frozen as an input sample for later Western blot analysis. In the meantime, magnetic beads against an epitope used in the IP (HA or FLAG) were transferred to a new reaction tube (50 µl of beads per 10 cm dish) and washed twice with IP buffer. The IP buffer and beads were then separate using the DynaMag-2 magnetic rack (ThermoFischer) and the IP buffer supernatant was then aspirated. Cell lysate was added on top of the beads and mixed by inverting the tube. The tube was put on a spinning wheel at 4 °C overnight to ensure maximal binding of the protein of interest to the beads. The next day, the reaction tube was taken out of the wheel and the beads were washed twice with fresh IP buffer. The beads were then suspended in 120 µl of 1x laemmli buffer and cooked for 5 minutes at 95 °C. Finally, the beads were separated from the supernatant and the supernatant was transferred to a new reaction tube and stored at -20 °C for Western blot analysis.

2.2.20 Membrane association assay

Two days prior to the experiment, $1 \cdot 10^7$ Huh7-T7 Lunet cells were seeded in a 15 cm dish with three 15 cm dishes per experimental condition. One day prior to the experiment, the cells were transfected with the corresponding plasmid to express the protein of interest according to section 2.2.10. On the day of the experiment, the cells were first washed twice with PBS and all supernatant was then aspirated from the cells. Around 1.5 ml of hypotonic buffer was added to each dish and the cells of the three 15 cm dishes corresponding to the same experimental condition were scraped and pooled in one reaction tube. Next, the cells were incubated on ice for at least 15 minutes, followed by lysis of the cells by passaging them through an 18 gauge needle for at least 20 times. To ensure all cells were lysed, the cell lysates were then subjected to

snap freezing in liquid nitrogen and thawed again in a 37 °C water bath. After the cells were thawed, the reaction tubes were centrifuged for 5 minutes at 1,000 g. The supernatant was transferred to a new reaction tube and supplemented with sucrose to reach a final concentration of 0.25 M. The reaction tubes were then centrifuged again at 9,000 g for at least 10 minutes to spin down the mitochondria. Following centrifugation, the supernatant was transferred to an ultracentrifuge tube (Beckman Coulter) and centrifuged for at least 40 minutes at a minimum of 100,000 g at 4 °C. Finally, a membrane pellet and a supernatant fraction were obtained and both could be handled for further analysis, such as a membrane extraction assay or a Western blot analysis.

2.2.21 Membrane extraction assay

After extraction of the membrane pellets as described before, the membrane pellets can be treated with a variety of buffers to extract membrane-associated proteins. As a negative control, one membrane pellet was incubated with NTE buffer. Extraction of peripheral membrane proteins was performed with either 1 M NaCl, 3 M urea, 6 M urea or 0.1 M Na_2CO_3 with one membrane pellet per buffer condition. Extraction of both peripheral and integral membrane proteins was performed with incubation of a membrane pellet in 1% Triton X-100. The membrane pellets were suspended in the correct buffer and incubated overnight at 4 °C. The next day, the suspensions were centrifuged for at least 1 hour at 21,000 g to obtain a supernatant and pellet fraction again. Small aliquots of the supernatant fraction were stored at -20°C for later Western blot analysis. The remaining supernatant was aspirated and the membrane pellet was air-dried, followed by resuspension of the pellet in a small amount of fresh NTE buffer and storage at -20 °C for later Western blot analysis.

2.2.22 Membrane sedimentation assay

Around $1 \cdot 10^7$ Huh7-T7 Lunet cells were seeded in a 15 cm dish two days prior to the experiment with three 15 cm dishes per experimental condition. One day prior to the experiment, cells were transfected with a plasmid encoding the protein of interest according to section 2.2.10. On the day of the experiment, cells were washed twice with PBS, after which 1.5 ml of hypotonic buffer was added to each 15 cm dish. The cells were then scraped from the dish and collected in a reaction tube, followed by

incubation of the cell suspension at ice for at least 15 minutes. After this incubation, the cells were passed at least 20 times through an 18 gauge needle to promote cell lysis. To ensure all cells were lysed, the cells were snap frozen in liquid nitrogen and then again thawed in a 37 °C water bath. Next, the lysates were centrifuged for 5 minutes at 1,000 g to remove all major debris. The supernatant was collected and poured on top of an ultracentrifuge tube filled with an iodixanol gradient (OptiPrep™) with 30% iodixanol at the bottom and 10% at the top in approximately 10 steps of 2% each. The gradient with lysate was then centrifuged for 4 hours at 4 °C and 200,000 g. After centrifugation, small fractions of approximately 1 ml were taken from the tube with fraction 1 having the highest density until the last fraction having the lowest density. Finally, the different density fractions were stored at -20 °C for Western blot analysis.

2.2.23 Immunofluorescence

Glass coverslips were placed in a 24-well plate and around $1.5 \cdot 10^4$ cells were seeded per well two days prior to the experiment, followed by transfection of the cells with a plasmid encoding the protein of interest the next day. On the day of the experiment, the coverslips were washed twice with PBS and were then fixed for 20 min at room temperature with 4% paraformaldehyde (PFA). After fixation, the coverslips were washed again twice with PBS and permeabilized with PBS supplemented with 0.5% Triton X-100 for 20 minutes at room temperature. Next, the coverslips were washed twice with PBS and then incubated in filtered PBS supplemented with 3% bovine serum albumin (BSA) at room temperature for at least 30 minutes. This blocking process was followed by pipetting droplets of 100 µl of filtered PBS supplemented with 3% BSA and primary antibodies on parafilm and incubating the coverslips with the cell layer side down on these droplets for at least 1 hour at room temperature. Next, the coverslips were washed twice again with PBS and were then incubated in filtered PBS supplemented with 3% BSA and secondary antibodies and/or LipidTOX Deep Red Neutral Lipid Stain (ThermoFischer) for at least 40 minutes at room temperature, followed by two PBS washings, one washing with distilled water and mounting with Fluoromount-G® (SouthernBiotech) on a microscope slide. The microscope slides were stored in the dark at 4 °C and were imaged with the Leica SP8 AOBS Point Scanning Confocal Microscopa (Leica Microsystems).

2.2.24 Electron microscopy

Huh7-T7 Lunet cells were seeded on glass coverslips in a 24-well plate with $1 \cdot 10^4$ cells per well . One day after seeding, the cells were transfected with a plasmid encoding a fusion protein of GFP and a protein sequence of GII.4 New Orleans human norovirus. One day after transfection, cells were washed twice with PBS, followed by fixation for 30 minutes at room temperature with the EM fixative solution. After fixation, the cells were washed with 50 mM cacodylate buffer for at least 5 times and incubated in the dark in 50 mM cacodylate buffer supplemented with 2% osmium tetroxide for 40 minutes on ice, followed by overnight washing with distilled water. The next day, the cells were treated with 0.5% uranyl acetate for half an hour at room temperature, followed by a short wash with distilled water and a subsequent dehydration series in graded ethanol at room temperature for 5 minutes per step (40% to 80% with 10% per step). The cells were then incubated in 95% ethanol for 20 minutes, followed by incubation in 100% ethanol for 20 minutes as well. Finally, the cells were covered with 100% propylene oxide and embedded in an Araldite-Epon solution (Electron Microscopy Sciences). Polymerization was promoted by incubating the cells with Araldite-Epon at 60 °C for 2 days. After polymerization, the coverslips were separated from the cell monolayers and sections were cut from the cell monolayers with a Leica Ultracut UCT microtome (Leica) and a diamond knife. Sections were mounted on a slot grid and then counterstained with 3% uranyl acetate dissolved in 70% methanol for 5 minutes and then with distilled water supplemented with 2% lead citrate for 2 minutes. The sections could now be investigated under the transmission electron microscope Jeol JEM-1400 (Jeol Ltd.).

2.2.25 Low-precision correlative light-electron microscopy

Huh7-T7 Lunet cells were seeded on glass bottom dishes with a grid coverslip (Mat-Tek) with a density of $4 \cdot 10^4$ cells per dish. The next day, cells were transfected with a plasmid encoding a fusion protein of GFP with a protein sequence of GII.4 New Orleans human norovirus. Around 48 hours after seeding, the cells were fixed with PBS supplemented with 4% PFA and 0.2% glutaraldehyde and the cells were examined with a Nikon Eclipse Ti-E Inverted fluorescence microscope (Nikon) to capture GFP-positive cells and their corresponding location on the grid coverslip. The cells were then fixed with EM fixative and handled as an EM sample as described

before. The Jeol JEM-1400 electron microscope was used to track the GFP-positive cells identified under the Nikon fluorescence microscope.

Chapter 3

Results

"*An experiment is a question which science poses to Nature and a measurement is the recording of Nature's answer.*"

— Max Planck (1858-1947), *Scientific Autobiography and Other Papers*

---

3 Results

3.1 Homology and conservation of NS4 among different genogroups

NS4 is known to be one of the least conserved norovirus nonstructural proteins with only minor sequence relatedness to other calicivirus homologues (83). Since no reverse genetics system is available for human noroviruses, the importance of conserved amino acids of NS4 for the replication cycle of these viruses remains difficult to address. Therefore, in the following section, I aimed to use MNV as a surrogate model for human norovirus in order to assess the significance of conserved amino acid residues in NS4 for viral replication.

3.1.1 Structural analysis and amino acid alignment of NS4 of different genogroups

Firstly, a PSIPRED analysis was performed in order to identify structural domains in GII.4 New Orleans NS4 (Figure 3.1A) and GV MNV CW-1 NS4 (Figure 3.1B). In line with a previous publication in our lab, three structural regions in GII.4 New Orleans NS4 were identified (Figure 3.1A), starting with the structured region (SR) which is composed of three alpha helices (AH1, AH2 and AH3) and beta strands and covers the region from the first amino acid until the threonine at position 80. This SR is followed by a large alpha helix (AH4) covering the region from amino acid position 81 to position 137. The last region is the nonstructured region (NSR) spanning the region from the asparagine at position 138 until the last amino acid of GII.4 New Orleans NS4. Interestingly, a highly identical structural organization for GV MNV CW-1 NS4 was found (Figure 3.1B), where the SR is covering the region of the first amino acid until amino acid position 84 and contains three alpha helices as well as beta strands. The AH4 in GV MNV CW-1 NS4 starts at position 85 and ends at position 130 and the NSR is mapped from residue position 131 until the last amino acid.

Secondly, to pinpoint amino acid residues within NS4 which are conserved among different norovirus genogroups, an amino acid alignment was performed for the documented sequences of genogroups capable of infecting humans (GI, GII, GIV), mice (GV) and the sequence of GII.4 New Orleans (Figure 3.1C). Seventeen amino

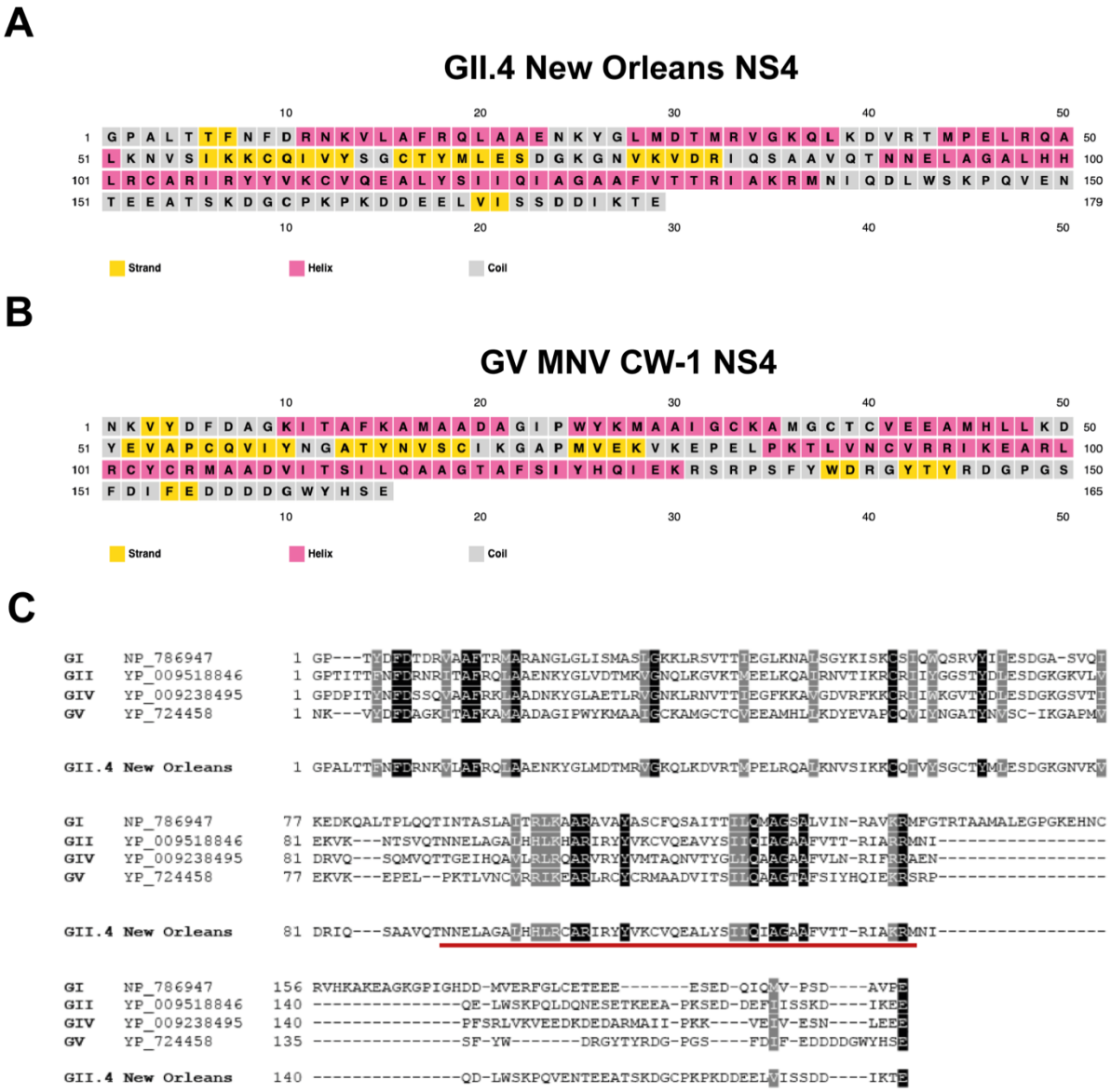

Figure 3.1 PSIPRED analysis of norovirus NS4 among different genogroups

(A) A PSIPRED analysis was performed (http://bioinf.cs.ucl.ac.uk/psipred/) for norovirus GII.4 New Orleans NS4 and for (B) GV MNV CW-1 NS4 to visualize the secondary structures of the proteins. (C) Concensus sequences of NS4 of norovirus GI, GII, GIV and GV and GII.4 New Orleans were aligned using (https://www.ebi.ac.uk/Tools/msa/tcoffee/). The predicted large, center alpha helix is underscored in red.

acids were found to be conserved among these genogroups: eight conserved amino acids were detected within the SR, eight amino acids were conserved in AH4 (underlined in red) and one glutamic acid was conserved within the NSR. However, this glutamic acid is the last amino acid of NS4 and is thus required for the proteolytic cleavage of NS4 from the polyprotein precursor, providing an explanation for the

conservation at this position. Furthermore, in addition to the eight conserved amino acids within AH4, seven amino acids were partially conserved based on polarity and charge, possible hinting at an amphipathic character of AH4.

3.1.2 Alanine scanning of conserved residues in GV MNV CW-1 NS4

Since MNV can replicate in cell culture and viral titers can be quantified with a $TCID_{50}$ assay, GV MNV CW-1 can be used as a surrogate model for the replication of human

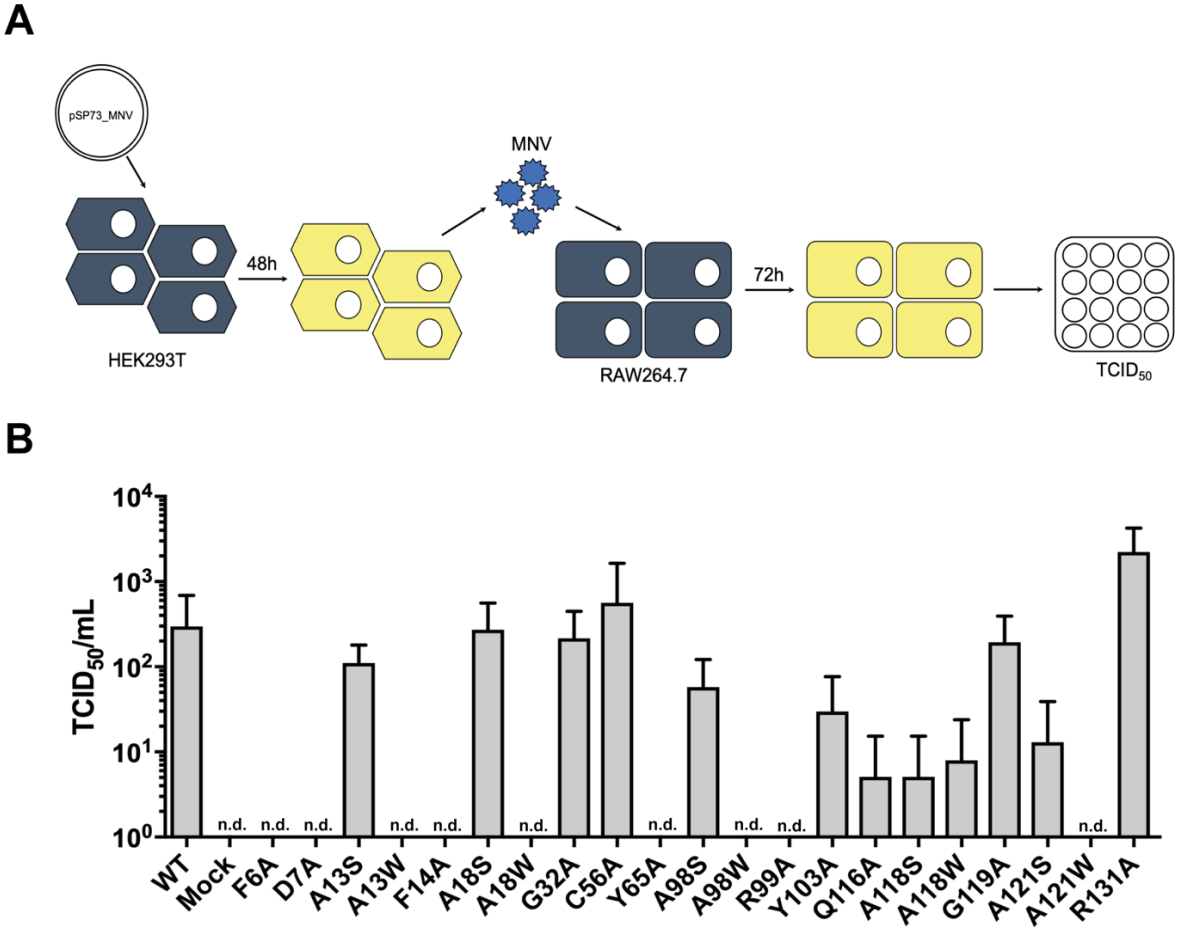

Figure 3.2 Production of infectious MNV particles and $TCID_{50}$ of NS4 mutants

(A) Infectious MNV particles are produced by transfecting HEK 293T cells with a pSP73_MNV plasmid encoding the entire GV MNV CW-1 genome under the influence of a minimal CMV promotor. After 48 hours of transfection, WT MNV or mutant MNV can be harvested and titrated on a $TCID_{50}$ plate seeded with murine RAW264.7 cells. After 72 hours of infection, the $TCID_{50}$ plates can be stained using crystal violet and viral titers can be calculated. (B) MNV with specific mutations within NS4 were produced and titrated using $TCID_{50}$. Most mutations concerned conserved residues among genogroups. In the case of a conserved alanine, a serine or a tryptophane substitution was introduced to either mimic or abolish secondary structure.

noroviruses (Figure 3.2A). In order to assess the importance of the identified conserved amino acids within NS4 for the replication of noroviruses, an alanine scanning of the conserved residues of NS4 in the context of GV MNV CW-1 was performed. Since multiple alanine residues were conserved as well, a conserved alanine was mutated into a serine to retain or into a tryptophan to disrupt the secondary structure. Of note, the conserved glutamic acid in the last position of NS4 was not mutated, since conservation of this residue is crucial for proteolytic cleavage. Mutations for this alanine scanning were generated in the pSP73_MNV vector, containing the whole GV MNV CW-1 genome under the transcriptional control of a minimal CMV promoter, and obtained viral particles were used to infect murine RAW264.7 cells of macrophage origin for a $TCID_{50}$ assay. In this assay, nine mutations were found to completely abolish replication (F6A, D7A, A13W, F14A, A18W, Y65A, A98W, R99A and A121W) (Figure 3.2B). In addition, at least five mutations were able to greatly impair replication (Y103A, Q116A, A118S, A118W and A121S). Taken together, this implies that the residues at position 6, 7, 14, 65, 99, 103, 116, 118 and 121 are also functionally conserved and cannot be mutated into an alanine (or serine in case of a conserved alanine). Finally, to validate the relevance of these residues for the membranous localization of NS4, I expressed these mutations in the context of the full-length GII.4 New Orleans NS4 and the ORF1 polyprotein. However, very little effect on NS4 localization was observed (data not shown).

In conclusion, conserved amino acid residues in NS4 of norovirus are primarily located in the large, center alpha helix (AH4), with few conserved sites in the N-terminal structured region and none in the unstructured C-terminus. Mutation of a few conserved amino acids, both in the structured region and AH4, abrogated or greatly impaired viral replication. However, mutation of these amino acid sites in a GFP-tagged NS4 construct did not significantly alter the membranous localization of NS4.

3.2 Molecular characterization of NS4

Since AH4 of NS4 contains many important conserved residues and might be important for the membranous localization of NS4, I next aimed to molecularly and biochemically characterize the different domains of NS4.

3.2.1 Subcellular localization of NS4 domains

Although norovirus NS4 is not well conserved on the amino acid level, NS4 is structurally quite related between genogroup GII and GV and the protein can be divided into three different domains, a characterization of the subcellular localization of these three domains was performed. GFP was fused N-terminally to the SR, AH4 and NSR of GII.4 New Orleans NS4 or GV MNV-1.CW1 and these fusion proteins were expressed in Huh7-T7 Lunet cells (Figure 3.3B and 3C). As expected, GFP was localized diffusely within the Huh7-T7 cells whereas the GFP-NS4 chimera was localized in a membrane-associated matter. Moreover, the expression of GFP-NS4 seems to be particularly dense around lipid droplets. Expression of the fusion proteins of GFP and SR or NSR of both GII.4 and GV norovirus resulted in an expression pattern resembling that of expression of GFP only with a diffuse GFP expression that is also visible within the nucleus. Of note, the expression of the chimera GFP-SR leads to rapid cell death after eight hours of expression. In contrast to SR and NSR, expression of the chimera GFP-AH4 displayed a membrane-associated localization pattern similar to GFP-NS4. Comparable to GFP-NS4, expression of GFP-AH4 was surrounding lipid droplets in the perinuclear region. AH4 might therefore be the domain of GII.4 New Orleans NS4 and GV MNV-1.CW1 NS4 responsible for association to cellular membranes.

To confirm the immunofluorescence data, the domains of GII.4 New Orleans NS4 were fused to GFP and expressed in Huh7-T7 Lunet cells to perform a membrane sedimentation experiment. Cells were lysed 16 hours after transfection and ultracentrifugation was performed on the cell lysate. Cytosolic supernatant fractions and membrane pellet fractions were obtained and blotted using Western blot (Figure 3.4A). The positive control HCV NS4B, which is an integral membrane protein, was visible only in the input and membrane pellet fraction, whereas GFP alone was detected in the input and supernatant fraction, indicating that membrane proteins and cytosolic proteins were separated. In line with the immunofluorescence data, only full-length GII.4 NS4 and the AH4 of GII.4 NS4 showed a detectable band in the membrane pellet fraction, suggesting that indeed the AH4 of GII.4 NS4 is responsible for the association of NS4 to membranes (Figure 3.4B).

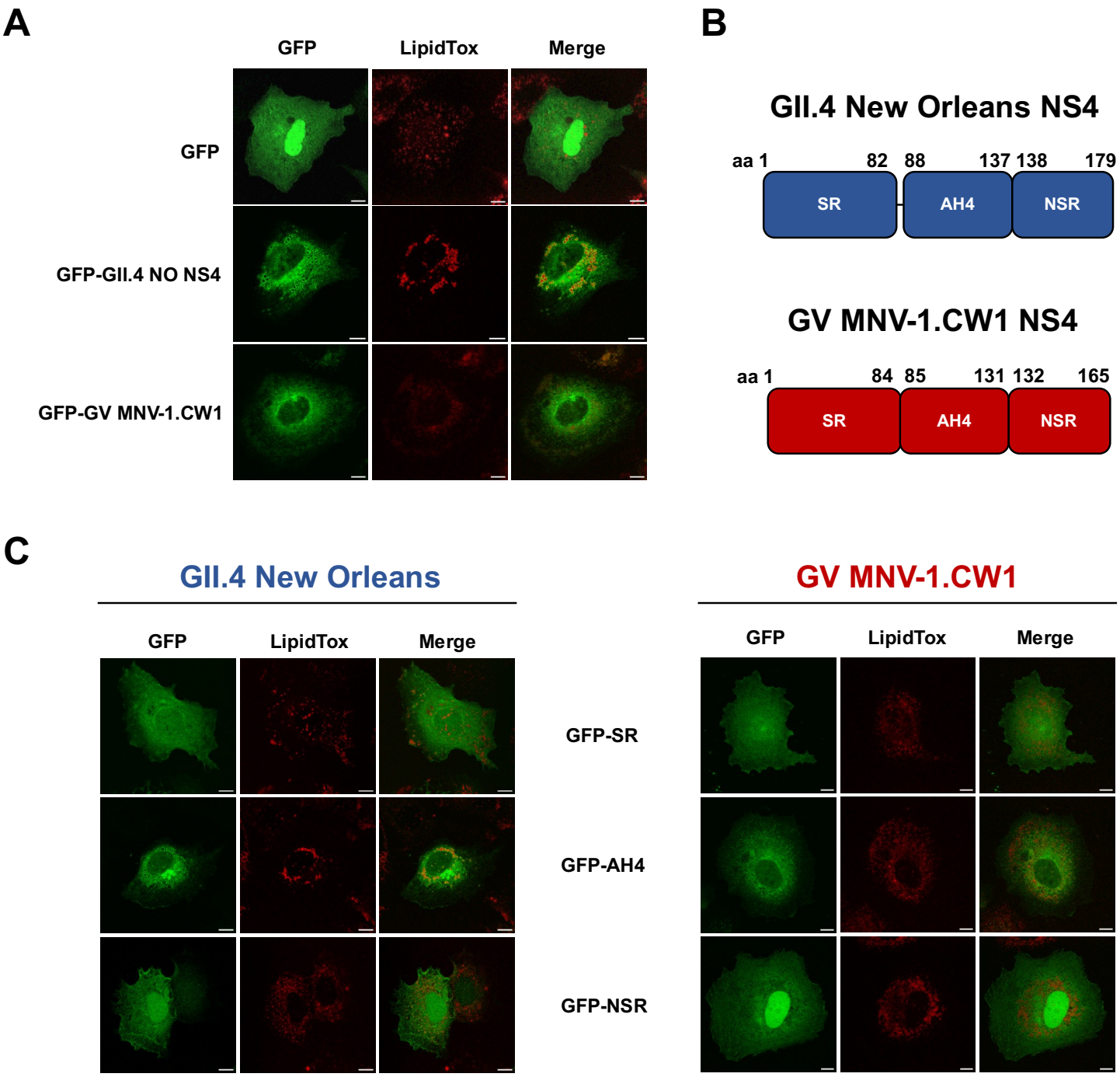

Figure 3.3 Localization of different NS4 domains

(A) Schematic overview of the domains of GII.4 NO NS4. (B) GFP was fused N-terminally to NS4 of GII.4 New Orleans or GV MNV-1.CW1 and expressed in Huh7-T7 Lunet cells. GFP localization and lipid droplet localization (LipidTox) were visualized using fluorescent microscopy. (C) Domains of NS4 of GII.4 and GV were fused to GFP and expressed in Huh7-T7 Lunet cells to visualize the localization of these NS4 domains. Scale bars represent ten micrometer.

3.2.2 Molecular characterization of the amphipathicity of AH4 in NS4

Many viruses employ alpha helices with an amphipathic character to tether their proteins to membranes and to induce membrane curvature. A HeliQuest prediction was performed for GII.4 New Orleans NS4 to assess the amphipathicity of AH4. A strong hydrophobic moment was predicted for AH4 which was particularly high in the center of AH4. Interestingly, this region, covering approximately amino acid position 100 to 120, contains several residues conserved on charge and polarity. To investigate the importance of this amphipathicity for membrane association, four amphipathic mutants of GII.4 New Orleans NS4 were generated and fused to GFP (Figure 3.5A). Two mutants, K111V_V113E_E115V and V113E_E115V, have a low hydrophobic moment, whereas the mutant V113L_E115D has a similar amphipathicity to wild-type NS4 and A116V_Y118T has a slightly higher hydrophobic moment than wild-type NS4. Expression of these fusion proteins in Huh7-T7 Lunet cells reveal that the two mutants with a lower amphipathicity are localized diffusely, whereas the mutants that mimic or even increase the hydrophobic moment could still associate to membranes (Figure 3.5B). Amphipathicity of AH4 at this position in GII.4 New Orleans seems therefore crucial for docking of NS4 at membranes.

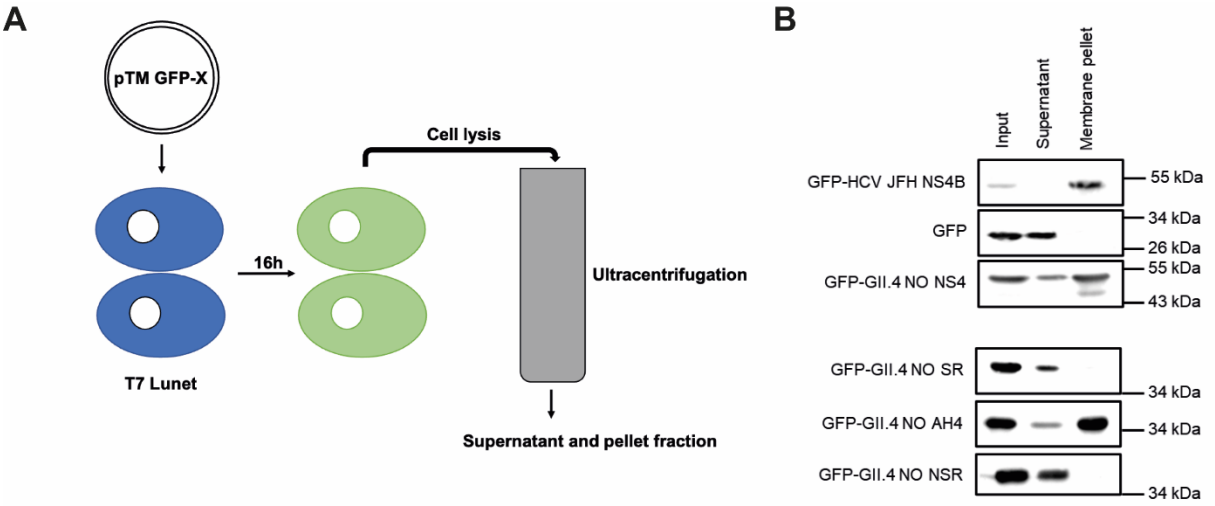

Figure 3.4 Membrane association of different NS4 domains

(A) In order to identify the membrane-associating domain of NS4, GFP was fused N-terminally to GII.4 NS4 or domains and expressed in Huh-T7 lunet cells. After 16 hours of expression in Huh7-T7 Lunet cells, the cells were lysed by freeze-thawing and ultracentrifuged to obtain a supernatant fraction and a membrane pellet fraction. (B) Supernatant and membrane pellet fractions of different constructs were visualized using Western Blot. GFP-HCV NS4B was used as a positive control for the membrane pellet fraction and GFP alone as a negative control for the supernatant fraction.

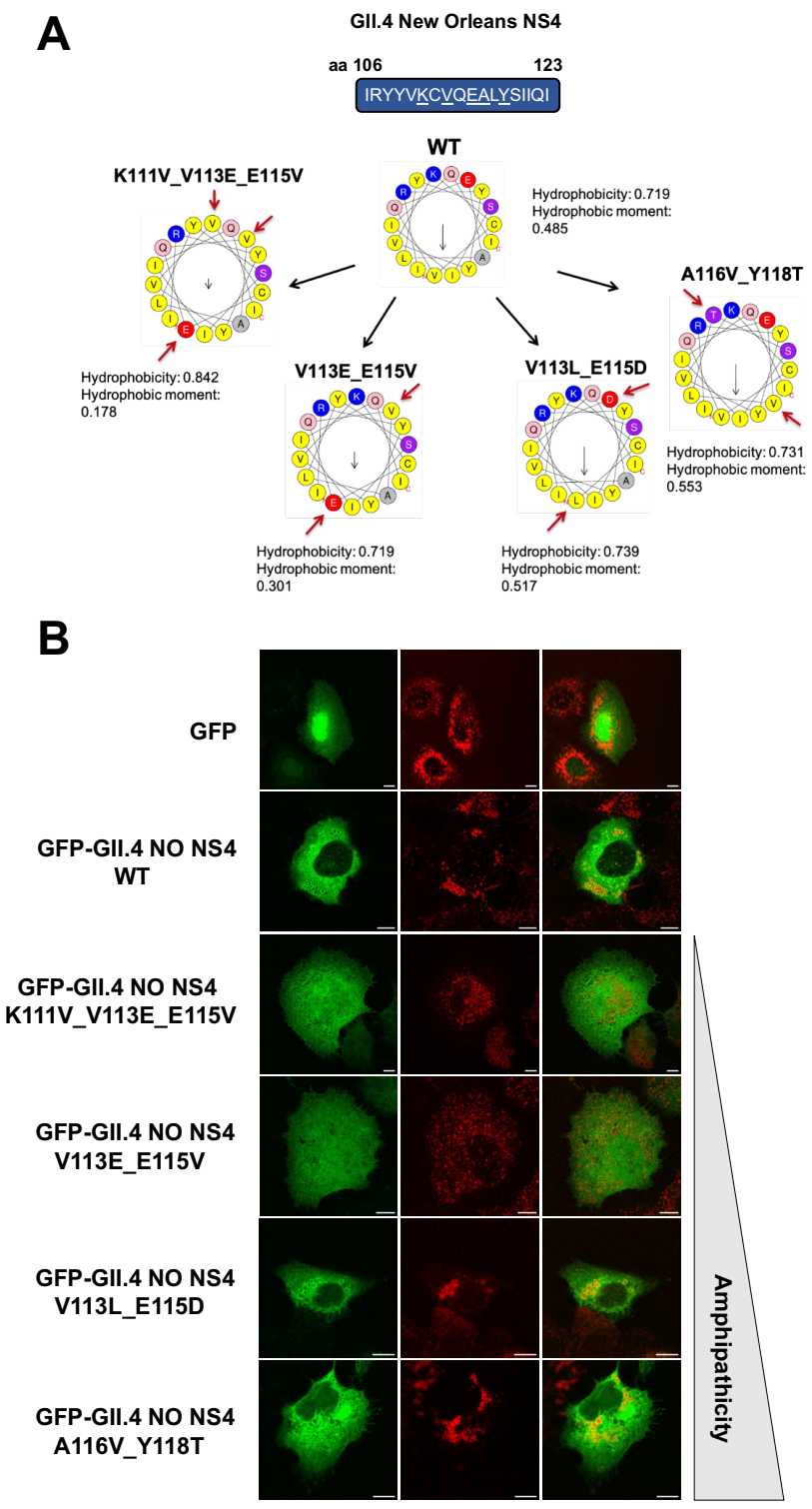

Figure 3.5 The amphipathic moment of AH4 is essential for membrane association of GII.4 NO NS4

(A) Careful mutation of AH4 was performed based on HeliQuest predictions to either abolish (K111V_V113E_E115V), reduce (V113E_E115V), mimick (V113L_E115D) or increase (A116V_Y118T) the amphiphatic moment of AH4 within the context of full-length GII.4 NS4. (B) GFP was N-terminally fused to GII.4 NO NS4 or an amphiphatic mutant and expressed in Huh7-T7 Lunet cells. GFP localization and lipid droplet localization (LipidTox) were visualized using fluorescent microscopy. Scale bars represent 10 micrometer.

3.2.3 Functional relevance of the amphipathicity of AH4 to MNV replication

In light of the structural similarities of GII and GV NS4, a HeliQuest prediction was performed to assess the amphipathicity of the AH4 of GV MNV-1.CW1. Strikingly, a very similar hydrophobic moment was found for MNV AH4 (Figure 3.6A). Two amphipathic mutants of MNV NS4 were generated in the context of GV MNV-1.CW1

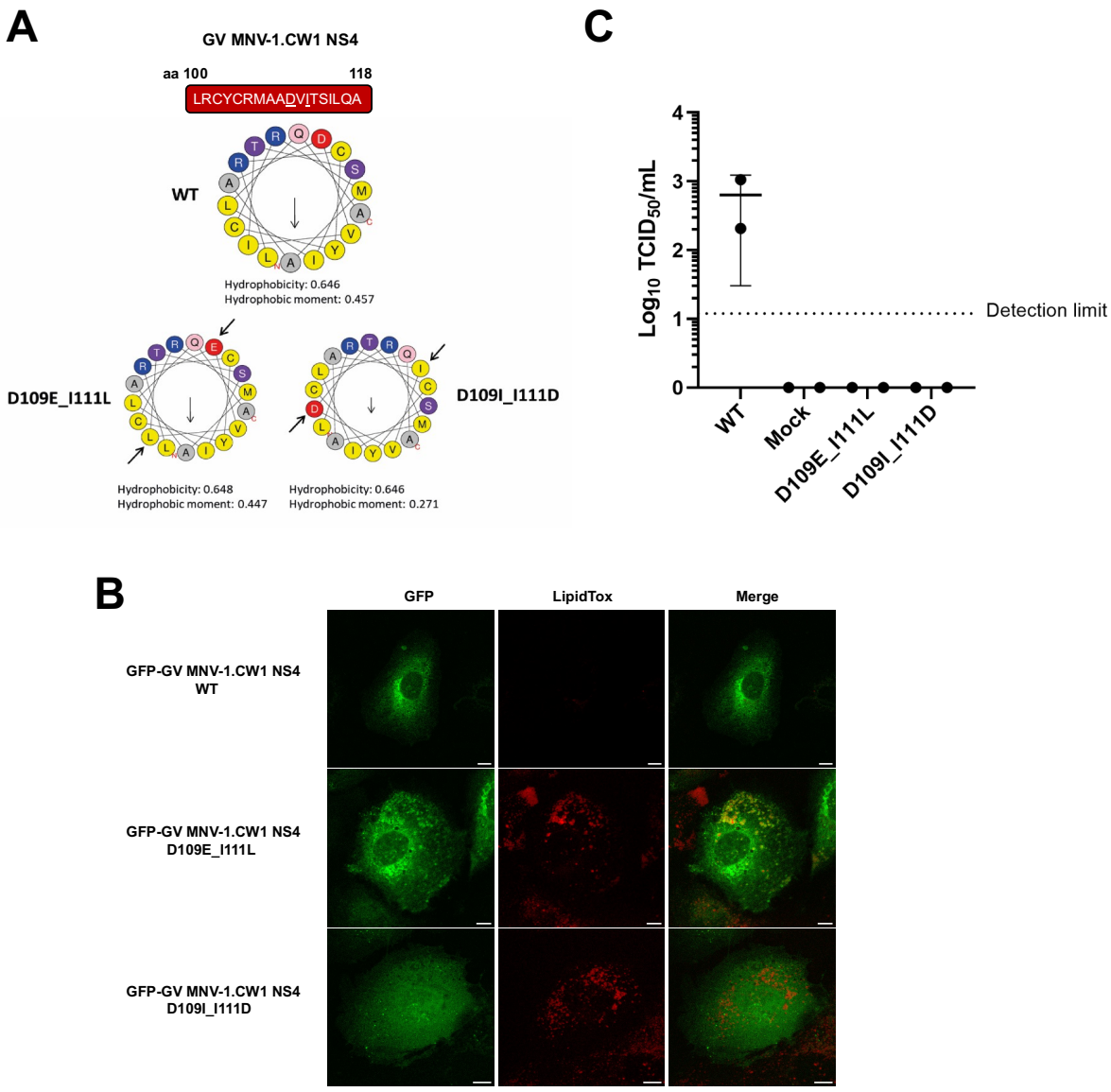

Figure 3.6 The amphipathic moment of AH4 is required for replication of GV MNV CW-1

(A) AH4 was mutated based on HeliQuest predictions to mimic (D109E_I111L) or reduce (D109I_I111D) the amphipathic moment of AH4 within the context of full-length GV MNV-1.CW1 NS4. Fusion proteins of GFP and wild-type NS4 or MNV NS4 amphipathic mutants were expressed in Huh7-T7 Lunet cells to visualize the localization of these proteins. (C) A $TCID_{50}$ was performed on WT MNV or two amphipathic mutants to assess the impact of amphipathicity of AH4 on the replication of MNV. Scale bars represent ten micrometer.

in order to investigate the importance of AH4 amphipathicity for MNV replication (Figure 3.6A). One mutant, D109I_I111D, was designed to have a reduced hydrophobic moment, whereas the mutant D109E_I111L was generated to contain a hydrophobic moment similar to the wild-type. In line with the findings for GII.4 NS4, expression in Huh7-T7 Lunet cells of MNV NS4 amphipathic mutants reveal loss of membrane association for the amphipathic mutant with a reduced amphipathicity (Figure 3.6B). After production of viral particles in HEK 293T cells and infection on RAW264.7 cells, the $TCID_{50}$ of these mutants was calculated. Although the mutant with a similar hydrophobic moment compared to wild-type was replication-defective, replication was also completely abolished for the mutant with a lower amphipathicity (Figure 3.6C). These combined results suggest that the amphipathicity of AH4 in the context of GV MNV CW-1 is important for viral replication, although this region might serve addition functions beyond membrane association as well.

3.2.4 Biochemical characteristics of NS4 and NS4-associated membranes

I next aimed to study the membrane association of NS4 via its amphipatic alpha helix in greater detail. I first aimed to verify biochemically that the mutations changing the amphipatic moment of NS4 indeed abrogate its association to membranes. Therefore, GFP fusion proteins were expressed in Huh7-T7 Lunet cells and subjected to ultracentrifugation after cell lysis to obtain a cytoplasmic supernatant fraction and a membrane pellet fraction (Figure 3.7A). Since HCV NS4B is a well-described transmembrane protein, a GFP fusion protein of HCV NS4B was expressed and used as a positive control in this experiment, whereas GFP alone served as a negative control. In addition, GFP fused N-terminally to wild-type GII.4 New Orleans NS4 and GFP fused N-terminally to the amphipathic mutant V113E_E115V were expressed to investigate biochemically whether the hydrophobic moment within AH4 of NS4 is essential for membrane association. As expected, GFP-HCV NS4B was found almost exclusively in the membrane pellet, whereas GFP alone was found solely in the supernatant fraction (Figure 3.7B). GFP-WT NS4 was detected in both the supernatant and membrane pellet fraction. Although this might be slightly surprising at first, the expression of the pTM vector in Huh7-T7 Lunet cells is typically very high, possibly leading to overexpression of WT NS4 and oversaturation of membranes with WT NS4. By contrast, the amphipathic mutant with a low hydrophobic moment, GFP-

V113E_E115V, was only visible in the supernatant fraction, confirming that the amphipathicity of AH4 is essential for the binding of NS4 to membranes.

To further elucidate the nature of the membranes that NS4 associates with, a membrane sedimentation assay was performed (Figure 3.8A). Huh7-T7 Lunet cells were transfected so that either GFP-WT GII.4 New Orleans NS4 or the amphipathic mutant GFP-V113E_E115V was expressed. After 16 hours of transfection, cells were lysed

using a hypotonic solution and passaging through a syringe. The cell lysis was loaded on a 10-30% iodixanol gradient and ultracentrifuged overnight. Thirteen density samples were collected and were subsequently subjected to a Western blot for further analysis (Figure 3.8B). The ER marker calnexin (CANX) was detected mostly in higher density fractions (fractions 5-9), whereas the cytoplasmic marker glyceraldehyde-3-phosphate dehydrogenase (GAPDH) was visible mostly in the lower density fractions (fractions 10-12). By contrast, the Golgi marker 130 kDa cis-Golgi matrix protein (GM130) was faintly visible starting from fraction 4 until fraction 12 with a peak in fraction 11 (Figure 3.8C). The GFP fusion protein of wild-type NS4 protein was found in many fractions with high expression starting from fraction 6 until fraction 11.

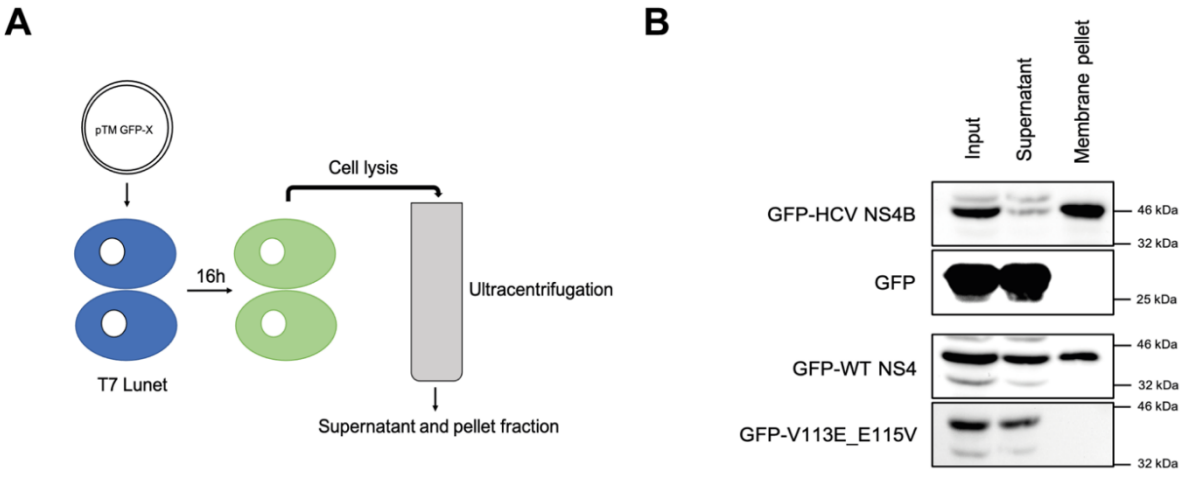

Figure 3.7 Loss of amphipathicity in AH4 renders NS4 in the supernatant fraction

(A) Different constructs with an N-terminal GFP tag were expressed in Huh7-T7 Lunet cells for 16 hours. Subsequently, the cells were lysed by freeze-thawing and ultracentrifugated to obtain a supernatant and a membrane pellet fraction. (B) (D) Supernatant and membrane pellet fractions of different constructs were visualized using Western Blot. GFP-HCV NS4B was used as a positive control for the membrane pellet fraction and GFP alone as a negative control for the supernatant fraction.

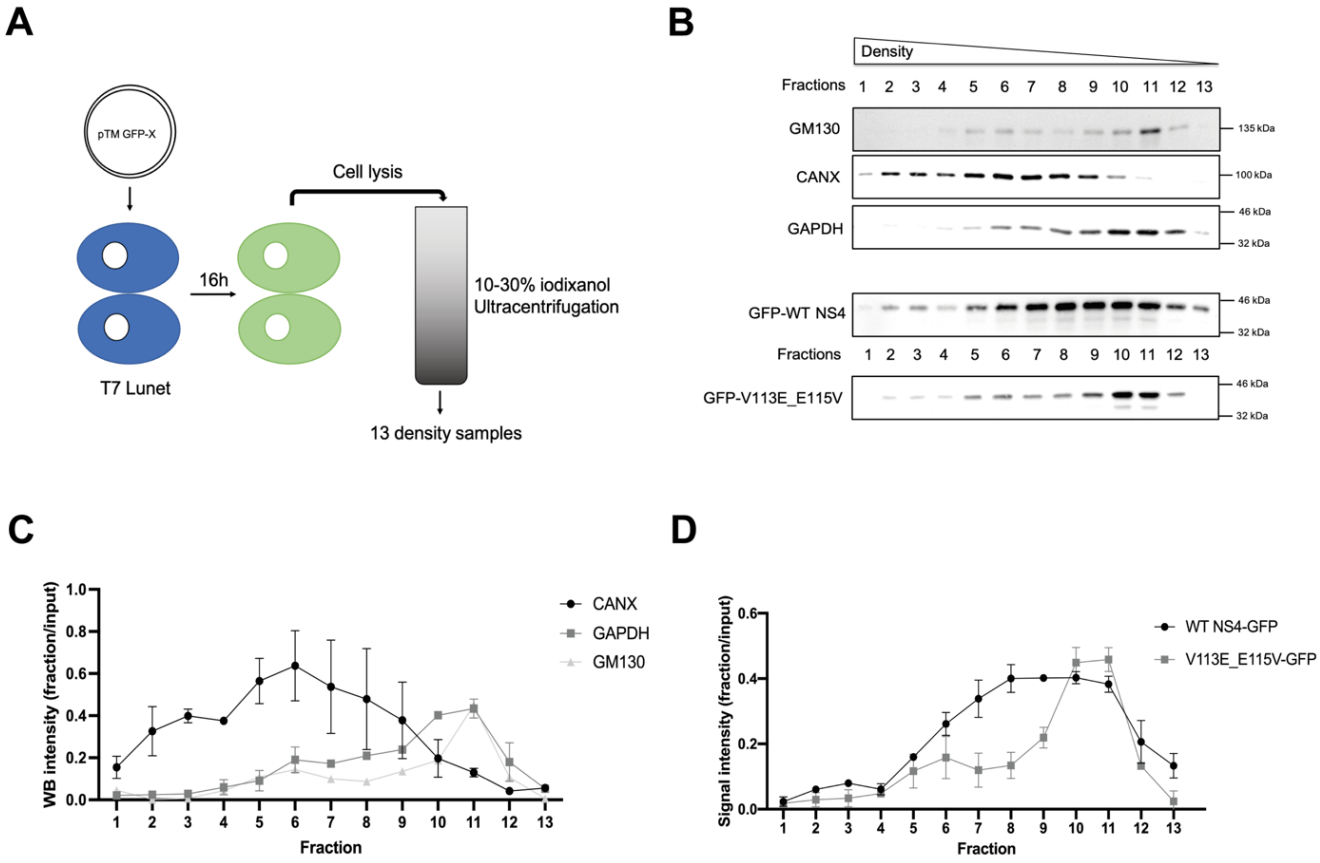

Figure 3.8 Membrane sedimentation assay for NS4-associated membranes

(A) Different constructs with an N-terminal GFP tag were expressed in Huh7-T7 Lunet cells for 16 hours and subsequently lysed using freeze-thawing. The cell lysis was loaded on top of a 10-30% iodixanol gradient and ultracentrifuged overnight. The following day, 13 density samples were taken from the bottom to the top of the ultracentrifuge tube. (B) The density gradients with the different constructs were loaded on a Western Blot. GM130 served as a marker for membranes of golgi origin, CANX for membranes of ER origin and GAPDH as a marker for the cytosolic fraction. (C) Quantification of different markers reveal ER marker in higher density samples. (D) Quantification of WT GII.4 NO NS4 and the amphipathic mutant V113E_E115V.

However, the amphipathic mutant GFP-V113E_E115V was found predominantly in the fractions 10 and 11, resembling the peak fractions of the cytoplasmic marker GAPDH (Figure 3.8D). These results support the previous findings that amphipathicity of AH4 is essential for the association of NS4 to membranes. Furthermore, these findings also indicate that NS4 associates to membranes containing CANX and/or GM130, which might suggest that NS4 associates predominantly to membranes of ER and/or Golgi origin.

Since amphipathic alpha helices often facilitate the peripheral attachment of proteins to membranes, a membrane extraction assay was performed to determine whether GII.4 NO NS4 behaves as an integral or peripheral membrane protein. Huh7-T7 Lunet cells were transfected with constructs containing either HCV NS4B, HCV NS5A, HAV 2B residues 145-251 or GII.4 NO NS4 fused to GFP. HCV NS5A contains an N-terminal amphipathic alpha helix as well, which is responsible for the association of NS5A to the ER membrane and to membrane monolayers associated with LDs (250–253). It is thought to attach to membranes via the amphipathic alpha helix, but in some aspects biochemically rather behaves as an integral membrane protein (254,255). By contrast, HAV 2B contains an amphipathic alpha helix, reported to behave as a peripheral membrane protein (256). Together with the integral membrane protein HCV NS4B, these proteins therefore served as additional controls. After 24 hours, the cells were lysed using freeze-thawing and ultracentrifuged to obtain a membrane pellet. The membrane pellets were subsequently treated with different buffers. The next day, these buffers were centrifuged again and a pellet and membrane fraction were obtained for each construct and buffer condition (Figure 3.9A).

As expected, the integral membrane protein HCV NS4B was resistant against all buffer treatments except for 1% Triton X-100 (Figure 3.9B). HCV NS5A, which has been reported to behave like an integral membrane protein, was slightly stripped from the membranes with 6M urea and 1% Triton X-100, whereas the peripheral membrane protein HAV 2B was stripped more heavily under these conditions and in the 100 mM sodium carbonate buffer. Although not all protein could be stripped under the condition of 1% Triton X-100, potentially because of aggregate formation, NS4 could be easily stripped of the membranes using 3M urea, 6M urea and 100 mM sodium carbonate, indicating that NS4 is indeed behaving like a peripheral membrane protein in this assay.

3.2.5 Importance of AH4 for the induction of membrane rearrangements

One of the most important functions of norovirus NS4 is the induction of membrane rearrangements to form the replication complex. Amphipathic alpha helices have been well described to be able to curve membranes resulting in membrane alterations (257). These membrane rearrangements are often clustered in close proximity to lipid

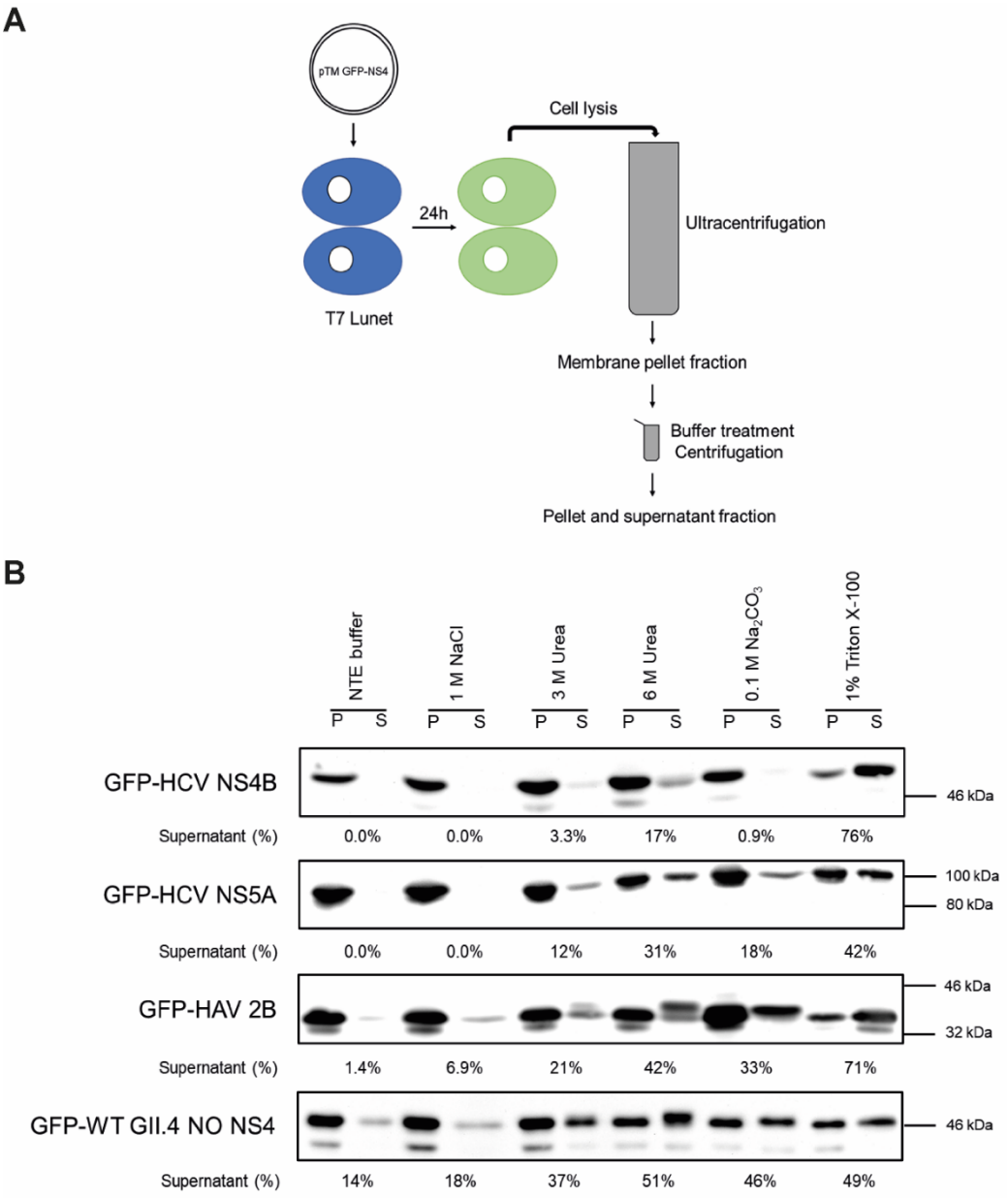

Figure 3.9 Membrane protein extraction assay of GII.4 NO NS4

(A) Different GFP-fusion proteins were expressed in Huh7-T7 Lunet cells for 24 hours and subsequently lysed by freeze-thawing the cells. After ultracentrifugation for one hour, the membrane pellet fractions were taken and incubated overnight in different buffer conditions. The next day, suspensions were centrifuged again and the supernatant and pellet fraction were separated and prepared for Western blot analysis. (B) Pellet and supernatant fractions of different GFP-fusion proteins were subjected to Western blot analysis to evaluate the strength of membrane association. Typically, 1M NaCl, urea and sodium carbonate are capable of extracting most peripheral membrane proteins from the pellet fraction to the supernatant fraction. Incubation with 1% Triton X-100 strips integral membrane proteins. GFP-HCV NS4B serves here as a known integral membrane protein and GFP-HAV 2B residues 145-251 serves as a known peripheral membrane protein.

droplets, where NS4 induces a tight association between lipid droplets and membranes (56). To elucidate the role of AH4 in the association between lipid droplets and membranes, GFP-GII.4 New Orleans NS4 and the amphipathic mutants GFP-V113E_E115V and GFP-V113L_E115D were expressed in Huh7-T7 Lunet cells and subjected to low precision correlative light and electron microscopy (CLEM). Upon

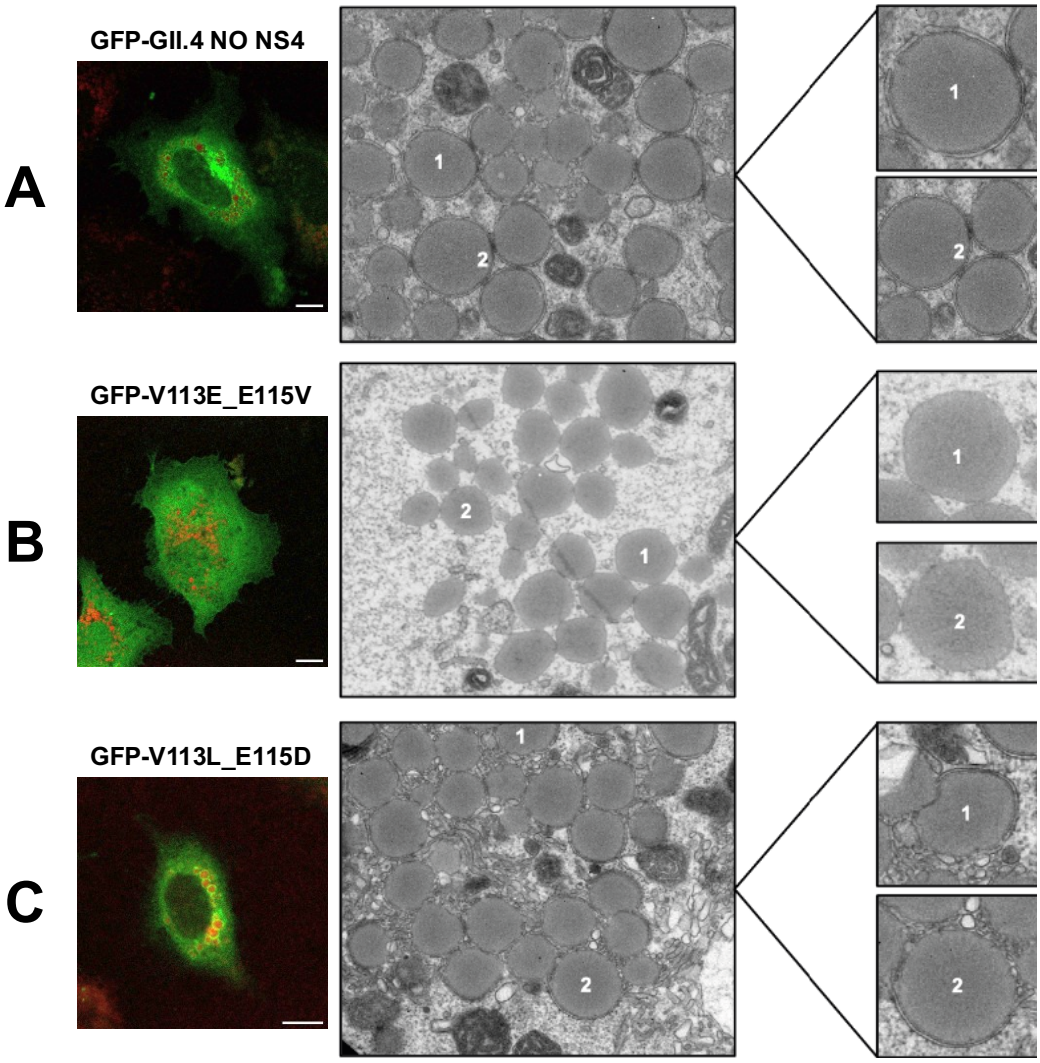

Figure 3.10 Amphipathicity of AH4 facilitates membrane enwrapment of lipid droplets

(A) GII.4 New Orleans NS4 tagged N-terminally with GFP was expressed in Huh7-T7 Lunet cells and treated for visualization with electron microscopy. A lipid bilayer around the lipid droplets 1 and 2 is visible. (B) The amphipathic mutant V113E_E115V, which display reduced amphipathicity in AH4, was fused N-terminally to GFP and expressed in Huh7-T7 Lunet cells. The cells were subsequently treated for low-precision correlative light electron microscopy. Lipid droplets were not enwrapped by a lipid bilayer (close-up 1 and 2). (C) The amphipathic mutant V113L_E114D, which mimics the wild-type amphipathicity in AH4, was fused N-terminally to GFP and expressed in Huh7=T7 Lunet cells. The cells were treated for electron microscopy. Lipid droplet enwrapment was detectable (close-up 1 and 2).

expression of wild-type NS4, wrapping of lipid droplets by a lipid bilayer was observed (Figure 3.10A). By contrast, expression of the amphipathic mutant V113E_E115V, in which the hydrophobic moment of AH4 is reduced, did not show wrapping of membranes around lipid droplets (Figure 3.10B). Interestingly, the amphipathic mutant V113L_E115D with a hydrophobic moment similar to wild-type NS4 was able to enwrap lipid droplets with a lipid bilayer comparable to wild-type NS4 (Figure 3.10C). These results indicate that a hydrophobic moment within AH4 is essential for the remodeling of intracellular membranes and the wrapping of a lipid bilayer around lipid droplets.

To verify the importance of AH4 for membrane enwrapment of LDs, GFP was fused to either GII.4 NO NS4 or AH4 and expressed in Huh7-T7 Lunet cells. Using low precision CLEM, expression of GFP-AH4 was found to induce LD clustering (Figure 3.11A). LDs were often found in close proximity to a membrane that probably originates from the

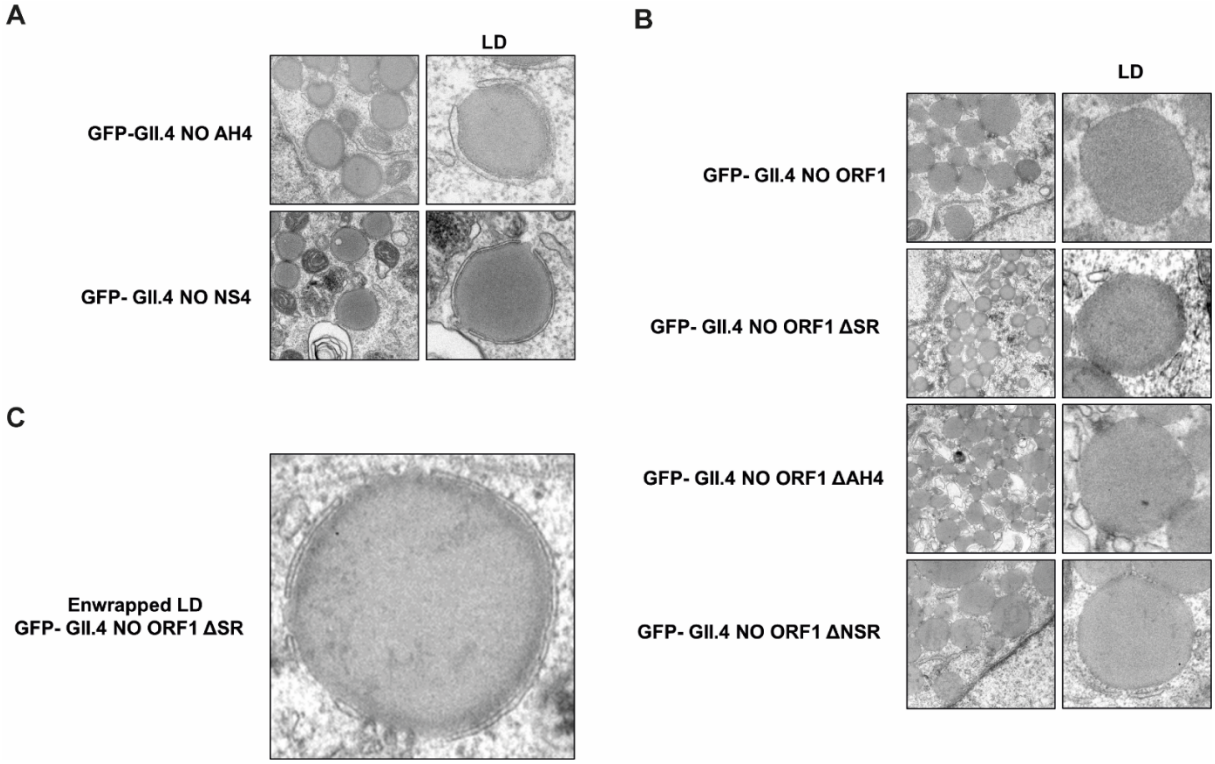

Figure 3.11 Membrane enwrapment of lipid droplets is rare in the ORF1 polyprotein context
(A) GFP fused to GII.4 NO NS4 or AH4 was expressed in Huh7-T7 Lunet cells, following subsequent EM analysis. (B) EM analysis of Huh7-T7 Lunet cells expressing GFP fused to GII.4 NO ORF1 or deletion mutants. LD enwrapment is rarely observed in the ORF1 polyprotein context . (C) EM picture of membrane enwrapment of a LD in cells expressing GFP-GII.4 NO ORF1 ΔSR.

ER. In some cases, LDs were almost completed engulfed by this membrane, reminiscent of the membrane enwrapment of LDs upon NS4 expression. These observations suggest that AH4 is the key inducer of membrane enwrapment of LDs, although other parts of NS4 most likely contribute to this phenomenon as well.

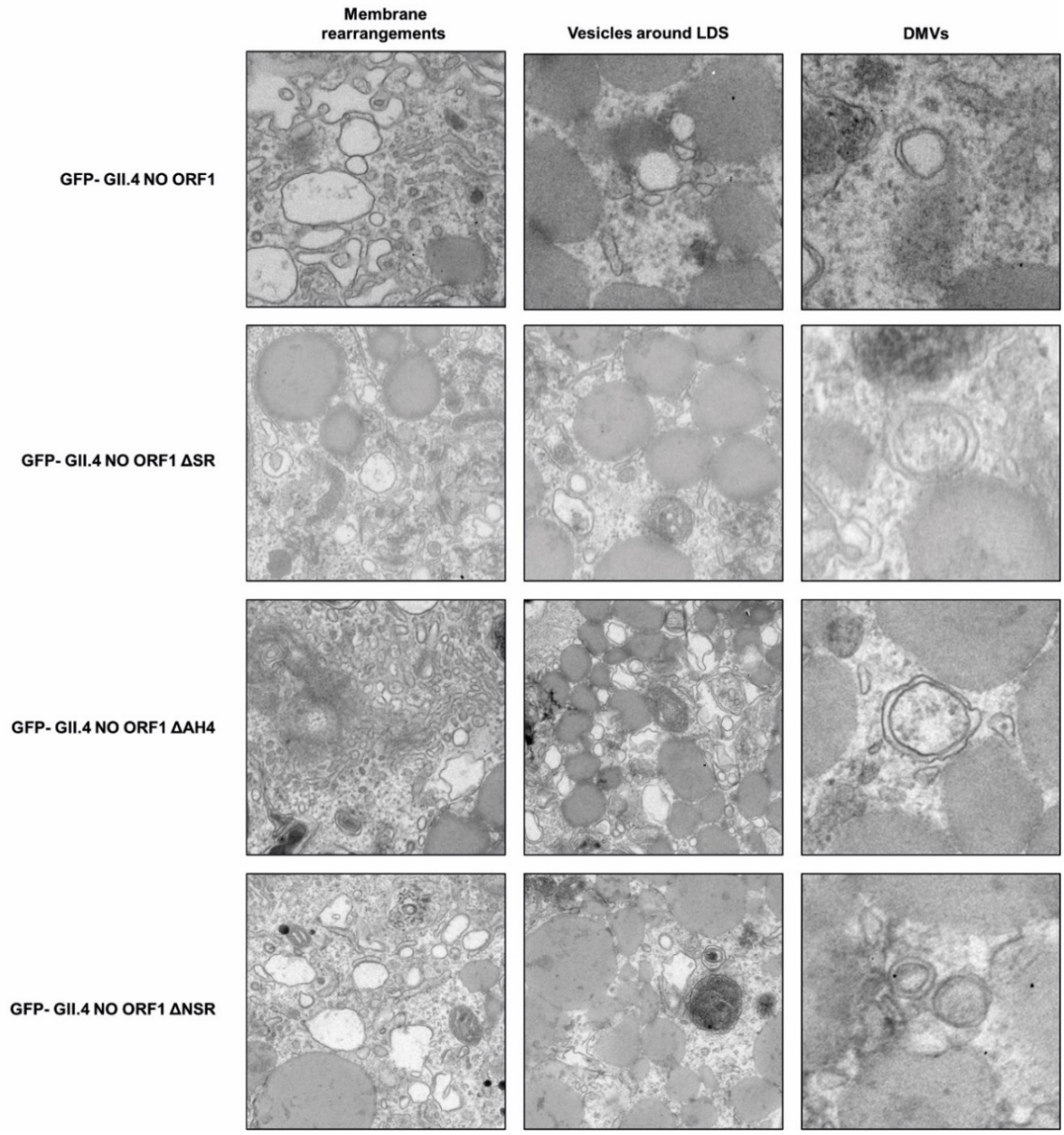

Figure 3.12 NS4 deletion mutants and membrane rearrangements in the ORF1 polyprotein context

EM analysis of Huh7-T7 Lunet cells expressing GFP fused to GII.4 NO ORF1 or deletion mutants. Many membranous structures were present in the perinuclear region and in close proximity to clusters of LDs. SMVs and DMVs were present in all expressed constructs.

Since GII.4 NO NS4 is present with the other proteins in the GII.4 NO ORF1 polyprotein during infection, GFP-ORF1 and deletion mutants were generated, in which either SR, AH4 or NSR were deleted from the ORF1 polyprotein. Huh7-T7 Lunet cells expression these constructs were subjected to low precision CLEM (Figure 3.11B). Surprisingly, LD clustering was observed upon expression of the deletion mutants, while LD enwrapment was very rare and only observed in one cell expressing GFP-ORF1 without SR (Figure 3.11C). Therefore, membrane enwrapment of LDs seems to be a feature that occurs only upon sole overexpression of NS4. However, at the same time, membrane rearrangements such as SMVs and DMVs were observed in all ORF1 constructs, even in the absence of AH4 (Figure 3.12), challenging the view that NS4 is the main protein responsible for membrane alterations during norovirus infection.

In conclusion, AH4 seems essential for the membrane-associating and membrane-rearranging properties of NS4. Furthermore, the amphipathic moment of AH4 determines its ability to associate to membranes, induce membrane alterations and might be crucial for viral replication in MNV as well. In addition, NS4 can be stripped from membranes by non-detergents such as urea and sodium carbonate, indicating that NS4 behaves as a peripheral membrane protein. However, within the context of the ORF1 polyprotein, deletion of AH4 appears to have very little effect on the overall induction of membrane rearrangements.

3.3 NS4 binding to NS1-2

As for many other viruses, NS4 is likely to interact with other norovirus nonstructural proteins. Of note, several interactions between NS1-2, NS3 and NS4 have been reported already, but very little is known about the exact biochemical nature of these interactions, nor about the function (61,79). In the next section, I aimed to examine the interaction of NS4 with NS1-2, NS3 and itself and to further investigate the potential interaction between NS4 and these nonstructural proteins.

3.3.1 Interaction of NS4 with other nonstructural proteins

Since the nonstructural proteins NS1-2, NS3 and NS4 have been shown to play a key role in the formation of the norovirus replication complex, interaction between these

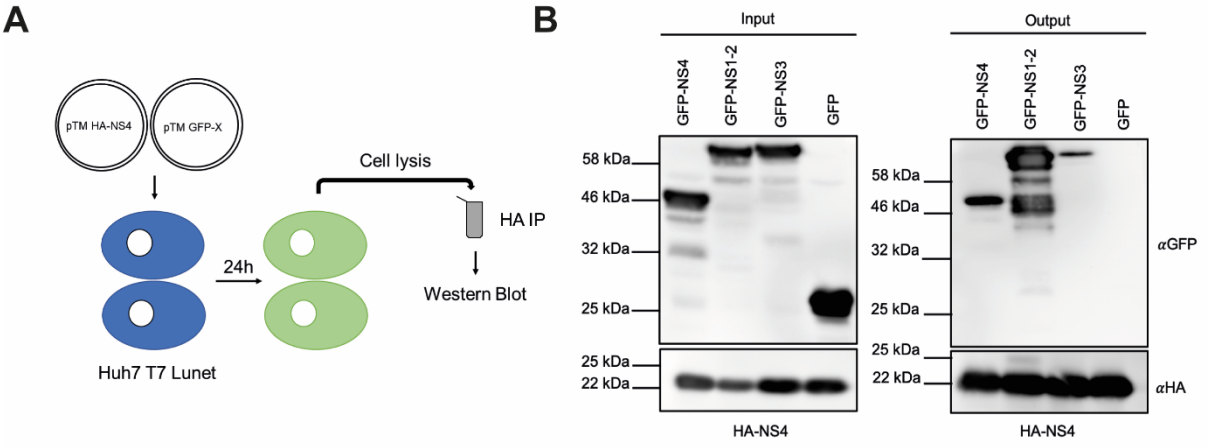

Figure 3.13 Co-immunoprecipitation of GII.4 NO NS4 and other nonstructural proteins

(A) HA-NS1-2 of GII.4 NO was co-expressed with another N-terminally GFP tagged nonstructural protein of GII.4 NO in Huh7-T7 Lunet cells. After 24 hours of expression, cells were lysed and the cell lysates were subjected to HA immunoprecipitation and Western blot analysis. (B) Western Blot analysis of the HA immunoprecipitation was performed using an anti-HA and anti-GFP antibody. GFP co-expressed with HA-NS4 serves here as a negative control.

nonstructural proteins was investigated (56). HA-tagged NS4 of the GII.4 New Orleans strain was co-expressed with either GFP-tagged NS4, NS1-2, NS3 and GFP alone in Huh7-T7 Lunet cells. After 24 hours of transfection, cells were lysed and a HA IP was performed with subsequent Western Blot to detect potential interaction of partners with HA-NS4 (Figure 3.13A). As indicated by the Western Blot, HA-NS4 was able to bind GFP-NS4, GFP-NS1-2 and GFP-NS3, but not the negative control GFP alone (Figure 3.13B). In particular, the binding between NS4 and NS1-2 appeared to be strong and highly specific.

3.3.2 Self-interaction of NS4

To demonstrate whether NS4 can dimerize or even oligomerize, HA-NS4 of the New Orleans strain was co-expressed with one of the three domains of NO NS4 fused to GFP (Figure 3.14A). HA-IP and Western blot were performed to demonstrate interaction between the domains and full-length NS4. Although the interaction appeared and was only visible after overexposure, The large center alpha helix seems responsible for the self-interaction of NS4 (Figure 3.14B).

3.3.3 Molecular characterization of NS4 binding to NS1-2

To determine whether the amphipathicity of AH4 is important for the binding between

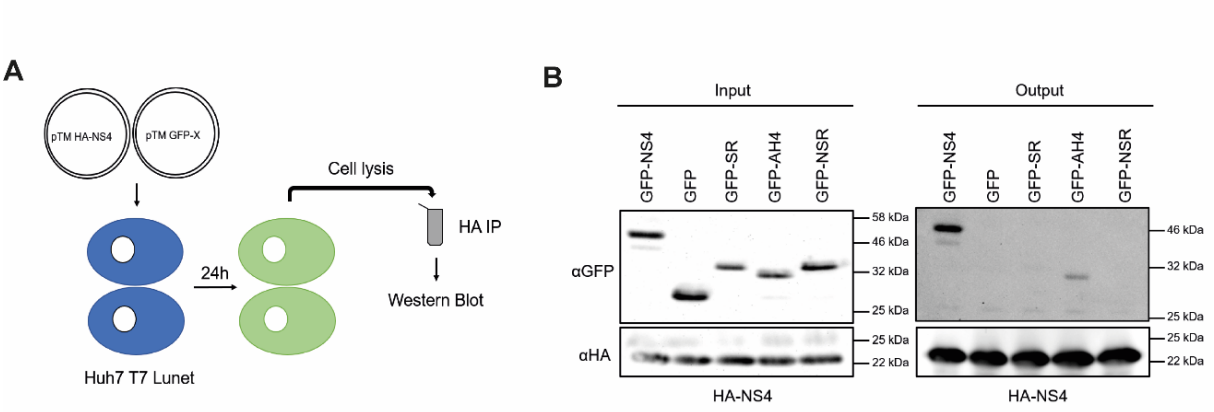

Figure 3.14 Self-interaction of GII.4 NO NS4 is facilitated by AH4

(A) HA-NS4 was co-expressed in Huh7-T7 Lunet cells with different domains of GII.4 NO NS4 with an N-terminal GFP tag. After 24 hours of expression, cells were lysed using a lysis buffer containing NP40 and the cell lysate was subjected to HA immunoprecipitation and subsequent Western blot analysis. (B) Western blot analysis of GII.4 NO NS4 and different domains of NS4. GFP-NS4 served as a positive control, whereas co-expression with GFP alone served as a negative control.

NS4 and NS1-2, HA-NS1-2 was expressed together with GFP fused to GII.4 NO NS4 or an amphipathic mutant (Figure 3.15A). Subsequently, HA-IP was performed to investigate the importance of the amphipathicity of AH4 for the binding between NS1-2 and NS4. Interestingly, all amphipathic mutants of GII.4 NO NS4 could bind to NS1-2, indicating that the amphipathicity and therefore membrane association of AH4 does not seem to impact the interaction between NS1-2 and NS4 (Figure 3.15B). To identify the NS4 domain responsible for the binding to NS1-2, HA-NS1-2 and GFP fused to NS4 or domains of both GII.4 NO and GV MNV-1.CW1 were expressed in Huh7-T7 Lunet cells (Figure 3.16A). Strikingly, for both GII.4 NO and GV MNV-1, only AH4 was capable of binding to NS1-2 (Figure 3.16B and 3.16C). Since the large center alpha helix is fifty amino acids long in GII.4 NO, a series of deletion mutations were generated to map the residues binding to NS1-2. Subsequent deletion series of 10 amino acids from the N-terminal part of NO AH4 (Δ1-10, Δ1-20, Δ1-30 and Δ1-40) and from the C-terminal part (Δ40-50, Δ30-50, Δ20-50 and Δ10-50) were constructed and GFP was fused to these small peptides and co-expressed with HA-NS1-2 in Huh7-T7 Lunet cells (Figure 3.17A). HA-IP and Western blot were performed to determine the binding capacity of these deletion mutants (Figure 3.17B). Strikingly, the first twenty amino acid residues of the AH4 in GII.4 NO could be deleted without severely disrupting the

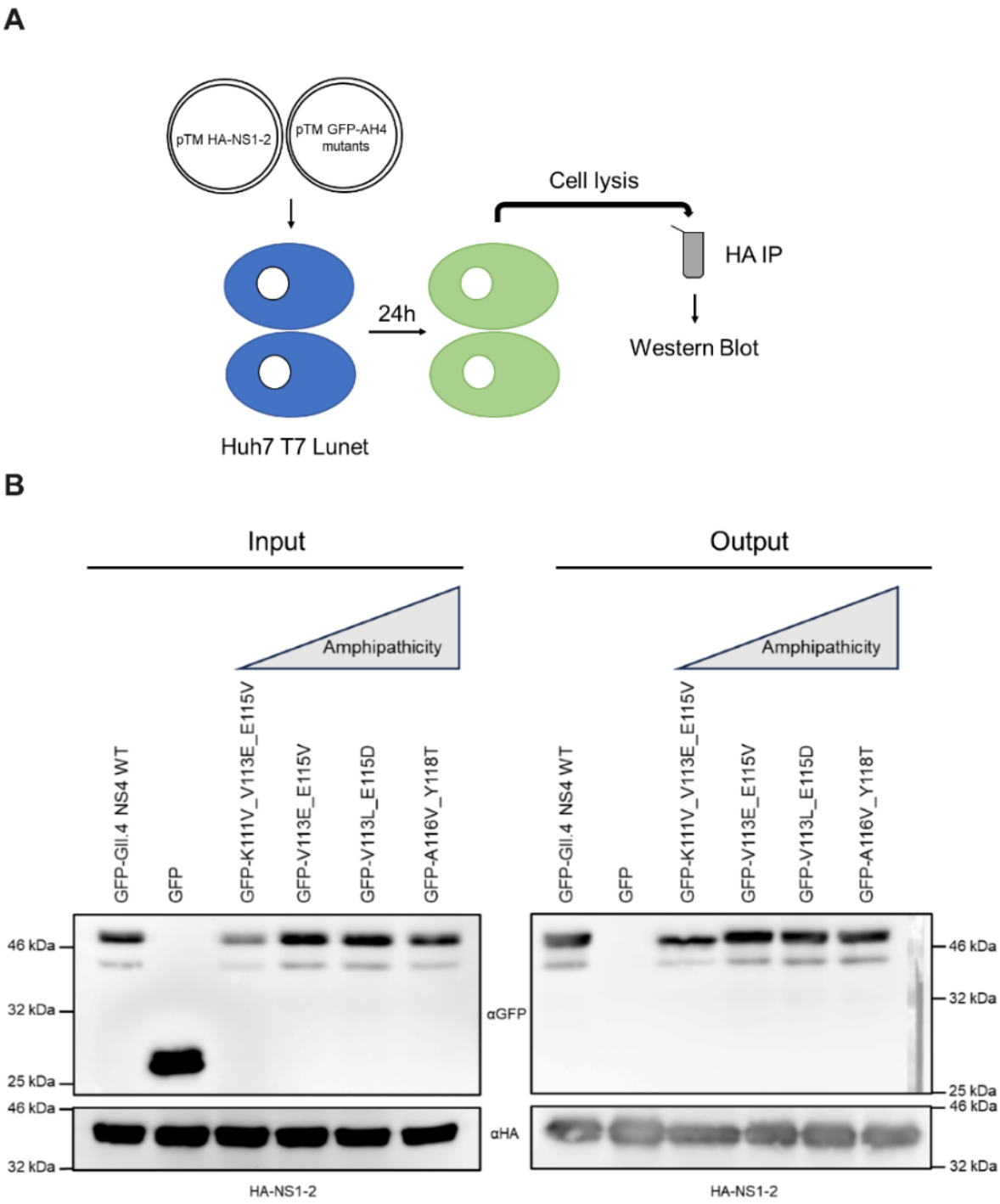

Figure 3.15 Amphipathicity of AH4 of GII.4 NS4 does not affect the binding to NS1-2

(A) HA-NS1-2 and GFP-NS4 or GFP fused N-terminally to an amphipathic mutant of NS4 were co-expressed in Huh7-T7 lunet cells. After 24 hours of transfection, the Huh7-T7 Lunet cells were lysed using a solution containing NP40 and HA IP was performed, followed by Western blot analysis. (B) Western blot analysis of the HA IP of NS1-2 and NS4 amphipathic mutants.

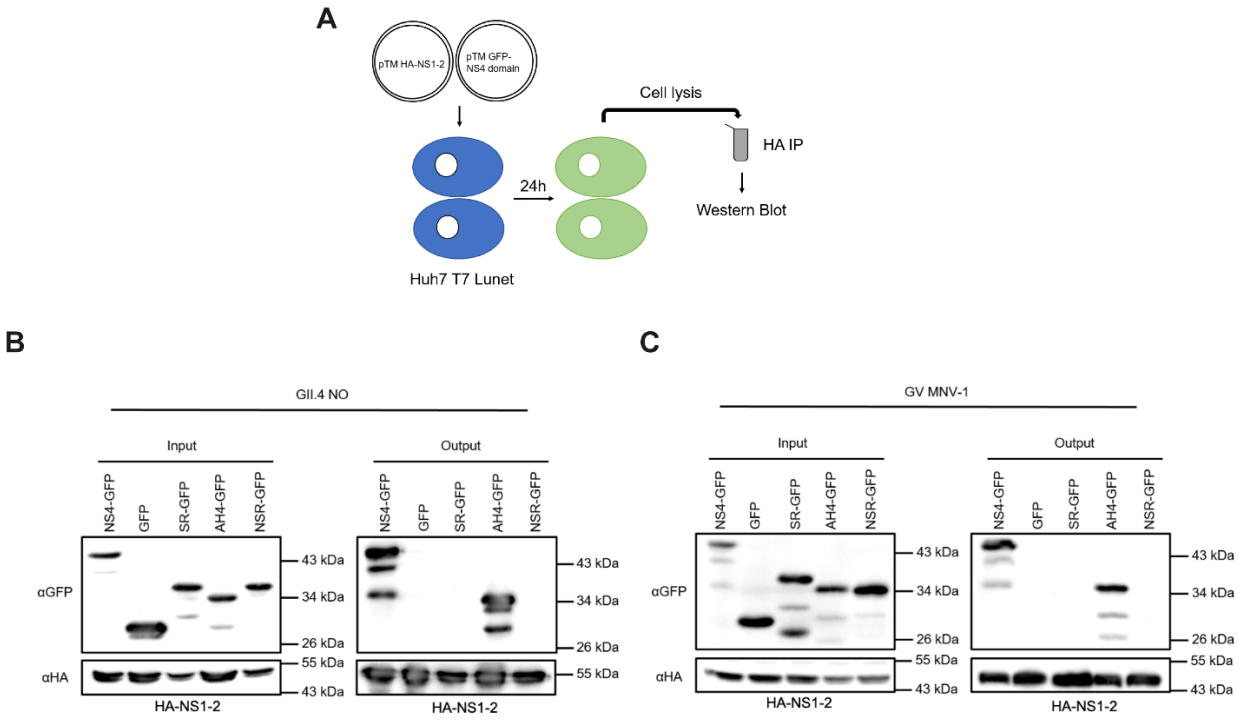

Figure 3.16 Interaction between norovirus NS1-2 and NS4 is mediated via the AH4 of NS4

(A) HA-NS1-2 and GFP-NS4 or GFP fused N-terminally to a domain of NS4 were co-expressed in Huh7-T7 lunet cells. After 24 hours of transfection, the Huh7-T7 Lunet cells were lysed using a solution containing NP40 and HA IP was performed, followed by Western blot analysis. (B) Western blot analysis of the HA IP of NS1-2 and domains of GII.4 New Orleans NS4 amphipathic mutants. (C) Western blot analysis of the HA IP of NS1-2 and domains of NS4 of GV MNV CW-1.

association to NS1-2. However, the C-terminal thirty amino acids seem crucial for binding to NS1-2 (Figure 3.17C). Furthermore, expression and IF of the deletion mutations in Huh7-T7 Lunet cells showed that the Δ1-10 construct was still able to accumulate lipid droplets in the perinuclear region, whereas the other constructs lost this phenotype (Figure 3.18). Notably, the Δ40-50 is not detectable in both the IP and the IF, suggesting that this construct might be unstable. In addition, although the Δ1-20 construct showed a more diffuse expression pattern than Δ1-10, membrane interaction might still be present for this construct.

To further identify important amino acid residues withing AH4 responsible for the binding to NS1-2, alanine scanning was performed of the Δ1-20. Alanine mutants were fused to GFP and co-expressed with HA-NS1-2 in Huh7-T7 Lunet cells. Western blot was performed to visualize the binding efficiency of the different alanine mutants. Of

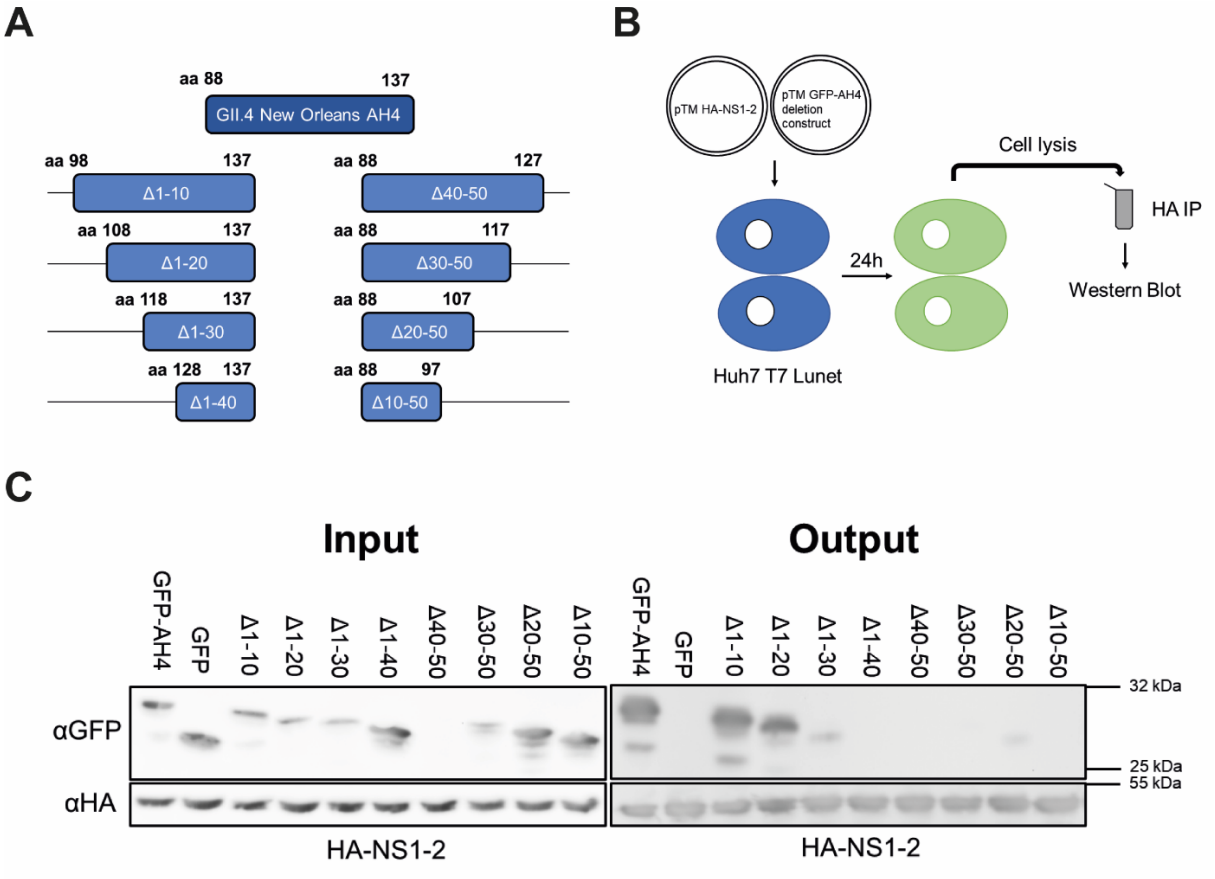

Figure 3.17 Deletion analysis of AH4 of GII.4 NO NS4

(A) Deletion constructs of GII.4 New Orleans NS4 AH4 were constructed and N-terminally tagged with GFP for further analaysis. (B) HA-NS1-2 and the deletion constructs of GFP-AH4 of GII.4 NO NS4 were expressed in Huh7-T7 Lunet cells for 24 hours and subsequently lysed using NP-40, followed by an HA-IP and Western blot analysis. (C) Western blot analysis of the HA-IP of several deletion constructs. GFP was fused N-terminally to multiple deletion constructs of AH4 of GII.4 NO NS4. AH4 is fifty residues in length and, thus, four N-terminal deletion constructs and four C-terminal deletion mutants were made with each mutant deleting ten additional residues.

note, the amino acid nomenclature of the full-length GII.4 NO NS4 protein was used for these Δ1-20 mutants to enable consistent comparison (Figure 3.19A). From the Western blots, five mutants of the Δ1-20 construct (F128A, V129A, R132A, I133A and R136A) seemed to reduce binding of this construct to NS1-2. These five amino acid residues might therefore contribute to the binding NS4 to NS1-2 (Figure 3.19B). Interestingly, many of these five residues show a degree of conservation among the different norovirus genogroups (Figure 3.20A). In addition, all of these residues are in close proximity when regarding the helical structure of AH4 (Figure 3.20B). In particular, the two arginine residues at position 132 and 136 are conserved in many

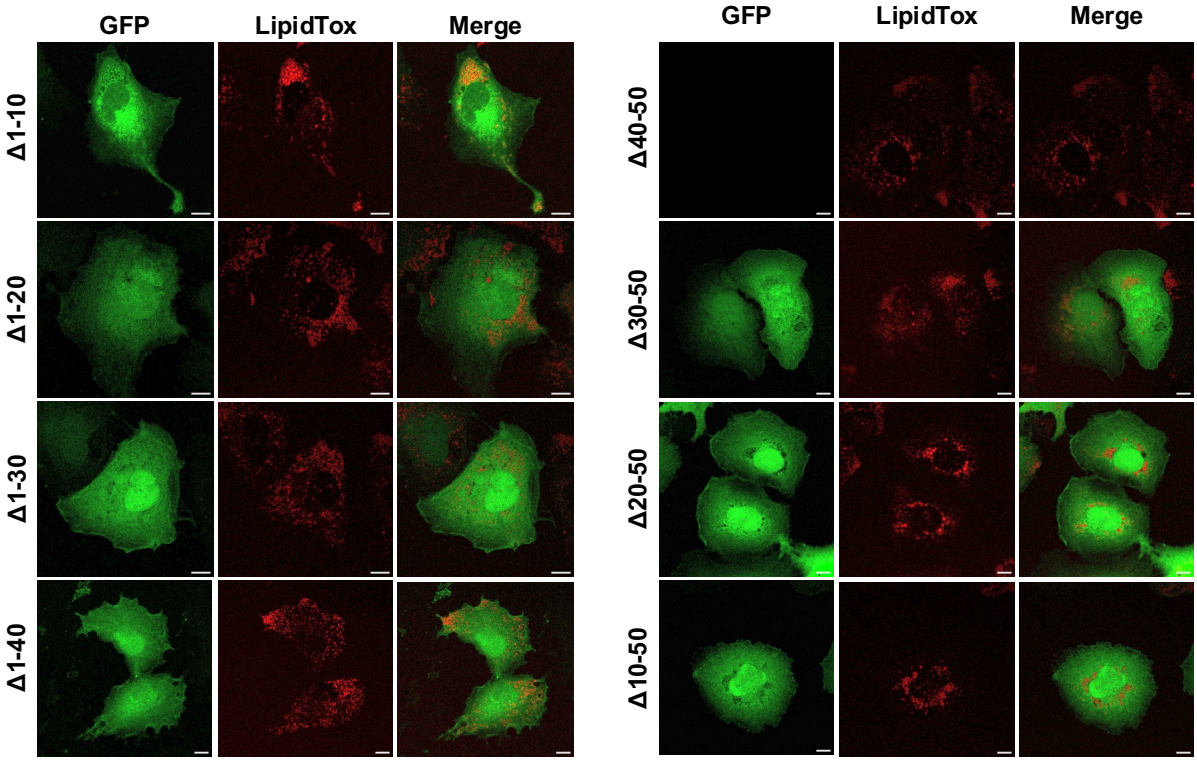

Figure 3.18 Expression of deletion mutants of GII.4 AH4

Deletion constructs of GII.4 New Orleans NS4 AH4 were constructed and N-terminally tagged with GFP and expressed in Huh7-T7 Lunet cells for IF analysis. Delta 1-10 showed a wildtype phenotype, whereas the other deletion mutations appeared to be reduced in membrane localization. Expression of delta 40-50 was not detectable, corresponding with the Western blot data.

genogroups and are almost juxtaposed in the helical conformation of AH4. To test the impact of multiple mutations on the binding capacity of Δ1-20, combinations of mutations were generated and co-expressed with HA-NS1- 2 in Huh7-T7 Lunet cells as described before. HA IP and Western blot analysis revealed that a combination of mutations reduced the binding capacity of Δ1-20 even further (Figure 3.20C). Of note, the R132ER136E mutation, resulting in a negative charge change, almost obliterated the binding to NS1-2. Interestingly, the R132KR136K mutation, resulting in conservation of positive charge, did not rescue binding to NS1-2, indicating that the arginine residues at these positions might be important both in structure and charge for the binding to NS1-2. In order to confirm these findings, immunofluorescence was performed to visualize colocalization between the wildtype Δ1-20 construct and mutants upon co-expression with mCherry-NS1-2 in Huh7-T7 Lunet cells (Figure 3.21A). As has been shown previously, GFP-NS4 shows a perinuclear pattern, whereas GFP- Δ1-20 displays a more diffuse localization pattern. In addition, mCherry-

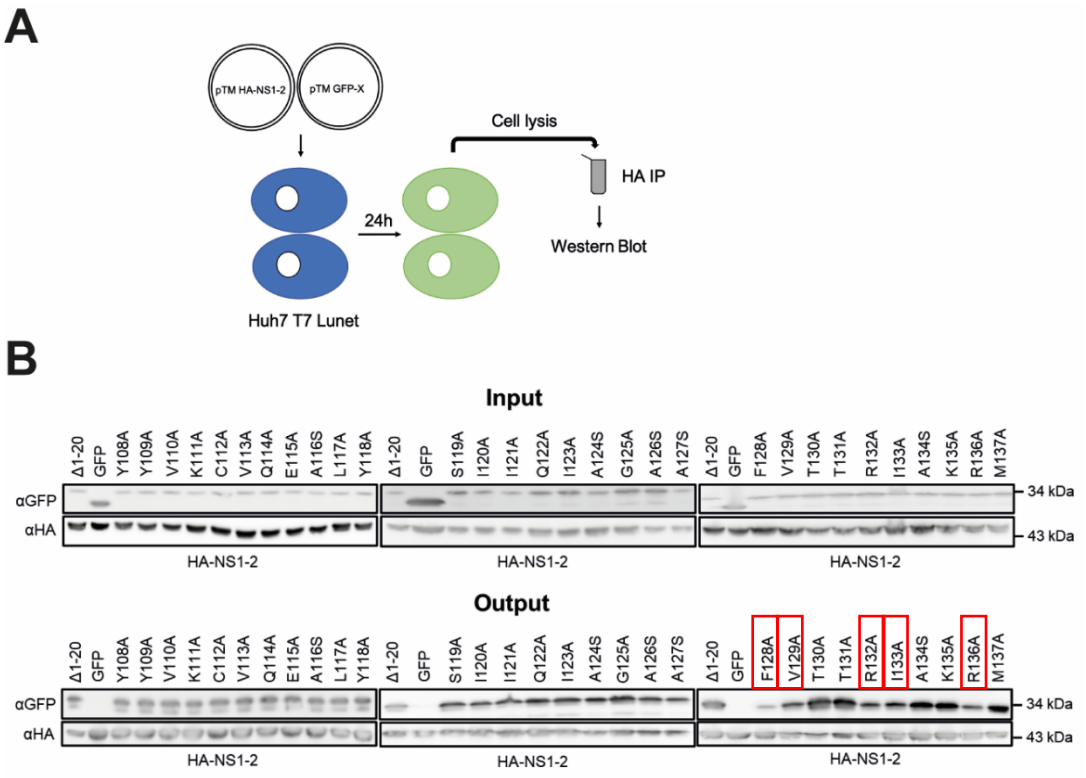

Figure 3.19 Alanine scanning of Δ1-20 of AH4 identifies five residues responsible for binding to NS1-2

(A) HA-NS1-2 and different GFP-tagged alanine mutants of Δ1-20 of AH4 of GII.4 NO NS4 were co-expressed in Huh7-T7 Lunet cells for 24 hours, followed by cell lysis using NP40 and a subsequent HA IP and Western blot analysis. (B) Western blot analysis of the alanine scanning of Δ1-20 of AH4. Five residues were identified as potentially involved in the binding with NS1-2 (red boxes).

NS1-2 showed a localization pattern that was very reminiscent of ER localization (Figure 3.21B). Co-expression of both mCherry-NS1-2 and GFP showed little colocalization, whereas co-expression with GFP-NS4 and GFP-Δ1-20 did demonstrate colocalization (Figure 3.21C). Interestingly, co-expression with loss-of-binding mutants GFP-R132AR136A or GFP-F128AV129AI133A showed a significantly smaller degree of colocalization, suggesting that mutation of these residues might impair the interaction with NS1-2 (Figure 3.21D).

3.3.4 Molecular characterization of NS1-2 binding to NS4

Since NS4 is capable of binding to NS1-2 in a highly specific manner, specific domains and residues in NS1-2 might facilitate this binding. Mapping of four of the five identified

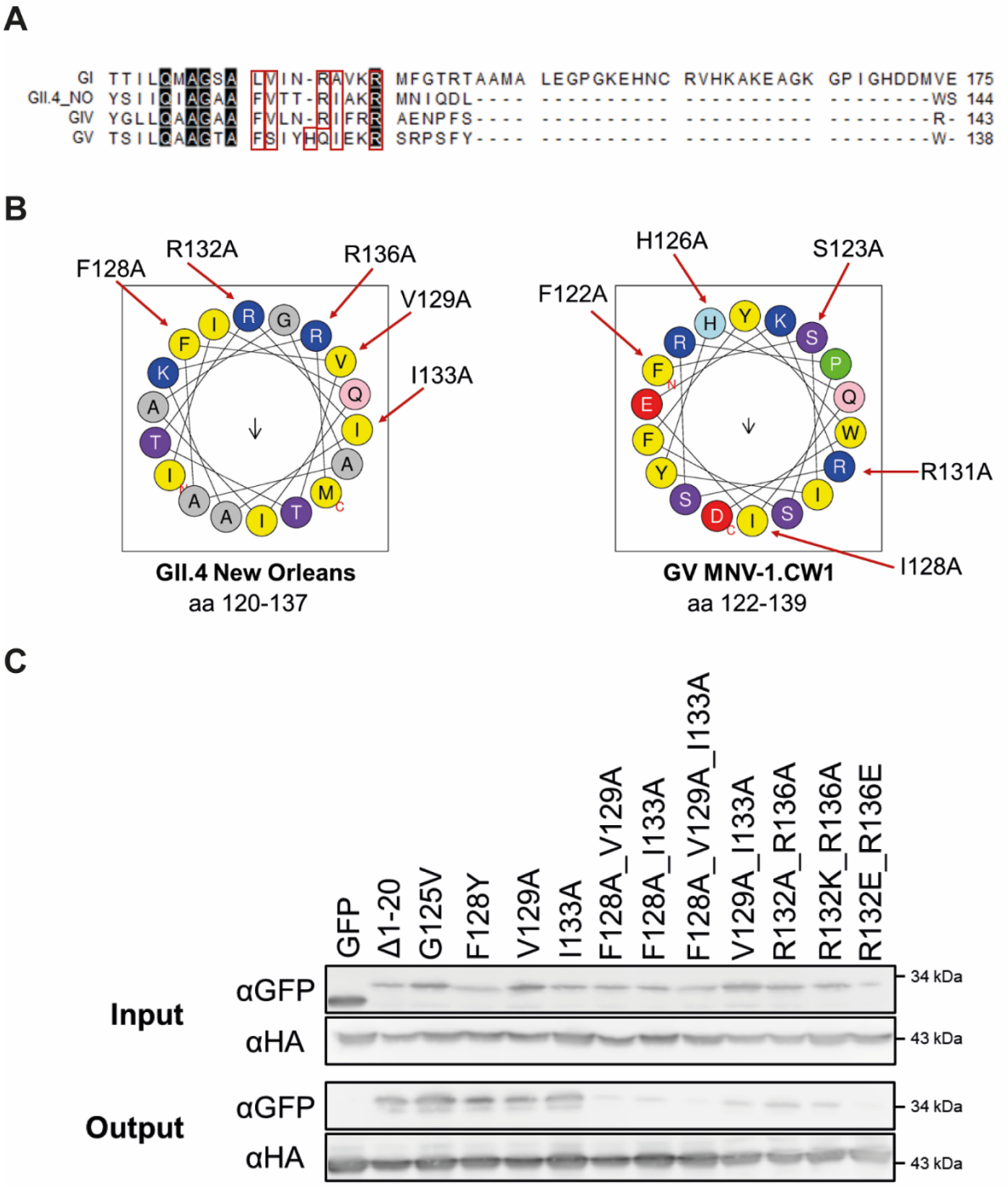

Figure 3.20 Combined mutation of multiple GII.4 NS4 binding residues disrupt the interaction between NS1-2 and NS4

(A) Five residues within GII.4 NS4 were identified as potentially facilitating the binding to NS1-2 (red boxes). Many of these residues were conserved on charge or hydrophobicity. Black background indicates full conservation at this site. (B) Potential binding residues shown on the helical wheel of GII.4 New Orleans and GV MNV-1.CW1 AH4 as depicted by HeliQuest. (C) HA-NS1-2 and GFP-tagged mutants of Δ1-20 of AH4 of GII.4 NO NS4 were co-expressed in Huh7-T7 Lunet cells, followed by cell lysis and a subsequent HA IP and Western blot analysis. Combining mutations of the potential binding residues greatly impaired the interaction between NS1-2 and NS4.

binding residues in NS4 reveal that these residues are in close proximity in AH4 (Figure 3.22A). Furthermore, AlphaFold modeling of NS1-2 and NS4 with subsequent *in silico* docking of the two proteins reveals that the NS1-2 domain ranging from amino acid 276 to 308 might be the minimal required domain to facilitate binding to NS4 (Figure 3.22B). DNA constructs encoding GFP fused to this region or even smaller regions were co-expressed with NO HA-NS4 in Huh7-T7 Lunet cells. Subsequent HA IP and Western blot were performed to confirm the binding of this domain to NS4 (Figure

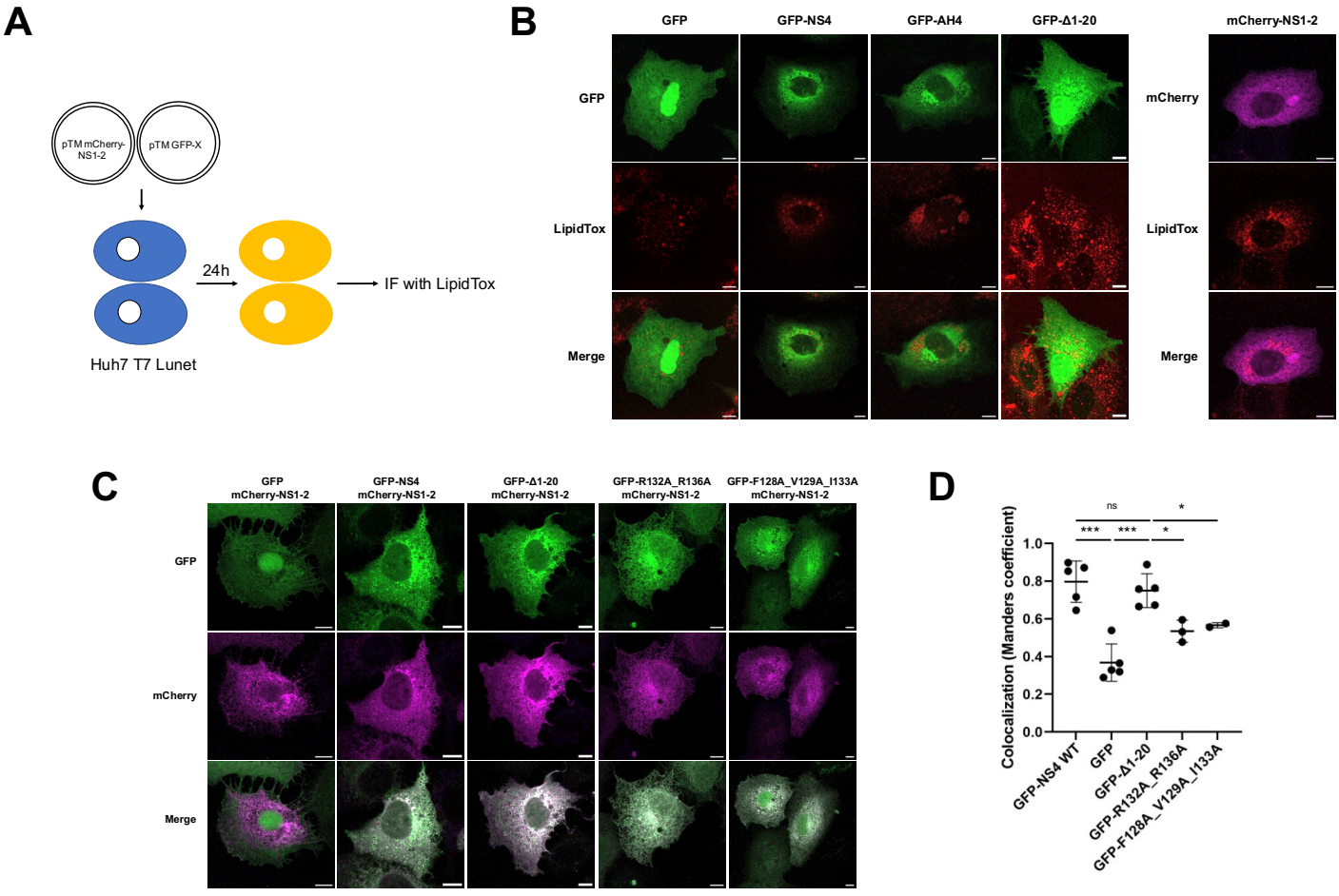

Figure 3.21 Co-expression of NS1-2 and Δ1-20 of AH4 show high colocalization

(A) mCherry-NS1-2 and different GFP-fusion proteins were co-expressed in Huh7-T7 Lunet cells and fixed for immunofluorescence microscopy after 24 hours of transfection. LipidTox was used to visualize lipid droplet localization. (B) Sole expression of GFP, GFP-NS4, GFP-Δ1-20 and mCherry-NS1-2 in Huh7-T7 Lunet cells. (C) Co-expression of mCherry-NS1-2 with either GFP, GFP-GII.4 NS4, GFP-Δ1-20, GFP-R45AR49A or GFP-F41AV42AI46A in Huh7-T7 Lunet cells was visualized using fluorescence microscopy to image colocalization of NS1-2 and the different GFP-tagged constructs. (D) Quantification of the colocalization between the fusion proteins and NS1-2 using the Manders coefficient, which measures the percentage of GFP signal that overlaps with the mCherry signal. *** $p<0.001$, * $p<0.05$. Scale bars represent ten micrometer.

3.22C). In line with the AlphaFold model, all constructs containing at least amino acids 277 to 313 of NS1-2 were able to bind efficiently to NS4. In addition, the domain of amino acid 290 to 326 was also capable of associating to NS4, although this association seems to be weaker than the domain ranging from residues 277 to 313 (Figure 3.22D).

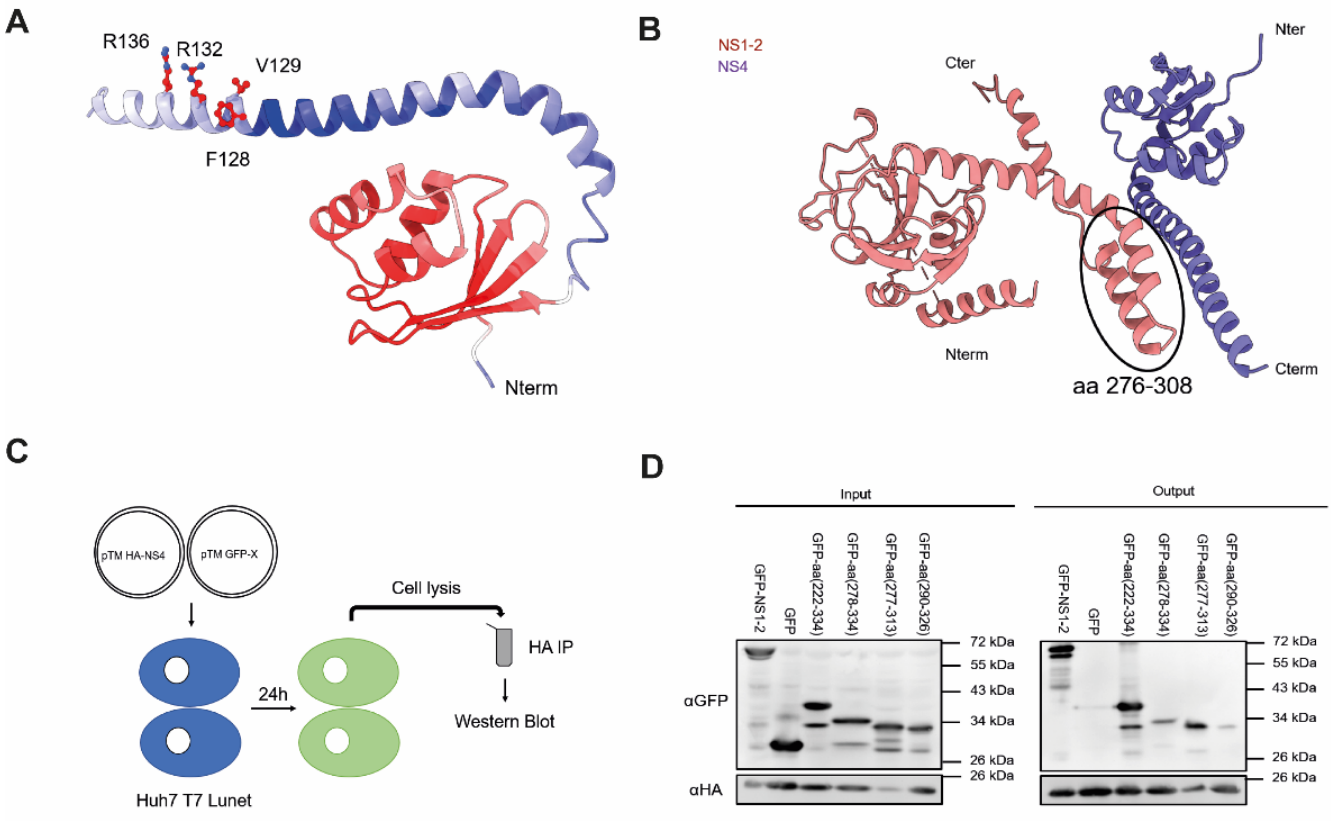

Figure 3.22 Identification of the NS4-associating domain of NS1-2

(A) Modeling of the N-terminal SR (red) and AH4 (blue) of GII.4 NO NS4 in AlphaFold. Binding partners to NS1-2 are indicated with the residue position within full-length NS4. Work performed by the Bressanelli group. (B) Docking of the AlphaFold models of NS1-2 (red) and NS4 (blue) using HADDOCK. Indicated binding domain of NS1-2 is encircled. Work performed by the Bressanelli group. (C) HA-NS4 of GII.4 NO and NS1-2 or different domains of NS1-2 with a N-terminal GFP tag were expressed in Huh7-T7 Lunet cells for 24 hours, followed by cell lysis and a HA IP and Western blot analysis. (D) Western blot analysis of the HA IP of HA-NS4 and different domains of NS1-2.

Closer examination of the interaction between NS1-2 and NS4 using AlphaFold2 proposed a very specific interaction, where C-terminal part of AH4 of NS4 interacts with residues 276 to 308 of NS1-2 and the N-terminal part of AH4 interacts with the very C-terminus of NS1-2. In addition, the C-terminus of NS1-2 might even interact with the structural region of NS4 (Figure 3.23A). Consequently, this model proposes a sandwich-like enwrapping of NS4 by NS1-2, tethering the proteins strongly to one

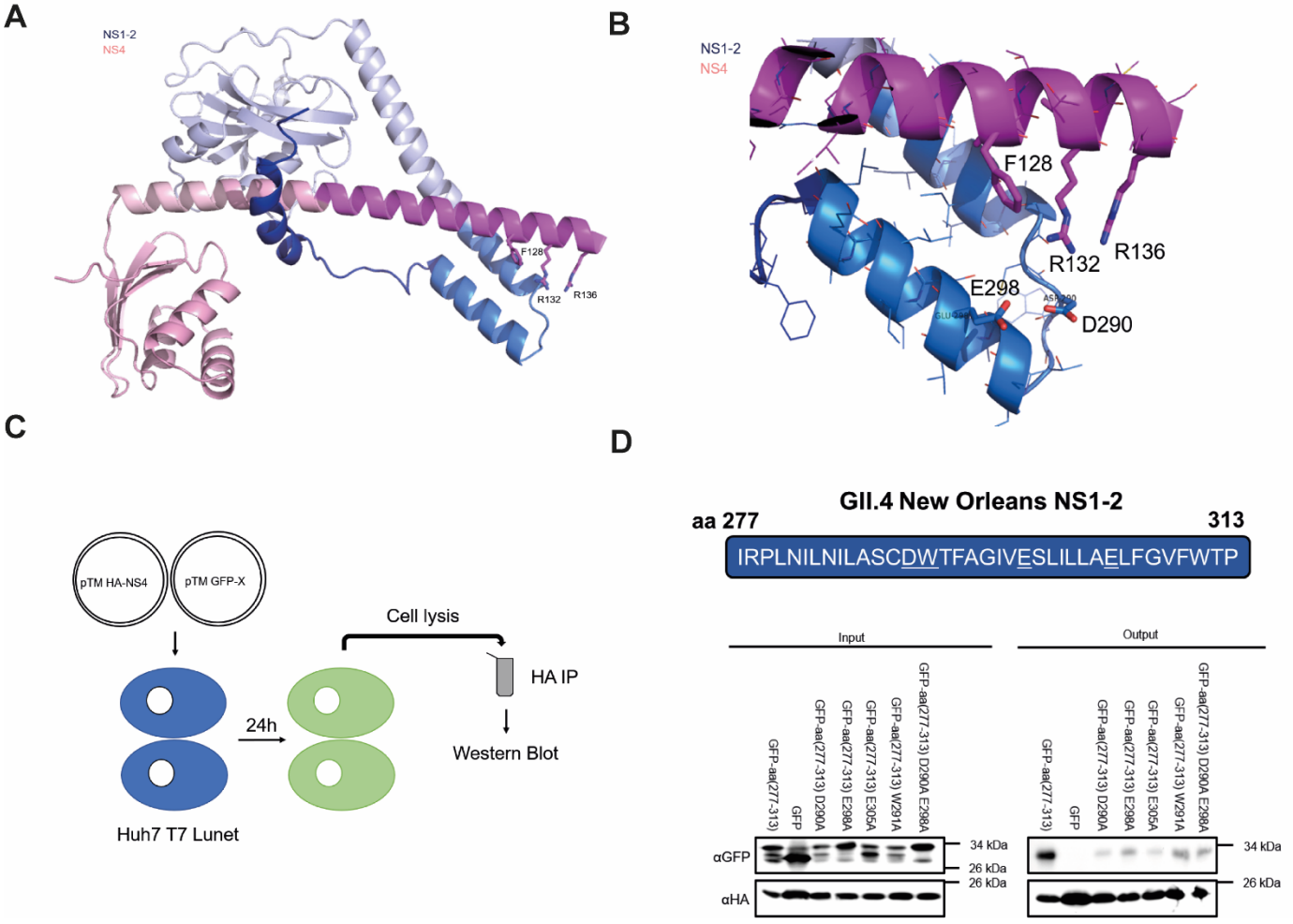

Figure 3.23 Identification of NS4-binding residues within NS1-2

(A) Co-modeling of NS1-2 and NS4 in AlphaFold2. Work performed by the Bressanelli group. (B) Potential binding partners within NS1-2 (E298 and D290) after co-modeling of NS1-2 and NS4. Modeling performed by the Bressanelli group. (C) HA-NS4 of GII.4 NO was co-expressed in Huh7-T7 Lunet cells with a constructing of GFP fused to residues 277 to 313 of NS1-2. Guided mutation of potential binding sites within this domain NS1-2 domain were also co-expressed with HA-NS4 to demonstrate the effect on binding efficiency. After 24 hours of transfection, the cells were lysed using NP40 and a HA IP and subsequent Western blot analysis were performed. (D) Western blot analysis of the HA IP with HA-NS4 and GFP fused to the NS4-associating domain of NS1-2 (minimal binding domain of NS1-2) and mutants thereof.

another. Closer inspection of this AlphaFold2 model indicates potential interaction partners to the two arginine residues of AH4 of NS4, with the highest probability being D290 and E298 (Figure 3.23B).

To test whether these specific residues in NS1-2 are responsible for binding to NS4, residues 277-313 of NS1-2 were fused to GFP and co-expressed with HA-NS4 in Huh7-T7 Lunet cells. Subsequent HA IP and Western blot were performed to visualize binding efficiency (Figure 3.23C). Although with varying efficiency, the residues D290, W291, E298 and E305 seem to decrease binding efficiency (Figure 3.23D). In addition, a combination of the mutation D290A and E298A seems to reduce binding to NS4 substantially, indicating that these two amino acid residues might indeed play an important role in binding to AH4 of NS4, potentially to R132 and R136 in GII.4 NO NS4.

3.3.5 Binding of NS1-2 and NS4 during viral replication

To verify whether NS1-2 and NS4 show binding during viral replication, a full-genome of GV MNV-1 was cloned in a pSP73 plasmid under influence of a minimal CMV promoter. An HA-tag was inserted in NS1-2 and a FLAG-tag was inserted in NS4 in sites that were shown acceptable in previous publications (Figure 3.24A) (258). After transfection of this construct in HEK 293T cells, obtained virus was passaged three times in BV-2 cells to obtain a viable virus with the two tags (Figure 3.24B). The passage 3 virus was used to infect BV-2 cells and 72 hours after infection, HA and FLAG IP were performed (Figure 3.24C). Strikingly, HA-tagged NS1-2 was able to bind efficiently to FLAG-tagged NS4, which was confirmed in both the HA IP Western blot and the FLAG IP Western blot, whereas the negative control GAPDH was not pulled out (Figure 3.24D). Therefore, the double-tagged MNV virus seems to be not only viable after three passage, but retains both tags and show a interaction between NS1-2 and NS4 as shown previously for individually expressed NS1-2 and NS4 of GII.4 NO and GV MNV-1.CW1 norovirus.

Since five amino acids in AH4 of GII.4 NO NS4 might be responsible for binding to NS1-2 as shown previously, mutation of these residues in MNV-1.CW1 might abolish the binding of NS1-2 to NS4 (Figure 3.25A). The combination of H126A and R131A

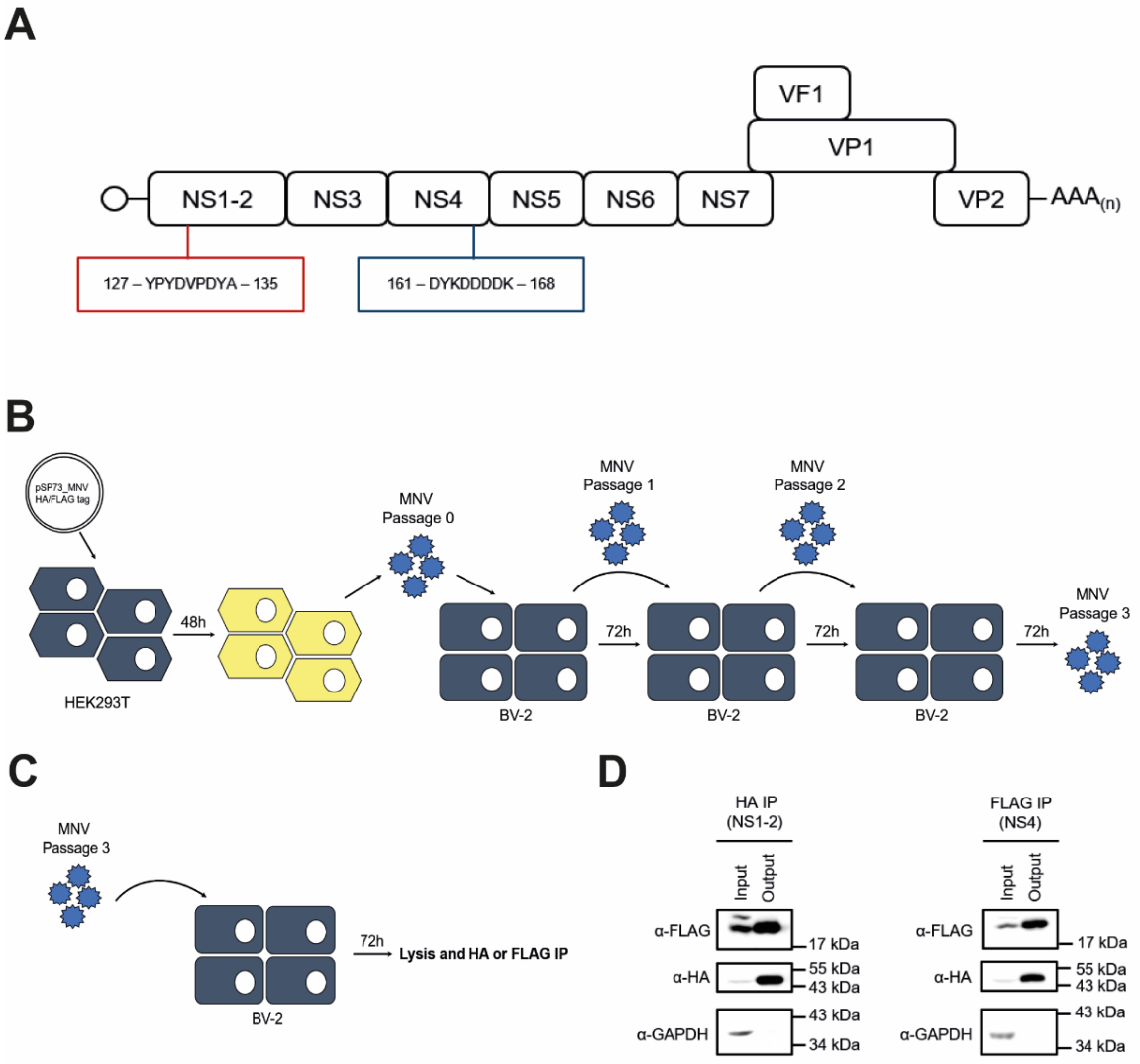

Figure 3.24 NS1-2 and NS4 bind strongly during replication of GV MNV CW-1

(A) Schematic overview of the GV MNV CW-1 genome and the introduction sites for the HA-tag (red box) and the FLAG-tag (blue box). (B) A pSP73 plasmid containing the double tagged MNV genome under the transcriptional control of a minimal CMV promotor was transfected into HEK 293T cells. After 48 hours, supernatant was harvested (passage 0) and passaged three times in murine BV-2 cells to obtain replication-competent double tagged MNV. (C) Passage 3 of the double tagged MNV was used to infected another round of BV-2 cells, which were infected for 72 hours and subsequently lysed and subjected to HA-IP and FLAG-IP and Western blot analysis to confirm the presence of the tags and the binding of NS1-2 and NS4 during replication. (D) Western blot analysis of the HA-IP and FLAG-IP of double-tagged MNV.

was introduced in the MNV context to resemble R132A_R136A in GII.4 NO NS4 and the combination of F122A, S123A and I128A was introduced to resemble F128A_V129A_I133A in GII.4 NO NS4. These sets of mutations were generated in

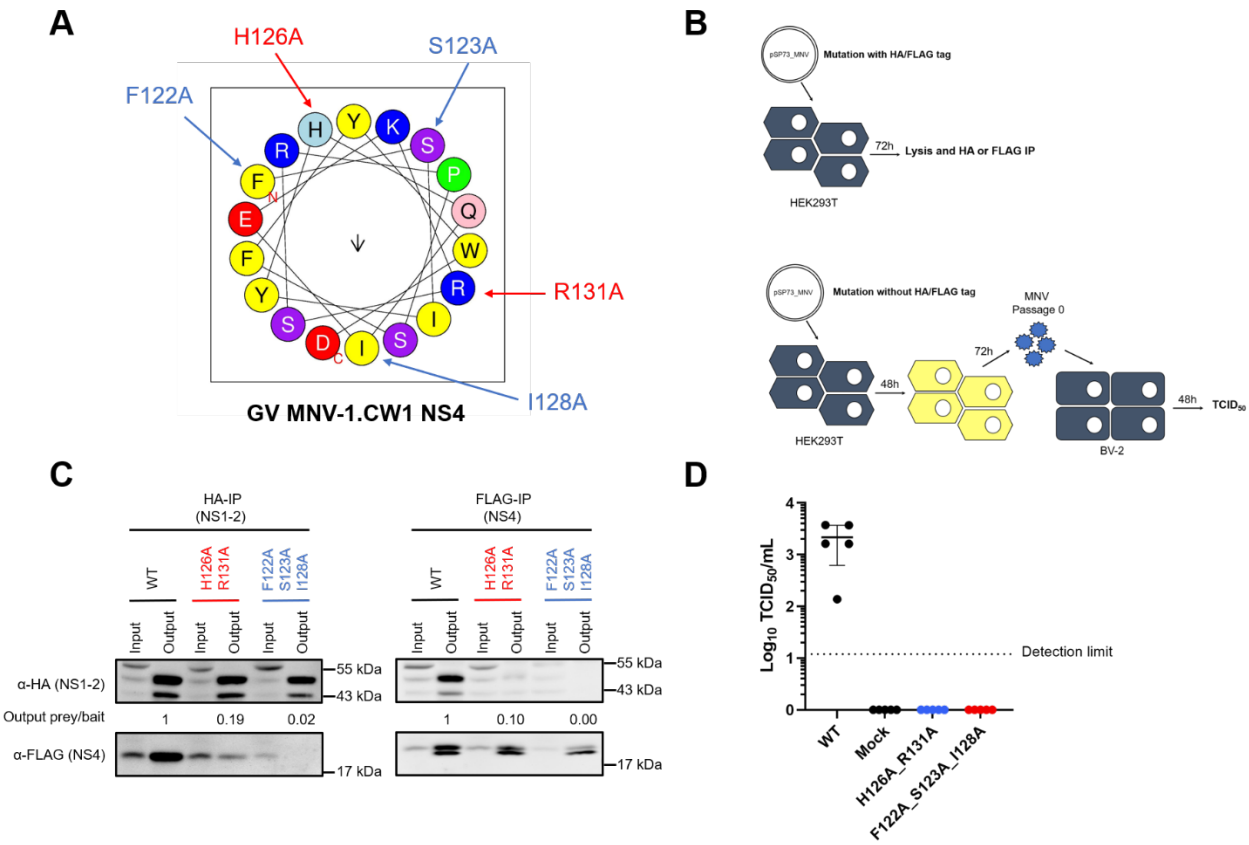

Figure 3.25 Disruption of NS4 binding to NS1-2 abolishes MNV replication

(A) Two sets of alanine scanning mutations were introduced in MNV (set AA with blue and set AAA with red arrows) using the five binding residues of AH4 of GII.4 NO NS4 for guidance of the mutations. (B) Double-tagged mutants were transfected into HEK 293T cells and incubated for 72 hours, followed by cell lysis and HA-IP and FLAG-IP. Western blot analysis was then performed to determine the binding efficiency of these mutants. Untagged mutants were used in a $TCID_{50}$ assay to determine the replication-competence of MNV after mutation. (C) Western blot analysis of the double-tagged MNV mutants and (D) $TCID_{50}$ of the untagged MNV mutants.

either the HA and FLAG-tagged MNV backbone for subsequent HA and FLAG IP to determine the binding efficiency or introduced in an untagged MNV backbone for $TCID_{50}$ analysis to investigate the viability of these binding mutants (Figure 3.25B).

HA and FLAG IP of these sets of mutations confirmed that both sets of mutations greatly impaired binding of NS1-2 to NS4 (Figure 3.25C), whereas wildtype MNV did show significant interaction between the two viral proteins. In addition, both sets of mutations were completely replication-deficient in the $TCID_{50}$ assay, indicating that the binding between NS1-2 and NS4 seems crucial for viral replication in this experimental setting (Figure 3.25D).

In addition to the amino acid sites in NS4, the residues within NS1-2 involved in the interaction between NS1-2 and NS4 were mutated in the context of MNV-1.CW1 as well (Figure 3.26A). The MNV site D301A represents GII.4 NO D290, whereas the MNV N309 site represents GII.3 NO E298. Both mutants and a combination mutant, D301A_N309A, were expressed in the HA and FLAG-tagged MNV construct and the MNV constructs without tags to demonstrate potential loss-of-binding and the effect on viral replication (Figure 3.26B). Interestingly, the D301A, N309A and the combination mutant all showed reduced binding between NS1-2 and NS4 in the HA IP, but this reduction was not clearly present in the FLAG IP (Figure 3.26C). Moreover, the single mutants and in particular the double mutant show less NS1-2 and NS4 present in the samples, indicating that these mutations might destabilize the polyprotein. Still, all mutants were replication-deficient (Figure 3.26D).

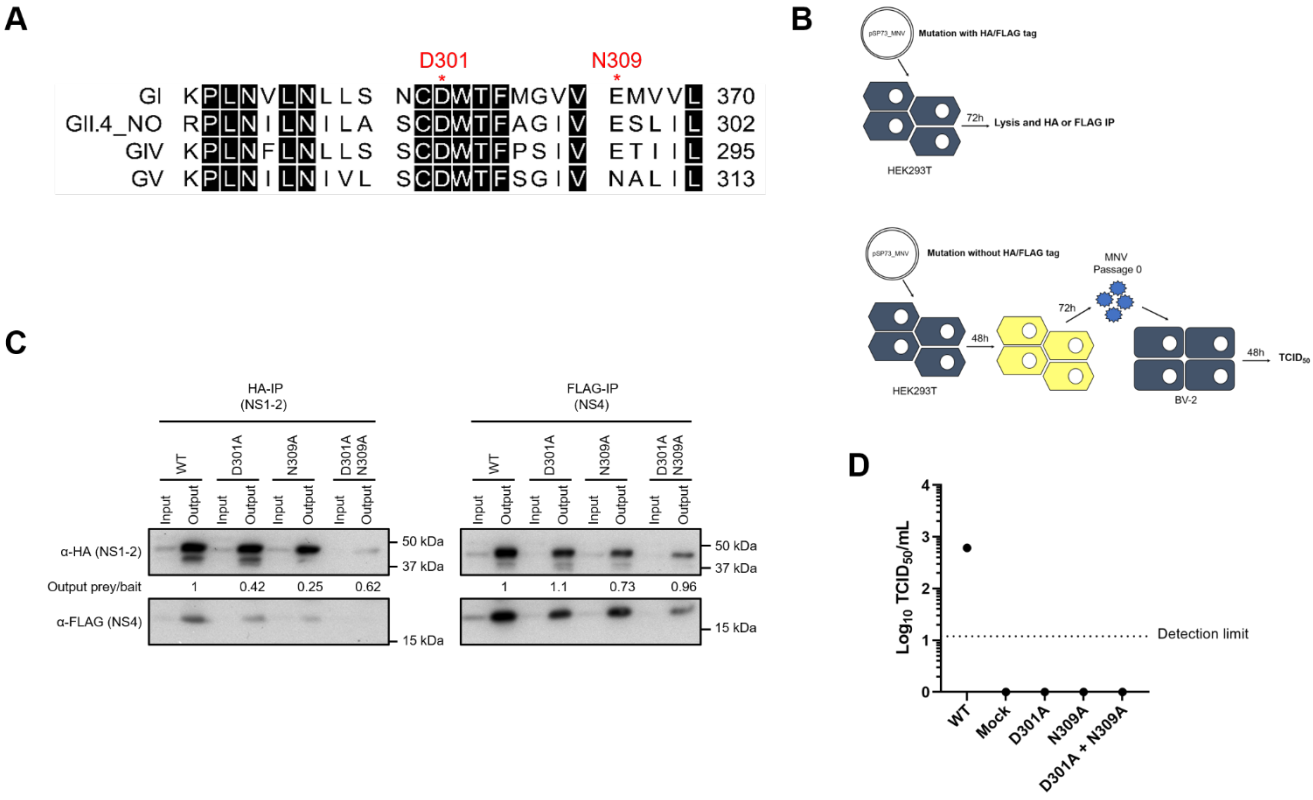

Figure 3.26 NS1-2 mutation in the MNV context and the effect on NS4 binding and viral replication
(A) Two point mutants and a combination mutant were generated in MNV-1.CW1 using the two main binding residues of GII.4 NO NS1-2 for guidance of the mutations. (B) Double-tagged mutants were transfected into HEK 293T cells and incubated for 72 hours, followed by cell lysis and HA-IP and FLAG-IP. Western blot analysis was then performed to determine the binding efficiency of these mutants. Untagged mutants were used in a $TCID_{50}$ assay to determine the replication-competence of MNV after mutation. (C) Western blot analysis of the double-tagged MNV mutants and (D) $TCID_{50}$ of the untagged MNV mutants.

In conclusion, NS4 interacts with NS1-2 and NS3 upon co-expression and forms homodimers upon sole expression of NS4. In particular, the interaction between NS1-2 and NS4 appears highly specific. Further mapping reveals AH4 of NS4 as the domain responsible for the interaction with NS1-2, although amphipathicity of AH4 appears to play no role in this interaction. Mapping of the interacting residues in NS4 identifies five amino acids responsible for this interaction. In addition, NS1-2 and NS4 strongly interact in replication-competent MNV and abrogation of the binding between NS1-2 and NS4 by means of mutation in MNV abolishes replication. Finally, the binding domain of NS1-2 was identified in the C-terminal hydrophobic region of NS1-2. Mutations of potential binding residues in this site diminished the interaction between NS1-2 and NS4 in GII.4, NO and possibly also in MNV, although these mutations seemed to potentially destabilize the polyprotein.

Chapter 4

Discussion

"*We must consider it, however, in the light not only of our conclusion and our premises, but also of what is commonly said about it; for with a true view all the data harmonize, but with a false one the facts soon clash.*"

— Aristotle (384-322 BCE), *Nicomachean Ethics*

---

4 Discussion

In this thesis, the role of norovirus nonstructural protein 4 in the viral life cycle is examined. First, the homology of NS4 among different norovirus genogroups was determined and the importance of conserved residues for viral replication was assessed by alanine scanning of MNV NS4. Second, the NS4 itself was molecularly characterized using various assays to determine the subcellar localization of NS4 and to examine the membrane-associating properties of NS4. Third, the interaction between norovirus NS4 and NS1-2 was explored for the first time and specific residues within GII.4 New Orleans NS4 and NS1-2 were found to facilitate this interaction, which was crucial for viral replication.

4.1 Conservation of NS4

4.1.1 Secondary structure prediction, amino acid alignment and homology

In order to obtain a prediction of the secondary structure of NS4, a PSIPRED analysis was performed on NS4 of GII.4 NO as well as GV MNV-1.CW1. In addition, since human noroviruses can belong to many different genogroups and genotypes, I performed an amino acid alignment on NS4 consensus sequences of GI, GII, GIV, GV (MNV-1.CW1) and GII.4 (New Orleans). Although other genogroups can infect humans as well, such as GVIII and GIX, the selected genogroups contain the most important pathogenic human noroviruses (30,259,260). GV MNV-1.CW1 was included in this analysis to allow for alanine scanning in a reverse genetics cell culture model available for this strain. The former pandemic strain GII.4 New Orleans was included as a prototype GII.4 norovirus, since plasmids encoding nonstructural proteins of this strain were readily available, allowing for mutagenesis in GII.4 NO NS4.

The PSIPRED secondary structure prediction indicated a large alpha helix (AH4) in the center of NS4. This indication is in line with previous studies predicting an alpha helix within the NS4 protein of various human noroviruses and MNV, roughly corresponding with the predicted membrane association domain of norovirus NS4 (83,249). Therefore, the results of this thesis indicating that AH4 is responsible for membrane

association of NS4 fit well with the *in silico* predictions. Furthermore, an alpha helix as membrane association domain would match with the general description of NS4 as a '3A-like protein' in the literature, since the enterovirus protein 3A contains an important alpha-helical membrane association domain as well (261,262). Interestingly, although the amino acid alignment indicated low homology of NS4 among different genogroups, almost half of all conserved residues were found within AH4. This emphasizes the importance of AH4 for the function of NS4 in the viral life cycle.

4.1.2 Alanine scanning of conserved residues in NS4

The amino acid alignment indicated seventeen conserved amino acid residues among the selected genogroups. One of the conserved residues was the last amino acid in the NS4 protein of all genogroups. This glutamic acid residue is crucial for proper polyprotein cleavage of NS4-NS5 and mutagenesis at this site results in altered proteolytic cleavage of the ORF1 polyprotein (181,182,263). The mutational flexibility of the other sixteen conserved amino acids is unknown and these residues were therefore subjected to alanine scanning in the MNV-1.CW1 reverse genetics system. The conserved amino acid residues intolerable for mutagenesis were mostly clustered in two regions. First, single mutation of three residues in the N-terminal region of NS4 (F6A, D7A, F14A) seems to render MNV replication-deficient. Second, multiple conserved residues within the heart of AH4 are intolerable to mutagenesis as well, most notably Q116A, A118S and A121S. Although functional assays for NS4 do not exist, EM analysis of cells expressing these single mutants could assess the effect of these mutations on membrane rearrangements. To this end, I tried to express both individual NS4 mutants and NS4 mutants in the context of the ORF1 polyprotein in Huh7-T7 Lunet cells and subject those cells to IF and EM analysis (data not shown). Unfortunately, there were no striking differences observed between the single mutants in both NS4 alone or the ORF1 polyprotein, suggesting that single mutation alone might not be sufficient to break the membrane-rearranging properties of NS4, even though these single mutants are replication-deficient in $TCID_{50}$. Still, combinations of mutations could be tried in both NS4 alone and the ORF1 polyprotein context to assess the importances of these amino acid residues for the function of NS4. Since deletion of AH4 from the ORF1 polyprotein does not seem to drastically impact membrane rearrangements, these combinations of mutations might have a more detectable

phenotype when introduced in NS4 alone, in which the amphipathic mutant V113E_E115V displays a prominent phenotype on membrane association as well.

4.2 Biochemical characterization of NS4

4.2.1 AH4 of NS4 facilitates membrane association

Previous studies have indicated that NS4 behaves as a membrane-associated protein and colocalizes with molecular markers of ER, Golgi and lipid droplets (56,66,67,79,80,83,249). Despite this well-described membranous localization, it remained poorly understood which domain of NS4 facilitates this localization and how this localization is established. In correspondence with the secondary structure prediction, experiments in this thesis show that fusion of GII.4 AH4 to GFP seems to be sufficient to mimic the wild-type membranous localization of NS4. Furthermore, in spite of low homology on the amino acid level, AH4 of MNV-1.CW1 appears to exert the same effect on localization as its human homolog. Of note, the reported MERES of human NS4 lies outside of AH4 and does not seem to play a role in membrane localization (249). These findings support the notion that norovirus NS4 tethers itself to membranes via its alpha helix AH4, similar to membrane proteins of other positive-sense, single-stranded RNA viruses, such as HCV NS5A and poliovirus 3A (253–255,261,262). Interestingly, alpha helices of related viruses, such as HCV and the related GB virus B, are sometimes interchangeable without rendering the chimeric virus replication-deficient, which would be intriguing to explore in the context of the reverse genetics model of MNV-1.CW1 (264–267).

4.2.2 Classification of NS4 as a peripheral membrane protein

Whereas some viral membrane proteins, such as HCV NS4B or dengue virus (DENV) NS4A, behave as an integral membrane protein by spanning their alpha helices through the membrane leaflet, other viral membrane proteins like HCV NS5A or HAV 2B act as a peripheral membrane protein and do not seem to cross the lipid bilayer (253–256,268–273). Reported *in silico* models suggest that NS4 belongs to the latter category of membrane proteins, although no study has proven or even addressed this experimentally (56). Unfortunately, the membrane protein extraction assays in this thesis did not provide a clear-cut answer on whether norovirus NS4 is an integral

membrane protein or a peripheral membrane protein, probably due to buffer conditions and protein aggregation. However, since a large proportion of NS4 could be extracted from the membranes with urea and sodium carbonate, these assays seem to indicate that norovirus NS4 indeed acts as a peripheral membrane protein (274). Caution is warranted, however, since some transmembrane proteins can be susceptible to sodium carbonate extraction as well (275). Strikingly, almost identical experiments with norovirus NS1-2 suggest that this protein behaves as an integral membrane protein (68). Although TV NS1-2 and RHDV p23 might possess a transmembrane domain, predictions about a putative transmembrane domain in human norovirus NS1-2 remain inconclusive (55,57,61,62). Alternatively, the behavior of NS1-2 as an integral membrane protein might be explained by its tight binding to the host protein VAPA (68,69). In that case, combined with the finding of this thesis that NS4 behaves in a matter consistent with a peripheral membrane protein, norovirus ORF1 might not encode a transmembrane protein to facilitate membrane anchoring of the RC, which is supported by revisited *in silico* models of GII.4 NO NS1-2, NS3 and NS4 (Figure 4.1). Although some viruses like CHIKV and SINV express only monotopic membrane

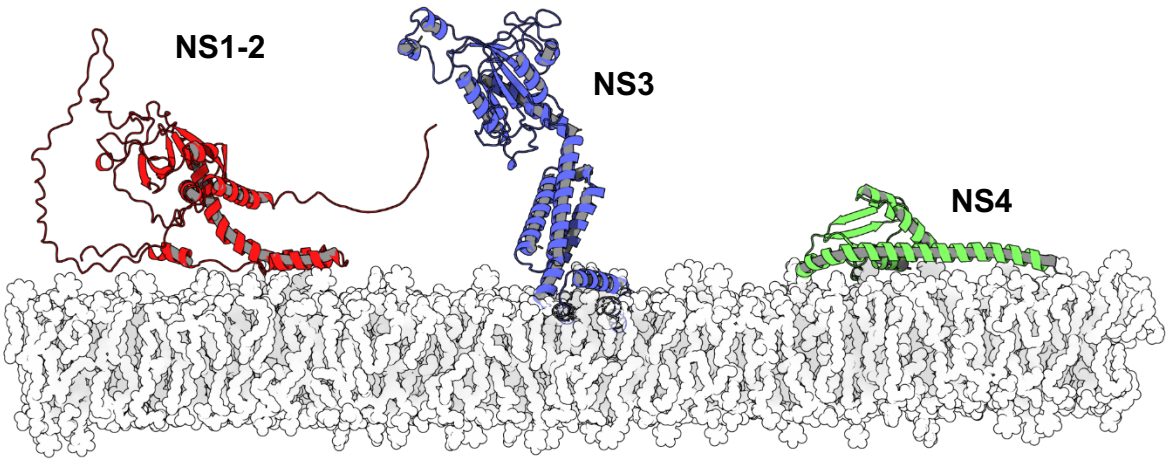

Figure 4.1 Revisited *in silico* models of GII.4 NO NS1-2, NS3 and NS4

With the advancement of AI-guided modeling of proteins by programs such as AlphaFold2, predictions of the structure of the nonstructural proteins of GII.4 NO can be generated with higher accuracy. Predications based on AlphaFold2 no longer model NS1-2, NS3 or NS4 as potential transmembrane proteins, but all seem to favor the models where these proteins are tethered to intracellular membranes monotopically by their alpha helices. Unstructured regions of NS1-2 (N-terminus) and NS4 (C-terminus) are not shown. Modeling performed by the Bressanelli group.

proteins, most positive-sense, single-stranded RNA viruses do express at least one transmembrane protein that is involved in membrane rearrangement and RC biogenesis (238,276–282). Additional biochemical experiments focusing on the membranous nature of norovirus NS1-2, NS3 and NS4 are needed to investigate the existence of a transmembrane domain in NS1-2 and to elucidate the mechanisms by which these three norovirus proteins are localized to subcellular membranes.

4.2.3 Importance of the amphipathicity of AH4 for GII.4 and GV NS4

Amphipathicity is an important property of alpha helices that determines their ability to interact with lipids and to curve membranes (257,283). Many viral membrane proteins therefore contain at least one amphipathic alpha helix to facilitate membrane association or membrane curvature, such as HCV NS5A, poliovirus 2C or DENV NS4A (252,284–290). This raises the question whether the amphipathicity of AH4 of norovirus NS4 is important for membrane association and the induction of membrane rearrangements. The findings in this thesis provide evidence that the amphipathicity of AH4 of human norovirus GII.4 NO NS4 is indeed crucial for membrane association. Swapping of a pair of amino acids from the hydrophobic and the hydrophilic face of AH4 (V113E_E115V) seems sufficient to reduce amphipathicity and to abolish membrane association in IF. This finding is very reminiscent of the N-terminal amphipathic alpha helix in HCV NS5A, where mutation of three uncharged residues into charged amino acids has been shown to lower amphipathicity and to disrupt membrane localization (252,253). In addition to membrane localization, the effect of amphipathicity of AH4 on the induction of membrane alterations was assessed using low precision CLEM. As shown in previous studies, sole expression of wild-type GII.4 NS4 induces membrane alterations including SMVs that are believed to harbor norovirus RCs during infection (56,67). Strikingly, whereas membrane association seems absent in Huh7-T7 Lunet cells expressing a mutant of GII.4 NS4 with a reduced amphipathicity (V113E_E115V), membrane association and lipid droplet enwrapment was detectable in cells expressing a mutant of GII.4 NS4 with a similar amphipathicity as wild-type (V113L_E115D). These findings suggest that a reduction in the amphipathicity of AH4 results in nullification of membrane association and might disrupt the rearrangements of membranes, although the lack of membrane alterations can be explained by the abrogation of membrane association alone as well. Separating

the capacity to induce membrane rearrangements from membrane association requires both biochemical and EM analyses as performed in this thesis, however, no such mutants have been identified in this thesis. In-depth biochemical and structural analyses could shed more light on the exact residues involved in membrane association and/or membrane rearrangement, as has been done before for other membrane proteins with a prominent amphipathic alpha helix (284,291–299).

Since a reverse genetics model for human noroviruses is lacking, the importance of the amphipathicity of AH4 for viral replication is only demonstrable for murine noroviruses. To this end, the reverse genetics model of MNV-1.CW1 was used in this thesis to study the effect of amphipathic mutations on membrane association and viral replication. One set of amphipathic mutations (D109I_I111D) appears to break the membrane association of MNV-1.CW1 NS4, whereas the corresponding control (D109E_I111L) retains membrane localization. Strikingly, this set of MNV-1.CW1 amphipathic mutations aligns well with a set of mutations that abolishes membrane association in GII.4 NO NS4 (V113E_E115V). Both the MNV-1.CW1 amphipathic mutant and its control seem to be replication-deficient in $TCID_{50}$ assays, making it difficult to draw definite conclusions on the necessity of membrane association of NS4 for norovirus replication. Still, these findings strongly resemble the reports in literature on other viral membrane proteins, such as HCV NS5A, Semliki Forest virus (SFV) nsP1 and poliovirus 2B (253,285,298–301). For many of these viral membrane proteins, membrane association can be abrogated by mutating residues in the hydrophobic face of the amphipathic alpha helix, although mutations in the polar face can loosen membrane attachment as well. Evaluating more sets of mutations with appropriate controls in the MNV-1.CW1 reverse genetics model could therefore help to demonstrate precisely which amino acids in AH4 are required for membrane association and how this relates to viral replication.

4.2.4 NS4 promotes ER wrapping and clustering of LDs

In this thesis, strong expression of NS4-GFP is reported around LDs, similar to the donut-like expression pattern reported in literature (56). Furthermore, expression of GII.4 NO NS4 in Huh7-T7 Lunet cells resulted in enwrapment of LDs by a lipid bilayer that probably originates from the ER membrane. A very similar phenomenon has been

described in literature for HCV, where NS5A interacts with the ubiquitously expressed LD protein Rab18 to promote ER apposition to LDs, although other factors are implicated in this process as well (250,251,302–305). Since the HCV core protein is localized on LDs, the tight wrapping of LDs by ER membranes is an important step in the formation of HCV assembly sites (306–308). Moreover, contact between LDs and the ER membrane has been observed during enterovirus infection and the ER is an important site for RC biogenesis in flaviviruses as well (235,247,309–311). The potential role of norovirus NS4 in ER wrapping of LDs as observed in this thesis seems therefore in line with the role of related membrane proteins of other positive-sense, single-stranded RNA viruses. Even more, although expression of GII.4 NO AH4-GFP in Huh7-T7 Lunet cells did not result in wrapping of LDs to the same extent as expression of full-length NS4-GFP, close contact points between the LDs and the ER membrane were still abundantly present. This might indicate that AH4 is the key inducer of ER wrapping of LDs, although other parts of NS4 most likely enhance this process. Nevertheless, some caution should be considered when interpreting these results, since eGFP used in these experiments can sometimes form homodimers, resulting in membranous artefacts when fused to membrane proteins. Furthermore, expression of GII.4 NO and MNV-1.CW1 ORF1 does not seem to induce ER wrapping of LDs, although this might be explained by lower expression levels of NS4 and the interaction of NS4 with other nonstructural proteins, most notably NS1-2 (56). Future experiments should therefore try to swap eGFP for a true monomeric fluorescent protein, such as mCherry, to verify these interesting findings.

Besides ER wrapping, perinuclear clustering of LDs was also observed in Huh7-T7 Lunet cells expressing full-length NS4-GFP as well as AH4-GFP. Vesicular membrane rearrangements such as SMVs and DMVs were observed in close proximity to these LD clusters, strongly resembling LD accumulation described for enterovirus and HCV infection (56,247,307,310,312–315). During enterovirus infection, perinuclear clusters of LDs fuel RC biogenesis by supplying fatty acids required for phospholipid synthesis, implying that enterovirus RC biogenesis relies more on membrane synthesis rather than remodeling of pre-existing membranes (235,247,310). For HCV, LDs are primarily serving as a site of virus assembly, although some evidence suggest that the lipid content of LDs might be consumed as well during virus assembly (302). Other viruses,

such as flaviviruses, induce lipophagy of LDs to enhance β-oxidation and provide ATP for viral replication (316–318). The involvement of lipid droplets is therefore a diverse but well-described hallmark of many positive-sense, single-stranded RNA viruses. Although the necessity of LDs in norovirus replication has not been demonstrated so far, MNV NS1-2 and NS3 have been found to contain LD-targeting domains (61,79). MNV NS1-2 seems to even induce LD enlargement (61). Thus, the LD clustering properties of NS4 seem fitting in the context of both positive-sense, single-stranded RNA virus replication as well as norovirus replication.

This thesis did not address the mechanism by which norovirus NS4 accumulates LDs in the perinuclear region. For enteroviruses, the self-interacting ability of the C-terminal helix of 2C seems crucial for LD clustering (247,319). Interestingly, the findings in this thesis suggest that AH4 might mediate homodimerization of NS4, albeit via a relatively weak self-association. Alternatively, LD clustering might be explained as a membranous artifact of eGFP when fused to NS4 or AH4. This seems unlikely, however, since MNV infection itself can induce LD accumulation in certain cell types as well (56). Still, switching eGFP for mCherry for furture experiments would help to exclude the possibility of LD clustering as an artifact.

4.2.5 Deletion of AH4 in ORF1 does not affect membrane alterations

Since norovirus NS4 promotes membrane rearrangements and the findings in this thesis suggest that the NS4 domain AH4 might facilitate this process, AH4 and other domains were deleted from GII.4 NO ORF1 and these deletion mutants were expressed in Huh7-T7 Lunet cells for subsequent low precision CLEM analysis. Surprisingly, neither AH4 deletion nor SR or NSR deletion from ORF1 had a significant impact on membrane rearrangements or lipid droplet clustering. This finding appears to be at odds with the proposition that AH4 facilitates the role of NS4 as the key inducer of membrane alterations during norovirus infection. An explanation for this observation could be found in the presence of other norovirus membrane proteins during ORF1 expression. Of note, NS1-2 and NS3 are both known to localize to membranes and to induce membrane alterations when expressed individually (56,61,79). These two proteins might act cooperatively when expressed in the ORF1 context, causing functional redundancy with regards to the induction of membrane alterations.

Supporting this explanation, NS1-2, NS3 and NS4 have been shown to interact with each other and form complexes in close proximity to aggregated LDs, resembling the norovirus RC (61). Still, deletion of any NS4 domain from the norovirus genome is likely to disrupt the function of NS4 and to abrogate viral replication. As an alternative approach for future experiments, the effect of deletion or mutation of NS4 domains on membrane rearrangements could be assessed in the context of concurrent expression of NS1-2, NS3 and NS4 instead of complete ORF1 polyprotein expression.

4.3 Interaction between NS1-2 and NS4

4.3.1 NS4 binds NS1-2 during co-expression and MNV infection via AH4

Sparse experimental evidence for an interaction between norovirus NS1-2 and NS4 can be found in literature. For example, FCV p32, p39 and p30, the respective homologues of norovirus NS1-2, NS3 and NS4, have been shown to localize to the ER to initiate RC biogenesis (72,74). LUMIER assays have reported a very strong interaction between NS1-2 and NS4 for GV MNV-1, GI.1 and GII.4 noroviruses (50). Other expression systems have verified the binding of GII.4 NS1-2 to NS3 and NS4 as well as the interaction between NS3 and NS4 (61,79). Although these experiments shed some light on the interaction between NS1-2 and NS4, the specific NS4 domain required for this association remains to be determined. Furthermore, it is still unclear whether this binding occurs during natural norovirus infection as well. To this end, experiments in this thesis make use of a double-tagged MNV-1.CW1 variant with an HA-tag inserted into the NS1-2 protein and a FLAG-tag inserted into the NS4 protein, according to previously reported tolerable sites (258). Interestingly, the double-tagged MNV required a few initial rounds of passaging before being detectable in TCID50, whereas single-tagged MNV typically replicates like WT immediately. This might reflect the necessity of compensatory mutations for double-tagged MNV in order to become a fully replication-competent virus. Still, HA- and FLAG-tags were detectable after these initial rounds of replication, suggesting that the compensatory mutations did not significantly affect these tags.

In line with previous studies, co-expression experiments in this thesis suggest that GII.4 NO NS4 interacts strongly with NS1-2 and to a lesser extent with NS3 as well. The results of this thesis also indicates a moderate self-interactions of GII.4 NO NS4 via AH4. Moreover, the NS4 domain AH4 imparts the ability to interact with NS1-2 in both GII.4 and GV norovirus. In addition, NS1-2 and NS4 seem to associate strongly during the replication of double-tagged MNV-1.CW1. These findings confirm the data from other studies in literature and suggest that NS4 might form a multiprotein complex with the other two norovirus membrane proteins NS1-2 and NS3, reflecting the initiation of RC biogenesis in FCV (72,74). Since the binding of NS1-2 to NS4 is mediated by AH4 in both GII.4 and GV norovirus, this interaction might be a conserved feature among all norovirus genogroups. These findings advocate for a dual function of AH4: on the one hand, AH4 docks NS4 to intracellular membranes and promotes the formation of membrane rearrangements, while one the other hand, AH4 facilitates the specific interaction between NS1-2 and NS4, most likely crucial for the formation of the norovirus RC. Interestingly, several studies suggest that NS4 is often present in viral precursor proteins during early to middle stages of infection, most notably NS4-NS5, NS4-NS6 and NS4-NS7, resembling the proteolytic processing of the P3 domain of the poliovirus polyprotein (49,50,182,320–322). This is in stark contrast with NS1-2 and NS3, which are cleaved off rapidly after translation by the proteolytic active site within NS6 (49,50,182,320,323,324). Since NS5, NS6 and NS7 appear to lack membrane localization, NS4 could target these nonstructural proteins to intracellular membranes when present in the same precursor protein (50). Taking the NS1-2-NS4 and NS3-NS4 interactions into consideration as well, these observations would propose a theoretical and spatiotemporal model of the formation of the norovirus RC, in which all nonstructural proteins are recruited to the same membranous site. In this model, NS1-2 and NS3 are cleaved off from the norovirus ORF1 polyprotein directly after translation of the norovirus genome, followed by translocation of NS1-2, NS3 and the precursor protein NS4-NS7 to intracellular membranes. Although the exact origin of these membranes remains speculative, the ER membrane might be a potential candidate for GII.4 norovirus, since GII.4 NS1-2, NS3 and NS4 have been shown to colocalize with markers of the ER when expressed individually, similar to the FCV homologues of these proteins (56,61,72,79,80). NS1-2, NS3 and NS4, still mostly present in the precursor protein NS4-7, will interact at this membranous site and

orchestrate the induction of membrane alterations to progress the RC formation. At the same time, NS6-7 and NS7 alone start to be cleaved off significantly from the precursor protein NS4-7 in order to produce active forms of RNA-dependent RNA polymerase, initiating negative-sense RNA synthesis in the developing RCs (101). Some experimental evidence suggests that NS7 interacts with NS1-2 directly, further maturing the RC (50). In addition, NS3 and NS4 might adhere to the LD membrane as well, resulting in recruitment and clustering of LDs in the perinuclear region and in close proximity of the RCs (61,79,80). The precise function of these lipid droplets in norovirus replication remains obscure, but related viruses exploit LDs as a source of lipids and energy to rearrange the host membrane architecture, enhance viral replication or assembly new virus particles (235,247,306,310,316). Finally, probably during the middle stages of viral infection, cleavage of the last precursor protein, NS4-NS5, gives rise to sufficient amounts of mature VPg, enabling positive-sense RNA synthesis (49,50,182). Subgenomic RNA can now be transcribed and translated to produce the structural proteins VP1 and VP2, leading to virus assembly and ultimately viral egress through induced cell death in later stages of infection (81).

This hypothetical model fits well in the literature on replication of positive-sense, single-stranded RNA viruses, but additional research and extensive experimental testing is required to further explore, correct and most importantly verify this theory. For example, in addition to the proposed model, human norovirus NS4 is known to disrupt normal COPII-mediated trafficking via a MERES, resulting in Golgi disassembly (83,249). This process might promote accumulation of vesicles belonging to the secretory pathway, giving rise to membranous structures similar to those associated with the MNV RC (67). This stresses the possibility of alternative pathways and explanations for the induction of membrane alterations and norovirus RC biogenesis.

4.3.2 Binding of NS4 to NS1-2 is mediated by specific residues in AH4

Since AH4 imparts the ability to interact with NS1-2, the amphipathicity of AH4 might play a role in this binding. However, since amphipathic mutants of NS4 were capable of binding to NS1-2 even when membrane association was disrupted, the amphipathicity of AH4 does not seem to influence the interaction between NS4 and NS1-2. As a consequence, these findings favor the hypothesis of a direct and highly

specific interaction between NS4 and NS1-2 rather than an indirect and nonspecific association that could arise when both proteins are highly expressed in close proximity on the same membrane. Such a specific protein-protein interaction most likely requires distinct amino acid residues, which are located in AH4 in this case. The experiments in this thesis address this point and indicate that especially the last thirty amino acids of GII.4 NS4 AH4 (Δ1-20 or minimal region domain of NS4) are implicated in the binding to NS1-2. In addition, five specific residues in this minimal binding region were identified that facilitate the interaction between NS4 and NS1-2. Strikingly, all of these residues displayed a significant degree of homology among genogroup I, II.4, IV and V, suggesting these residues are of high importance to the replication of noroviruses belonging to these genogroups. Interestingly, one of these residues, R136A, was mutated previously in this thesis in MNV (R131A) during alanine scanning, although this mutation alone did not result in a significant reduction in TCID50. When analyzing the five identified residues, two different groups can be categorized: three residues are mostly hydrophobic in nature (F128, V129 and I133A in GII.4; F122, S123 and I128 in GV) and two residues are positively charged (R132 and R136 in GII.4; H126 and R131 in GV). These hydrophobic residues in NS4 might interact with other hydrophobic residues in NS1-2, whereas the positively charged amino acids in NS4 might interact with negatively charged residues in NS1-2 to form strong salt bridges to link the two proteins together. For proteins of other positive-sense, single-stranded RNA viruses, such as HCV NS5A, coxsackievirus 3A and SARS-CoV-2 nsp5, hydrophobic interactions or salt bridges are described to promote protein dimerization, which is often crucial for protein function and viral replication (325–328). Interestingly, mutation of the two arginine residues into lysine residues in GII.4 did not fully rescue the interaction between the minimal binding region of NS4 and full-length NS1-2, suggesting that a positive charge is not the only prerequisite for the interaction of these residues with NS1-2. In addition, the hydrophobic interacting residues in the minimal binding region of GII.4 NS4 could be switched through conservative mutation by other hydrophobic residues without apparent loss-of-binding to NS1-2, indicating that the nonpolar nature of these amino acids is indeed critical for the interaction with NS1-2.

4.3.3 NS4 interacts with residues in the C-terminal domain of NS1-2

Besides careful mutagenesis, which revealed five specific residues within the minimal binding region of NS4 that facilitate binding between NS4 and NS1-2, *in silico* and *in vitro* experiments in this thesis provide insights in the binding domain of NS1-2 as well. First, the interaction between GII.4 NO NS1-2 and NS4 was modeled *in silico* using AlphaFold and HADDOCK. These models suggested a strong interaction between AH4 of NS4 and the membrane-associating C-terminus of NS1-2, specifically amino acid residues 276 to 308. In addition, *in silico* modeling using AlphaFold2 again pointed to the same region in NS1-2 as interacting partner for NS4, but in these models, the more N-terminal region of AH4 of NS4 seems to interact with the NS1-2 hydrolase domain as well (Figure 4.2). In strong agreement with these models, deletion mutagenesis indicated a minimal binding region of NS1-2 spanning from amino acids 277 to 313. This minimal binding region contains an aspartic acid at amino acid position 290 and a glutamic acid at position 298, which are both juxtaposed to the two arginine residues within AH4 in these models, emphasizing the possibility of salt bridge formation between these residues in NS1-2 and NS4. In addition, alanine scanning of D290 and E298 in the minimal binding region of NS1-2 seems to reduce the interaction with NS4. However, mutation of these two amino acid residues also destabilize the expression of the ORF1 polyprotein, potentially via misfolding of the NS1-2 protein. Moreover, due to the aromatic nature of the C-terminus of GII.4 NO NS1-2, cation-π interactions between R132 and/or R136 of GII.4 NO NS4 and aromatic residues in the C-terminus of GII.4 NO NS1-2 could also occur. Caution is therefore warranted when drawing definite conclusions about these two amino acid residues as interacting sites. Nevertheless, amino acid sequence alignments of the NS1-2 protein argue for high homology of D290 and E298 among multiple norovirus genogroups. Even more, the one exception in conservation of E298 in NS1-2 pairs with the exception in homology of R132 in NS4: in genogroup V, E298 of NS1-2 is present as an asparagine, while its interacting partner R132 is present as a histidine in this genogroup. Such an amino acid change might reflect a co-evolutionary pattern as described for other viral protein-protein interactions (329–331). Additional co-evolution analyses with more genogroups and genotypes could shed light on the conservation of these amino acid residues and their potential interaction.

4.3.4 Loss-of-binding between NS1-2 and NS4 abolishes MNV replication

Since the amino acid residues within GII.4 NS1-2 and NS4 responsible for the interaction between NS1-2 and NS4 have been identified in this thesis, the binding between NS1-2 and NS4 can be disrupted experimentally in the MNV context to assess the effect on viral replication. Combined mutation of H126 and R131 in NS4 of MNV-1.CW1 abolished viral replication as measured in TCID50 and the interaction between NS1-2 and NS4 as measured in an IP experiment. Similarly, combined mutation of

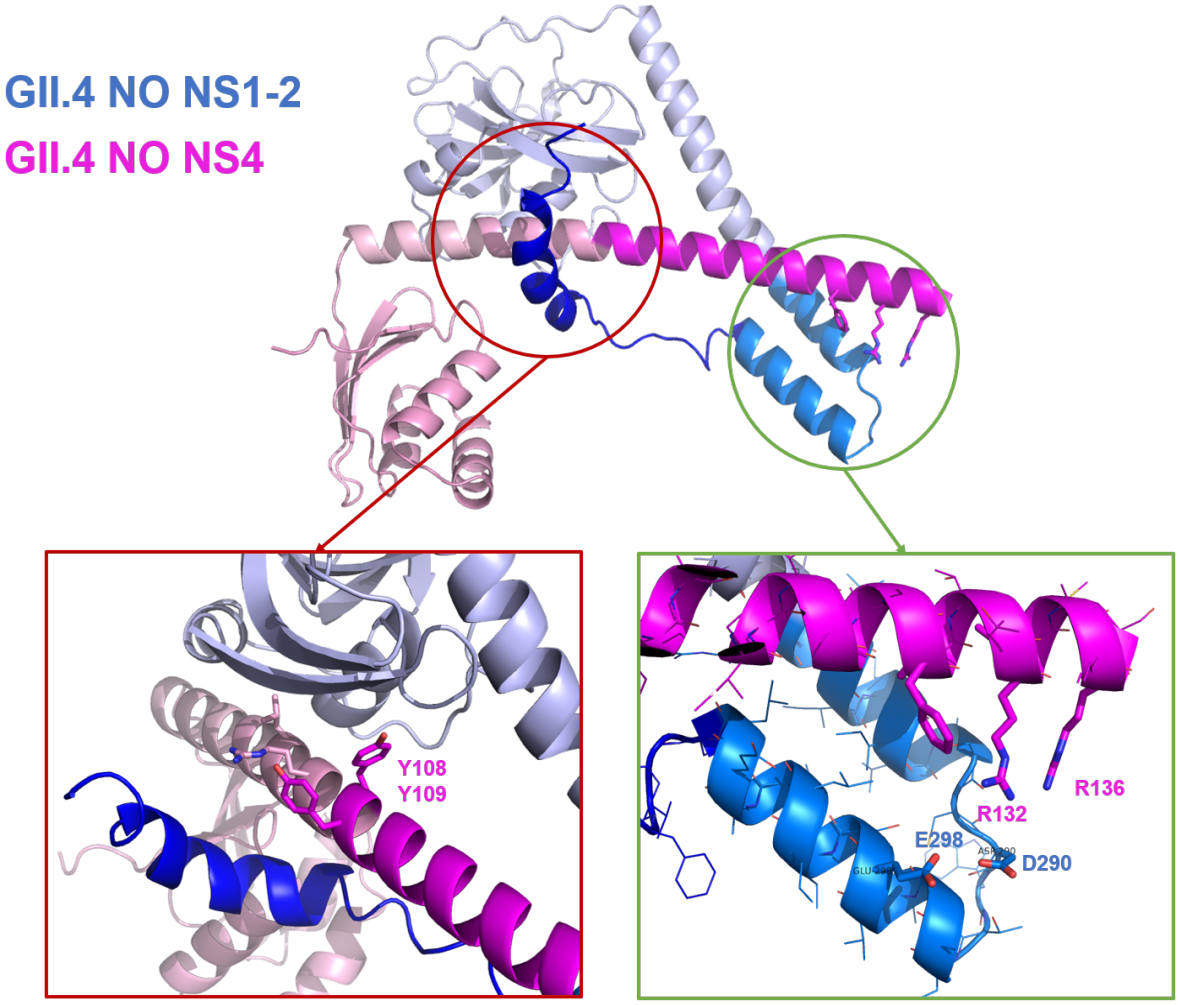

Figure 4.2 *In silico* AlphaFold2 model of the interaction between GII.4 NO NS1-2 and NS4
More recent AlphaFold2 predictions of the interaction between GII.4 NO NS1-2 and NS4 highlights the interaction identified and explored in this thesis (green box), but also an interaction between the more N-terminal part of AH4 of NS4 (amino acid residues 101-111) and the hydrolase domain of NS1-2 (red box). Although the co-immunoprecipitation experiments described in this thesis did not find evidence for this interaction, experiments with more specific constructs could shed more light on the existence and biological relevance of this interaction. Modeling performed by the Bressanelli group.

F122, S123 and I128 in NS4 of MNV-1.CW1 nullifies viral replication and breaks the interaction between NS1-2 and NS4. These findings do not only confirm that NS1-2 and NS4 interact during viral replication, but also indicate that this interaction is imperative for viral replication to take place. In addition to the interacting residues in NS4, this thesis also provides evidence that two amino acid residues in GII.4 NO NS1-2, D290 and E298, might be involved in the interaction to NS4. However, the polyprotein stability was significantly impaired by mutation of either of these two amino acid sites, making additional experiments to confirm these results paramount. Nevertheless, essential interactions between nonstructural proteins are known for many other positive-sense, single-stranded RNA viruses as well, such as DENV and HCV (332,333). Blocking these viral protein-protein interactions could pave the way for novel antivirals. For example, pan-serotype DENV inhibitors of the NS3-NS4B interaction have recently been identified as promising drug candidates (334–336). Therefore, future experiments should explore the potential of the interaction between norovirus NS1-2 and NS4 as a druggable target. Screenings for compounds that inhibit the interaction between norovirus NS1-2 and NS4, such as AlphaScreen-based assays, could aid the identification of interesting pharmaceutical candidates (337).

4.3.5. Scientific outlook

Although the work presented in this thesis lays the groundwork for future studies on norovirus NS4, many aspects of the function of NS4 remain to be elucidated. First, the role of certain amino acid residues of NS4 in the induction of membrane rearrangements is still elusive. This thesis provides compelling evidence that certain amino acid residues are involved in membrane association of NS4, as can be concluded from the V113E_E115V mutation in GII.4 NO NS4 and the D109I_I111D mutation in GV MNV-1.CW1 NS4. However, whether other amino acid residues within NS4 contribute to the induction of membrane alterations, such as SMVs or DMVs, could not be concluded from EM data (not shown). Since these membrane alterations likely function as active sites of norovirus replication, future projects should aim to study these membranous structures in greater detail. Especially mutations in the ORF1 polyprotein would be physiologically relevant to investigate, even though the effects of such mutations on the induction of membrane rearrangements are very subtle and therefore hard to quantify. Nevertheless, the identification of these amino acid sites will

significantly enhance our understanding of the mechanism by which NS4 subverts the intracellular membranous organization.

In addition to the membranous rearrangements seen upon NS4 expression, NS4 seems to interact with LDs as well. The EM analyses presented in this thesis provide evidence for the enwrapment of the LDs by NS4, probably by a membrane of ER origin. Even more, expression of NS4 in Huh7-T7 Lunet cells results in perinuclear accumulation of LDs in live-cell imaging (data not shown). Although these effects are far less pronounced in the ORF1 polyprotein context, LDs might still play an important role in the induction of membrane alterations in these settings. Similar to enteroviruses, noroviruses might use LDs as intracellular sources of phospholipids to promote membrane remodeling (235,247). Therefore, future studies should address the physiological relevance of these lipid droplets for membrane rearrangements as observed during norovirus replication. Since such studies are readily available for enteroviruses, the same experimental approaches can be adopted for future norovirus research.

The experiments performed for this thesis provide an in-depth insight in the molecular interaction between norovirus NS1-2 and NS4. Still, due to polyprotein instability issues, it remains difficult to draw hard conclusions on the interacting amino acid sites on the NS1-2 side. Although D290 and E298 seem to play a role in this interaction on the NS1-2 side, it is impossible to rule out the involvement of other, possibly aromatic amino acid residues. Moreover, a tight interaction between AH4 of NS4 and the hydrolase domain of NS1-2 has been modelled as well (Figure 4.2). This model not only involves Y108 and Y109 of NS4, but also L101 and R105 of NS4, of which some are highly conserved among different norovirus genogroups. Functionally investigating these sites by means of reverse genetics and co-IP experiments would constitute a fruitful approach for the betterment of our understanding of the interaction between norovirus NS1-2 and NS4.

Finally, since the results of this thesis provide minimal binding regions of both NS1-2 and NS4, screening experiments for antiviral drug development could be designed and performed. Different screening assays exist for this purpose, such as AlphaScreens, Fluorescence Resonance Energy Transfer (FRET)-based assays and cell-based high-throughput screenings. Given the hydrophobic nature of NS4, it might be challenging to synthesize NS4-derived peptides directly, although full-length GII.4 NO NS4 has

been expressed and purified from *E. coli* before. These assays could provide potential antiviral compounds that can be further validated using co-IP experiments, the GI replicon model, the MNV replication system and GII.4 infection in human intestinal enteroid models. In this way, the characterization of the interaction between norovirus NS1-2 and NS4 as reported in this thesis might pave the way for the development for novel antiviral compounds against norovirus infection.

Chapter 5

References

"*If I have seen further, it is by standing on the shoulders of giants.*"

— Isaac Newton (1643-1727), *Letter to Robert Hooke*

---

5 References

1. Zahorsky J. Hyperemesis hiemis or the winter vomiting disease. Arch Pediatr. 1929;46:391–5.

2. Adler JL, Zickl R. Winter vomiting disease. J Infect Dis. 1969 Jun;119(6):668–73.

3. Dolin R, Blacklow NR, DuPont H, Formal S, Buscho RF, Kasel JA, et al. Transmission of acute infectious nonbacterial gastroenteritis to volunteers by oral administration of stool filtrates. J Infect Dis. 1971 Mar;123(3):307–12.

4. Dolin R, Blacklow NR, DuPont H, Buscho RF, Wyatt RG, Kasel JA, et al. Biological properties of Norwalk agent of acute infectious nonbacterial gastroenteritis. Proc Soc Exp Biol Med. 1972 Jun;140(2):578–83.

5. Kapikian AZ, Wyatt RG, Dolin R, Thornhill TS, Kalica AR, Chanock RM. Visualization by immune electron microscopy of a 27-nm particle associated with acute infectious nonbacterial gastroenteritis. J Virol. 1972 Nov;10(5):1075–81.

6. Pires SM, Fischer-Walker CL, Lanata CF, Devleesschauwer B, Hall AJ, Kirk MD, et al. Aetiology-Specific Estimates of the Global and Regional Incidence and Mortality of Diarrhoeal Diseases Commonly Transmitted through Food. PLoS One. 2015;10(12):e0142927.

7. Bartsch SM, O'Shea KJ, Lee BY. The Clinical and Economic Burden of Norovirus Gastroenteritis in the United States. J Infect Dis. 2020;222(11):1910–9.

8. Glass RI, Parashar UD, Estes MK. Norovirus gastroenteritis. N Engl J Med. 2009 Oct 29;361(18):1776–85.

9. Teunis PFM, Moe CL, Liu P, Miller SE, Lindesmith L, Baric RS, et al. Norwalk virus: how infectious is it? J Med Virol. 2008 Aug;80(8):1468–76.

10. Lee RM, Lessler J, Lee RA, Rudolph KE, Reich NG, Perl TM, et al. Incubation periods of viral gastroenteritis: a systematic review. BMC Infect Dis. 2013 Sep 25;13:446.

11. Miura F, Matsuyama R, Nishiura H. Estimating the Asymptomatic Ratio of Norovirus Infection During Foodborne Outbreaks With Laboratory Testing in Japan. J Epidemiol. 2018;28(9):382–7.

12. Kaplan JE, Gary GW, Baron RC, Singh N, Schonberger LB, Feldman R, et al. Epidemiology of Norwalk gastroenteritis and the role of Norwalk virus in outbreaks of acute nonbacterial gastroenteritis. Ann Intern Med. 1982 Jun;96(6 Pt 1):756–61.

13. Arness MK, Feighner BH, Canham ML, Taylor DN, Monroe SS, Cieslak TJ, et al. Norwalk-like viral gastroenteritis outbreak in U.S. Army trainees. Emerg Infect Dis. 6(2):204–7.

14. Tseng CY, Chen CH, Su SC, Wu FT, Chen CC, Hsieh GY, et al. Characteristics of norovirus gastroenteritis outbreaks in a psychiatric centre. Epidemiol Infect. 2011 Feb;139(2):275–85.

15. Lopman BA, Reacher MH, Vipond IB, Sarangi J, Brown DWG. Clinical manifestation of norovirus gastroenteritis in health care settings. Clin Infect Dis. 2004 Aug 1;39(3):318–24.

16. Roddie C, Paul JP v, Benjamin R, Gallimore CI, Xerry J, Gray JJ, et al. Allogeneic hematopoietic stem cell transplantation and norovirus gastroenteritis: a previously unrecognized cause of morbidity. Clin Infect Dis. 2009 Oct 1;49(7):1061–8.

17. Schorn R, Höhne M, Meerbach A, Bossart W, Wüthrich RP, Schreier E, et al. Chronic norovirus infection after kidney transplantation: molecular evidence for immune-driven viral evolution. Clin Infect Dis. 2010 Aug 1;51(3):307–14.

18. Westhoff TH, Vergoulidou M, Loddenkemper C, Schwartz S, Hofmann J, Schneider T, et al. Chronic norovirus infection in renal transplant recipients. Nephrol Dial Transplant. 2009 Mar;24(3):1051–3.

19. Roos-Weil D, Ambert-Balay K, Lanternier F, Mamzer-Bruneel MF, Nochy D, Pothier P, et al. Impact of norovirus/sapovirus-related diarrhea in renal transplant recipients hospitalized for diarrhea. Transplantation. 2011 Jul 15;92(1):61–9.

20. Saif MA, Bonney DK, Bigger B, Forsythe L, Williams N, Page J, et al. Chronic norovirus infection in pediatric hematopoietic stem cell transplant recipients: a cause of prolonged intestinal failure requiring intensive nutritional support. Pediatr Transplant. 2011 Aug;15(5):505–9.

21. Bok K, Green KY. Norovirus gastroenteritis in immunocompromised patients. N Engl J Med. 2012 Nov 29;367(22):2126–32.

22. Xi JN, Graham DY, Wang KN, Estes MK. Norwalk virus genome cloning and characterization. Science. 1990 Dec 14;250(4987):1580–3.

23. Greenberg HB, Valdesuso JR, Kalica AR, Wyatt RG, McAuliffe VJ, Kapikian AZ, et al. Proteins of Norwalk virus. J Virol. 1981 Mar;37(3):994–9.

24. Okada S, Sekine S, Ando T, Hayashi Y, Murao M, Yabuuchi K, et al. Antigenic characterization of small, round-structured viruses by immune electron microscopy. J Clin Microbiol. 1990 Jun;28(6):1244–8.

25. Lambden PR, Caul EO, Ashley CR, Clarke IN. Sequence and genome organization of a human small round-structured (Norwalk-like) virus. Science. 1993 Jan 22;259(5094):516–9.

26. Zheng DP, Ando T, Fankhauser RL, Beard RS, Glass RI, Monroe SS. Norovirus classification and proposed strain nomenclature. Virology. 2006 Mar 15;346(2):312–23.

27. Dolin R, Reichman RC, Roessner KD, Tralka TS, Schooley RT, Gary W, et al. Detection by immune electron microscopy of the Snow Mountain agent of acute viral gastroenteritis. J Infect Dis. 1982 Aug;146(2):184–9.

28. Thornhill TS, Wyatt RG, Kalica AR, Dolin R, Chanock RM, Kapikian AZ. Detection by immune electron microscopy of 26- to 27-nm viruslike particles associated with two family outbreaks of gastroenteritis. J Infect Dis. 1977 Jan;135(1):20–7.

29. Wyatt RG, Dolin R, Blacklow NR, DuPont HL, Buscho RF, Thornhill TS, et al. Comparison of three agents of acute infectious nonbacterial gastroenteritis by cross-challenge in volunteers. J Infect Dis. 1974 Jun;129(6):709–14.

30. Chhabra P, de Graaf M, Parra GI, Chan MCW, Green K, Martella V, et al. Updated classification of norovirus genogroups and genotypes. J Gen Virol. 2019;100(10):1393–406.

31. Wu X, Han J, Chen L, Xu D, Shen Y, Zha Y, et al. Prevalence and genetic diversity of noroviruses in adults with acute gastroenteritis in Huzhou, China, 2013-2014. Arch Virol. 2015 Jul;160(7):1705–13.

32. Cannon JL, Bonifacio J, Bucardo F, Buesa J, Bruggink L, Chan MCW, et al. Global Trends in Norovirus Genotype Distribution among Children with Acute Gastroenteritis. Emerg Infect Dis. 2021;27(5):1438–45.

33. Hoa Tran TN, Trainor E, Nakagomi T, Cunliffe NA, Nakagomi O. Molecular epidemiology of noroviruses associated with acute sporadic gastroenteritis in children: global distribution of genogroups, genotypes and GII.4 variants. J Clin Virol. 2013 Mar;56(3):185–93.

34. Bull RA, Eden JS, Rawlinson WD, White PA. Rapid evolution of pandemic noroviruses of the GII.4 lineage. PLoS Pathog. 2010 Mar 26;6(3):e1000831.

35. Eden JS, Tanaka MM, Boni MF, Rawlinson WD, White PA. Recombination within the pandemic norovirus GII.4 lineage. J Virol. 2013 Jun;87(11):6270–82.

36. Winder N, Gohar S, Muthana M. Norovirus: An Overview of Virology and Preventative Measures. Viruses. 2022 Dec 16;14(12).

37. Tohma K, Lepore CJ, Gao Y, Ford-Siltz LA, Parra GI. Population Genomics of GII.4 Noroviruses Reveal Complex Diversification and New Antigenic Sites Involved in the Emergence of Pandemic Strains. mBio. 2019 Sep 24;10(5).

38. Vinjé J. Advances in laboratory methods for detection and typing of norovirus. J Clin Microbiol. 2015 Feb;53(2):373–81.

39. Eden JS, Hewitt J, Lim KL, Boni MF, Merif J, Greening G, et al. The emergence and evolution of the novel epidemic norovirus GII.4 variant Sydney 2012. Virology. 2014 Feb;450–451:106–13.

40. Desai R, Hembree CD, Handel A, Matthews JE, Dickey BW, McDonald S, et al. Severe outcomes are associated with genogroup 2 genotype 4 norovirus outbreaks: a systematic literature review. Clin Infect Dis. 2012 Jul;55(2):189–93.

41. de Graaf M, van Beek J, Koopmans MPG. Human norovirus transmission and evolution in a changing world. Nat Rev Microbiol. 2016;14(7):421–33.

42. Ludwig-Begall LF, Mauroy A, Thiry E. Noroviruses-The State of the Art, Nearly Fifty Years after Their Initial Discovery. Viruses. 2021;13(8).

43. Ajami NJ, Barry MA, Carrillo B, Muhaxhiri Z, Neill FH, Prasad BVV, et al. Antibody responses to norovirus genogroup GI.1 and GII.4 proteases in volunteers administered Norwalk virus. Clin Vaccine Immunol. 2012 Dec;19(12):1980–3.

44. Lun JH, Hewitt J, Sitabkhan A, Eden JS, Enosi Tuipulotu D, Netzler NE, et al. Emerging recombinant noroviruses identified by clinical and waste water screening. Emerg Microbes Infect. 2018 Mar 29;7(1):50.

45. Clarke IN, Estes MK, Green KY, Hansman GS, Knowles NJ, Koopmans MK, et al. Virus taxonomy: classification and nomenclature of viruses: ninth report of the International Committee on Taxonomy of Viruses. King, AMQ, Adams, MJ, Carstens, EB, Lefkowitz, EJ, Eds. 2012;977–86.

46. McFadden N, Bailey D, Carrara G, Benson A, Chaudhry Y, Shortland A, et al. Norovirus regulation of the innate immune response and apoptosis occurs via the product of the alternative open reading frame 4. PLoS Pathog. 2011 Dec;7(12):e1002413.

47. Alhatlani B, Vashist S, Goodfellow I. Functions of the 5' and 3' ends of calicivirus genomes. Virus Res. 2015 Aug 3;206:134–43.

48. Burroughs JN, Brown F. Presence of a covalently linked protein on calicivirus RNA. J Gen Virol. 1978 Nov;41(2):443–6.

49. Sosnovtsev S V, Belliot G, Chang KO, Prikhodko VG, Thackray LB, Wobus CE, et al. Cleavage map and proteolytic processing of the murine norovirus nonstructural polyprotein in infected cells. J Virol. 2006 Aug;80(16):7816–31.

50. Emmott E, de Rougemont A, Hosmillo M, Lu J, Fitzmaurice T, Haas J, et al. Polyprotein processing and intermolecular interactions within the viral replication complex spatially and temporally control norovirus protease activity. J Biol Chem. 2019;294(11):4259–71.

51. Lin X, Thorne L, Jin Z, Hammad LA, Li S, Deval J, et al. Subgenomic promoter recognition by the norovirus RNA-dependent RNA polymerases. Nucleic Acids Res. 2015 Jan;43(1):446–60.

52. Yunus MA, Lin X, Bailey D, Karakasiliotis I, Chaudhry Y, Vashist S, et al. The murine norovirus core subgenomic RNA promoter consists of a stable stem-loop that can direct accurate initiation of RNA synthesis. J Virol. 2015 Jan 15;89(2):1218–29.

53. Napthine S, Lever RA, Powell ML, Jackson RJ, Brown TDK, Brierley I. Expression of the VP2 protein of murine norovirus by a translation termination-reinitiation strategy. PLoS One. 2009 Dec 22;4(12):e8390.

54. Lateef Z, Gimenez G, Baker ES, Ward VK. Transcriptomic analysis of human norovirus NS1-2 protein highlights a multifunctional role in murine monocytes. BMC Genomics. 2017;18(1):39.

55. Fernandez-Vega V, Sosnovtsev S V, Belliot G, King AD, Mitra T, Gorbalenya A, et al. Norwalk virus N-terminal nonstructural protein is associated with disassembly of the Golgi complex in transfected cells. J Virol. 2004 May;78(9):4827–37.

56. Doerflinger SY, Cortese M, Romero-Brey I, Menne Z, Tubiana T, Schenk C, et al. Membrane alterations induced by nonstructural proteins of human norovirus. PLoS Pathog. 2017 Oct;13(10):e1006705.

57. Strtak AC, Perry JL, Sharp MN, Chang-Graham AL, Farkas T, Hyser JM. Recovirus NS1-2 Has Viroporin Activity That Induces Aberrant Cellular Calcium Signaling To Facilitate Virus Replication. mSphere. 2019 Sep 18;4(5).

58. Hyser JM, Collinson-Pautz MR, Utama B, Estes MK. Rotavirus disrupts calcium homeostasis by NSP4 viroporin activity. mBio. 2010 Nov 30;1(5).

59. Pham T, Perry JL, Dosey TL, Delcour AH, Hyser JM. The Rotavirus NSP4 Viroporin Domain is a Calcium-conducting Ion Channel. Sci Rep. 2017 Mar 3;7:43487.

60. van Kuppeveld FJM, de Jong AS, Melchers WJG, Willems PHGM. Enterovirus protein 2B po(u)res out the calcium: a viral strategy to survive? Trends Microbiol. 2005 Feb;13(2):41–4.

61. Hung CH, Yen JB, Chang PJ, Chen LW, Huang TY, Tsai WJ, et al. Characterization of Human Norovirus Nonstructural Protein NS1.2 Involved in the Induction of the Filamentous Endoplasmic Reticulum, Enlarged Lipid Droplets, LC3 Recruitment, and Interaction with NTPase and NS4. Viruses. 2023 Mar 22;15(3).

62. Smertina E, Carroll AJ, Boileau J, Emmott E, Jenckel M, Vohra H, et al. Lagovirus Non-structural Protein p23: A Putative Viroporin That Interacts With Heat Shock Proteins and Uses a Disulfide Bond for Dimerization. Front Microbiol. 2022;13:923256.

63. Robinson BA, van Winkle JA, McCune BT, Peters AM, Nice TJ. Caspase-mediated cleavage of murine norovirus NS1/2 potentiates apoptosis and is required for persistent infection of intestinal epithelial cells. PLoS Pathog. 2019;15(7):e1007940.

64. Mirabelli C, Jones MK, Young VL, Kolawole AO, Owusu I, Shan M, et al. Human Norovirus Triggers Primary B Cell Immune Activation In Vitro. mBio. 2022 Apr 26;13(2):e0017522.

65. Nice TJ, Strong DW, McCune BT, Pohl CS, Virgin HW. A single-amino-acid change in murine norovirus NS1/2 is sufficient for colonic tropism and persistence. J Virol. 2013 Jan;87(1):327–34.

66. Hyde JL, Mackenzie JM. Subcellular localization of the MNV-1 ORF1 proteins and their potential roles in the formation of the MNV-1 replication complex. Virology. 2010 Oct 10;406(1):138–48.

67. Hyde JL, Sosnovtsev S V, Green KY, Wobus C, Virgin HW, Mackenzie JM. Mouse norovirus replication is associated with virus-induced vesicle clusters originating from membranes derived from the secretory pathway. J Virol. 2009 Oct;83(19):9709–19.

68. Ettayebi K, Hardy ME. Norwalk virus nonstructural protein p48 forms a complex with the SNARE regulator VAP-A and prevents cell surface expression of vesicular stomatitis virus G protein. J Virol. 2003 Nov;77(21):11790–7.

69. McCune BT, Tang W, Lu J, Eaglesham JB, Thorne L, Mayer AE, et al. Noroviruses Co-opt the Function of Host Proteins VAPA and VAPB for Replication via a Phenylalanine-Phenylalanine-Acidic-Tract-Motif Mimic in Nonstructural Viral Protein NS1/2. mBio. 2017;8(4).

70. Tu H, Gao L, Shi ST, Taylor DR, Yang T, Mircheff AK, et al. Hepatitis C virus RNA polymerase and NS5A complex with a SNARE-like protein. Virology. 1999 Oct 10;263(1):30–41.

71. Eyre NS, Fiches GN, Aloia AL, Helbig KJ, McCartney EM, McErlean CSP, et al. Dynamic imaging of the hepatitis C virus NS5A protein during a productive infection. J Virol. 2014 Apr;88(7):3636–52.

72. Bailey D, Kaiser WJ, Hollinshead M, Moffat K, Chaudhry Y, Wileman T, et al. Feline calicivirus p32, p39 and p30 proteins localize to the endoplasmic reticulum to initiate replication complex formation. J Gen Virol. 2010 Mar;91(Pt 3):739–49.

73. Green KY, Mory A, Fogg MH, Weisberg A, Belliot G, Wagner M, et al. Isolation of enzymatically active replication complexes from feline calicivirus-infected cells. J Virol. 2002 Sep;76(17):8582–95.

74. Kaiser WJ, Chaudhry Y, Sosnovtsev S V, Goodfellow IG. Analysis of protein-protein interactions in the feline calicivirus replication complex. J Gen Virol. 2006 Feb;87(Pt 2):363–8.

75. Han KR, Lee JH, Kotiguda GG, Jung KH, Chung MS, Kang S, et al. Nucleotide triphosphatase and RNA chaperone activities of murine norovirus NS3. J Gen Virol. 2018;99(11):1482–93.

76. Pfister T, Wimmer E. Polypeptide p41 of a Norwalk-like virus is a nucleic acid-independent nucleoside triphosphatase. J Virol. 2001 Feb;75(4):1611–9.

77. Li TF, Hosmillo M, Schwanke H, Shu T, Wang Z, Yin L, et al. Human Norovirus NS3 Has RNA Helicase and Chaperoning Activities. J Virol. 2018;92(5).

78. Xia H, Wang P, Wang GC, Yang J, Sun X, Wu W, et al. Human Enterovirus Nonstructural Protein 2CATPase Functions as Both an RNA Helicase and ATP-Independent RNA Chaperone. PLoS Pathog. 2015 Jul;11(7):e1005067.

79. Yen JB, Chen LW, Wei LH, Hung CH, Wang SS, Lin CL, et al. Identification and Characterization of Human Norovirus NTPase Regions Required for Lipid Droplet Localization, Cellular Apoptosis, and Interaction with the Viral P22 Protein. Microbiol Spectr. 2021;9(1):e0042221.

80. Yen JB, Wei LH, Chen LW, Chen LY, Hung CH, Wang SS, et al. Subcellular Localization and Functional Characterization of GII.4 Norovirus-Encoded NTPase. J Virol. 2018;92(5).

81. Wang G, Zhang D, Orchard RC, Hancks DC, Reese TA. Norovirus MLKL-like protein initiates cell death to induce viral egress. Nature. 2023 Mar 29;

82. Sharp TM, Guix S, Katayama K, Crawford SE, Estes MK. Inhibition of cellular protein secretion by norwalk virus nonstructural protein p22 requires a mimic of an endoplasmic reticulum export signal. PLoS One. 2010 Oct 18;5(10):e13130.

83. Sharp TM, Crawford SE, Ajami NJ, Neill FH, Atmar RL, Katayama K, et al. Secretory pathway antagonism by calicivirus homologues of Norwalk virus nonstructural protein p22 is restricted to noroviruses. Virol J. 2012 Sep 3;9:181.

84. Eruera AR, McSweeney AM, McKenzie-Goldsmith GM, Ward VK. Protein Nucleotidylylation in +ssRNA Viruses. Viruses. 2021 Aug 5;13(8).

85. Belliot G, Sosnovtsev S V, Chang KO, McPhie P, Green KY. Nucleotidylylation of the VPg protein of a human norovirus by its proteinase-polymerase precursor protein. Virology. 2008 Apr 25;374(1):33–49.

86. Medvedev A, Viswanathan P, May J, Korba B. Regulation of human norovirus VPg nucleotidylylation by ProPol and nucleoside triphosphate binding by its amino terminal sequence in vitro. Virology. 2017;503:37–45.

87. McSweeney AM, Young VL, Ward VK. Norovirus VPg Binds RNA through a Conserved N-Terminal K/R Basic Patch. Viruses. 2021;13(7).

88. Olspert A, Hosmillo M, Chaudhry Y, Peil L, Truve E, Goodfellow I. Protein-RNA linkage and posttranslational modifications of feline calicivirus and murine norovirus VPg proteins. PeerJ. 2016;4:e2134.

89. Chung L, Bailey D, Leen EN, Emmott EP, Chaudhry Y, Roberts LO, et al. Norovirus translation requires an interaction between the C Terminus of the genome-linked viral protein VPg and eukaryotic translation initiation factor 4G. J Biol Chem. 2014 Aug 1;289(31):21738–50.

90. Hosmillo M, Lu J, McAllaster MR, Eaglesham JB, Wang X, Emmott E, et al. Noroviruses subvert the core stress granule component G3BP1 to promote viral VPg-dependent translation. Elife. 2019 Aug 12;8.

91. Zeitler CE, Estes MK, Venkataram Prasad B V. X-ray crystallographic structure of the Norwalk virus protease at 1.5-A resolution. J Virol. 2006 May;80(10):5050–8.

92. Viskovska MA, Zhao B, Shanker S, Choi JM, Deng L, Song Y, et al. GII.4 Norovirus Protease Shows pH-Sensitive Proteolysis with a Unique Arg-His Pairing in the Catalytic Site. J Virol. 2019 Mar 15;93(6).

93. Muzzarelli KM, Kuiper B, Spellmon N, Brunzelle J, Hackett J, Amblard F, et al. Structural and Antiviral Studies of the Human Norovirus GII.4 Protease. Biochemistry. 2019 Feb 19;58(7):900–7.

94. Zhao B, Hu L, Song Y, Patil K, Ramani S, Atmar RL, et al. Norovirus Protease Structure and Antivirals Development. Viruses. 2021 Oct 14;13(10).

95. Leen EN, Baeza G, Curry S. Structure of a murine norovirus NS6 protease-product complex revealed by adventitious crystallisation. PLoS One. 2012;7(6):e38723.

96. Guo J, Douangamath A, Song W, Coker AR, Chan AWE, Wood SP, et al. In crystallo-screening for discovery of human norovirus 3C-like protease inhibitors. J Struct Biol X. 2020;4:100031.

97. Rocha-Pereira J, Nascimento MSJ, Ma Q, Hilgenfeld R, Neyts J, Jochmans D. The enterovirus protease inhibitor rupintrivir exerts cross-genotypic anti-norovirus activity and clears cells from the norovirus replicon. Antimicrob Agents Chemother. 2014 Aug;58(8):4675–81.

98. Van Dycke J, Dai W, Stylianidou Z, Li J, Cuvry A, Roux E, et al. A Novel Class of Norovirus Inhibitors Targeting the Viral Protease with Potent Antiviral Activity In Vitro and In Vivo. Viruses. 2021 Sep 16;13(9).

99. Emmott E, Sweeney TR, Goodfellow I. A Cell-based Fluorescence Resonance Energy Transfer (FRET) Sensor Reveals Inter- and Intragenogroup Variations in Norovirus Protease Activity and Polyprotein Cleavage. J Biol Chem. 2015 Nov 13;290(46):27841–53.

100. Deval J, Jin Z, Chuang YC, Kao CC. Structure(s), function(s), and inhibition of the RNA-dependent RNA polymerase of noroviruses. Virus Res. 2017 Apr 15;234:21–33.

101. Belliot G, Sosnovtsev S V, Chang KO, Babu V, Uche U, Arnold JJ, et al. Norovirus proteinase-polymerase and polymerase are both active forms of RNA-dependent RNA polymerase. J Virol. 2005 Feb;79(4):2393–403.

102. Smertina E, Urakova N, Strive T, Frese M. Calicivirus RNA-Dependent RNA Polymerases: Evolution, Structure, Protein Dynamics, and Function. Front Microbiol. 2019;10:1280.

103. Lin X, Thorne L, Jin Z, Hammad LA, Li S, Deval J, et al. Subgenomic promoter recognition by the norovirus RNA-dependent RNA polymerases. Nucleic Acids Res. 2015 Jan;43(1):446–60.

104. Lin X, Thorne L, Jin Z, Hammad LA, Li S, Deval J, et al. Subgenomic promoter recognition by the norovirus RNA-dependent RNA polymerases. Nucleic Acids Res. 2015 Jan;43(1):446–60.

105. Zamyatkin DF, Parra F, Alonso JMM, Harki DA, Peterson BR, Grochulski P, et al. Structural insights into mechanisms of catalysis and inhibition in Norwalk virus polymerase. J Biol Chem. 2008 Mar 21;283(12):7705–12.

106. Alam I, Lee JH, Cho KJ, Han KR, Yang JM, Chung MS, et al. Crystal structures of murine norovirus-1 RNA-dependent RNA polymerase in complex with 2-thiouridine or ribavirin. Virology. 2012 May 10;426(2):143–51.

107. Ng KKS, Pendás-Franco N, Rojo J, Boga JA, Machín A, Alonso JMM, et al. Crystal structure of norwalk virus polymerase reveals the carboxyl terminus in the active site cleft. J Biol Chem. 2004 Apr 16;279(16):16638–45.

108. Lee JH, Alam I, Han KR, Cho S, Shin S, Kang S, et al. Crystal structures of murine norovirus-1 RNA-dependent RNA polymerase. J Gen Virol. 2011 Jul;92(Pt 7):1607–16.

109. Högbom M, Jäger K, Robel I, Unge T, Rohayem J. The active form of the norovirus RNA-dependent RNA polymerase is a homodimer with cooperative activity. J Gen Virol. 2009 Feb;90(Pt 2):281–91.

110. Zamyatkin DF, Parra F, Machín A, Grochulski P, Ng KKS. Binding of 2'-amino-2'-deoxycytidine-5'-triphosphate to norovirus polymerase induces rearrangement of the active site. J Mol Biol. 2009 Jul 3;390(1):10–6.

111. Jin Z, Tucker K, Lin X, Kao CC, Shaw K, Tan H, et al. Biochemical Evaluation of the Inhibition Properties of Favipiravir and 2'-C-Methyl-Cytidine Triphosphates against Human and Mouse Norovirus RNA Polymerases. Antimicrob Agents Chemother. 2015 Dec;59(12):7504–16.

112. Rocha-Pereira J, Jochmans D, Dallmeier K, Leyssen P, Nascimento MSJ, Neyts J. Favipiravir (T-705) inhibits in vitro norovirus replication. Biochem Biophys Res Commun. 2012 Aug 10;424(4):777–80.

113. Arias A, Thorne L, Goodfellow I. Favipiravir elicits antiviral mutagenesis during virus replication in vivo. Elife. 2014 Oct 21;3:e03679.

114. Rocha-Pereira J, Jochmans D, Dallmeier K, Leyssen P, Cunha R, Costa I, et al. Inhibition of norovirus replication by the nucleoside analogue 2'-C-methylcytidine. Biochem Biophys Res Commun. 2012 Nov 2;427(4):796–800.

115. Kolawole AO, Rocha-Pereira J, Elftman MD, Neyts J, Wobus CE. Inhibition of human norovirus by a viral polymerase inhibitor in the B cell culture system and in the mouse model. Antiviral Res. 2016 Aug;132:46–9.

116. Rocha-Pereira J, Jochmans D, Debing Y, Verbeken E, Nascimento MSJ, Neyts J. The viral polymerase inhibitor 2'-C-methylcytidine inhibits Norwalk virus replication and protects against norovirus-induced diarrhea and mortality in a mouse model. J Virol. 2013 Nov;87(21):11798–805.

117. Rocha-Pereira J, Kolawole AO, Verbeken E, Wobus CE, Neyts J. Post-exposure antiviral treatment of norovirus infections effectively protects against diarrhea

and reduces virus shedding in the stool in a mortality mouse model. Antiviral Res. 2016 Aug;132:76–84.

118. Rocha-Pereira J, Jochmans D, Neyts J. Prophylactic treatment with the nucleoside analogue 2'-C-methylcytidine completely prevents transmission of norovirus. J Antimicrob Chemother. 2015 Jan;70(1):190–7.

119. Mastrangelo E, Pezzullo M, Tarantino D, Petazzi R, Germani F, Kramer D, et al. Structure-based inhibition of Norovirus RNA-dependent RNA polymerases. J Mol Biol. 2012 Jun 8;419(3–4):198–210.

120. Croci R, Pezzullo M, Tarantino D, Milani M, Tsay SC, Sureshbabu R, et al. Structural bases of norovirus RNA dependent RNA polymerase inhibition by novel suramin-related compounds. PLoS One. 2014;9(3):e91765.

121. Costantini VP, Whitaker T, Barclay L, Lee D, McBrayer TR, Schinazi RF, et al. Antiviral activity of nucleoside analogues against norovirus. Antivir Ther. 2012;17(6):981–91.

122. Tarantino D, Pezzullo M, Mastrangelo E, Croci R, Rohayem J, Robel I, et al. Naphthalene-sulfonate inhibitors of human norovirus RNA-dependent RNA-polymerase. Antiviral Res. 2014 Feb;102:23–8.

123. Kaplan G, Racaniello VR. Construction and characterization of poliovirus subgenomic replicons. J Virol. 1988 May;62(5):1687–96.

124. Lohmann V, Körner F, Koch J, Herian U, Theilmann L, Bartenschlager R. Replication of subgenomic hepatitis C virus RNAs in a hepatoma cell line. Science. 1999 Jul 2;285(5424):110–3.

125. He X, Quan S, Xu M, Rodriguez S, Goh SL, Wei J, et al. Generation of SARS-CoV-2 reporter replicon for high-throughput antiviral screening and testing. Proc Natl Acad Sci U S A. 2021 Apr 13;118(15).

126. Chang KO, Sosnovtsev S V, Belliot G, King AD, Green KY. Stable expression of a Norwalk virus RNA replicon in a human hepatoma cell line. Virology. 2006 Sep 30;353(2):463–73.

127. Enosi Tuipulotu D, Fumian TM, Netzler NE, Mackenzie JM, White PA. The Adenosine Analogue NITD008 has Potent Antiviral Activity against Human and Animal Caliciviruses. Viruses. 2019 May 30;11(6).

128. Arthur SE, Sorgeloos F, Hosmillo M, Goodfellow IG. Epigenetic Suppression of Interferon Lambda Receptor Expression Leads to Enhanced Human Norovirus Replication In Vitro. mBio. 2019 Oct 1;10(5).

129. Li Y, Yu P, Qu C, Li P, Li Y, Ma Z, et al. MDA5 against enteric viruses through induction of interferon-like response partially via the JAK-STAT cascade. Antiviral Res. 2020 Apr;176:104743.

130. Wobus CE, Karst SM, Thackray LB, Chang KO, Sosnovtsev S V, Belliot G, et al. Replication of Norovirus in cell culture reveals a tropism for dendritic cells and macrophages. PLoS Biol. 2004 Dec;2(12):e432.

131. Orchard RC, Wilen CB, Doench JG, Baldridge MT, McCune BT, Lee YCJ, et al. Discovery of a proteinaceous cellular receptor for a norovirus. Science. 2016;353(6302):933–6.

132. Haga K, Fujimoto A, Takai-Todaka R, Miki M, Doan YH, Murakami K, et al. Functional receptor molecules CD300lf and CD300ld within the CD300 family enable murine noroviruses to infect cells. Proc Natl Acad Sci U S A. 2016;113(41):E6248–55.

133. Orchard RC, Sullender ME, Dunlap BF, Balce DR, Doench JG, Virgin HW. Identification of Antinorovirus Genes in Human Cells Using Genome-Wide CRISPR Activation Screening. J Virol. 2019 Jan 1;93(1).

134. Mears H V, Emmott E, Chaudhry Y, Hosmillo M, Goodfellow IG, Sweeney TR. Ifit1 regulates norovirus infection and enhances the interferon response in murine macrophage-like cells. Wellcome Open Res. 2019;4:82.

135. Jones MK, Watanabe M, Zhu S, Graves CL, Keyes LR, Grau KR, et al. Enteric bacteria promote human and mouse norovirus infection of B cells. Science. 2014 Nov 7;346(6210):755–9.

136. Green KY. Editorial Commentary: Noroviruses and B Cells. Clin Infect Dis. 2016 May 1;62(9):1139–40.

137. Ettayebi K, Crawford SE, Murakami K, Broughman JR, Karandikar U, Tenge VR, et al. Replication of human noroviruses in stem cell-derived human enteroids. Science. 2016;353(6306):1387–93.

138. Costantini V, Morantz EK, Browne H, Ettayebi K, Zeng XL, Atmar RL, et al. Human Norovirus Replication in Human Intestinal Enteroids as Model to Evaluate Virus Inactivation. Emerg Infect Dis. 2018 Aug;24(8):1453–64.

139. Overbey KN, Zachos NC, Coulter C, Schwab KJ. Optimizing Human Intestinal Enteroids for Environmental Monitoring of Human Norovirus. Food Environ Virol. 2021 Dec;13(4):470–84.

140. Desdouits M, Polo D, Le Mennec C, Strubbia S, Zeng XL, Ettayebi K, et al. Use of Human Intestinal Enteroids to Evaluate Persistence of Infectious Human Norovirus in Seawater. Emerg Infect Dis. 2022 Jul;28(7):1475–9.

141. Chan MCW, Cheung SKC, Mohammad KN, Chan JCM, Estes MK, Chan PKS. Use of Human Intestinal Enteroids to Detect Human Norovirus Infectivity. Emerg Infect Dis. 2019 Sep;25(9):1730–5.

142. Ward VK, McCormick CJ, Clarke IN, Salim O, Wobus CE, Thackray LB, et al. Recovery of infectious murine norovirus using pol II-driven expression of full-length cDNA. Proc Natl Acad Sci U S A. 2007 Jun 26;104(26):11050–5.

143. Yunus MA, Chung LMW, Chaudhry Y, Bailey D, Goodfellow I. Development of an optimized RNA-based murine norovirus reverse genetics system. J Virol Methods. 2010 Oct;169(1):112–8.

144. Harrington PR, Lindesmith L, Yount B, Moe CL, Baric RS. Binding of Norwalk virus-like particles to ABH histo-blood group antigens is blocked by antisera from infected human volunteers or experimentally vaccinated mice. J Virol. 2002 Dec;76(23):12335–43.

145. Marionneau S, Ruvoën N, le Moullac-Vaidye B, Clement M, Cailleau-Thomas A, Ruiz-Palacois G, et al. Norwalk virus binds to histo-blood group antigens present on gastroduodenal epithelial cells of secretor individuals. Gastroenterology. 2002 Jun;122(7):1967–77.

146. Huang P, Farkas T, Marionneau S, Zhong W, Ruvoën-Clouet N, Morrow AL, et al. Noroviruses bind to human ABO, Lewis, and secretor histo-blood group antigens: identification of 4 distinct strain-specific patterns. J Infect Dis. 2003 Jul 1;188(1):19–31.

147. Cao S, Lou Z, Tan M, Chen Y, Liu Y, Zhang Z, et al. Structural basis for the recognition of blood group trisaccharides by norovirus. J Virol. 2007 Jun;81(11):5949–57.

148. Singh BK, Leuthold MM, Hansman GS. Human noroviruses' fondness for histo-blood group antigens. J Virol. 2015 Feb;89(4):2024–40.

149. Shanker S, Czako R, Sankaran B, Atmar RL, Estes MK, Prasad BVV. Structural analysis of determinants of histo-blood group antigen binding specificity in genogroup I noroviruses. J Virol. 2014 Jun;88(11):6168–80.

150. Huang P, Farkas T, Zhong W, Tan M, Thornton S, Morrow AL, et al. Norovirus and histo-blood group antigens: demonstration of a wide spectrum of strain specificities and classification of two major binding groups among multiple binding patterns. J Virol. 2005 Jun;79(11):6714–22.

151. Tan M, Xia M, Chen Y, Bu W, Hegde RS, Meller J, et al. Conservation of carbohydrate binding interfaces: evidence of human HBGA selection in norovirus evolution. PLoS One. 2009;4(4):e5058.

152. Thorven M, Grahn A, Hedlund KO, Johansson H, Wahlfrid C, Larson G, et al. A homozygous nonsense mutation (428G-->A) in the human secretor (FUT2) gene provides resistance to symptomatic norovirus (GGII) infections. J Virol. 2005 Dec;79(24):15351–5.

153. Currier RL, Payne DC, Staat MA, Selvarangan R, Shirley SH, Halasa N, et al. Innate Susceptibility to Norovirus Infections Influenced by FUT2 Genotype in a United States Pediatric Population. Clin Infect Dis. 2015 Jun 1;60(11):1631–8.

154. Miura T, Sano D, Suenaga A, Yoshimura T, Fuzawa M, Nakagomi T, et al. Histo-blood group antigen-like substances of human enteric bacteria as specific adsorbents for human noroviruses. J Virol. 2013 Sep;87(17):9441–51.

155. Almand EA, Moore MD, Jaykus LA. Characterization of human norovirus binding to gut-associated bacterial ligands. BMC Res Notes. 2019 Sep 23;12(1):607.

156. Almand EA, Moore MD, Outlaw J, Jaykus LA. Human norovirus binding to select bacteria representative of the human gut microbiota. PLoS One. 2017;12(3):e0173124.

157. Kilic T, Koromyslova A, Hansman GS. Structural Basis for Human Norovirus Capsid Binding to Bile Acids. J Virol. 2019;93(2).

158. Lindesmith LC, Brewer-Jensen PD, Mallory ML, Jensen K, Yount BL, Costantini V, et al. Virus-Host Interactions Between Nonsecretors and Human Norovirus. Cell Mol Gastroenterol Hepatol. 2020;10(2):245–67.

159. Nelson CA, Wilen CB, Dai YN, Orchard RC, Kim AS, Stegeman RA, et al. Structural basis for murine norovirus engagement of bile acids and the CD300lf receptor. Proc Natl Acad Sci U S A. 2018;115(39):E9201–10.

160. Williams AN, Sherman MB, Smith HQ, Taube S, Pettitt BM, Wobus CE, et al. A Norovirus Uses Bile Salts To Escape Antibody Recognition While Enhancing Receptor Binding. J Virol. 2021;95(13):e0017621.

161. Rydell GE, Nilsson J, Rodriguez-Diaz J, Ruvoën-Clouet N, Svensson L, le Pendu J, et al. Human noroviruses recognize sialyl Lewis x neoglycoprotein. Glycobiology. 2009 Mar;19(3):309–20.

162. Taube S, Perry JW, Yetming K, Patel SP, Auble H, Shu L, et al. Ganglioside-linked terminal sialic acid moieties on murine macrophages function as attachment receptors for murine noroviruses. J Virol. 2009 May;83(9):4092–101.

163. Han L, Tan M, Xia M, Kitova EN, Jiang X, Klassen JS. Gangliosides are ligands for human noroviruses. J Am Chem Soc. 2014 Sep 10;136(36):12631–7.

164. Wegener H, Mallagaray Á, Schöne T, Peters T, Lockhauserbäumer J, Yan H, et al. Human norovirus GII.4(MI001) P dimer binds fucosylated and sialylated carbohydrates. Glycobiology. 2017;27(11):1027–37.

165. Stuart AD, Brown TDK. Alpha2,6-linked sialic acid acts as a receptor for Feline calicivirus. J Gen Virol. 2007 Jan;88(Pt 1):177–86.

166. Tan M, Wei C, Huang P, Fan Q, Quigley C, Xia M, et al. Tulane virus recognizes sialic acids as cellular receptors. Sci Rep. 2015 Jul 6;5:11784.

167. Kim DS, Hosmillo M, Alfajaro MM, Kim JY, Park JG, Son KY, et al. Both α2,3- and α2,6-linked sialic acids on O-linked glycoproteins act as functional receptors for porcine Sapovirus. PLoS Pathog. 2014 Jun;10(6):e1004172.

168. Creutznacher R, Maass T, Ogrissek P, Wallmann G, Feldmann C, Peters H, et al. NMR Experiments Shed New Light on Glycan Recognition by Human and Murine Norovirus Capsid Proteins. Viruses. 2021;13(3).

169. Grau KR, Roth AN, Zhu S, Hernandez A, Colliou N, DiVita BB, et al. The major targets of acute norovirus infection are immune cells in the gut-associated lymphoid tissue. Nat Microbiol. 2017 Dec;2(12):1586–91.

170. Wilen CB, Lee S, Hsieh LL, Orchard RC, Desai C, Hykes BL, et al. Tropism for tuft cells determines immune promotion of norovirus pathogenesis. Science. 2018 Apr 13;360(6385):204–8.

171. Karandikar UC, Crawford SE, Ajami NJ, Murakami K, Kou B, Ettayebi K, et al. Detection of human norovirus in intestinal biopsies from immunocompromised transplant patients. J Gen Virol. 2016;97(9):2291–300.

172. Green KY, Kaufman SS, Nagata BM, Chaimongkol N, Kim DY, Levenson EA, et al. Human norovirus targets enteroendocrine epithelial cells in the small intestine. Nat Commun. 2020;11(1):2759.

173. Perry JW, Taube S, Wobus CE. Murine norovirus-1 entry into permissive macrophages and dendritic cells is pH-independent. Virus Res. 2009 Jul;143(1):125–9.

174. Gerondopoulos A, Jackson T, Monaghan P, Doyle N, Roberts LO. Murine norovirus-1 cell entry is mediated through a non-clathrin-, non-caveolae-, dynamin- and cholesterol-dependent pathway. J Gen Virol. 2010 Jun;91(Pt 6):1428–38.

175. Ayyar BV, Ettayebi K, Salmen W, Karandikar UC, Neill FH, Tenge VR, et al. CLIC and membrane wound repair pathways enable pandemic norovirus entry and infection. Nat Commun. 2023 Feb 28;14(1):1148.

176. López-Manríquez E, Vashist S, Ureña L, Goodfellow I, Chavez P, Mora-Heredia JE, et al. Norovirus genome circularization and efficient replication are facilitated by binding of PCBP2 and hnRNP A1. J Virol. 2013 Nov;87(21):11371–87.

177. Gutiérrez-Escolano AL, Brito ZU, del Angel RM, Jiang X. Interaction of cellular proteins with the 5’ end of Norwalk virus genomic RNA. J Virol. 2000 Sep;74(18):8558–62.

178. Sanford TJ, Mears H v, Fajardo T, Locker N, Sweeney TR. Circularization of flavivirus genomic RNA inhibits de novo translation initiation. Nucleic Acids Res. 2019;47(18):9789–802.

179. Souii A, M’hadheb-Gharbi M ben, Gharbi J. Cellular Proteins Act as Bridge Between 5’ and 3’ Ends of the Coxsackievirus B3 Mediating Genome Circularization During RNA Translation. Curr Microbiol. 2015 Sep;71(3):387–95.

180. Wells SE, Hillner PE, Vale RD, Sachs AB. Circularization of mRNA by eukaryotic translation initiation factors. Mol Cell. 1998 Jul;2(1):135–40.

181. Belliot G, Sosnovtsev S V, Mitra T, Hammer C, Garfield M, Green KY. In vitro proteolytic processing of the MD145 norovirus ORF1 nonstructural polyprotein

yields stable precursors and products similar to those detected in calicivirus-infected cells. J Virol. 2003 Oct;77(20):10957–74.

182. May J, Korba B, Medvedev A, Viswanathan P. Enzyme kinetics of the human norovirus protease control virus polyprotein processing order. Virology. 2013 Sep;444(1–2):218–24.

183. Fukushi S, Kojima S, Takai R, Hoshino FB, Oka T, Takeda N, et al. Poly(A)- and primer-independent RNA polymerase of Norovirus. J Virol. 2004 Apr;78(8):3889–96.

184. Rohayem J, Robel I, Jäger K, Scheffler U, Rudolph W. Protein-primed and de novo initiation of RNA synthesis by norovirus 3Dpol. J Virol. 2006 Jul;80(14):7060–9.

185. Thorne LG, Goodfellow IG. Norovirus gene expression and replication. J Gen Virol. 2014 Feb;95(Pt 2):278–91.

186. Pettersson RF, Ambros V, Baltimore D. Identification of a protein linked to nascent poliovirus RNA and to the polyuridylic acid of negative-strand RNA. J Virol. 1978 Aug;27(2):357–65.

187. Subba-Reddy C V, Goodfellow I, Kao CC. VPg-primed RNA synthesis of norovirus RNA-dependent RNA polymerases by using a novel cell-based assay. J Virol. 2011 Dec;85(24):13027–37.

188. Arai H, Nishigaki K, Nemoto N, Suzuki M, Husimi Y. Characterization of norovirus RNA replicase for in vitro amplification of RNA. BMC Biotechnol. 2013 Oct 9;13:85.

189. Shimoike T, Hayashi T, Oka T, Muramatsu M. The predicted stem-loop structure in the 3'-end of the human norovirus antigenomic sequence is required for its genomic RNA synthesis by its RdRp. J Biol Chem. 2021;297(4):101225.

190. Borg C, Jahun AS, Thorne L, Sorgeloos F, Bailey D, Goodfellow IG. Murine norovirus virulence factor 1 (VF1) protein contributes to viral fitness during persistent infection. J Gen Virol. 2021;102(9).

191. Prasad B v, Rothnagel R, Jiang X, Estes MK. Three-dimensional structure of baculovirus-expressed Norwalk virus capsids. J Virol. 1994 Aug;68(8):5117–25.

192. Bertolotti-Ciarlet A, White LJ, Chen R, Prasad BVV, Estes MK. Structural requirements for the assembly of Norwalk virus-like particles. J Virol. 2002 Apr;76(8):4044–55.

193. Hu L, Salmen W, Chen R, Zhou Y, Neill F, Crowe JE, et al. Atomic structure of the predominant GII.4 human norovirus capsid reveals novel stability and plasticity. Nat Commun. 2022 Mar 10;13(1):1241.

194. Sosnovtsev S v, Belliot G, Chang KO, Onwudiwe O, Green KY. Feline calicivirus VP2 is essential for the production of infectious virions. J Virol. 2005 Apr;79(7):4012–24.

195. Vongpunsawad S, Venkataram Prasad B v, Estes MK. Norwalk Virus Minor Capsid Protein VP2 Associates within the VP1 Shell Domain. J Virol. 2013 May;87(9):4818–25.

196. Alonso C, Oviedo JM, Martín-Alonso JM, Díaz E, Boga JA, Parra F. Programmed cell death in the pathogenesis of rabbit hemorrhagic disease. Arch Virol. 1998;143(2):321–32.

197. Sosnovtsev S v, Prikhod'ko EA, Belliot G, Cohen JI, Green KY. Feline calicivirus replication induces apoptosis in cultured cells. Virus Res. 2003 Jul;94(1):1–10.

198. Bok K, Prikhodko VG, Green KY, Sosnovtsev S v. Apoptosis in murine norovirus-infected RAW264.7 cells is associated with downregulation of survivin. J Virol. 2009 Apr;83(8):3647–56.

199. Furman LM, Maaty WS, Petersen LK, Ettayebi K, Hardy ME, Bothner B. Cysteine protease activation and apoptosis in Murine norovirus infection. Virol J. 2009 Sep 10;6:139.

200. Troeger H, Loddenkemper C, Schneider T, Schreier E, Epple HJ, Zeitz M, et al. Structural and functional changes of the duodenum in human norovirus infection. Gut. 2009 Aug;58(8):1070–7.

201. Kaufman SS, Chatterjee NK, Fuschino ME, Morse DL, Morotti RA, Magid MS, et al. Characteristics of human calicivirus enteritis in intestinal transplant recipients. J Pediatr Gastroenterol Nutr. 2005 Mar;40(3):328–33.

202. Bok K, Green KY. Norovirus gastroenteritis in immunocompromised patients. N Engl J Med. 2012 Nov 29;367(22):2126–32.

203. Santiana M, Ghosh S, Ho BA, Rajasekaran V, Du WL, Mutsafi Y, et al. Vesicle-Cloaked Virus Clusters Are Optimal Units for Inter-organismal Viral Transmission. Cell Host Microbe. 2018 Aug 8;24(2):208-220.e8.

204. Enosi Tuipulotu D, Netzler NE, Lun JH, Mackenzie JM, White PA. TLR7 Agonists Display Potent Antiviral Effects against Norovirus Infection via Innate Stimulation. Antimicrob Agents Chemother. 2018 May;62(5).

205. Ponterio E, Mariotti S, Tabolacci C, Ruggeri FM, Nisini R. Virus like particles of GII.4 norovirus bind Toll Like Receptors 2 and 5. Immunol Lett. 2019 Nov;215:40–4.

206. Lee W, Kim M, Lee SH, Jung HG, Oh JW. Prophylactic efficacy of orally administered Bacillus poly-γ-glutamic acid, a non-LPS TLR4 ligand, against norovirus infection in mice. Sci Rep. 2018 Jun 6;8(1):8667.

207. MacDuff DA, Baldridge MT, Qaqish AM, Nice TJ, Darbandi AD, Hartley VL, et al. HOIL1 Is Essential for the Induction of Type I and III Interferons by MDA5 and Regulates Persistent Murine Norovirus Infection. J Virol. 2018 Dec 1;92(23).

208. McCartney SA, Thackray LB, Gitlin L, Gilfillan S, Virgin HW, Colonna M. MDA-5 recognition of a murine norovirus. PLoS Pathog. 2008 Jul 18;4(7):e1000108.

209. Jahun AS, Goodfellow IG. Interferon responses to norovirus infections: current and future perspectives. J Gen Virol. 2021 Oct;102(10).

210. Yu P, Li Y, Li Y, Miao Z, Wang Y, Peppelenbosch MP, et al. Murine norovirus replicase augments RIG-I-like receptors-mediated antiviral interferon response. Antiviral Res. 2020 Oct;182:104877.

211. Lee W, Lee SH, Kim M, Moon JS, Kim GW, Jung HG, et al. Vibrio vulnificus quorum-sensing molecule cyclo(Phe-Pro) inhibits RIG-I-mediated antiviral innate immunity. Nat Commun. 2018 Apr 23;9(1):1606.

212. Dang W, Xu L, Yin Y, Chen S, Wang W, Hakim MS, et al. IRF-1, RIG-I and MDA5 display potent antiviral activities against norovirus coordinately induced by different types of interferons. Antiviral Res. 2018 Jul;155:48–59.

213. Mumphrey SM, Changotra H, Moore TN, Heimann-Nichols ER, Wobus CE, Reilly MJ, et al. Murine norovirus 1 infection is associated with histopathological changes in immunocompetent hosts, but clinical disease is prevented by STAT1-dependent interferon responses. J Virol. 2007 Apr;81(7):3251–63.

214. Karst SM, Wobus CE, Lay M, Davidson J, Virgin HW. STAT1-dependent innate immunity to a Norwalk-like virus. Science. 2003 Mar 7;299(5612):1575–8.

215. Wang P, Zhu S, Yang L, Cui S, Pan W, Jackson R, et al. Nlrp6 regulates intestinal antiviral innate immunity. Science. 2015 Nov 13;350(6262):826–30.

216. Pattabhi S, Knoll ML, Gale M, Loo YM. DHX15 Is a Coreceptor for RLR Signaling That Promotes Antiviral Defense Against RNA Virus Infection. J Interferon Cytokine Res. 2019 Jun;39(6):331–46.

217. Jahun AS, Sorgeloos F, Chaudhry Y, Arthur SE, Hosmillo M, Georgana I, et al. Leaked genomic and mitochondrial DNA contribute to the host response to noroviruses in a STING-dependent manner. Cell Rep. 2023 Mar 28;42(3):112179.

218. Yu P, Miao Z, Li Y, Bansal R, Peppelenbosch MP, Pan Q. cGAS-STING effectively restricts murine norovirus infection but antagonizes the antiviral action of N-terminus of RIG-I in mouse macrophages. Gut Microbes. 2021;13(1):1959839.

219. Thackray LB, Duan E, Lazear HM, Kambal A, Schreiber RD, Diamond MS, et al. Critical role for interferon regulatory factor 3 (IRF-3) and IRF-7 in type I interferon-mediated control of murine norovirus replication. J Virol. 2012 Dec;86(24):13515–23.

220. Zhu S, Regev D, Watanabe M, Hickman D, Moussatche N, Jesus DM, et al. Identification of immune and viral correlates of norovirus protective immunity through comparative study of intra-cluster norovirus strains. PLoS Pathog. 2013;9(9):e1003592.

221. Niendorf S, Klemm U, Mas Marques A, Bock CT, Höhne M. Infection with the Persistent Murine Norovirus Strain MNV-S99 Suppresses IFN-Beta Release and Activation of Stat1 In Vitro. PLoS One. 2016;11(6):e0156898.

222. Baldridge MT, Lee S, Brown JJ, McAllister N, Urbanek K, Dermody TS, et al. Expression of Ifnlr1 on Intestinal Epithelial Cells Is Critical to the Antiviral Effects of Interferon Lambda against Norovirus and Reovirus. J Virol. 2017 Apr 1;91(7).

223. Nice TJ, Baldridge MT, McCune BT, Norman JM, Lazear HM, Artyomov M, et al. Interferon-λ cures persistent murine norovirus infection in the absence of adaptive immunity. Science. 2015 Jan 16;347(6219):269–73.

224. Qu L, Murakami K, Broughman JR, Lay MK, Guix S, Tenge VR, et al. Replication of Human Norovirus RNA in Mammalian Cells Reveals Lack of Interferon Response. J Virol. 2016 Oct 1;90(19):8906–23.

225. Lindesmith L, Moe C, Lependu J, Frelinger JA, Treanor J, Baric RS. Cellular and humoral immunity following Snow Mountain virus challenge. J Virol. 2005 Mar;79(5):2900–9.

226. Tacket CO, Sztein MB, Losonsky GA, Wasserman SS, Estes MK. Humoral, mucosal, and cellular immune responses to oral Norwalk virus-like particles in volunteers. Clin Immunol. 2003 Sep;108(3):241–7.

227. Newman KL, Moe CL, Kirby AE, Flanders WD, Parkos CA, Leon JS. Human norovirus infection and the acute serum cytokine response. Clin Exp Immunol. 2015 Nov;182(2):195–203.

228. Lin L, Han J, Yan T, Li L, Li J, Ao Y, et al. Replication and transcriptionomic analysis of human noroviruses in human intestinal enteroids. Am J Transl Res. 2019;11(6):3365–74.

229. Neufeldt CJ, Cortese M. Membrane architects: how positive-strand RNA viruses restructure the cell. J Gen Virol. 2022;103(8).

230. Nguyen-Dinh V, Herker E. Ultrastructural Features of Membranous Replication Organelles Induced by Positive-Stranded RNA Viruses. Cells. 2021;10(9).

231. Belov GA, van Kuppeveld FJM. (+)RNA viruses rewire cellular pathways to build replication organelles. Curr Opin Virol. 2012 Dec;2(6):740–7.

232. Neufeldt CJ, Joyce MA, van Buuren N, Levin A, Kirkegaard K, Gale M, et al. The Hepatitis C Virus-Induced Membranous Web and Associated Nuclear Transport Machinery Limit Access of Pattern Recognition Receptors to Viral Replication Sites. PLoS Pathog. 2016 Feb;12(2):e1005428.

233. Du X, Zhang Y, Zou J, Yuan Z, Yi Z. Replicase-mediated shielding of the poliovirus replicative double-stranded RNA to avoid recognition by MDA5. J Gen Virol. 2018;99(9):1199–209.

234. Knoops K, Kikkert M, Worm SHE van den, Zevenhoven-Dobbe JC, van der Meer Y, Koster AJ, et al. SARS-coronavirus replication is supported by a reticulovesicular network of modified endoplasmic reticulum. PLoS Biol. 2008 Sep 16;6(9):e226.

235. Viktorova EG, Nchoutmboube JA, Ford-Siltz LA, Iverson E, Belov GA. Phospholipid synthesis fueled by lipid droplets drives the structural development of poliovirus replication organelles. PLoS Pathog. 2018;14(8):e1007280.

236. Nagy PD, Strating JRPM, van Kuppeveld FJM. Building Viral Replication Organelles: Close Encounters of the Membrane Types. PLoS Pathog. 2016;12(10):e1005912.

237. Harak C, Lohmann V. Ultrastructure of the replication sites of positive-strand RNA viruses. Virology. 2015 May;479–480:418–33.

238. Gottipati K, Woodson M, Choi KH. Membrane binding and rearrangement by chikungunya virus capping enzyme nsP1. Virology. 2020;544:31–41.

239. Frolova EI, Gorchakov R, Pereboeva L, Atasheva S, Frolov I. Functional Sindbis virus replicative complexes are formed at the plasma membrane. J Virol. 2010 Nov;84(22):11679–95.

240. Belov GA, Nair V, Hansen BT, Hoyt FH, Fischer ER, Ehrenfeld E. Complex dynamic development of poliovirus membranous replication complexes. J Virol. 2012 Jan;86(1):302–12.

241. Jackson WT. Poliovirus-induced changes in cellular membranes throughout infection. Curr Opin Virol. 2014 Dec;9:67–73.

242. Limpens RWAL, van der Schaar HM, Kumar D, Koster AJ, Snijder EJ, van Kuppeveld FJM, et al. The transformation of enterovirus replication structures: a three-dimensional study of single- and double-membrane compartments. mBio. 2011;2(5).

243. Romero-Brey I, Merz A, Chiramel A, Lee JY, Chlanda P, Haselman U, et al. Three-dimensional architecture and biogenesis of membrane structures associated with hepatitis C virus replication. PLoS Pathog. 2012;8(12):e1003056.

244. Romero-Brey I, Berger C, Kallis S, Kolovou A, Paul D, Lohmann V, et al. NS5A Domain 1 and Polyprotein Cleavage Kinetics Are Critical for Induction of Double-Membrane Vesicles Associated with Hepatitis C Virus Replication. mBio. 2015 Jul 7;6(4):e00759.

245. Cotton BT, Hyde JL, Sarvestani ST, Sosnovtsev S v, Green KY, White PA, et al. The Norovirus NS3 Protein Is a Dynamic Lipid- and Microtubule-Associated Protein Involved in Viral RNA Replication. J Virol. 2017 Feb 1;91(3).

246. Dias SSG, Soares VC, Ferreira AC, Sacramento CQ, Fintelman-Rodrigues N, Temerozo JR, et al. Lipid droplets fuel SARS-CoV-2 replication and production of inflammatory mediators. PLoS Pathog. 2020;16(12):e1009127.

247. Laufman O, Perrino J, Andino R. Viral Generated Inter-Organelle Contacts Redirect Lipid Flux for Genome Replication. Cell. 2019;178(2):275-289.e16.

248. Viktorova EG, Nchoutmboube JA, Ford-Siltz LA, Iverson E, Belov GA. Phospholipid synthesis fueled by lipid droplets drives the structural development of poliovirus replication organelles. PLoS Pathog. 2018;14(8):e1007280.

249. Sharp TM, Guix S, Katayama K, Crawford SE, Estes MK. Inhibition of cellular protein secretion by norwalk virus nonstructural protein p22 requires a mimic of an endoplasmic reticulum export signal. PLoS One. 2010 Oct 18;5(10):e13130.

250. Vogt DA, Camus G, Herker E, Webster BR, Tsou CL, Greene WC, et al. Lipid droplet-binding protein TIP47 regulates hepatitis C Virus RNA replication through interaction with the viral NS5A protein. PLoS Pathog. 2013;9(4):e1003302.

251. Salloum S, Wang H, Ferguson C, Parton RG, Tai AW. Rab18 binds to hepatitis C virus NS5A and promotes interaction between sites of viral replication and lipid droplets. PLoS Pathog. 2013;9(8):e1003513.

252. Cho NJ, Cheong KH, Lee C, Frank CW, Glenn JS. Binding dynamics of hepatitis C virus' NS5A amphipathic peptide to cell and model membranes. J Virol. 2007 Jun;81(12):6682–9.

253. Elazar M, Cheong KH, Liu P, Greenberg HB, Rice CM, Glenn JS. Amphipathic helix-dependent localization of NS5A mediates hepatitis C virus RNA replication. J Virol. 2003 May;77(10):6055–61.

254. Brass V, Pal Z, Sapay N, Deléage G, Blum HE, Penin F, et al. Conserved determinants for membrane association of nonstructural protein 5A from hepatitis C virus and related viruses. J Virol. 2007 Mar;81(6):2745–57.

255. Brass V, Bieck E, Montserret R, Wölk B, Hellings JA, Blum HE, et al. An amino-terminal amphipathic alpha-helix mediates membrane association of the hepatitis C virus nonstructural protein 5A. J Biol Chem. 2002 Mar 8;277(10):8130–9.

256. Jecht M, Probst C, Gauss-Müller V. Membrane permeability induced by hepatitis A virus proteins 2B and 2BC and proteolytic processing of HAV 2BC. Virology. 1998 Dec 5;252(1):218–27.

257. Drin G, Antonny B. Amphipathic helices and membrane curvature. FEBS Lett. 2010 May 3;584(9):1840–7.

258. Thorne L, Bailey D, Goodfellow I. High-resolution functional profiling of the norovirus genome. J Virol. 2012 Nov;86(21):11441–56.

259. Chen Y, Wu Q, Li G, Li H, Li W, Li H, et al. Identification and genetic characterization of a minor norovirus genotype, GIX.1[GII.P15], from China. BMC Genom Data. 2022 Jul 6;23(1):50.

260. Parra GI. Emergence of norovirus strains: A tale of two genes. Virus Evol. 2019 Jul;5(2):vez048.

261. Fujita K, Krishnakumar SS, Franco D, Paul A V, London E, Wimmer E. Membrane topography of the hydrophobic anchor sequence of poliovirus 3A and 3AB proteins and the functional effect of 3A/3AB membrane association upon RNA replication. Biochemistry. 2007 May 1;46(17):5185–99.

262. Towner JS, Ho T V, Semler BL. Determinants of membrane association for poliovirus protein 3AB. J Biol Chem. 1996 Oct 25;271(43):26810–8.

263. May J, Viswanathan P, Ng KKS, Medvedev A, Korba B. The p4-p2' amino acids surrounding human norovirus polyprotein cleavage sites define the core sequence regulating self-processing order. J Virol. 2014 Sep;88(18):10738–47.

264. Hu B, Siche S, Möller L, Veit M. Amphipathic Helices of Cellular Proteins Can Replace the Helix in M2 of Influenza A Virus with Only Small Effects on Virus Replication. J Virol. 2020 Jan 17;94(3).

265. Teterina NL, Gorbalenya AE, Egger D, Bienz K, Rinaudo MS, Ehrenfeld E. Testing the modularity of the N-terminal amphipathic helix conserved in picornavirus 2C proteins and hepatitis C NS5A protein. Virology. 2006 Jan 20;344(2):453–67.

266. Perera R, Navaratnarajah C, Kuhn RJ. A heterologous coiled coil can substitute for helix I of the Sindbis virus capsid protein. J Virol. 2003 Aug;77(15):8345–53.

267. Lee H, Liu Y, Mejia E, Paul A V, Wimmer E. The C-terminal hydrophobic domain of hepatitis C virus RNA polymerase NS5B can be replaced with a heterologous domain of poliovirus protein 3A. J Virol. 2006 Nov;80(22):11343–54.

268. Vives-Adrián L, Garriga D, Buxaderas M, Fraga J, Pereira PJB, Macedo-Ribeiro S, et al. Structural basis for host membrane remodeling induced by protein 2B of hepatitis A virus. J Virol. 2015 Apr;89(7):3648–58.

269. Lundin M, Monné M, Widell A, Von Heijne G, Persson MAA. Topology of the membrane-associated hepatitis C virus protein NS4B. J Virol. 2003 May;77(9):5428–38.

270. Miller S, Kastner S, Krijnse-Locker J, Bühler S, Bartenschlager R. The non-structural protein 4A of dengue virus is an integral membrane protein inducing membrane alterations in a 2K-regulated manner. J Biol Chem. 2007 Mar 23;282(12):8873–82.

271. Hügle T, Fehrmann F, Bieck E, Kohara M, Kräusslich HG, Rice CM, et al. The hepatitis C virus nonstructural protein 4B is an integral endoplasmic reticulum membrane protein. Virology. 2001 May 25;284(1):70–81.

272. Cortese M, Mulder K, Chatel-Chaix L, Scaturro P, Cerikan B, Plaszczyca A, et al. Determinants in Nonstructural Protein 4A of Dengue Virus Required for RNA Replication and Replication Organelle Biogenesis. J Virol. 2021 Oct 13;95(21):e0131021.

273. Gouttenoire J, Montserret R, Kennel A, Penin F, Moradpour D. An amphipathic alpha-helix at the C terminus of hepatitis C virus nonstructural protein 4B mediates membrane association. J Virol. 2009 Nov;83(21):11378–84.

274. Fujiki Y, Hubbard AL, Fowler S, Lazarow PB. Isolation of intracellular membranes by means of sodium carbonate treatment: application to endoplasmic reticulum. J Cell Biol. 1982 Apr;93(1):97–102.

275. Kim H, Botelho SC, Park K, Kim H. Use of carbonate extraction in analyzing moderately hydrophobic transmembrane proteins in the mitochondrial inner membrane. Protein Sci. 2015 Dec;24(12):2063–9.

276. Einav S, Elazar M, Danieli T, Glenn JS. A nucleotide binding motif in hepatitis C virus (HCV) NS4B mediates HCV RNA replication. J Virol. 2004 Oct;78(20):11288–95.

277. Paul D, Romero-Brey I, Gouttenoire J, Stoitsova S, Krijnse-Locker J, Moradpour D, et al. NS4B self-interaction through conserved C-terminal elements is required for the establishment of functional hepatitis C virus replication complexes. J Virol. 2011 Jul;85(14):6963–76.

278. Zou J, Xie X, Wang QY, Dong H, Lee MY, Kang C, et al. Characterization of dengue virus NS4A and NS4B protein interaction. J Virol. 2015 Apr;89(7):3455–70.

279. Oostra M, Hagemeijer MC, van Gent M, Bekker CPJ, te Lintelo EG, Rottier PJM, et al. Topology and membrane anchoring of the coronavirus replication complex: not all hydrophobic domains of nsp3 and nsp6 are membrane spanning. J Virol. 2008 Dec;82(24):12392–405.

280. Wolff G, Limpens RWAL, Zevenhoven-Dobbe JC, Laugks U, Zheng S, de Jong AWM, et al. A molecular pore spans the double membrane of the coronavirus replication organelle. Science. 2020 Sep 11;369(6509):1395–8.

281. Jones R, Bragagnolo G, Arranz R, Reguera J. Capping pores of alphavirus nsP1 gate membranous viral replication factories. Nature. 2021 Jan;589(7843):615–9.

282. Jones R, Hons M, Rabah N, Zamarreño N, Arranz R, Reguera J. Structural basis and dynamics of Chikungunya alphavirus RNA capping by nsP1 capping pores. Proc Natl Acad Sci U S A. 2023 Mar 21;120(12):e2213934120.

283. Drin G, Casella JF, Gautier R, Boehmer T, Schwartz TU, Antonny B. A general amphipathic alpha-helical motif for sensing membrane curvature. Nat Struct Mol Biol. 2007 Feb;14(2):138–46.

284. Penin F, Brass V, Appel N, Ramboarina S, Montserret R, Ficheux D, et al. Structure and function of the membrane anchor domain of hepatitis C virus nonstructural protein 5A. J Biol Chem. 2004 Sep 24;279(39):40835–43.

285. Varkey J, Zhang J, Kim J, George G, He G, Belov G, et al. An Amphipathic Alpha-Helix Domain from Poliovirus 2C Protein Tubulate Lipid Vesicles. Viruses. 2020 Dec 18;12(12).

286. Hung YF, Schwarten M, Hoffmann S, Willbold D, Sklan EH, Koenig B. Amino Terminal Region of Dengue Virus NS4A Cytosolic Domain Binds to Highly Curved Liposomes. Viruses. 2015 Jul 21;7(7):4119–30.

287. Hung YF, Schwarten M, Schünke S, Thiagarajan-Rosenkranz P, Hoffmann S, Sklan EH, et al. Dengue virus NS4A cytoplasmic domain binding to liposomes is sensitive to membrane curvature. Biochim Biophys Acta. 2015 May;1848(5):1119–26.

288. Martyna A, Bahsoun B, Badham MD, Srinivasan S, Howard MJ, Rossman JS. Membrane remodeling by the M2 amphipathic helix drives influenza virus membrane scission. Sci Rep. 2017 Mar 20;7:44695.

289. Miller S, Krijnse-Locker J. Modification of intracellular membrane structures for virus replication. Nat Rev Microbiol. 2008 May;6(5):363–74.

290. Rossman JS, Jing X, Leser GP, Lamb RA. Influenza virus M2 protein mediates ESCRT-independent membrane scission. Cell. 2010 Sep 17;142(6):902–13.

291. Nishimura T, Lazzeri G, Mizushima N, Covino R, Tooze SA. Unique amphipathic α helix drives membrane insertion and enzymatic activity of ATG3. Sci Adv. 2023 Jun 23;9(25):eadh1281.

292. Boucrot E, Pick A, Çamdere G, Liska N, Evergren E, McMahon HT, et al. Membrane fission is promoted by insertion of amphipathic helices and is restricted by crescent BAR domains. Cell. 2012 Mar 30;149(1):124–36.

293. Milstein ML, Kimler VA, Ghatak C, Ladokhin AS, Goldberg AFX. An inducible amphipathic helix within the intrinsically disordered C terminus can participate in membrane curvature generation by peripherin-2/rds. J Biol Chem. 2017 May 12;292(19):7850–65.

294. Khattree N, Ritter LM, Goldberg AFX. Membrane curvature generation by a C-terminal amphipathic helix in peripherin-2/rds, a tetraspanin required for photoreceptor sensory cilium morphogenesis. J Cell Sci. 2013 Oct 15;126(Pt 20):4659–70.

295. Herlo R, Lund VK, Lycas MD, Jansen AM, Khelashvili G, Andersen RC, et al. An Amphipathic Helix Directs Cellular Membrane Curvature Sensing and Function of the BAR Domain Protein PICK1. Cell Rep. 2018 May 15;23(7):2056–69.

296. Romero-García J, Biarnés X, Planas A. Essential Mycoplasma Glycolipid Synthase Adheres to the Cell Membrane by Means of an Amphipathic Helix. Sci Rep. 2019 May 8;9(1):7085.

297. Sapay N, Montserret R, Chipot C, Brass V, Moradpour D, Deléage G, et al. NMR structure and molecular dynamics of the in-plane membrane anchor of

nonstructural protein 5A from bovine viral diarrhea virus. Biochemistry. 2006 Feb 21;45(7):2221–33.

298. Lampio A, Kilpeläinen I, Pesonen S, Karhi K, Auvinen P, Somerharju P, et al. Membrane binding mechanism of an RNA virus-capping enzyme. J Biol Chem. 2000 Dec 1;275(48):37853–9.

299. Komatsu K, Sasaki N, Yoshida T, Suzuki K, Masujima Y, Hashimoto M, et al. Identification of a Proline-Kinked Amphipathic α-Helix Downstream from the Methyltransferase Domain of a Potexvirus Replicase and Its Role in Virus Replication and Perinuclear Complex Formation. J Virol. 2021 Sep 27;95(20):e0190620.

300. Spuul P, Salonen A, Merits A, Jokitalo E, Kääriäinen L, Ahola T. Role of the amphipathic peptide of Semliki forest virus replicase protein nsP1 in membrane association and virus replication. J Virol. 2007 Jan;81(2):872–83.

301. Roberts KL, Leser GP, Ma C, Lamb RA. The amphipathic helix of influenza A virus M2 protein is required for filamentous bud formation and scission of filamentous and spherical particles. J Virol. 2013 Sep;87(18):9973–82.

302. Lee JY, Cortese M, Haselmann U, Tabata K, Romero-Brey I, Funaya C, et al. Spatiotemporal Coupling of the Hepatitis C Virus Replication Cycle by Creating a Lipid Droplet- Proximal Membranous Replication Compartment. Cell Rep. 2019;27(12):3602-3617.e5.

303. Ozeki S, Cheng J, Tauchi-Sato K, Hatano N, Taniguchi H, Fujimoto T. Rab18 localizes to lipid droplets and induces their close apposition to the endoplasmic reticulum-derived membrane. J Cell Sci. 2005 Jun 15;118(Pt 12):2601–11.

304. Camus G, Herker E, Modi AA, Haas JT, Ramage HR, Farese R V, et al. Diacylglycerol acyltransferase-1 localizes hepatitis C virus NS5A protein to lipid droplets and enhances NS5A interaction with the viral capsid core. J Biol Chem. 2013 Apr 5;288(14):9915–23.

305. Nevo-Yassaf I, Yaffe Y, Asher M, Ravid O, Eizenberg S, Henis YI, et al. Role for TBC1D20 and Rab1 in hepatitis C virus replication via interaction with lipid droplet-bound nonstructural protein 5A. J Virol. 2012 Jun;86(12):6491–502.

306. Miyanari Y, Atsuzawa K, Usuda N, Watashi K, Hishiki T, Zayas M, et al. The lipid droplet is an important organelle for hepatitis C virus production. Nat Cell Biol. 2007 Sep;9(9):1089–97.

307. Vieyres G, Pietschmann T. HCV Pit Stop at the Lipid Droplet: Refuel Lipids and Put on a Lipoprotein Coat before Exit. Cells. 2019 Mar 12;8(3).

308. Barba G, Harper F, Harada T, Kohara M, Goulinet S, Matsuura Y, et al. Hepatitis C virus core protein shows a cytoplasmic localization and associates to cellular lipid storage droplets. Proc Natl Acad Sci U S A. 1997 Feb 18;94(4):1200–5.

309. Melia CE, Peddie CJ, de Jong AWM, Snijder EJ, Collinson LM, Koster AJ, et al. Origins of Enterovirus Replication Organelles Established by Whole-Cell Electron Microscopy. mBio. 2019 Jun 11;10(3).

310. Belov GA, van Kuppeveld FJM. Lipid Droplets Grease Enterovirus Replication. Cell Host Microbe. 2019 Aug 14;26(2):149–51.

311. Gillespie LK, Hoenen A, Morgan G, Mackenzie JM. The endoplasmic reticulum provides the membrane platform for biogenesis of the flavivirus replication complex. J Virol. 2010 Oct;84(20):10438–47.

312. Depla M, Uzbekov R, Hourioux C, Blanchard E, Le Gouge A, Gillet L, et al. Ultrastructural and quantitative analysis of the lipid droplet clustering induced by hepatitis C virus core protein. Cell Mol Life Sci. 2010 Sep;67(18):3151–61.

313. Boulant S, Douglas MW, Moody L, Budkowska A, Targett-Adams P, McLauchlan J. Hepatitis C virus core protein induces lipid droplet redistribution in a microtubule- and dynein-dependent manner. Traffic. 2008 Aug;9(8):1268–82.

314. Akil A, Peng J, Omrane M, Gondeau C, Desterke C, Marin M, et al. Septin 9 induces lipid droplets growth by a phosphatidylinositol-5-phosphate and microtubule-dependent mechanism hijacked by HCV. Nat Commun. 2016 Jul 15;7:12203.

315. Shavinskaya A, Boulant S, Penin F, McLauchlan J, Bartenschlager R. The lipid droplet binding domain of hepatitis C virus core protein is a major determinant for efficient virus assembly. J Biol Chem. 2007 Dec 21;282(51):37158–69.

316. Zhang J, Lan Y, Li MY, Lamers MM, Fusade-Boyer M, Klemm E, et al. Flaviviruses Exploit the Lipid Droplet Protein AUP1 to Trigger Lipophagy and Drive Virus Production. Cell Host Microbe. 2018 Jun 13;23(6):819-831.e5.

317. Jordan TX, Randall G. Dengue Virus Activates the AMP Kinase-mTOR Axis To Stimulate a Proviral Lipophagy. J Virol. 2017 Jun 1;91(11).

318. Heaton NS, Randall G. Dengue virus-induced autophagy regulates lipid metabolism. Cell Host Microbe. 2010 Nov 18;8(5):422–32.

319. Guan H, Tian J, Qin B, Wojdyla JA, Wang B, Zhao Z, et al. Crystal structure of 2C helicase from enterovirus 71. Sci Adv. 2017 Apr;3(4):e1602573.

320. Scheffler U, Rudolph W, Gebhardt J, Rohayem J. Differential cleavage of the norovirus polyprotein precursor by two active forms of the viral protease. J Gen Virol. 2007 Jul;88(Pt 7):2013–8.

321. Franco D, Pathak HB, Cameron CE, Rombaut B, Wimmer E, Paul A V. Stimulation of poliovirus synthesis in a HeLa cell-free in vitro translation-RNA replication system by viral protein 3CDpro. J Virol. 2005 May;79(10):6358–67.

322. Xiang W, Cuconati A, Hope D, Kirkegaard K, Wimmer E. Complete protein linkage map of poliovirus P3 proteins: interaction of polymerase 3Dpol with VPg and with genetic variants of 3AB. J Virol. 1998 Aug;72(8):6732–41.

323. Takahashi D, Kim Y, Lovell S, Prakash O, Groutas WC, Chang KO. Structural and inhibitor studies of norovirus 3C-like proteases. Virus Res. 2013 Dec 26;178(2):437–44.

324. Herod MR, Prince CA, Skilton RJ, Ward VK, Cooper JB, Clarke IN. Structure-based design and functional studies of novel noroviral 3C protease chimaeras offer insights into substrate specificity. Biochem J. 2014 Dec 15;464(3):461–72.

325. Zhang L, Lin D, Sun X, Curth U, Drosten C, Sauerhering L, et al. Crystal structure of SARS-CoV-2 main protease provides a basis for design of improved α-ketoamide inhibitors. Science. 2020 Apr 24;368(6489):409–12.

326. Wessels E, Notebaart RA, Duijsings D, Lanke K, Vergeer B, Melchers WJG, et al. Structure-function analysis of the coxsackievirus protein 3A: identification of residues important for dimerization, viral rna replication, and transport inhibition. J Biol Chem. 2006 Sep 22;281(38):28232–43.

327. Shanmugam S, Nichols AK, Saravanabalaji D, Welsch C, Yi M. HCV NS5A dimer interface residues regulate HCV replication by controlling its self-interaction, hyperphosphorylation, subcellular localization and interaction with cyclophilin A. PLoS Pathog. 2018 Jul;14(7):e1007177.

328. Love RA, Brodsky O, Hickey MJ, Wells PA, Cronin CN. Crystal structure of a novel dimeric form of NS5A domain I protein from hepatitis C virus. J Virol. 2009 May;83(9):4395–403.

329. Douam F, Fusil F, Enguehard M, Dib L, Nadalin F, Schwaller L, et al. A protein coevolution method uncovers critical features of the Hepatitis C Virus fusion mechanism. PLoS Pathog. 2018 Mar;14(3):e1006908.

330. Champeimont R, Laine E, Hu SW, Penin F, Carbone A. Coevolution analysis of Hepatitis C virus genome to identify the structural and functional dependency network of viral proteins. Sci Rep. 2016 May 20;6:26401.

331. Yin C, Yau SST. A coevolution analysis for identifying protein-protein interactions by Fourier transform. PLoS One. 2017;12(4):e0174862.

332. Płaszczyca A, Scaturro P, Neufeldt CJ, Cortese M, Cerikan B, Ferla S, et al. A novel interaction between dengue virus nonstructural protein 1 and the NS4A-2K-4B precursor is required for viral RNA replication but not for formation of the membranous replication organelle. PLoS Pathog. 2019 May;15(5):e1007736.

333. David N, Yaffe Y, Hagoel L, Elazar M, Glenn JS, Hirschberg K, et al. The interaction between the hepatitis C proteins NS4B and NS5A is involved in viral replication. Virology. 2015 Jan 15;475:139–49.

334. Kaptein SJF, Goethals O, Kiemel D, Marchand A, Kesteleyn B, Bonfanti JF, et al. A pan-serotype dengue virus inhibitor targeting the NS3-NS4B interaction. Nature. 2021 Oct;598(7881):504–9.

335. Ackaert O, Vanhoutte F, Verpoorten N, Buelens A, Lachau-Durand S, Lammens L, et al. Safety, Tolerability, and Pharmacokinetics of JNJ-1802, a Pan-serotype Dengue Direct Antiviral Small Molecule, in a Phase 1, Double-Blind, Randomized, Dose-Escalation Study in Healthy Volunteers. Clin Infect Dis. 2023 Sep 18;77(6):857–65.

336. Goethals O, Kaptein SJF, Kesteleyn B, Bonfanti JF, Van Wesenbeeck L, Bardiot D, et al. Blocking NS3-NS4B interaction inhibits dengue virus in non-human primates. Nature. 2023 Mar;615(7953):678–86.

337. Yasgar A, Jadhav A, Simeonov A, Coussens NP. AlphaScreen-Based Assays: Ultra-High-Throughput Screening for Small-Molecule Inhibitors of Challenging Enzymes and Protein-Protein Interactions. Methods Mol Biol. 2016;1439:77–98.

Chapter 6

Acknowledgments

"*Science is not only a disciple of reason but also one of romance and passion.*"

— Stephan Hawking (1942-2018), *Q&A Parade*

---

6 Acknowledgments

First and foremost, the work presented in this thesis could not have been accomplished without the continuous help and support of Dr. Volker Lohmann. He accepted me in his research group as a master student back in 2016 and later as a PhD student in 2017 and mentored me throughout my scientific career. Our scientific discussions have always been most valuable to me and have been essential for the experiments performed for this doctoral thesis. Besides scientific matters, Volker was always willing to lend a listening ear to my personal issues and has been one of the most caring and understanding group leaders that I ever had the pleasure of working with.

Second, I would like to express my greatest gratitude to the members of my TAC committee, Dr. Steeve Boulant, Dr. Mirko Cortese and Prof. Dr. Ralf Bartenschlager, who have provided my project with excellent scientific input over the years. They have really helped me shape my project during discussions, meetings, seminars and retreats. In addition, I feel deeply in debt to Dr. Brett Lindenbach, Dr. Peter Bredenbeek and Dr. Freek Weidema for the academic and professional support they have given me during my scientific career.

Third, I am thankful to all our scientific collaborators, in particular dr. Stéphane Bressanelli and his group members at the Paris-Saclay University, for aiding me in my scientific process and providing me with such detailed and excellent modeling data. Thanks to their input and work, we are a step closer towards understanding the replication of norovirus and the molecular interaction between norovirus NS1-2 and NS4.

Fourth, I would like to thank all my former and present colleagues of the Lohmann lab, in particular Ombretta Colasanti, Cong Si Tran, Philipp Schult, Chris Heuss, Marit Lingemann, Arthur Lang, Rahel Klein and Tengfeng Li, for creating such an amiable and supportive atmosphere, both inside and outside of the lab. Thanks to you, Heidelberg felt like home. In addition to the members of the Lohmann lab, I would also like to thank other members of the institute that made my stay in Germany so

enjoyable, especially Yannick Stahl, Julia Welsch, Vera Magg, Dominik Kiemel, Sarah Göllner, Katja Kopp, Philipp Klein and Berati Cerikan.

Ten vijfde wil ik mijn vrienden in Nederland bedanken voor de steun en toeverlaat die zij in de afgelopen jaren voor mij vormden. Ik zal altijd een gevoel van nostalgische genegenheid koesteren bij alle mensen uit het Westland met wie ik sinds de middelbare school of zelfs daarvoor al bevriend ben. Ook betuig ik grote dank aan mijn vrienden van de universitaire studie in Leiden, in het bijzonder Jente van Staalduinen, Hessel Honkoop en Chris Stavast, voor de luchtige, maar ook vakinhoudelijke gesprekken en borrels van de afgelopen jaren. Tot slot wil ik mijn dankbaarheid uiten aan de leden van de JOVD Baronie van Breda, in het bijzonder ir. Stijn Clarijs, voor de warme manier waarop ik in Breda ontvangen ben.

Ten zesde prijs ik mijzelf gelukkig met mijn familie. Zonder de onvoorwaardelijke steun van hen, in het bijzonder mijn vader en moeder, was ik nooit op de plek terechtgekomen waar ik mij nu bevind. Ook opa en oma Veenstra en opa en oma Geldhof zijn altijd belangrijke steunpilaren voor mij geweest. Daarnaast ben ik ongelooflijk trots op mijn broertje en zusje en bedank ik hen voor alle steun die ze mij de afgelopen jaren gegeven hebben.

Als laatste wil ik mijn vriendin, Mirthe Dolk, de meest liefdevolle dankbaarheid betuigen. Zonder haar steun zouden de afgelopen paar jaren niet hetzelfde zijn geweest en zou ik de tegenslagen die inherent horen bij een wetenschappelijke carrière alleen hebben moeten trotseren. Ik ben ontzettend blij dat we nu samenwonen en we samen – met Winston en Cleo – de toekomst tegemoet gaan.